

**Cytoskeleton proteins involved in  
chromosome segregation and cell division in  
*Corynebacterium glutamicum***

Inaugural-Dissertation  
zur  
Erlangung des Doktorgrades  
der Mathematisch-Naturwissenschaftlichen Fakultät  
der Universität zu Köln

vorgelegt von  
**Catriona Donovan**  
aus Tralee, Irland

Köln, March 2012





Berichtersteller: Prof. Dr. Reinhard Krämer  
Institut für Biochemie der Universität zu Köln

Prof. Dr. Marc Bramkamp  
Institut für Biochemie der Universität zu Köln und  
Biozentrum, Department Biologie I, Ludwig-Maximilians Universität, München

Tag der mündlichen Prüfung: 11-06-2012

**This dissertation is dedicated to my parents.**

**Index**

<b>I. Abstract</b>	<b>V</b>
<b>II. Zusammenfassung</b>	<b>VII</b>
<b>III. Abbreviations</b>	<b>IX</b>
<b>1. Introduction</b>	<b>1</b>
<b>Chapter I</b>	
1.1 DNA replication initiation	1
1.2 DNA partitioning systems	1
Plasmid partitioning systems	2
Chromosome encoded partitioning systems	3
Chromosome segregation in <i>Bacillus subtilis</i>	4
Chromosome segregation in <i>Caulobacter crescentus</i>	5
Chromosome segregation in <i>Vibrio cholerae</i>	6
1.3 Chromosome condensation - SMC and organization of chromosomes	7
1.4 Cell division	9
Spatial regulation of cytokinesis – negative regulation	9
Novel spatial and temporal regulation of cytokinesis	10
Spatial regulation of cytokinesis – positive regulators	10
1.5 Cell polarity – integrated temporal and spatial regulation	12
1.6 <i>Corynebacterium glutamicum</i> – cell division and chromosome segregation	13
<b>Chapter II</b>	
1.7 The bacterial cytoskeleton	17
Bacterial actin homologues – ParM	18
Divergent bacterial actin families – AlfA and Alf7A	18
1.8 Identification of a <i>C. glutamicum</i> actin-like protein	20
1.9 <i>C. glutamicum</i> prophages	21
1.10 Aim of the research	22
<b>2. Results</b>	<b>24</b>
<b>Chapter I</b>	
2.1 The Par chromosome segregation system of <i>C. glutamicum</i>	24
Phenotypes of <i>par</i> null deletion mutants	24
<i>In vivo</i> localization of ParA and PldP	27
Phenotypes of double <i>par</i> deletion mutants	28
ParA, unlike PldP, is necessary for polar localization of ParB	29
2.2 Polar tethering of the chromosome origins in <i>C. glutamicum</i>	30
DivIVA physically interacts with ParB, <i>in vivo</i>	31
DivIVA interacts with ParB, <i>in vitro</i>	33

## Index

---

The N-terminal domain of ParB interacts with DivIVA	33
In <i>C. glutamicum</i> , mutation of the conserved arginine (R21) of ParB significantly alters interaction with DivIVA	35
A central region of DivIVA is necessary for ParB interaction	37
In the synthetic <i>E. coli</i> system, ParB interacts with DivIVA via a diffusion-capture mechanism	39
The ParB-DivIVA interaction is conserved in Actinobacteria	39
ParA interacts with both ParB and DivIVA	42
2.3 Chromosome organization influences cell growth and division site selection	44
2.4 Characterization of the orphan ParA-like protein, PldP	49
PldP exists as a monomer in solution	49
PldP binds membranes via a putative C-terminal amphipathic helix	50
<i>In vivo</i> , PldP binds to the membrane	51
Identification of potential PldP interaction partners	52
<b>Chapter II</b>	
2.5 Does AlpC exhibit actin-like properties?	55
AlpC assembles into filaments, <i>in vivo</i>	55
AlpC filament dynamics	57
AlpC exists as a monodisperse species in solution	57
AlpC hydrolyzes both ATP and GTP	58
AlpC polymerization is nucleotide dependent, <i>in vitro</i>	58
2.6 What is the molecular role of AlpC in <i>C. glutamicum</i> ?	60
AlpC filament assembly requires a host specific factor	60
Attempts to identify an AlpC adaptor protein	60
Filament assembly of AlpC at physiological concentration	61
In the absence of <i>alpC</i> , prophage induction rate is reduced	61
<i>In vivo</i> co-visualization of the CGP3 prophage and AlpC	62
<b>3. Discussion</b>	<b>64</b>
<b>Chapter I</b>	
3.1 ParA and ParB: role in chromosome segregation	64
ParA has a possible additional role in regulation of chromosome replication initiation	67
Pleiotropic nature of <i>parA</i> and <i>parB</i> mutation – possible additional roles	68
3.2 Polar anchoring of the <i>oriC</i> is mediated by ParB-DivIVA interaction	70
The N-terminal of ParB interacts with DivIVA	73
ParA might support polar <i>oriC</i> anchoring	73
ParB interacts with a central region of DivIVA	74
In <i>C. glutamicum</i> , DivIVA truncation mutants are viable but acquire suppressor mutations	75

## Index

---

3.3 Regulation of cell division in <i>C. glutamicum</i>	76
PldP: role in cell division	77
PldP: possible role in regulation of ParA	78
Simultaneous deletion of PldP and ParB or ParA increases growth from ectopic sites	88
Orphan ParA-like proteins organize the bacterial subcellular environment	81
3.4 Proposed model for chromosome segregation in <i>C. glutamicum</i>	82
3.5 The ParB-DivIVA interaction is conserved in Actinobacteria	84
<b>Chapter II</b>	
3.6 AlpC is an actin-like protein	85
3.7 AlpC is necessary for efficient prophage induction	86
3.8 Host actin related proteins organize phage replication	87
<b>4. Experimental Procedures</b>	<b>89</b>
Table 4.1: Plasmids used in this study	89
Table 4.2: Oligonucleotides used in this study	92
Table 4.3: Bacterial strains used in this study	96
Table 4.4: Overview of <i>C. glutamicum</i> strains constructed in this study	97
4.1 Strain construction	98
4.2 Plasmid construction	98
4.3 Media and cultivation conditions	103
4.4 Molecular biological techniques	104
General cloning techniques	104
DNA amplification	104
Agarose gel electrophoresis and gel extraction	104
Sequencing	104
Site-directed mutagenesis	104
DNA quantification	105
Overlap extension PCR	105
Preparation of competent cells and transformation	105
Fluorescence microscopy	105
Time-lapse microscopy with microfluidic chamber	105
Bacterial Two-Hybrid and $\beta$ -galactosidase-assay	106
Determination of circular phage DNA using quantitative PCR	106
4.5 Biochemical methods	106
Polyacrylamid gel electrophoresis	106
Immunoblotting	106
Heterologous overexpression and protein purification	107
ParB purification	107
PldP purification	107
AlpC purification	108
Concentration by ultrafiltration	108
Nucleotide hydrolysis assay	108

## Index

---

Co-elution Assay	108
Pull Down Assay	109
PI3P membrane binding	109
Sodium carbonate extraction	110
<b>5. Literature</b>	<b>111</b>
<b>6. Supplementary Figures</b>	<b>125</b>
<b>7. Scientific Activities</b>	<b>131</b>
<b>8. Acknowledgements</b>	<b>132</b>
<b>9. Erklärung</b>	<b>133</b>
<b>10. Curriculum Vitae</b>	<b>134</b>

### I. Abstract

The chromosome partitioning system of the rod-shaped *actinomycete*, *Corynebacterium glutamicum* consists of the Walker-type ATPase (ParA), a DNA binding protein (ParB) and centromere-like *parS* sites, located at the origin-proximal region of the chromosome. ParB binds *parS* sites, specifically. ParA is recruited to the ParB-*parS* nucleoprotein complex, likely providing the driving force needed to relocate replicated *oriC*'s to the opposite cell pole. The ParB-*oriC* complex is then stably attached to the cell pole, where it remains and the cell divides in-between the segregated chromosomes. The phenotypic consequences of mutation of *parA* or *parB* include reduced growth rates, a high frequency of anucleate cells and altered cell lengths. Also, in the absence of *parA*, the *oriC* is mislocalized.

To date, polar origin tethering factors have been identified in only few bacteria. Thus, we wanted to identify and analyze the *Actinobacteria* chromosome polar targeting factor. A synthetic *in vivo* approach was employed to analyze the anchoring of the ParB-*oriC* nucleoprotein complex to the cell poles via interaction with DivIVA. It was shown that DivIVA is necessary and sufficient to recruit ParB, therefore also tether the *oriC* at the cell poles. With this synthetic system, in combination with mutational analysis, the interaction sites between ParB and DivIVA were mapped. In *Corynebacterium glutamicum*, mutation of the N-terminal of ParB showed reduced polar *oriC* localization. In addition, the interaction between ParB and DivIVA was demonstrated for other members of the Actinobacteria phylum, including the notorious pathogen *Mycobacterium tuberculosis* and *Streptomyces coelicolor*.

*Corynebacterium glutamicum*, which undergoes cell division between the segregated nucleoids but not necessarily precisely at midcell, does not possess the conventional positive or negative FtsZ regulators found in other rod-shaped bacteria. However, *Corynebacterium glutamicum* encodes an orphan *parA*-like gene (*pldP*, for ParA-like Division Protein). In this thesis a number of subtle differences between ParA and PldP were highlighted, showing that PldP is not involved in chromosome segregation, but probably in regulation of cytokinesis. Similar to the MinD protein of *B. subtilis*, PldP contains a putative C-terminal amphipathic helix. *In vivo*, PldP localizes, probably early, to the division septum and the localization pattern is highly reminiscent of MinD. Further *in vitro* analysis showed that PldP can bind membranes.

Contrary to the long-standing assumption, some *Corynebacterium glutamicum* strains encode an actin homologue. The *cg1890* (designated AlpC, for Actin-Like Protein Corynebacterium) gene was recently identified as a putative actin-like protein. At the sequence level, AlpC shares little homology with actin and other actin-like proteins, however, it does contain the actin signature motive involved in nucleotide binding and hydrolysis. *In vivo*, AlpC forms dynamic structures, which assemble into long straight filaments and disassemble into foci. *In vitro*, AlpC can hydrolyze both ATP and GTP and exhibits nucleotide dependent polymerization. Mutation of the actin signature motif (AlpCD301A) abolishes nucleotide hydrolysis but not polymerization. Thus, AlpC is a genuine member of the actin-like superfamily.

On the genome, *alpC* is one of the first on the CGP3 prophage region. This prophage no longer forms infectious phage particles and most of the coding regions show little homology to known

## Abstract

---

bacterial genes. The CGP3 prophage can excise from the bacterial chromosome and exist as multiple copies of circular DNA. *In vivo* co-visualization of induced prophage and AlpC filaments suggests that the *Corynebacterium glutamicum* actin-like protein is not involved in segregation of the prophage particles. However, in the absence of *alpC*, the frequency of prophage induction is drastically reduced. Thus, we speculate that AlpC plays a role in replication the CGP3 prophage.

### II. Zusammenfassung

Das Chromosom-Partitionierungs-System des keulenförmigen Aktinomyzets *Corynebacterium glutamicum* besteht aus einer „Walker-type“ ATPase (ParA), einem DNA-Bindeprotein (ParB) sowie zentromeren *parS*-Sequenzen, die sich an einer ursprungsnahen Region auf dem Chromosom befinden. ParB bindet spezifisch an *parS*-Sequenzen. ParA wird an den ParB-*parS* Nukleoprotein-Komplex rekrutiert und stellt dabei die treibende Kraft zur Verlagerung der replizierten *oriC*'s zum gegenüberliegenden Zellpol. Der ParB-*oriC* Komplex wird dann stabil an den Zellpol gebunden sodass die Zellteilung zwischen den getrennten Chromosomen stattfinden kann. Phänotypische Konsequenzen nach Mutationen von *parA* und *parB* sind reduziertes Wachstum, eine hohe Anzahl DNA-freier Zellen sowie veränderte Zelllängen. Des Weiteren ist die *oriC* in Abwesenheit von ParA misslokalisiert.

Bis heute wurden Mechanismen zur polaren Chromosomenbindung nur in wenigen Bakterien identifiziert. Ein Ziel dieser Arbeit ist die Identifizierung und Charakterisierung des Chromosomsegregations-Mechanismus in *Aktinobakterien*. Zur Untersuchung der polaren Verankerung des ParB-*oriC* Nukleoprotein-Komplexes als Folge einer Interaktion mit DivIVA wurde ein synthetischer *in vivo* Ansatz etabliert. Es konnte gezeigt werden, dass DivIVA nötig und ausreichend ist um ParB, und somit den *oriC*, an die Zellpole zu rekrutieren. Des Weiteren konnte in dem *in vivo* Assay, zusammen mit Mutationsanalysen, die Bindestellen von ParB und DivIVA identifiziert werden. In *Corynebacterium glutamicum* führte eine Mutation des N-Terminus von ParB zu einer reduzierten polaren *oriC*-Lokalisation. Darüber hinaus konnte die Interaktion zwischen ParB und DivIVA für weitere Mitglieder der Abteilung der Aktinobakterien gezeigt werden, inklusive dem Krankheitserreger *Mykobakterium tuberculosis* sowie *Streptomyces coelicolor*.

*Corynebacterium glutamicum*, dessen Zellteilung zwischen den getrennten Chromosomen aber nicht zwangsläufig an der exakten Zellmitte stattfindet, besitzt keine konventionellen positiven oder negativen FtsZ-Regulatoren, die man in anderen keulenförmigen Bakterien findet. Jedoch kodiert *Corynebacterium glutamicum* ein *parA*-ähnliches Gen (*pldP*, engl.: ParA-like Division Protein). In der vorliegenden Arbeit werden einige subtile Unterschiede zwischen ParA und PldP beschrieben, die zeigen, dass PldP keine Rolle in der Chromosomensegregation spielt, vermutlich aber in der Zellteilung. Ähnlich dem MinD Protein aus *Bacillus subtilis* enthält PldP eine mögliche C-terminale amphipatische Helix. *In vivo* lokalisiert PldP, wahrscheinlich zu einem frühen Zeitpunkt des Zellzyklus, an das Zellteilungsseptum und gleicht somit dem Lokalisationsverhalten von MinD. Außerdem haben *in vitro* Studien gezeigt, dass PldP an Membranen bindet.

Gegensätzlich langjähriger Annahmen kodieren einige *Corynebacterium glutamicum* Stämme ein Homolog zum eukaryotischen Aktin. Das Gen *cg1890* (umbenannt zu AlpC, engl.: Actin-like Protein Corynebacterium) wurde kürzlich als mögliches Aktin-ähnliches Protein identifiziert. Obwohl AlpC nur wenige Sequenzhomologien zum Aktin sowie anderen Aktin-ähnlichen Proteinen hat, enthält es das typische Aktinmotiv, dass in Nukleotidbindung und Hydrolyse involviert ist. *In vivo* bildet AlpC dynamische Strukturen die zu langen Filamenten assemblieren bzw. Foki disassemblieren können. *In*

## Zusammenfassung

---

*vitro* kann AlpC sowohl ATP als auch GTP hydrolysieren und nukleotidabhängig polymerisieren. Mutationen im Aktin-typischen Motiv verhindert Nukleotidhydrolyse jedoch nicht die Polymerisation. Somit ist AlpC ein Mitglied der Aktin-ähnlichen Superfamilie.

Im Genom ist *alpC* eines der ersten Gene der CGP3 Prophagenregion. Dieser Prophage ist nicht mehr in der Lage infektiöse Phagenpartikel zu formen und die meisten Kodierungsregionen zeigen wenig Homologie zu bekannten bakteriellen Genen. Der CGP3 Prophage kann sich vom bakteriellen Chromosom trennen und als vielfache Kopie zirkulärer DNA existieren. *In vivo* Co-Visualisierungen induzierter Prophagen- und AlpC-Filamente lässt vermuten, dass das Aktin-ähnliche Protein aus *Corynebacterium glutamicum* in der Segregation der Prophagenpartikel keine Rolle spielt. Jedoch ist in Abwesenheit von *alpC* die Häufigkeit der Prophageninduktion drastisch reduziert. Daher wird vermutet, dass AlpC eine Rolle in der CGP3 Prophagenreplikation spielt.

## Abbreviations

---

### III Abbreviations

ADP	adenosine-5'-diphosphate
ATP	adenosine-5'-triphosphate
Bp	base pairs
DAPI	4'-6-Diamidino-2-phenylindole
BCIP	5-Bromo-4-chloro-3-indolyl phosphate
CFP	cyan fluorescent protein
CGXII	minimal medium
DMSO	dimethyl sulfoxide
DNA	deoxyribonucleic acid
dNTP	deoxyribonucleotide
eCFP	enhanced cyan fluorescent protein
EDTA	ethylenediaminetetraacetic acid
GFP	green fluorescent protein
H <sub>2</sub> O <sub>d</sub>	deionized water
H <sub>2</sub> O <sub>dd</sub>	double deionized water
IPTG	isopropyl β-D-1-thiogalactopyranoside
kan <sup>R</sup>	kanamycin resistance
<i>K<sub>av</sub></i>	elution constant
kb	<i>kilo base pairs</i>
kDa	kilodalton
LB	Luria Bertani medium
mCHERRY	red fluorescent protein
MM1	minimal medium
MWCO	molecular weight cut-off
<i>n</i>	sample size
NBT	nitro blue tetrazolium chloride
OD <sub>600</sub>	optical Density at 600nm
PAGE	polyacrylamid-gel electrophoresis
PCR	polymerase chain reaction
PVDF	polyvinylidene fluoride
SDS	sodium dodecylsulfate
TAE	tris-Acetate / EDTA-buffer
Tris	tris-(hydroxymethyl)-aminomethane
V	volt
YFP	yellow fluorescent protein



### 1. Introduction

#### Chapter I

#### Cytoskeleton elements involved in chromosome segregation and cell division

Bacteria exhibit a high degree of intracellular organization, both in the timing of essential processes and in the placement of the chromosome, division site and regulatory proteins. The high accuracy of spatial and temporal regulators ensures that chromosome replication initiation along with chromosome segregation and condensation are coordinated with cell growth and division, ensuring that each daughter cell receives a complete copy of the genetic material. Recent advances in microscopy and cytological techniques along with structural and biochemical analysis have greatly advanced our knowledge on the organization and regulation of the bacterial cell.

#### 1.1 DNA replication initiation

Initiated from a single origin of replication (*oriC*), the bacterial chromosome is replicated bidirectionally and terminates at the opposite end of the chromosome (*terC*), where termination proteins disengage the replication machinery from the DNA (Sherratt, 2003). Replication initiation is mediated by a single initiator protein, DnaA, which specifically interacts with conserved motifs at the *oriC* (Messer, 2002; Kaguni, 2006). In the ATP bound state, DnaA forms high-ordered multimeric complexes and cooperatively binds to *oriC* (Nishida *et al.*, 2002). Binding of ATP-DnaA promotes local unwinding of the DNA duplex at AT-rich sequences, facilitating loading of the DNA helicase, and recruitment of other necessary initiator proteins (Sutton *et al.*, 1998).

Replication initiation is strictly coordinated with cell cycle progression. Depending on the organism, a variety of mechanisms regulate the activity of DnaA, including mechanisms that affect the cellular concentration of DnaA, nucleotide bound state and accessibility to binding sites. Recent evidence shows that replication initiation and elongation is directly linked with nutrient availability in *Escherichia coli* and *Bacillus subtilis* (Janniere *et al.*, 2007; Maciag *et al.*, 2011). However, in some organisms (for example, *E. coli*) replication can be initiated more than once per cell cycle, giving rise to daughter cells that inherit a semi-replicated chromosome (Cooper and Helmstetter, 1968; Niki and Hiraga, 1998; Nielsen *et al.*, 2007). Although this normally only occurs when there is an abundance of nutrients, regulation of multiple initiation events per cell cycle remains largely obscure.

#### 1.2 DNA partitioning systems

The organization and dynamic behavior of the bacterial chromosome is particularly evident during chromosome replication and segregation. In *E. coli* and vegetative *B. subtilis* cells the newly

## Introduction

---

duplicated origins rapidly move from the midcell to the cell quarter positions, sites which represent the predivisional site in each daughter cell (Niki and Hiraga, 1998; Webb *et al.*, 1998; Niki *et al.*, 2000). In *Caulobacter crescentus*, the *oriC* is positioned at the cell pole and after replication the sister origin is moved to the opposite cell pole (Mohl and Gober, 1997; Viollier *et al.*, 2004). More interestingly, in the gamma-proteobacterium *Vibrio cholerae*, which contains two circular chromosomes, the *oriC* of chromosome I (chrI) is segregated unidirectionally similar to *C. crescentus*, while the *oriC* of chromosome II (chrII) is found at the cell centre and is segregated bidirectionally similar to the chromosomes of *E. coli* and *B. subtilis* (Fogel and Waldor, 2005; Fiebig *et al.*, 2006). Irrespective of cellular localization and track of movement, common to all is the rapid and directed translocation of the *oriC* which occurs prior to completion of chromosome replication.

Thus, it appeared that, similar to the eukaryotic chromosome segregation apparatus, a mitotic-like apparatus could also exist in bacteria. As early as 1977, an active partitioning system was suggested for the low copy plasmid P1 prophage from *E. coli* due to its extremely efficient maintenance, despite often being present in as few as two copies prior to division (Prentki *et al.*, 1977). Indeed, the *parABS* locus was later identified and shown to be necessary and sufficient for stable maintenance of P1 prophage (Abeles *et al.*, 1985). Homologues of the *par* locus were subsequently identified on the bacterial chromosome, and found to be highly conserved, found across the bacterial domain and in many archaea, as well as in some chloroplasts and mitochondria (Gerdes *et al.*, 2000; Livny *et al.*, 2007). However, the chromosome of *E. coli* and *Mycoplasma* species are examples of the few exceptions.

### Plasmid partitioning systems

The genetic organization of *par* loci is similar for both chromosome and plasmid encoded systems. In general, the *par* locus entails two *trans*-acting proteins encoded in an operon (*parA* and *parB*, respectively) and *cis*-acting “centromere-like” elements. The centromere-binding protein (ParB) binds the centromere-like element (*parS*) forming a nucleoprotein complex (Funnell, 1987). The segrosomes are recognized and subsequently segregated by the action of dynamic cytoskeleton filaments composed of ParA protein, which, depending on the plasmid partitioning system, is either a Walker-A P loop ATPase (ParA, Type I), an actin-like ATPase (ParM, Type II) or a tubulin-like GTPase (TubZ, Type III) (Gerdes *et al.*, 2000, Larsen *et al.*, 2007). (Refer to chapter II for more details on type II plasmid partitioning systems).

The *par* loci of Type I plasmid partitioning systems are among the best characterized, including *E. coli* P1 and F plasmids (Ogura and Hiraga, 1983; Austin and Abele, 1983a; Austin and Abele, 1983b; Abeles *et al.*, 1985). Type I systems can be divided further into type Ia and Ib which differ in genetic organization and homology of the Par proteins encoded (Davis *et al.*, 1992; Hayes *et al.*, 1994; Radnedge *et al.*, 1998; Libante *et al.*, 2001). Both systems encode a Walker-type ATPase located upstream of the centromere-binding protein. In type Ia the centromere-like element is located downstream of the *par* operon, while in type Ib this element is found upstream, often in the promoter

region of the *par* operon. Type Ia ParA proteins contain a putative N-terminal helix-turn-helix (HTH) DNA binding motive and a C-terminal Walker box domain. The ParA protein can associate with the operator sequence of the *par* promoter to down-regulate transcription (Davis *et al.*, 1992; Davey and Funnell, 1994; Davey and Funnell, 1997). The putative DNA binding motive is absent in type Ib ParA proteins. However, the centromere-binding protein functions as a transcription regulator upon binding the centromere-like element, which is situated in the promoter region of the *par* operon. Thus, in both systems autoregulation maintains the correct stoichiometry of Par proteins which is essential for plasmid partitioning (Hirano *et al.*, 1998; Friedman and Austin, 1998).

The P1 and F plasmids exhibit very specific subcellular localizations. When only a single plasmid is present, midcell localization is observed, while in cells that contain two plasmids each plasmid is positioned at the cell quarter positions (Kim and Wang, 1999; Erdmann *et al.*, 1999). This rapid segregation is highly dependent on the Par system (Gordon *et al.*, 1997). Cooperative binding of ParB to the centromere-like element leads to the formation of higher ordered partition complexes. Although controversial, this interaction is thought to mediate plasmid pairing (Jensen *et al.*, 1998; Edgar *et al.*, 2001). Plasmid pairing ensures that plasmids that use similar replication or segregation mechanisms are incompatible and cannot coexist in the same cell (Austin and Nordstroem, 1990). Subsequent to nucleoprotein complex formation, a fully active segrosome is formed only when bound by ParA. The ParA protein forms dynamic gradients, oscillating over the bacterial nucleoid, directing the movement of the plasmid (Ringgaard *et al.*, 2009). The activity of ParA is modulated by ParB, regulating the nucleotide bound state of ParA and its affinity for the nucleoid or polymerization into filaments. Numerous models have been proposed in an attempt to explain the dynamic oscillating activities of ParA and the directed movement of replicated plasmids. A recent model proposed by Ringgaard and co-workers suggests that ATP hydrolysis and depolymerization of the ParA-ATP polymers is stimulated by interaction with ParB (Ringgaard *et al.*, 2009). However, the nucleoprotein complex remains attached to and follows the end of the retracting ParA filament. Released ParA monomers rebind ATP and polymerize in regions furthest away from the nucleoprotein complex. Another model suggests that ParA forms filaments that extend from pole to pole and again upon encountering the nucleoprotein complex, the depolymerizing ParA filament pulls the replicated plasmid to their correct subcellular position. Although the molecular mechanism has not been completely unraveled, it is clear that in the absence of one component of the Par system, plasmids are not stably maintained.

### **Chromosome encoded partitioning systems**

Chromosome encoded *par* loci are classified as Type I, encoding ParA ATPases which contain Walker A / B motifs that have low ATPase activity. The *parAB* locus and centromere-like elements are generally located in the origin-proximal region (Gerdes *et al.*, 2000; Livny *et al.*, 2007), suggesting a functional preservation among different bacterial species. Structural and biochemical analysis revealed that ParB (Spo0J) of *Thermus thermophilus* has four domains, a flexible N-terminal domain,

a central HTH domain followed by a linker domain and a C-terminal dimerization domain (Leonard *et al.*, 2004). It has been suggested that the C-terminal domain is the primary dimerization domain, while the N-terminal and HTH domains compose a secondary dimerization domain that is necessary for DNA binding. *In vitro*, Spo0J can stimulate the ATP hydrolysis of Soj (ParA), which is further enhanced in the presence of *parS* DNA (Leonard *et al.*, 2005). In some plasmid and chromosome encoded Par systems, the ParA interaction site has been mapped to a short but highly conserved part of the N-terminal of ParB / Spo0J (Surtees and Funnell, 1999; Figge *et al.*, 2003; Ravin *et al.*, 2003). *In vitro*, the hydrolysis rate of ParA can be specifically stimulated by the N-terminal 20 amino acid of ParB (Leonard *et al.*, 2005). Structural and biochemical analysis of *Thermus thermophilus* Soj revealed that upon binding ATP Soj dimerizes forming a “nucleotide sandwich dimer”. Only as an ATP bound dimer can Soj bind DNA, both of which are prerequisites for polymerization (Leonard *et al.*, 2005).

*B. subtilis*, *C. crescentus*, *E. coli* and *V. cholerae* have emerged as model organisms for studying the molecular mechanisms of chromosome segregation, to date. Although *E. coli* does not encode a Par system, segregation has been studied in detail in this organism (Reyes-Lamothe *et al.*, 2008; Wang and Sherratt, 2010). Despite the high degree of conservation at the levels of sequence and genetic organization, studies on chromosomal ParA and ParB revealed a lack of uniformity in their action in different organisms. New insights into the molecular role(s) of Par systems show an involvement in a number of overlapping systems and subsequent mutation of the Par system lead to pleiotropic phenotypes, making it difficult to decipher their precise role. However, a role in segregation is underlined by the fact that chromosomally encoded Par systems can stabilize unstable plasmids as long as the plasmid contains the cognate *parS* sequence (Lin and Grossman, 1998; Yamaichi and Niki, 2000; Godfrin-Estevenson *et al.*, 2007).

### Chromosome segregation in *Bacillus subtilis*

In *B. subtilis*, the ParB homologue (Spo0J) binds at least 8 *parS* sites found in the origin-proximal region of the chromosome and spreads latterly along the DNA to form foci that localize at the cell quarter positions, coinciding with the *oriC* region during vegetative growth (Lin *et al.*, 1997; Glaser *et al.*, 1997; Lin and Grossman, 1998; Murray *et al.*, 2006). The ParA homologue (Soj) exhibits two distinct localization patterns; as cytoplasmic foci which are dependent on Spo0J and septal localization that is dependent on the division site selection protein MinD. (Autret and Errington, 2003; Murray and Errington, 2008). In the absence of *spo0J*, Soj remains statically associated with the nucleoid (Marston and Errington, 1999; Quisel *et al.*, 1999; Murray and Errington, 2008).

On a molecular level, the interplay between Soj and Spo0J influences multiple processes. Upon binding ATP, Soj dimerizes and subsequently exhibit non-specific, cooperative DNA binding activity (Murray and Errington, 2008). Two positively charged residues of the N-terminal of Spo0J (amino acid 3 and 7, both lysine) can stimulate the ATPase activity of Soj, driving the Soj-ATP dimer to a monomer and subsequent release from DNA (Gruber and Errington, 2009). This cycle of DNA binding and ATP-hydrolysis is important for the regulation of replication initiation (Murray and

Errington, 2008; Scholefield *et al.*, 2011). In the monomeric form, Soj directly interacts with DnaA and inhibits DNA replication (Scholefield *et al.*, 2012). Positive regulation of DnaA by Soj requires its DNA binding activity. Although dimeric Soj also directly interacts with DnaA, the molecular mechanism of activation has not been elucidated, yet.

In vegetative cells, *soj* mutants do not exhibit any gross segregation defects (Ireton *et al.*, 1994; Webb *et al.*, 1998), while deletion of *sop0J* does not affect origin localization and dynamics, but does however result in mild segregation defects (approximately 2 % anucleate cells) (Lin and Grossman, 1998). In addition, contrary to other ParA homologues, assembly of Soj into filaments, either in the presence or absence of DNA, has not been observed (Scholefield *et al.*, 2011). However, Soj and Spo0J are involved in chromosome organization during sporulation. Under nutrient limitation *B. subtilis* cells can undergo a complex morphological developmental route leading to the production of endospores. Sporulation specific genes are transcribed, the chromosome adopts an elongated structure (called an axial filament) extended from pole to pole and an asymmetric septum forms close to one cell pole, forming the prespore compartment. Due to the relaxed configuration some of the axial filament becomes trapped in the prespore. Prior to closure of the septum, the remainder of the chromosome is pumped into the prespore compartment by the DNA translocase, SpoIIIE. Analysis of the organization of the axial filament revealed that the *oriC*, representing about one quarter of the chromosome, is positioned at the cell pole in the prespore compartment while the *terC* is in the mother cell (Wu and Errington, 1998; Sullivan *et al.*, 2009). In the absence of *soj* and *sop0J* the organization of the axial filament is dramatically altered, frequently resulting in prespores lacking the *oriC* (Wu and Errington, 1998; Lee *et al.*, 2003; Sullivan *et al.*, 2009).

Soj was suspected to act as a transcription regulator that negatively regulates sporulation specific genes (Ireton *et al.*, 1994). More recently, this block in sporulation was shown to be indirect, through the activation of the Sda replication checkpoint (Murray and Errington, 2008). In the absence of *sop0J* entry into the sporulation pathway is blocked as the nucleotide bound state of Soj is not regulated, which subsequently effects DnaA mediated replication initiation leading to activation of Sda. However, what remains to be understood is the consequence of the interaction between Soj and the cell division protein MinD (Autret and Errington, 2003; Murray and Errington, 2008). ATP bound Soj interacts with and is recruited by MinD to the division septa, and in the absence of *minD* Soj is diffused throughout the cytoplasm (Scholefield *et al.*, 2011). One could imagine that MinD fulfills a role similar to Spo0J, regulating the nucleotide bound state of Soj, perhaps to synchronize initiation of replication and cell division. However, in the absence of *minD* chromosome replication and organization is not affected (Marston *et al.*, 1998).

### **Chromosome segregation in *Caulobacter crescentus***

*C. crescentus* is an  $\alpha$ -proteobacterium that divides unequally into a swarmer cell and a sessile stalked cell, which, aside from distinct morphological features, have different cell fates. DNA replication is initiated only when the swarmer cell differentiates into a stalked cell (Jensen and Shapiro, 1999;

Jensen *et al.*, 2001). After origin duplication, the sister origin is translocated from the flagellated pole (old pole) to the opposite cell pole. Using high-resolution microscopy, retraction of ParA filaments was shown to coincide with the directed movement of the ParB bound origins (Ptacin *et al.*, 2010). Similar to the situation in *B. subtilis*, ParB regulates ParA activity by modulating the nucleotide bound state of ParA (Easter and Gober, 2002). ParA monomers bind ATP and dimerize, which subsequently result in DNA binding or polymerization (Ptacin *et al.*, 2010; Schofield *et al.*, 2010). ParA forms filaments that pull the replicated chromosome to the opposite cell pole. Upon interaction with ParB the ATPase activity of ParA is stimulated, hydrolyzing ATP and thereby releasing ParA units from the filament, resulting in shortening of the filament and subsequent pulling of the *oriC* to the opposite cell pole (Fig. 1.1A). Released ParA is recruited to the cell pole by interaction with TipN, preventing further interaction with ParB (Lam *et al.*, 2006). Together, TipN and PopZ hold ParA and the partitioning complex at the cell poles preventing additional rounds of replication initiation until completion of division. After completion of cell division, TipN relocates to the new cell pole, releasing ParA which can again polymerize restarting the cycle.

Although, the *parA* and *parB* genes are indispensable in *C. crescentus* and severe chromosome segregation defects result from overexpression of ParA or ParB, depletion of ParB or mutations in the ParA ATPase active site (Mohl *et al.*, 1997; Mohl *et al.*, 2001), ParA is not involved in regulation of replication. Instead, rapid degradation of DnaA at the end of every cell cycle regulates initiation of replication (Gorbatyuk and Marczynski, 2005). However, mutation of *parAB* additionally results in a block in cytokinesis (Mohl *et al.*, 2001; Figge *et al.*, 2003). Thus, the *parAB* locus of *C. crescentus* has multiple additional roles outside of chromosome segregation and the act of chromosome segregation itself serves as a check point for initiation of cell division.

### Chromosome segregation in *Vibrio cholerae*

*V. cholerae* is a Gram-negative, rod-shaped gamma-proteobacterium that contains two unequally sized circular chromosomes, chrI (2.96 Mb) and chrII (1.07 Mb). Although each chromosome encodes *parAB* genes, phylogenetic analysis suggests that ParAB from chrI (ParA1 and ParB1) cluster with chromosomal ParAB proteins, while the Par proteins encoded on chrII (ParA2 and ParB2) cluster with plasmid and phage Par proteins (Gerdes *et al.*, 2000; Heidelberg *et al.*, 2000; Yamaichi and Niki, 2000). The product of each encoded *par* system is necessary for segregation of the parental chromosome and is thought not to influence segregation of the other chromosome. Indeed, the nucleotide sequence of the centromere-like elements on chrI and chrII differs significantly. The nucleotide sequence of *parS2* is restricted to *Vibrio* and *Photobacteria* species and are only bound by their cognate ParB protein (Yamaichi *et al.*, 2007; Livny *et al.*, 2007). The origin of chrI exhibits a polar localization and sister origins are segregated to the opposite cell pole. ParA1 interacts with the ParB1-*parS1* nucleoprotein complex and functions to anchor the nucleoprotein at the cell pole and segregate the sister origin via a “pulling” mechanism (Fig. 1.1B) (Fogel and Waldor, 2006). Lack of *parBI* leads to reduced polar localization of the origins and also DNA replication overinitiation (Kadoya *et al.*, 2011).

Although overinitiation of replication was not observed for a *parA1* mutant, increased DNA content was seen upon overexpression of ParA1 in a *parAB1* mutant strain suggesting that ParB1 mediates its action through ParA1.

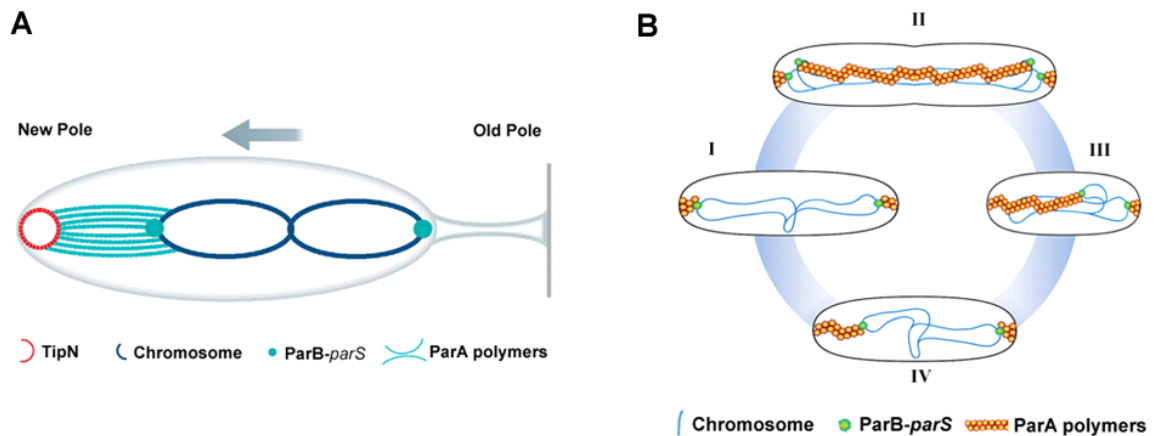


**Figure 1.1: Model of chromosome segregation in *C. crescentus* and *V. cholerae*.** In both organisms ParA polymerizes into filaments which depolymerize upon interaction with the ParB bound origin. A “pulling” mechanism has been proposed, whereby the retracting ParA filament pulls the replicated origin to the opposite cell pole. **(A)** In *C. crescentus*, the origin is positioned at the old pole in a newborn cell. The duplicated origin is bound by ParB and upon interaction with the ParA filament, which extends almost the entire length of the cell, ParB stimulates the hydrolysis of ParA-ATP. ParA subunits are released from the depolymerizing filament and held at the new cell pole through interactions with TipN, preventing further polymerization and / or interaction with ParB. After completion of cell division, ParA is released from the pole as TipN moves to the site of most recent division. **(B)** In the predivisional cell, *V. cholerae* ParA holds the *oriC* at the cell poles through interaction with an as-of-yet unidentified factor (I). After duplication of the origins ParA polymerization is initiated, which is possibly linked to assembly of the cell division apparatus or the inward growing septum (II). When the cell has completed division, one end of the ParA filament is attached to the cell pole and the other end interacts with the ParB-*oriC*. Again, ParB stimulates hydrolyses of the ParA bound ATP, causing the ParA filament to retract, pulling the sister origin to the opposite cell pole (III, IV). Models adopted from Kirkpatrick and Viollier, 2010; Fogel and Waldor, 2006, respectively.

Less is known about segregation of chrII. In contrast to chrI, chrII undergoes a symmetric division moving bidirectionally to the cell quarter positions. Null mutants of *parAB2* exhibit altered growth and localization of chrII, often leading to cells that lack chrII (Yamaichi *et al.*, 2007). In the absence of chrII, cells undergo one round of division before cell death.

### 1.3 Chromosome condensation - SMC and organization of chromosomes

In parallel to replication and also probably segregation of the *oriC*, the newly replicated DNA must be reorganized. One of the main players in chromosome organization and condensation is the highly conserved structural maintenance of chromosomes (SMC) protein, found across all three kingdoms of life. Bacterial cells normally encode a single SMC protein, which forms a coiled-coil protein with a

## Introduction

---

hinge domain at one end and an ABC-type ATPase domain at the other end (Saitoh *et al.*, 1994; Löwe *et al.*, 2001). Upon homodimerization, contacts of the hinge regions lead to a V-shaped dimer which can subsequently form a ring-like structure through ATP dependent interactions between the ATPase domains and / or associations with the kleisin family protein, ScpA and ScpB (Soppa *et al.*, 2002; Volkov *et al.*, 2003; Hirano and Hirano, 2004; Schwartz and Shapiro, 2011). These complexes are thought to interconnect different regions of the chromosome, stabilizing them in a twisted, condensed conformation (Hirano and Hirano, 2006). In *B. subtilis*, null mutant of *smc* display pleiotropic phenotypes, including growth defects, anucleate cells and unorganized chromosome with aberrant *oriC* and *terC* localization, less condensed and often guillotined chromosomes that have been chopped by the division septum (Britton *et al.*, 1998; Mascarenhas *et al.*, 2002; Soppa *et al.*, 2002). Simultaneous deletion of *smc* and *spo0J* exaggerates the phenotype of the single *smc* mutant (Autret *et al.*, 2001). Similarly, deletion of the origin-proximal *parS* sites led to a phenotype intermediate of the single mutants (Sullivan *et al.*, 2009).

In *B. subtilis*, SMC localization is dependent on complex formation with ScpA and ScpB (Lindow *et al.*, 2002). The finding that the SMC complex accumulates as foci around the *oriC* region gave the first hint that SMC proteins could be directly involved in chromosome segregation (Britton *et al.*, 1998). Indeed, recruitment of SMC to the *oriC* is dependent on Spo0J-*parS* nucleoprotein complex formation and subsequent lateral spreading of Spo0J on the chromosome (Sullivan *et al.*, 2009; Gruber and Errington, 2009). Thus, another role of Spo0J is as a chromosome loading factor for site specific recruitment of the SMC complex. Once in position at the *oriC*, SMC acts as an “organizing center” interacting with large regions of the chromosome, functioning in chromosome reorganization, condensation and also aiding segregation. However, in *B. subtilis* other recruitment factors must exist as deletion of *spo0J* does not lead to gross segregation defects (Lin and Grossman, 1998). Non-specific association of SMC with the chromosome is speculated to be sufficient for chromosome organization in the absence of *spo0J*, at least in vegetative cells. Such functionally redundant mechanisms ensure faithful chromosome segregation and can, at least partly, explain the mild *spo0J* mutant phenotype.

Spo0J plays a role in regulating the activities of Soj, which in turn regulate replication initiation, segregation of the *oriC* and transcription of early sporulation specific genes. Spo0J additionally marks the *oriC* priming it for loading of SMC, which functions in segregation of the bulk of the chromosome. Interestingly, mutant forms of Spo0J were isolated that are either defective in regulation of Soj or in the SMC pathway demonstrating that the different functions of Spo0J are independent from each other (Gruber and Errington, 2009).

*E. coli* does not encode homologues of SMC, ScpA or ScpB, however they encode the structurally and functionally related MukB, MukF and MukE proteins (Niki *et al.*, 1991; Yamanaka *et al.*, 1996). The characteristic architecture of SMC proteins is shared by MukB and MukF is classified as a kleisin (Fennell-Fezzie *et al.*, 2005). Mutation of either component causes atypical nucleoid localization, anucleate cells and temperature sensitive growth defects, all phenotypes that are indicative of a role in chromosome organization and segregation (Yamanaka *et al.*, 1996). Akin to *B.*

*subtilis* SMC, MukBEF complexes are targeted to the *oriC* regions (Danilova *et al.*, 2007). How this targeting occurs is not well understood. However, chromosome partitioning appears to be mediated through interaction with DNA topoisomerases IV, which is involved in DNA decatenation (Hayama and Mariani, 2010; Li *et al.*, 2010). A direct physical interaction is necessary for MukB function, but the molecular mechanisms have not been elucidated, yet.

### 1.4 Cell division

Once the chromosomes have been replicated and (partially) segregated, the bacterial cell will divide to produce two genetically identical daughter cells. Temporal control of cytokinesis ensures that cell division does not precede chromosome duplication and partitioning. The cell division apparatus is made up of a large number of proteins. The foundation for assembly of the division complex is laid down by the tubulin homologue FtsZ (Bi and Lutkenhaus, 1991; Wang and Lutkenhaus, 1993). Polymerization of FtsZ at the midcell region results in the formation of a ring-like structure. These Z-rings act as a scaffold for the assembly of additional proteins into the contractile Z-ring, forming a multisubunit complex, known as the divisome (Adams and Errington, 2009).

#### Spatial regulation of cytokinesis – negative regulation

Many organisms employ a dual mechanism to spatially regulate divisome positioning and assembly, including the Min system and nucleoid occlusion (Woldring *et al.*, 1990; Harry, 2001; Wu and Errington, 2004). The Min system of *E. coli* consists of MinC, MinD and MinE, all of which work collectively to prevent division sites from occurring at the cell poles (de Boer *et al.*, 1988; de Boer *et al.*, 1989). Upon binding ATP, MinD associates with the cell membrane and recruits MinC (de Boer *et al.*, 1991). MinC is a division inhibitor that prevents FtsZ from forming a stable cytokinetic ring (Hu *et al.*, 1999; Hu and Lutkenhaus, 2000). The third component, MinE, binds MinD stimulating ATP hydrolysis (Fu *et al.*, 2001). MinD-ADP disassociates from the membrane and as a consequence also MinC and MinE (Hu and Lutkenhaus, 1991). In the cytoplasm, nucleotide exchange results in reassembly of MinD-ATP at the cell membrane where MinE concentration is lowest, namely the opposite cell pole. This cycle of events results in a pole to pole oscillation of MinCD, leading to a MinCD gradient which is lowest at midcell, where FtsZ polymerizes.

The Min system of *B. subtilis* does not oscillate and consists of four proteins. The topological determinant, DivIVA, localizes to the curved membranes of the cell poles and is also recruited late to the assembling divisome (Cha and Stewart, 1997; Edwards and Errington, 1997). DivIVA recruits MinJ to the cell poles and division septa (Patrick and Kearns, 2008; Bramkamp *et al.*, 2008). MinJ is an adaptor protein necessary for recruitment of MinD and also indirectly for MinC. Contrary to the role of the Min system in *E. coli*, recent evidence suggests that the *B. subtilis* Min system is important for disassembly of the divisome machinery (van Baarle and Bramkamp, 2010). In the absence of MinCD or MinJ, division proteins remain associated to the divisome at the cell pole instead of localizing at

midcell. This subsequently leads to the initiation of a new round of cytokinesis close to the original cell division site, leading to rows of minicells.

Spatial regulation by the nucleoid occlusion system employs DNA binding proteins that bind to the nucleoid, inhibiting FtsZ polymerization over areas that contain DNA (Wu and Errington, 2004). Nucleoid occlusion may also provide a checkpoint-like mechanism for preventing division before replication and segregation of the sister chromosome has been completed. In *B. subtilis*, the Noc protein protects the nucleoid and in *E. coli* the unrelated SlmA carries out a similar role. *In vitro*, SlmA directly binds FtsZ, promoting polymer assembly (Bernhardt and de Boer, 2005; Cho *et al.*, 2011). It has been proposed that recruitment of FtsZ away from the membrane may compete with other FtsZ assembly proteins, thus inhibiting the formation of a functional cytokinetic ring. Interestingly, Noc is highly homologous to the partitioning protein ParB and in a similar mechanism Noc binds to a palindromic sequence found through out the chromosome (Wu *et al.*, 2009).

### **Novel spatial and temporal regulation of cytokinesis**

Not all bacteria that divide in a medial fashion have a Min or Noc system, for example *C. crescentus*. Thus, alternative spatial regulators must exist. In *C. crescentus*, a novel cell division protein, MipZ, spatially regulates FtsZ polymerization (Thanbichler and Shapiro, 2006). MipZ is a homologue of ParA and a member of the Walker A ATPase family. MipZ is highly conserved among  $\alpha$ -proteobacteria. In *C. crescentus*, MipZ is an essential protein. It forms a complex with the polar ParB-*oriC* nucleoprotein complex, but does not localize as tight foci. Instead, MipZ forms a gradient that peaks at the cell poles, where the origins are localized, and decreases towards midcell. *In vitro*, MipZ directly interacts with FtsZ stimulating its GTPase activity, inhibiting FtsZ polymerization. Interestingly, MipZ is distantly related to MinD, however the underlying mechanism of spatial regulation is different (see below).

Subsequent to cell division, the ParB-*oriC* nucleoprotein complex is found at the old cell pole, while FtsZ forms foci at the new cell pole (the site of most recent cell division) (Fig. 1.2 A). After initiation of chromosome replication and segregation, MipZ binds the origins through direct interaction with ParB. Depolymerizing ParA filaments translocate the sister origin to the opposite cell pole. Upon reaching the cell pole, MipZ stimulates the GTPase activity of FtsZ, displacing it from the cell pole. FtsZ subsequently moves to a region in the cell where MipZ concentration is lowest, namely midcell. Here, the divisome assembles and the cell divides. Depletion of MipZ leads to the formation of minicells and sporadic division events. Additionally, depletion of ParB or overexpression of ParA leads to a block in cell division resulting in long filamentous cells (Mohl *et al.*, 2001). Alterations in the ratio of ParA to ParB might lead to increase ParA-ADP, which binds DNA, possibly leading to repression of cell division genes (Mohl *et al.*, 2001). Thus, MipZ, together with ParA and ParB, spatially and temporally synchronizes cytokinesis with chromosome segregation.

### Spatial regulation of cytokinesis – positive regulators

Aside from negative regulators of division site placement, positive regulators of FtsZ polymerization have also been recently described for *Streptomyces coelicolor*. *S. coelicolor* is a member of the Actinobacteria family, which grows by tip extension and hyphal branching forming the mycelia of vegetative hyphae (Flårdh and Buttner, 2009). On occasion crosswalls form in vegetative hyphae separating the multigenomic compartments. Morphological differentiation into aerial hyphae is accompanied by increased chromosome replication resulting in numerous copies of non-segregated chromosomes filling the aerial hyphae. Cessation of growth is closely followed by development into endospore chains. During this development phase, chromosome segregation and condensation is closely followed by the assembly of regularly spaced FtsZ rings, marking the localization of sporulation septa (Schwedock *et al.*, 1997).

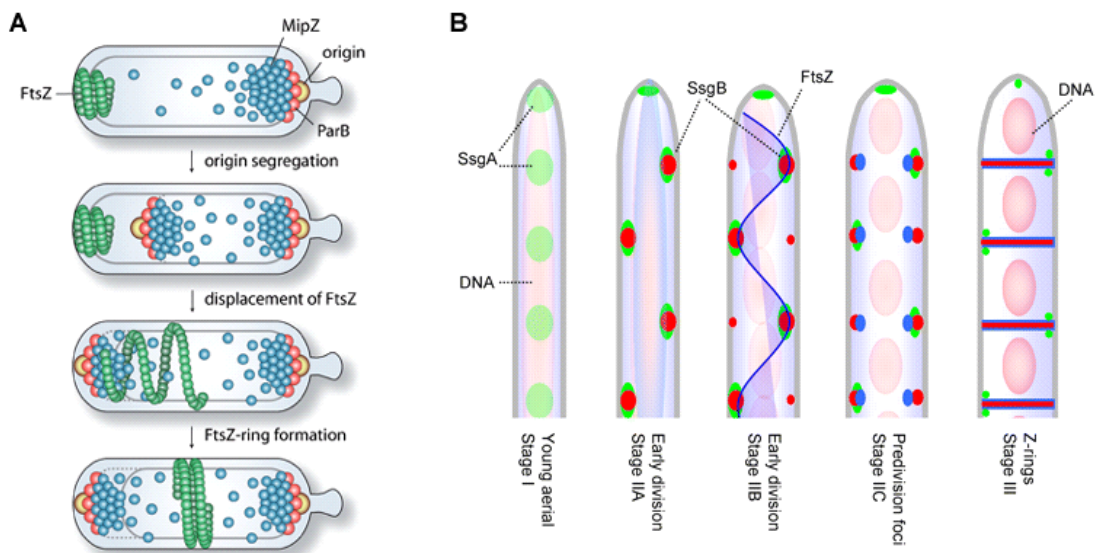


**Figure 1.2: Spatial and temporal regulation of FtsZ in *C. crescentus* and *S. coelicolor*.** (A) In *Caulobacter crescentus* MipZ is an inhibitor of FtsZ polymerization. MipZ forms a complex with the ParB bound origin at the old cell pole. After replication of the origin, ParA mediates translocation of the sister origin to the opposite cell pole, which is closely followed by MipZ. Upon reaching the opposite cell pole, MipZ displaces FtsZ. FtsZ reassembles where MipZ concentration is lowest. Thus, MipZ exploits origin segregation for its subcellular positioning and additionally spatially and temporally regulates cell division. (B) In *S. coelicolor* FtsZ and SsgB are diffused in young aerial hyphae, while SsgA forms foci (Stage I). SsgA dependent recruitment of SsgB in the pre-sporulation hyphae marks the predivisional sites. FtsZ uses SsgAB as landmarks for localization into long spiral-like filaments throughout the hyphae. SsgB interacts with the membrane and FtsZ, tethering FtsZ in position. Z-rings are formed and the divisome matures in coordination with chromosome segregation and condensation resulting in equally sized prespore compartments. As the prespore matures, SsgA remains localized at alternating sides of the division septum. Adopted from Thanbichler and Shapiro, 2006; Willemsen *et al.*, 2010.

Interestingly, in *S. coelicolor* deletion of *ftsZ* does not perturb growth in vegetative and aerial hyphae, which has not been reported for any other organism to date, however spore development defects are observed (McCormick *et al.*, 1994; McCormick and Losick, 1996). Similar to *C. crescentus*,

the canonical nucleoid occlusion and Min system are absent in *S. coelicolor*. Two novel positive regulators of FtsZ, SsgA and SsgB, were recently identified in *S. coelicolor* (Willemse *et al.*, 2010). Null mutants of *ssgA* and *ssgB* are blocked at stages preceding the onset of sporulation specific cell division (van Wezel *et al.*, 2000; Keijser *et al.*, 2003). In the absence of *ftsZ*, SsgA and SsgB still localize, however no septa are produced (Willemse *et al.*, 2010). In young aerial hyphae, SsgA expression is upregulated and, as development proceeds, SsgB is recruited by SsgA to alternating sides of the aerial hyphae membrane (Fig. 1.2 B). FtsZ begins to localize as spiraling filaments that are speculated to attach to the membrane bound SsgB. Subsequently, Z-rings form and sporulation septa develop. In light of these data, it is obvious that bacteria have developed multiple mechanisms to spatially and temporally organize cell division.

### 1.5 Cell polarity – integrated temporal and spatial regulation

Bacterial cells exhibit a high level of intercellular organization. Proteins or protein complexes are distinctly and selectively localized to specific subcellular regions, spatially organizing the cytoplasmic environment and in turn influencing temporal regulation. In rod-shaped bacteria, the cell poles have emerged as important sites for the intracellular localization of proteins, lipids and nucleic acids, affecting numerous cellular processes including chemotaxis, pole morphogenesis, symmetric and asymmetric cell division and chromosome segregation (Edwards and Errington, 1997; Goley *et al.*, 2007; Lam *et al.*, 2006; Ringgaard *et al.*, 2011). Polarity can be generated as a result of cell division. Cytokinesis in rod-shaped bacteria gives rise to offspring with differently organized cell poles (Lawler and Brun, 2007). Specific proteins are inherited at the site of most recent division (new pole) historically distinguishing the two poles, setting up spatial cues in the progeny cells that once again guide the cell through the cell cycle. In some bacteria, the *oriC* is a molecular marker of cell polarity, which is firmly localized to one cell pole, the old pole immediately after division (Webb *et al.*, 1997). Following chromosome replication, the newly replicated origin is translocated to the opposite cell pole and is subsequently attached to the opposite cell pole.

Although polar localization of the *oriC* is not common for all bacteria, *Caulobacter crescentus* and sporulating *Bacillus subtilis* exhibit polar attachment of the origin. In *C. crescentus*, a multimeric self-organizing protein (PopZ) was recently identified as a chromosome origin tethering factor (Fig. 1.3 A) (Bowman *et al.*, 2008; Ebersbach *et al.*, 2008). Polar localized PopZ sets up a polar epicenter that not only anchors the chromosome origins, but also stabilizes bipolar gradients of the cell division inhibitor MipZ (Thanbichler and Shapiro, 2006) and mediates the localization of morphogenic and cell cycle regulating proteins (Bowman *et al.*, 2010). However, PopZ is not highly conserved and many bacterial species exhibit polar localization of chromosome origins. Thus, the mechanism of polar origin anchoring must differ in unrelated bacteria.

In *B. subtilis*, upon entry into sporulation rearrangements of the chromosome lead to anchoring of the *oriC* regions at the cell pole where asymmetric division will occur. Tethering the

chromosome requires the sporulation specific factor, RacA and the coiled-coil protein, DivIVA (Fig. 1.3 B) (Ben-Yehuda *et al.*, 2003; Wu and Errington, 2003). RacA has a classical HTH motif and binds specific sequences of DNA located around the *oriC* (*ram* sites). Mutants deleted for *racA* sporulate almost as efficiently as wild type, unlike deletion of *divIVA*. A more severe phenotype is, however, observed upon simultaneous deletion of *soj* or *spo0J*. The current model proposes that Soj / Spo0J deliver the origin to the cell pole, where interaction of RacA with *ram* sites and Soj via Spo0J *parS* domain fix the origin at the cell poles. Polar anchoring of the chromosome might provide a signal for entry into sporulation and subsequent efficient DNA translocase activity.

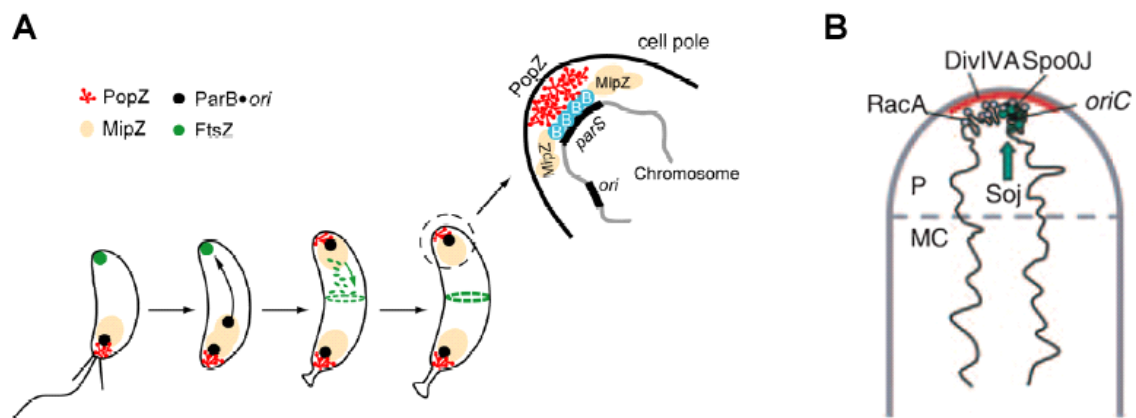


**Figure 1.3: Chromosome tethering factors in *C. crescentus* and sporulating *B. subtilis*.** The localization of the bacterial chromosome origin, dictated by interaction with polar tethering factors can establish cell polarity which plays a role in spatial and temporal regulation of cell cycle events. (A) In *C. crescentus* the polymeric protein PopZ interacts with the ParB bound origin, tethering the chromosome at the old cell pole. Shortly after initiation of replication, PopZ assembles at the origin-free pole preparing the pole for chromosome anchoring. (B) In sporulating *B. subtilis* cells, Spo0J and Soj play a role in organizing the axial filament, orientating the *oriC* towards the cell poles. Tethering of the origin in position requires DivIVA and RacA which binds to “*ram*” sites located around the *oriC*. Soj, through interactions with Spo0J *parS*, is also speculated to help anchor the chromosome. Models adopted from Erbsbach *et al.*, 2008 and Wu and Errington, 2003, respectively.

### 1.6 *Corynebacterium glutamicum* – cell division and chromosome segregation

*Corynebacterium glutamicum* is a non-sporulating, Gram-positive, soil-dwelling microorganism. It is a member of the Actinobacteria phylum and thus, closely related to the notorious pathogens such as *Mycobacterium tuberculosis*, *Mycobacterium leprae*, and *Corynebacterium diphtheriae*. A remarkable feature of corynebacteria and their close relatives is a special cell wall that has, in addition to the common peptidoglycan, an arabino-galactan and a mycolic acid layer (McNeil and Brennan, 1991). In the biotechnology sector, *C. glutamicum* is extremely important for the production of amino acids, such as L-glutamate and L-lysine. Therefore, *C. glutamicum* has been studied extensively and has emerged as a model organism in the study of metabolism and transport. However, the cell biology of *C. glutamicum* is severely lagging behind. As *C. glutamicum* is related to a number of pathogens,

## Introduction

---

understanding the fundamental cell biology aspects of this organism is important. In the past decade, some advances have been made.

*C. glutamicum* is classified as a rod-shaped organism. However, the morphology of this organism is largely dependent on growth medium, and is often more club shaped rather than symmetrically rod-shaped. The shape of the *C. glutamicum* cell is likely a consequence of its mode of growth, which differs from the conventional model organisms. In rod-shaped bacteria such as *E. coli* and *B. subtilis*, cell division gives rise to hemispherical cell poles, which after their formation largely remain inert (de Pedro *et al.*, 1997). Bacterial cell elongation involves extension of the lateral cell wall, which, in most rod-shaped bacteria, occurs by intercalation of new peptidoglycan into the lateral cell wall. This process requires the assembly of MreB, an actin homologue, into the helical cytoskeleton that is distributed throughout the cell (Kruse *et al.*, 2005). Therefore, in most rod-shaped bacteria, cells elongate along the lateral cell wall in a process that requires the actin cytoskeleton. The mode of cell elongation for members of the Actinobacteria phylum differs greatly. Intercalation of new cell wall material occurs at the cell poles, giving rise to an apical mode of cell elongation (Gray *et al.*, 1990; Letek *et al.*, 2008). The DivIVA protein has been identified as an organizer of apical growth (Letek *et al.*, 2008). In *C. glutamicum* and other members of the Actinobacteria phylum, DivIVA is an essential protein. Overexpression of DivIVA results in cells with bulging cell pole, while knock-down mutants have coccoidal morphology (Letek *et al.*, 2008). Heterologous expression of DivIVA from *B. subtilis* or *Streptococcus pneumoniae* does not complement the *C. glutamicum* DivIVA knock-down phenotype, suggesting that DivIVA functions differently in the two main phylogenetic lines of gram-positive bacteria (Letek *et al.*, 2008). In *C. glutamicum*, DivIVA localizes at the septum after cell wall synthesis had started and the nucleoids had already segregated, and was therefore, suggested that in *C. glutamicum* DivIVA is not involved in cell division or chromosome segregation (Letek *et al.*, 2008).

Electron microscopy images of corynebacteria suggest that septa placement is not always precisely at midcell, dissimilar to other rod-shaped organisms, such as *B. subtilis* or *E. coli*. Thus, regulation of the division site placement must differ from the conventional model organisms. Indeed, a genome wide blast for conventional FtsZ interacting factors from other Gram-positive bacteria revealed that *C. glutamicum* lack the eminent positive / negative FtsZ regulators found in conventional rod-shaped bacteria (A. Schwaiger and M. Bramkamp). The situation is similar for other members of the Actinobacteria phylum, e.g. *S. coelicolor* and *M. tuberculosis*. Although some candidates for cell division regulation have been identified in *S. coelicolor* and *M. tuberculosis*, these proteins do not appear to be highly conserved. Nevertheless, *C. glutamicum* possesses a *parAB* operon and an orphan *parA*-like gene. The *parAB* operon is located in the vicinity of the origin of replication (*oriC*) between 99.85 and 99.88 minutes on the *C. glutamicum* chromosome, while the orphan *parA*-like gene (renamed PldP) is located almost on the opposite site of the chromosome, without a *parB*-like gene in its vicinity. Additionally, three consensus *parS* sequences were identified in the origin proximal region, which is in agreement with the proposed two to four *parS* sites described previously (Livny *et al.*, 2007). While one site matches the consensus *parS* sequence perfectly, the other two have one mismatch each. Although no classical Min or nucleoid occlusion system was identified for *C.*

## Introduction

*glutamicum*, it was hypothesized that chromosome segregation might be spatially and temporally linked with cell division. This theory is not unrealistic as the *B. subtilis* nucleoid occlusion protein Noc is homologous to ParB proteins and MinD is evolutionarily related to ParA proteins.

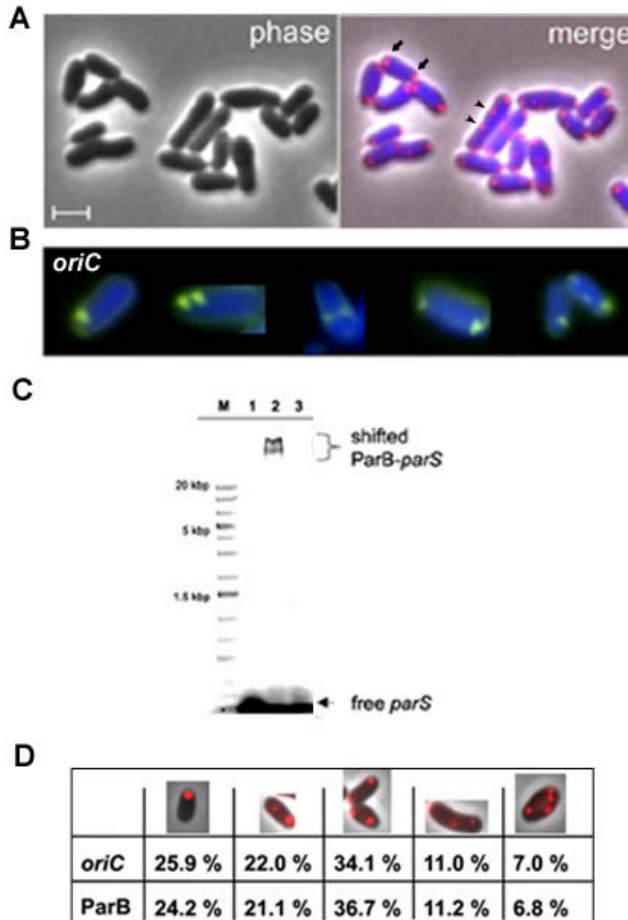


**Figure 1.4: Polar localization of *oriC* and ParB in *C. glutamicum*.** (A) ParB-GFP forms foci localized at the cell poles (arrows) and in cells with multifork replication, additional foci are seen in between the polar foci (arrowheads). ParB-GFP (red) and DNA (blue). (B) The *oriC* is positioned at the cell poles. Up to four *oriC* foci per cell were observed. DNA staining (blue) and *oriC* foci (yellow). (C) Purified ParB binds *parS* DNA. (M, molecular mass standard; 1, *parS* DNA; 2, *parS* plus 20  $\mu$ g of ParB. (D) ParB and *oriC* exhibit highly similar localization patterns. The localization of ParB-GFP and *oriC* were analyzed and categorized as one polar focus, two foci, with one polar focus and one focus somewhere in the cytoplasm, foci at both poles, three foci, and four foci. Scale bar, 2  $\mu$ m. (Adopted from Donovan *et al.*, 2010)

In our lab, it was established that the *C. glutamicum* *oriC* is localized at the cell pole, similar to the situation in *C. crescentus* (Fig. 1.4 B) (Schwaiger, 2009). Interestingly, the number of origins was dependent on the growth medium and up to four *oriC* foci per cell were seen. Thus, *C. glutamicum* can initiate multifork replication when ample nutrients are available. Similarly, ParB-GFP localizes as foci at the cell poles (Fig. 1.4 A). Again, up to four foci per cell could be detected. *In vitro*, it was shown that ParB binds its cognate *parS* DNA (Fig. 1.4 C). Although direct colocalization was not carried out, statistical analysis of ParB-GFP and the *oriC* localization revealed a highly similar pattern (Fig. 1.4 D). Thus, in *C. glutamicum* ParB binds the origin-proximal *parS* sites and this nucleoprotein complex is then positioned at the cell poles in cells undergoing one round of replication per cell cycle. In cells undergoing multifork replication additional foci are often found near the midcell region, probably close to where the divisome assembles.

## Introduction

In line with the notion that the Par proteins might also have a role in regulating cell division, a bacterial-two-hybrid approach was used to test the interaction between the ParAB, PldP and FtsZ proteins (Fig. 1.5 A). Strong self-interaction was observed for FtsZ, ParA and PldP whereas ParB showed no homodimerization. Analysis of pair-wise interactions revealed that ParB interacts with FtsZ, ParA, and PldP, interacting strongest with PldP. Also, an interaction between ParA and PldP could be observed. However, no interaction was observed between FtsZ and ParA or PldP. The finding that the ParB-*oriC* nucleoprotein complex is situated at the cell poles suggested that the chromosome might be held in position by a polar localized protein, analogous to polar anchoring of the *oriC* in *C. crescentus*. A potential candidate for tethering the *oriC* region of the chromosome at the cell poles was DivIVA. Again a bacterial-two-hybrid approach hinted that ParAB and PldP could interact with DivIVA (Fig. 1.5 B).

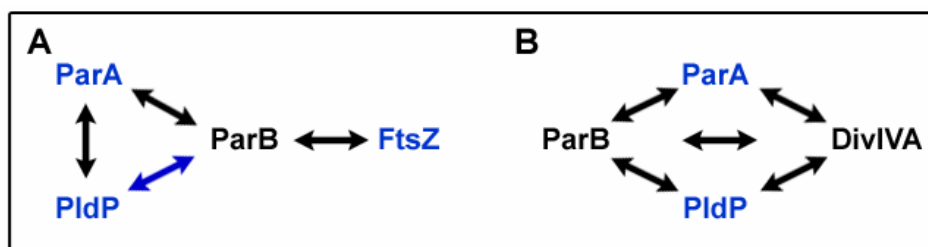


**Figure 1.5: Bacterial two-hybrid analysis of protein-protein interactions of ParAB and PldP.** Both homodimerization and heterologous interaction between different protein pairs was studied. Based on the two-hybrid data an interaction map was built that shows the interaction between (A) the Par proteins and FtsZ and (B) the Par proteins and DivIVA. Blue script indicates strong self-interactions and black script indicates weak self-interactions. Blue arrows indicate strong interaction and black arrows indicate weaker interaction. Note that homodimerization of DivIVA was not tested.

Although ParA and the orphan ParA (PldP) exhibit similar interactions, the genetic organization of both loci differ in that the orphan ParA lacks a centromere-binding protein. Orphan *parA*-like genes are not uncommon and have been shown to be involved in diverse cellular processes in different organisms. In cyanobacteria, carboxysomes, proteinaceous structures that enclose the carbon-fixing enzymes, have defined subcellular positions which is important for inheritance into daughter cells. ParA is necessary for segregation of these structures (Savage *et al.*, 2010). In the absence of *parA*, the carboxysomes are not segregated properly during cell division leading to cells lacking carboxysomes and, thus, impaired carbon fixation. Orphan ParA proteins have also been shown to be involved in localization of chemoreceptors (Thompson *et al.*, 2006; Ringgaard *et al.*, 2011), or in the positioning of cellulose biosynthesis machinery (Le and Ghigo, 2009). These observations suggest that orphan ParA proteins are also involved in correct positioning of protein complexes. In *C. glutamicum* the function of PldP is unknown. It remains to be seen if PldP, in collaboration with ParA/ParB, is involved in chromosome segregation or if it functions similar to MipZ in *C. crescentus*.

### Chapter II A prophage encoded cytoskeleton protein

#### 1.7 The bacterial cytoskeleton

Polymerizing proteins have key roles in numerous biological processes, for example ParA proteins of the chromosome segregation system or components of the cytoskeleton. The discovery that prokaryotic cells also possess a cytoskeleton dramatically challenged the passive diffusion model and the view that bacterial cells are unorganized bags of enzymes. Bacterial cells have counterparts of actin, tubulin and intermediate filaments, and more recently, numerous prokaryotic specific proteins have emerged as candidates for cytoskeleton elements (Bork *et al.*, 1992; Erickson *et al.*, 1996; Ausmees *et al.*, 2003; Derman *et al.*, 2009). Identification of prokaryotic cytoskeleton proteins was compounded by the lack of primary sequence similarity with eukaryotic counterparts. However, crystal structures together with *in vivo* and *in vitro* characterization have confirmed that a number of proteins are components of the bacterial cytoskeleton, for example MreB, FtsA or FtsZ (Löwe and Amos, 1998; van de Ent and Löwe, 2000; van den Ent *et al.*, 2002). Interestingly, structural data has now revealed that even structurally similar cytoskeletal proteins have widely differing properties and functions. Nevertheless, an intrinsic property and functional prerequisite of bacterial cytoskeleton proteins is their ability to form dynamic filamentous structures. The bacterial cytoskeleton is involved in organizing the cytoplasmic environment, playing crucial roles in cell division, plasmid and chromosome segregation, positioning of intracellular organelle-like structures, maintaining cell shape and cell polarity (Bi and Lutkenhaus, 1991; Jones *et al.*, 2001; Carballido-Lopez and Errington, 2003; Figge *et al.*, 2004; Savage *et al.*, 2010; Ptacin *et al.*, 2010). In light of the fact that ParA proteins assemble into dynamic filaments, aiding the subcellular organization of the bacterial chromosome, it was proposed that members of this protein family should also be classified as components of the bacterial cytoskeleton.

To date, characterized bacterial cytoskeleton proteins include the essential cell division protein and tubulin homologue FtsZ, intermediate filament-like proteins such as crescentin that is a mediator of curved morphology in *C. crescentus*, and actin homologues such as MreB, which is an essential protein, involved in numerous cellular roles (Bi and Lutkenhaus, 1991; Jones *et al.*, 2001; Ausmees *et al.*, 2003). Actin is the most abundant protein of the eukaryotic cytoskeleton and is involved in fundamental processes like cell mobility and remodeling, endocytosis and cytokinesis. At the sequence level, eukaryotic actin is well conserved from human to yeast and is a member of a large superfamily, including the 70 kDa heat shock proteins (Hsp70) and sugar kinases (Bork *et al.*, 1992; Kabsch and Holmes, 1995). The crystal structures of three prokaryotic actin-like proteins, (FtsA, MreB and ParM) have been resolved and confirm their classification as members of the actin family (van de Ent and Löwe, 2000; van den Ent *et al.*, 2001; van den Ent *et al.*, 2002). More recently, a phylogenetic analysis identified a large number of potential novel actin-like protein families (Derman *et al.*, 2009). To date, only a few of these candidates have been studied so it remains to be seen if the prokaryotic cytoskeleton is as well represented as its eukaryotic counterpart.

### Bacterial actin homologues – ParM

The motor protein of type II plasmid partitioning system is an actin homologue. This system entails three core elements; a *cis*-acting DNA sequence (*parC*), a motor protein (ParM) and an adaptor protein (ParR) (Gerdes and Molin, 1986; Dam and Gerdes, 1994). Detailed *in vivo* and *in vitro* analysis has led to a comprehensive understanding of its mechanism of action. ParM binds and hydrolyses both ATP and GTP, with approximately ten-fold preference for ATP (Galkin *et al.*, 2009). *In vivo*, ParM forms either foci or curved filamentous structures, indicative of dynamic behavior, and the tips of growing filaments are always associated with plasmids (Møller-Jensen *et al.*, 2002; Møller-Jensen *et al.*, 2003). ParM filaments exhibit extreme dynamic instability, switching from bidirectional polymerization to catastrophic endwise disassembly (Garner *et al.*, 2004). The stability of ParM filaments is regulated by ATP hydrolysis, as addition of ParM hydrolysis mutants to wild type ParM significantly stabilizes the filaments. Similar to actin, ParM assembly begins with the formation of a small and stable filament nucleus, which then elongates. ParM nucleation is about 300 times faster than actin and the disassociation rate is about 100 times faster (Garner *et al.*, 2004). These properties probably allow ParM to spontaneously form short-lived filaments as it randomly seeks out ParR-*parC* bound plasmids. These data led to the model that ParM filaments are stabilized by ParR-*parC*, leading to growth of the ParM filament and “pushing” of plasmids to opposite cell poles (Fig. 1.6 A and B). *In vitro* reconstitution of ParM and ParB-*parC* coated microspheres demonstrated that, in the presence of ATP, ParM filaments grow and shrink rapidly, consistent with its dynamic instability property (Garner *et al.*, 2007). However, when both ends of the ParM filament are capped with a ParB-*parC* coated bead, the filament stabilizes and then elongates, pushing the beads apart. Later it could be shown that elongation of ParM filaments is exclusively from their ParB-*parC* bound ends (Salje and Löwe, 2008). Further structural and biochemical data suggest that ParM filaments are bundled and that multiple plasmids might cap the ends of ParM filament bundles *in vivo*.

### Divergent bacterial actin families – AlfA and Alf7A

More recently, representatives of distinct bacterial actin families have been identified. One of the few characterized members, AlfA, is involved in segregation of the *B. subtilis* pLS32 plasmid (Becker *et al.*, 2006). Again, nucleotide hydrolysis (ATP or GTP) appears to be essential for both dynamics of the curved filaments, which run along the long axis of cells, and plasmid segregation (Fig. 1.6 D). The gene downstream of the *alfA*, *alfB*, is proposed to encode an adaptor-like protein, which binds three tandem repeats found upstream of *alfA* (Becker *et al.*, 2006; Polka *et al.*, 2009; Tanaka, 2010). However, mechanistic differences exist compared to the ParM system, as AlfA does not exhibit dynamic instability (Polka *et al.*, 2009). Upon bleaching a central region of an AlfA filament, recovery is symmetrical from both sides (Becker *et al.*, 2006). The architecture of AlfA is also distinct from ParM filament, forming bundles with mixed polarity (Polka *et al.*, 2009). Two novel modes of action have subsequently been proposed (Polka *et al.*, 2009). The first model proposes that the end of an AlfA

## Introduction

filament interacts with the AlfB-bound plasmid and grows along an existing AlfA bundle delivering the plasmid to the cell pole. Although such a model can explain polar distribution of plasmids, it does not account for segregation of plasmids. The second model suggests lateral interaction of plasmids with the AlfA bundles and subsequent treadmilling of subunits to move the plasmids apart. Plasmids are thought to be maintained at the cell poles by another factor, possibly host cell factors. At least in sporulating *Bacillus* cells, RacA helps maintain the pLS32 plasmid (Becker *et al.*, 2006).

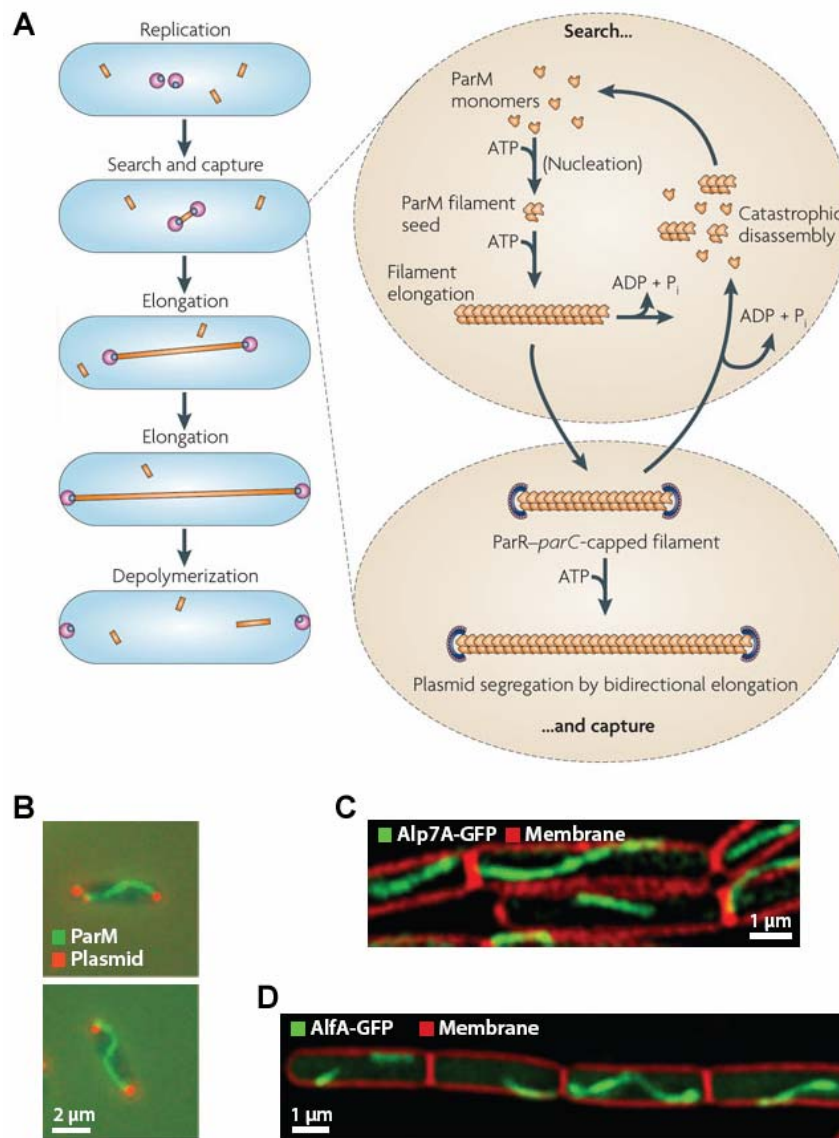


**Figure 1.6: Bacterial actin homologues involved in plasmid partitioning.** (A) Model of ParMRC mediated plasmid segregation. ParR bound plasmids are shown in pink, ParM filaments are shown in yellow. (B) *In vivo* localization of ParM filaments capped with ParR-parC bound plasmid. (C and D) Alp7A and AlfA form long curved filaments *in vivo*. (Adopted from Salje *et al.*, 2010; Møller-Jensen *et al.*, 2003; Derman *et al.*, 2009 and Becker *et al.*, 2006, respectively).

Recently, multiple rounds of BLAST searches, starting from the AlfA sequence, uncovered more than 35 additional phylogenetically distinct and diverse bacterial actin homologues (Derman *et al.*, 2009). On the sequence level, these actin families are extremely divergent from known actins. However, each new actin family contains the five actin signature motives of amino acids involved in the binding and hydrolysis of ATP and were hence, designated actin-like proteins (Alps) (Bork *et al.*, 1992). While a few of these novel actin-like proteins are found on the bacterial chromosome, most appear on phage genomes, plasmids or integrating conjugative elements. *In vivo*, at least three Alps from different families form long curved filaments that extended longitudinally through several cells causing the cells to grow as chains, when produced in *E. coli*. Thus, it appears that at least some of the identified proteins exhibit actin-like properties. Alp7A from *Bacillus subtilis natto* plasmid pLS20, was studied in more detail. The genetic organization of the Alp7A family member is similar to other plasmid stability determinants. The *alp7A* gene is found in an operon and is co-transcribed with the downstream *alp7R* gene. The downstream *alp7R* codes for a 134 amino acid protein whose small size and high percentage of charged residues resemble the DNA binding protein ParR of the ParMRC plasmid partitioning system. Thus, a role in plasmid partitioning was proposed for Alp7A. Indeed, Alp7A formed filaments within the cell and these filaments exhibited dynamic instability and treadmilling (Fig. 1.6 C). Mutation analysis revealed that Alp7A must polymerize into filaments with dynamic properties in order to function as a plasmid partitioning protein. Furthermore, filaments were detected at physiological concentrations of Alp7A only in the presence of DNA that contains both the *alp7R* gene and the 165 bp directly upstream of the *alp7* initiation codon. Additionally, Alp7A filaments colocalized with the plasmid containing the *alp7R* gene and the region upstream of *alp7A*. Consequently, an Alp7A plasmid partitioning model has been proposed, the mechanism of which resembles fundamentally the ParM partitioning mechanism.

### 1.8 Identification of a *C. glutamicum* actin-like protein

The phylogenetic analysis carried out by Derman *et al.*, 2009 identified the *C. glutamicum* *cg1890* gene as an actin-like protein (Fig 1.7). On the chromosome, *cg1890* is one of the first genes on the CGP3 bacteriophage. The genetic organization of *cg1890* is dissimilar to other studied actin-like proteins involved in plasmid stability / segregation. Cg1890 is not co-transcribed from an operon containing an adaptor protein and no tandem repeats are found near this gene. However, it should be noted that, to date, no study has been carried out on an actin-like protein found on an integrated prophage. According to the phylogenetic analysis *cg1890* groups almost perfectly between Alf7A and Alp7, both of which are quiet separated from ParM and MreB (Derman *et al.*, 2009). The *C. glutamicum* Alp (here renamed AlpC) is grouped with an actin-like protein (*Isl1868*) from *Lactobacillus salivarius* UCC118. Interestingly, the *L. salivarius*, *Isl1860* gene is not in the vicinity of a bacteriophage and encodes a hypothetical protein of unknown function.

	Phosphate 1	Connect 1	Phosphate 2
beta Actin	LVVDN <b>GS</b> GMCK	VAIQAVLS	TGIV <b>MD</b> SGDGVTHTVPI
MreB	LGID <b>LG</b> TANTL	PIE <b>EP</b> FAA	GSMV <b>VD</b> IGGGTTEVAH
ParM	VFID <b>DG</b> STNIK	VM <b>PE</b> SIPA	SL <b>LI</b> DLGGTTLDISQV
AlfA	TVID <b>IG</b> NFSTK	MAA <b>EL</b> LGA	NCVIV <b>D</b> AGSKTLNVLYL
Alf7A	MNV <b>DF</b> GNSMYM	CRI <b>ES</b> EVA	DVV <b>FC</b> DLGGGTDDLVL
AlpC	AGL <b>DI</b> GNGYVK	KAE <b>Q</b> ELSK	HTIG <b>VD</b> VGEGTVNFPVF

**Figure 1.7: Alignment of the phosphate 1, connect and phosphate 2 regions of human beta-actin and other members of the actin superfamily.** Conserved residues are highlighted in red and blue. Aligned are; human beta-actin, *B. subtilis* MreB, *E. coli* plasmid R1 ParM, *B. subtilis natto* plasmid pLS32 AlfA, *B. subtilis natto* plasmid Alp7A and *C. glutamicum* AlpC (Cg1890).

### 1.9 *C. glutamicum* prophages

The genome of *C. glutamicum* contains three putative prophage elements, designated CGP1-3, which are highly diverse in size and degeneration (Kalinowski, 2005). Prophages CGP1 and CGP2 are relatively small and, most probably, highly degenerated. The larger putative prophage CGP3 encodes a number of bacteriophage protein homologues e.g. a phage primase and phage-type integrases. The CGP3 prophage is bordered on one side by a cluster of tRNA genes, flanked by a 26 bp direct repeat and on the other side by a phage-type integrase, *int2*. Integrase enzymes catalyze site-specific recombination between phage recognition sites (*attP*) and short sequences of bacterial DNA (*attB*) (Williams, 2002). However, most of the coding regions lack any significant similarities to known bacterial genes, with the exception of three genes of a restriction-modification system (*cgIIM*, *cgIIR* and *cgIIIR*), genes encoding transposases and putative recombination enzymes (Frunzke *et al.*, 2008).

In an unrelated study, deletion of the *dtxR* gene was observed to result in an increase in the mRNA levels of many genes located within the CGP3 region (genes between *cg1890* to *cg2071*) (Frunzke *et al.*, 2008). The DtxR protein, first identified in *C. diphtheriae*, represses the transcription of the phage gene *tox*, encoding the diphtheria toxin, and a variety of genes involved in iron homeostasis (Brune *et al.*, 2006). In *C. glutamicum*, DtxR is the master regulator controlling iron homeostasis (Wennerhold and Bott, 2006). It was shown that CGP3 prophage can excise from the chromosome and exist as a circular double stranded DNA molecule. In the *dtxR* mutant, induction of the CGP3 prophage is likely triggered by a general SOS response due to the elevated intracellular iron concentration. *In vivo* visualization of the CGP3 prophage in wild type *C. glutamicum* cells showed that most of the cells contained up to four foci, representing chromosome-inserted prophages synchronized with chromosomal replication (Frunzke *et al.*, 2008). However, a small population of cells contained between four and eight foci, which probably represent induced CGP3 prophages and replication of its genome. Whether fully functional phage particles are formed remains unclear. However, as homologues of the typical phage morphogenic genes, (genes encoding coat proteins, tail fibers or shaft-building proteins), could not be identified on the CGP3 prophage, it seems unlikely (Frunzke *et al.*, 2008). Interestingly, *C. glutamicum* cells retain the CGP3 prophage. Either essential

genes or addiction molecules might contribute to maintenance of the CGP3 prophage. Type II restriction-modification system, similar to those found on CGP3 prophage, have been shown to serve as addiction molecules (Naito *et al.*, 1995). However, the identification of a putative actin homologue encoded on the CGP3 prophage raised the possibility that, similar to indigenous plasmids, an active segregation system might help maintain the *C. glutamicum* prophage.

### 1.10 Aim of the research

#### Chapter I

#### Cytoskeleton elements involved in chromosome segregation and cell division

The main aim of this research was to further our understanding of the cell biology, in terms of cell division and chromosome segregation, of *C. glutamicum*. Although homologues of the ParAB chromosome segregation system could be identified in *C. glutamicum*, positive and negative regulators of cell division found in the canonical rod-shaped model organisms, such as *B. subtilis* and *E. coli*, are absent in *C. glutamicum*. Thus, regulation of cell division must be different in this organism. The ParAB segregation system has been shown in numerous organisms to be necessary for partitioning of the chromosome origins, and thus, is central to chromosome organization. Furthermore, the mode of action of this system varies in the different organisms. Thus, we aimed to determine, first of all if and how the Par system functions in chromosome segregation and secondly, if the process of chromosome segregation and cell division are linked in *C. glutamicum*. We aimed to generate null deletion mutants of the *par* system and analyze the phenotypic consequences. As *C. glutamicum* encodes a second *parA*-like gene, designated *pldP*, we wanted to determine if both ParA proteins function in chromosome segregation or if each protein fulfills a different role.

The *oriC* region is positioned at the cell poles in *C. glutamicum*. In other organisms that exhibit a similar chromosome organization, specific factors have been identified that tether the origin regions at the cell poles. We aspired to identify the *C. glutamicum* polar tethering factor. As a previous interaction analysis hinted that the polar growth determinant, DivIVA interacts with components of the Par system, the interaction potential should be tested further. Additionally, we aimed to determine the domains or residues that are necessary for interaction.

Furthermore, the mode of cell growth differs from the classical cell division and chromosome segregation model organisms. Thus, we aimed to determine if the subcellular organization of the chromosome, mediated by the action of the Par system, influences cell growth and cell division.

### Chapter II A prophage encoded cytoskeleton protein

AlpC is a novel, putative actin-like protein that is found on the CGP3 prophage of the *C. glutamicum* genome. AlpC was identified in a phylogenetic study that identified in total 35 new actin families. However, to date, only few of these proteins have been characterized. As these proteins share little sequence homology with each other and other members of the actin superfamily, we firstly aimed to determine if AlpC is a bona fide actin-like protein. Thus, we wanted to determine if AlpC exhibits actin-like properties, such as assembling into dynamic filaments *in vivo* and nucleotide hydrolysis.

The CGP3 prophage can excise from the *C. glutamicum* chromosome and exist as a double stranded circular DNA molecule. Although induction of the CGP3 prophage is only observed in a small population of cells, interestingly, *C. glutamicum* cells always retain this prophage. Thus, we speculated that, similar to some plasmids, the CGP3 prophage might be equipped with its own segregation machinery. An ideal candidate for such a role would be AlpC. Therefore, we wanted to determine if AlpC plays a role in partitioning of the excised CGP3 prophages. In collaboration with the group of Julia Frunzke (FZ, Jülich), we planned to co-visualize the subcellular localization of AlpC and induced prophages, to determine if AlpC filaments physically segregate these particles. Additionally, the phenotypic consequences of an *alpC* null deletion mutant will be tested in relation to prophage induction efficiency.

## 2. Results

### Chapter I

### Cytoskeleton elements involved in chromosome segregation and cell division

#### 2.1 The Par chromosome segregation system of *C. glutamicum*

The ParAB partitioning system is highly conserved, involved in segregation of newly replicated origins and organization of the chromosome in the cytoplasmic environment. Although the function of the Par system in *C. crescentus* and *B. subtilis* is quite well understood, the molecular role(s) of this system varies in the different organisms. A role in chromosome segregation appears to be universal, however, involvement of the Par system in a number of overlapping systems, such as replication initiation or division site placement, is not common to the different organisms (Murray and Errington, 2008; Scholefield *et al.*, 2012; Thanbichler and Shapiro, 2006). Our model organism, *C. glutamicum*, shares only few similarities with *C. crescentus* and *B. subtilis* and thus, understanding the cell biology of this organism is beneficial. Similar to *C. crescentus*, *C. glutamicum* encode an orphan *parA*-like gene, thus we wanted to determine if both ParA proteins function in chromosome segregation or if the orphan ParA protein fulfills a different role. Furthermore, we aimed to determine if the ParAB system plays a role in organization of the chromosome origins.

#### Phenotypes of *par* null deletion mutants

We began deciphering the role of the Par system in *C. glutamicum* by generating markerless null mutant strains of *parA*, *parB* and *pldP*. While wild type *C. glutamicum* cells are on average 2  $\mu\text{m}$  in length and can be easily identified by the characteristic snapping division, mutants deleted for *parA*, *parB* or *pldP* exhibited aberrant cell morphology, altered cell lengths and varying frequency of anucleate cell production (Fig. 2.1 A). The consequence of the specific mutation was subsequently analyzed in growth experiments. *C. glutamicum* cells are capable of rapid growth, to extremely high optical densities. Growth in minimal media supplemented with 4 % glucose (MM1) revealed that loss of *parA* or *parB* result in drastically reduced growth rates, compared to wild type cells (Fig. 2.1 C). In contrast, the mutant deleted for *pldP* grew at a rate comparable to wild type cells. Interestingly, when cultured in medium that supports slower growth (LB medium) all deletion mutants grew at a rate comparable to wild type cells (Fig. 2.1 C). Wild type cells have a doubling time of approximately 97 min in MM1 medium, whereas the doubling time is increased to 152 min in LB medium. Hence, it appears that slower growth rates can partly compensate for the loss of *parA* or *parB*. Also, under conditions that support rapid growth, multiple rounds of chromosome replication can be initiated prior to the completion of cell division (Cooper and Helmstetter, 1968; Niki and Hiraga, 1998; Nielsen *et al.*, 2007; Schwaiger, 2009). Thus, it seems plausible that cells defect in chromosome segregation would have a severe disadvantage under such growth conditions. These results indicate that *parA* and *parB*

## Results

mutants have defective chromosome replication initiation or chromosome segregation, which is not the case for the *pldP* mutant.

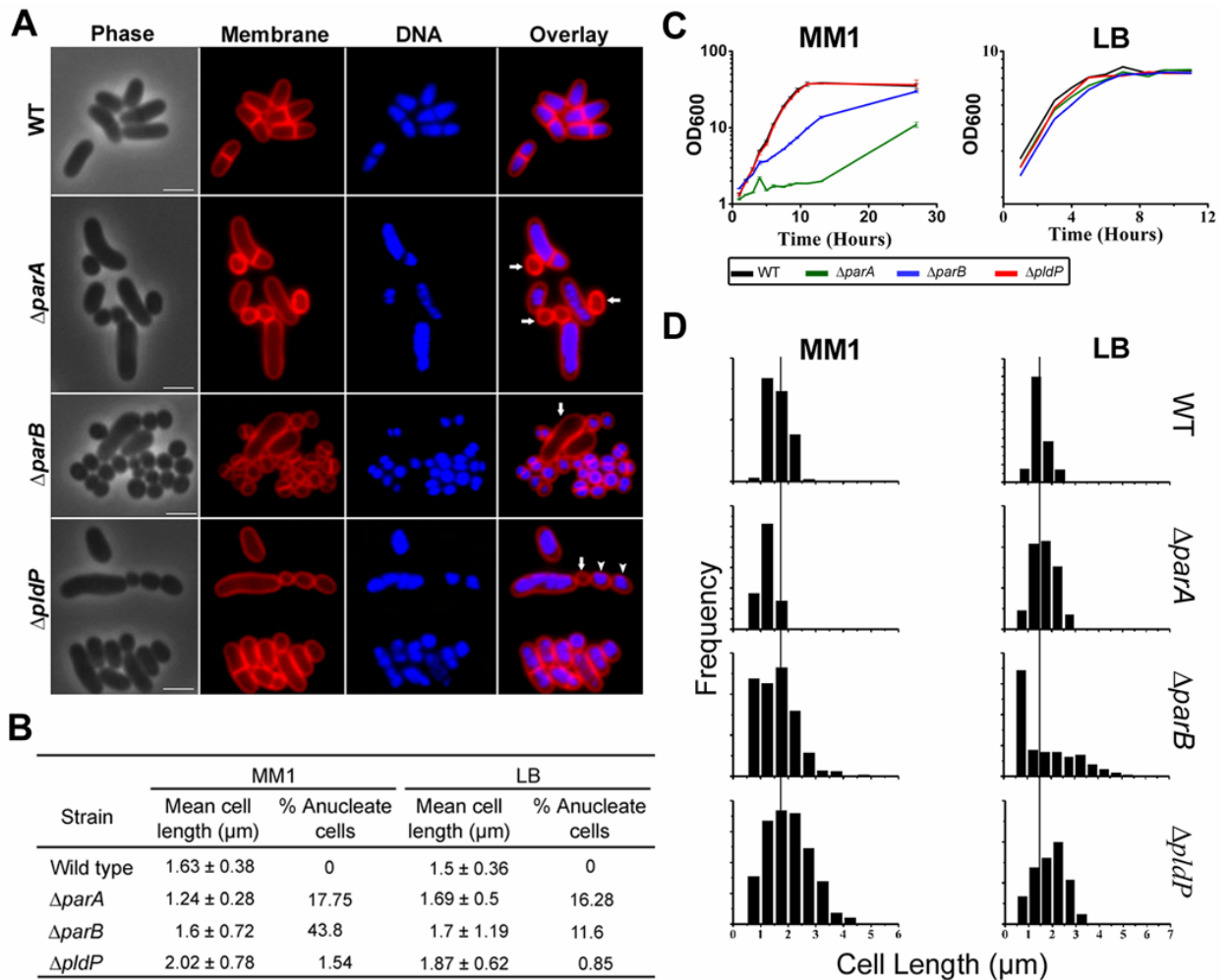


**Figure 2.1: Phenotypes of *C. glutamicum* *parA*, *parB* and *pldP* null mutants. (A)** Microscopic images of *parA*, *parB* and *pldP* null mutants grown in MM1 medium with 4 % glucose. Shown are phase contrast images (Phase), membrane stain with Nile Red (Membrane), DNA stain with Hoechst dye (DNA), and an overlay. Anucleate cells are indicated with arrows. Minicells are indicated with arrowheads. **(B)** Statistical analysis of the *parA*, *parB* and *pldP* deletion mutants. Cell lengths were measured using Nile Red as a membrane stain and values are expressed as mean cell lengths ± the standard deviation. Anucleate cells were measured by staining DNA with Hoechst dye. For each strain, more than 200 cells were counted ( $n \geq 200$ ). **(C)** Growth analysis of the *parA*, *parB* and *pldP* deletion mutants in MM1 supplemented with 4 % glucose (left side) and LB medium (right side). Values are the means of three growth experiments. The standard deviations are shown. **(D)** Histograms showing the distribution of cell lengths of wild type and mutant strains grown in MM1 medium (left panel) and LB medium (right panel). The black lines indicate the mean cell length of wild type cells. Scale bar, 2 μm.

The phenotypes of the deletion mutants cultured in the various media were analyzed further in terms of cell length and anucleate cell production (Fig. 2.1 B and D). This analysis highlighted clear differences between the *parA* and *pldP* mutants. The maximum frequency of anucleate cell production

## Results

was approximately 1.5 % for the *pldP* mutant. The number of DNA free cells did not vary much with growth medium in cells that lack *parA*, 17.75 % when grown in MM1 medium and 16.28 % when grown in LB medium (Fig. 2.1 B). Interestingly, this staggering number of anucleate cells has not been observed previously for *parA* deletion mutants in other bacteria, e.g. deletion of *parA* (*soj*) in *B. subtilis* (Ireton *et al.*, 1994; Webb *et al.*, 1998). The cell length distributions were altered for both the *parA* and *pldP* mutants, ranging from very small to slightly elongated, however the average cell length of the *pldP* mutant was significantly longer than wild type cells,  $2.02 \pm 0.78$  and  $1.63 \pm 0.38$ , respectively.

The most drastic phenotype was observed for the *parB* deletion mutant. While some cells were elongated, up to 5  $\mu\text{m}$  in length, a large number of cells of this mutant strain were coccoidal in shape (Fig. 2.1 A). The coccoidal cells contained, what appeared to be, extremely compact chromosomes, while the elongated cells were often DNA free. In addition, the coccoidal shaped cells appeared to be defect in apical growth. Interestingly, a similar coccoidal morphology has been previously described for a DivIVA knock-down mutant (Letek *et al.*, 2008). The severe phenotypic consequence of the *parB* mutant is underlined by the degree of anucleate cell production (Fig. 2.1 B). Cultured in medium that supports rapid growth (MM1), almost 44 % of the cells lacked a chromosome. In comparison, growth in medium that supports slower growth (LB) resulted in a reduced rate of anucleate cell production (11.6 %), however, still considerably high.

Vancomycin labeled with fluorescein on its only amide group (Van-FL) has been used to show regions of cells where active peptidoglycan synthesis occurs (Daniel and Errington, 2003). Vancomycin is an antibiotic that inhibits cell wall synthesis by forming stable complexes with the C-terminal D-Ala-D-Ala residues present in the lipid II-linked disaccharide pentapeptide cell wall precursors and in the nascent, uncrosslinked peptidoglycan (Sheldrick *et al.*, 1978). This binding can inhibit transpeptidase activity, either directly or indirectly. *C. glutamicum* cells stained with Van-FL exhibits fluorescence at the cell poles and division septa (Letek *et al.*, 2008), (Fig 2.2). In comparison, cells deleted for *parB* are uniformly stained, showing that the normal mode of growth is perturbed.

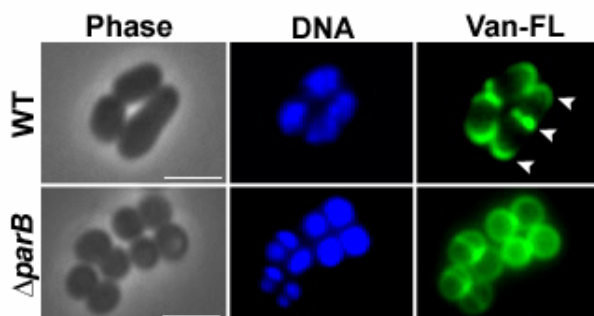


**Figure 2.2: Mutants deleted for *parB* have an altered mode of growth.** Wild type cells stained with Van-FL exhibit polar and septal staining. In comparison, uniform staining is observed in cells deleted for *parB*. Scale bar, 2 $\mu\text{m}$ .

Taken together these data indicate that ParA and ParB are involved in chromosome segregation and also possibly chromosome replication initiation. In addition, the reduced apical growth of the *parB* mutant indicate that chromosome segregation or anchoring of the chromosome at the cell poles might be coupled to cell growth. The low frequency of anucleate cells, unaltered growth and cell

## Results

length distribution of the *pldP* mutant would suggest that this orphan ParA-like protein is not involved in chromosome replication initiation and segregation.

### *In vivo* localization of ParA and PldP

In order to examine the subcellular localization of ParA and PldP at physiological concentrations, strains were constructed whereby the native alleles were replaced by *cfp* fusion genes, placing the expression of the CFP fusion proteins under the control of the native promoter. These fusion proteins were deemed functional based on the lack of anucleate cell production and cells lengths similar to wild type cells. Again, analysis of the subcellular localization of ParA-CFP and PldP-CFP highlighted subtle differences between these two proteins (Fig. 2.3). ParA-CFP often localized as foci to areas of DNA closest to the cell poles (Fig. 2.3, top panel). As ParA and ParB have been shown to interact in other organisms (Leonard *et al.*, 2005; Scholefield *et al.*, 2011; Easter and Gober, 2002), it could be assumed that these polar ParA-CFP foci are interacting with the ParB-*oriC* nucleoprotein complexes. ParA-CFP also localized as large cloud-like structures, covering part of the nucleoid. These diverse localization patterns would suggest that ParA-CFP is dynamic, consistent with a role in chromosome segregation.

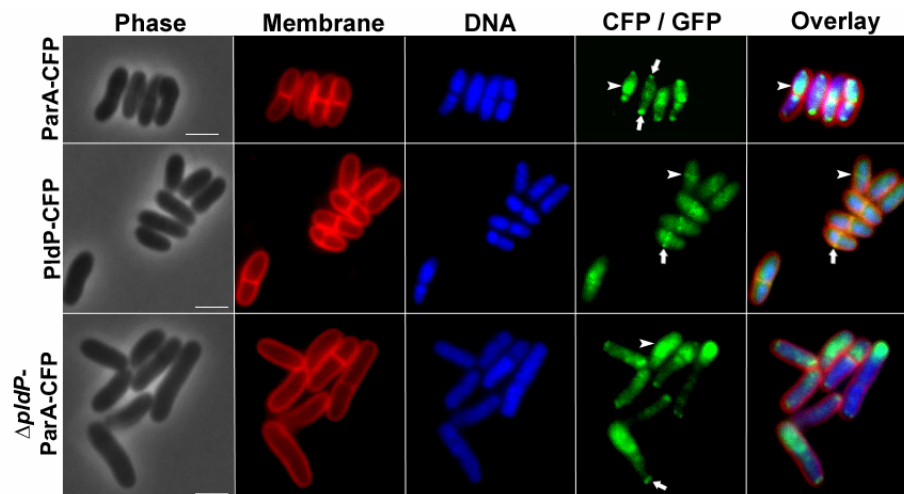


**Figure 2.3: Subcellular localization of ParA-CFP and PldP-CFP in *C. glutamicum*.** The subcellular localization of ParA and PldP was analyzed using strains where the native allele was replaced by *cfp* fusion genes. Shown are phase contrast images (Phase), membrane stain (Membrane), DNA stain with Hoechst dye (DNA), CFP fluorescence (CFP, false color in green), and an overlay. ParA-CFP forms either polar foci (arrows) or cloud-like structures that bind the nucleoid (arrowhead) (upper panel). PldP localizes as either a band-like structure around midcell prior to inward growth of the division septum (arrowhead) or as foci at the midcell region prior to completion of septation (arrow). In the absence of *pldP*, ParA-CFP still localizes as polar foci (arrow) and larger patches which often concentrate at the opposite pole (arrowhead). Scale bar, 2  $\mu$ m.

PldP-CFP, on the other hand, exhibited two distinct localization patterns, which differed greatly from ParA-CFP localization. In approximately 45 % of cells, PldP-CFP localized as discrete foci to the

## Results

---

mature (or maturing) division septum, as determined by a Nile red membrane stain (Fig. 2.3, middle panel). PldP-CFP formed a band-like structure around the midcell region, in approximately 50 % of cells prior to inward growth of the division septum. Thus, it appears that PldP is recruited relatively early to the division site. To rule out that ParA and the orphan ParA-like protein function cooperatively, the localization of ParA-CFP was analyzed in the absence of *pldP*. Although the cells were slightly elongated, ParA-CFP still localized as foci to the cell poles and as patches over the chromosome in the *pldP* mutant (Fig. 2.3, lower panel).

### Phenotypes of double *par* deletion mutants

Numerous attempts were made to simultaneously delete *parA* and *parB* in *C. glutamicum*, however it appears that deletion of both *par* genes is lethal. Nonetheless, mutants deleted for *pldP* in combination with *parA* or *parB* could be generated. Similar to the single null deletion mutants, mutants deleted for *pldP* and *parA* or *parB* grew identical to wild type cells when grown in LB medium (Fig. 2.4 B). Simultaneous deletion of *pldP* did not alter growth rates compared to the single deletion mutants, when cultured in MM1 medium (Fig. 2.4 B). However, the morphology of the double deletion mutants was dramatically altered (Fig. 2.4 A). Aside from altered cell lengths and production of anucleate cells, growth from ectopic sites along the lateral axis of the cell was observed. A similar branching phenotype was also observed for the single deletion mutants, however at a much lower frequency. Interestingly, growth from ectopic sites was only observed when cells were grown in LB medium and the frequency of branching was slightly increased in the *parB-pldP* mutant (6.4 %) compared to the *parA-pldP* mutant (4.25 %).

In *E. coli*, altered cell morphology has also been observed in mutants of cell division, *ftsZ* and *ftsL* mutations, and also mutants that are defective in chromosome replication or nucleoid separation, which often continue to divide, resulting in the formation of filaments, minicells and anucleate cells, in addition to normal cells (Woldringh *et al.*, 1994; Gullbrand *et al.*, 1999; Young, 2003; Potluri *et al.*, 2010, Potluri, *et al.*, 2012). In particular, mutation of components of the Min system form branching cells under certain growth conditions (Akerlund *et al.*, 1993). Overexpression of DivIVA can induce growth from ectopic sites in *C. glutamicum* (Letek *et al.*, 2008). We also observed a branching phenotype in a *C. glutamicum* strain expressing a partially non-functional FtsZ-mCHERRY translational fusion from its native locus (see discussion and Fig. S7). Although the underlying mechanism that leads to this phenotype is not understood, it might be a consequence of defects in cell division and / or cell wall synthesis, along with a defect in chromosome segregation. In any case, simultaneous deletion of *pldP* and *parA* or *parB* greatly enhances growth from ectopic sites.

Another consequence of these double deletion mutants was uncontrolled septum formation and placement, resulting in severe guillotining of the chromosome. In figure 2.4 A (lower panel, arrow) an example is shown where four septa, positioned close together have severed the nucleoid, compartmentalizing pieces of DNA. However, the chromosome exists as a continuous, unsegregated

## Results

mass of DNA in branching cells. Remarkably, these mutants can maintain a growth rate similar to wild type cells, when grown in LB medium.

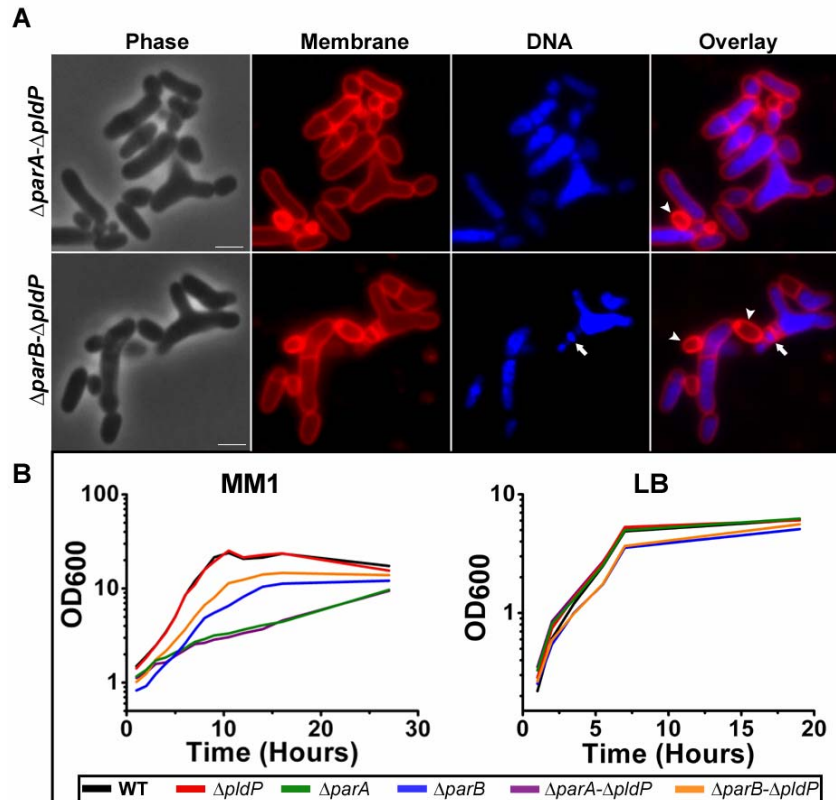


**Figure 2.4. Mutants deleted for *pldP* and *parA* or *parB* have altered cell morphology and aberrant septum placement.** (A) Microscopic examination of  $\Delta parA-\Delta pldP$  and  $\Delta parB-\Delta pldP$  mutants. Both double deletion mutants exhibit altered cell lengths, a high frequency of anucleate cells, growth from ectopic sites and aberrant septum placement. The arrowheads indicate anucleate cells and the arrow shows a branching cell in which numerous septa have chopped the nucleoid into small pieces. Shown are phase contrast images (Phase), Nile red membrane stain (Membrane), DNA stain with Hoechst dye (DNA) and an overlay. (B) Growth analysis of the  $\Delta parA-\Delta pldP$  and  $\Delta parB-\Delta pldP$  mutants. Both double deletion mutants grow at a rate comparable to wild type in LB medium. In minimal medium supplemented with 4 % glucose (MM1), simultaneous deletion *pldP* did not drastically alter the growth rate compared to the single *parA* and *parB* deletion mutants. Scale bar, 2 $\mu$ m.

### ParA, unlike PldP, is necessary for polar localization of ParB

The movement of the *oriC* is a rapid and directed process. In *C. crescentus* and *V. cholerae* the directed movement of the newly replicated origin is influenced by ParA (Ptacin *et al.*, 2010; Fogel and Waldor, 2006). Thus, we wanted to determine if ParA alone or both ParA and PldP influence polar localization of ParB-*parS* nucleoprotein complexes in *C. glutamicum*. Thereby, the subcellular localization of ParB-CFP foci was analyzed in wild type cells and compared to mutants deleted for *parA* or *pldP*. ParB-CFP was expressed from a pEKEX2 plasmid in the wild type and mutant backgrounds. The localization of ParB-CFP foci was classified as polar (unipolar or bipolar), midcell or

## Results

cell quarter positions. When expressed in the wild type background, more than 80 % of the ParB-CFP foci were localized at the cell poles, with an average number of 2.2 foci per cell (Table. 2.1). This result is consistent with the localization pattern of chromosomally expressed ParB-GFP (Fig. 1.4). Even though the number of polar foci was reduced, a similar localization pattern was observed when ParB-CFP was expressed in the *pldP* mutant background (Table. 2.1). In contrast, in the absence of *parA* the number of polar ParB-CFP foci decreased dramatically (28 %) (Table 2.1). In the *parA* mutant background, the majority of the ParB-CFP foci were found at the cell quarter positions (48.8 %). Moreover, the number of ParB foci increased to 3.22 per cell, which was not observed in the *pldP* mutant background. Again, this result highlights a clear difference between ParA and PldP. The data suggests that ParA, and not PldP, helps to segregate the newly replicated *oriC* to the opposite cell pole. In addition, the increased number of ParB foci, and hence, increased number of origins, observed in the absence of *parA*, could suggest that ParA plays an additional role in the regulation of chromosome replication initiation, similar to the situation in *B. subtilis* (Murray and Errington, 2008; Scholefield *et al.*, 2012).

**Table 2.1: Influence of *parA* or *pldP* deletion on the localization of ParB, *in vivo*.**

Strain	Mean cell length ( $\mu\text{m}$ )	% ParB-CFP localization ( $n \leq 170$ )			Mean no. of foci / cell
		Polar	Midcell	Cell quarters	
ParB-CFP	2.15 $\pm$ 0.5	81.9	9	9.1	2.21
$\Delta\textit{parA}$ ParB-CFP	3.2 $\pm$ 0.9	27.6	23.6	48.8	3.22
$\Delta\textit{pldP}$ ParB-CFP	3.19 $\pm$ 0.9	67.6	11.6	20.8	2.68

<sup>a</sup> Cells were grown in LB medium at 30°C. Cell length was measured using Nile Red as a membrane stain. DNA was stained with Hoechst dye. Polar localization of at least one focus was counted as “polar.”

### 2.2 Polar tethering of the chromosome origins in *C. glutamicum*

In *C. glutamicum*, chromosome organization is similar to *C. crescentus* where the *oriC* is localized at the cell pole, and newly replicated origins are segregated to the opposite cell pole (Mohl and Gober, 1997; Viollier *et al.*, 2004). In *C. crescentus*, the polymeric protein PopZ helps anchor the ParB bound origin at the cell pole (Bowman *et al.*, 2008; Ebersbach *et al.*, 2008). A similar mechanism has been postulated for *V. cholerae*, however the polar factor necessary for tethering the origin has not been identified, yet. Based on the similar mutant phenotype, namely impaired apical growth, of a DivIVA knock-down mutant and a *parB* null mutant, we speculated that DivIVA could play a role in analogous to PopZ in *C. crescentus*. A bacterial two-hybrid interaction analysis demonstrated that ParB and DivIVA might interact (Fig. 1.5).

### DivIVA physically interacts with ParB, *in vivo*

Members of the Actinobacteria phylum, many of which do not encode a prokaryotic actin homologue (*mreB*), require DivIVA to coordinate apical growth and determine cell shape (Letek *et al.*, 2008). In *Corynebacterium*, *Mycobacterium* and *Streptomyces*, DivIVA localizes to cell poles, division septa and emerging branches, which are all areas of active growth (Flårdh, 2003; Nguyen *et al.*, 2007; Letek *et al.*, 2008; Kang *et al.*, 2008; Hempel *et al.*, 2008). In *C. glutamicum*, cells overexpressing DivIVA have bulging cell poles, while knock-down mutants have coccoidal morphology (Letek *et al.*, 2008). Therefore, a *C. glutamicum* DivIVA-mCHERRY expressing strain was constructed. In this strain DivIVA-mCHERRY is chromosomally expressed as a single copy from its native promoter (Fig. 2.5 C). Growth rate and morphology of this strain was identical to wild type, suggesting that the DivIVA-mCHERRY construct is fully functional. Upon analysis of this strain it became apparent that DivIVA forms polar localized polymers that are partly intruding into the cytoplasm, to some extent resembling the localization of the functionally analogous PopZ protein in *C. crescentus*.

Since DivIVA is essential in *C. glutamicum* and slight alterations in the expression level alter cell morphology (Letek *et al.*, 2008), the *in vivo* interaction between ParB and DivIVA was tested further by reconstitution in *E. coli* cells. The heterologous *E. coli* system is particularly advantageous as *E. coli* does not encode homologues of *divIVA* and the *parAB* chromosome partitioning system. *E. coli* strains were constructed in which DivIVA-GFP and ParB-CFP are expressed, either individually or in combination, from an IPTG inducible vector. Similar to other DivIVA homologues, DivIVA-GFP localized to the curved membranes at the cell poles and sites of septation, in *E. coli* cells (Fig. 2.5 A). In both *C. glutamicum* and *E. coli*, DivIVA associates to the pole membrane, partially intruding into the cytoplasm, and is also targeted to the division site. Thus, in the heterologous *E. coli* system, DivIVA behaves similar as in the native host and polar localization of DivIVA in *E. coli* is not the result of accumulation of insoluble material.

We tested interaction between ParB-CFP and DivIVA-GFP in the presence and absence of plasmid containing *parS* DNA. When DivIVA-GFP and ParB-CFP were co-expressed in *E. coli*, ParB-CFP was recruited to the cell poles and septa by interaction with DivIVA (Fig. 2.5 A). To exclude unspecific interactions, ParB-CFP was co-expressed with DivIVA lacking a fluorescent tag (for detection purposes DivIVA contains a C-terminal S-tag). Similarly, ParB-CFP was recruited by the native DivIVA (data not shown). Also, in the presence of *parS* DNA ParB-CFP was recruited by DivIVA to the cell poles and division septa; however, the localization of ParB-CFP sometimes resembled an assembly of ParB-CFP foci (Fig. 2.5 A). Thus, the ParB-DivIVA interaction also occurs in complex with *parS* DNA. Together, these results demonstrate that ParB and DivIVA physically interact under *in vivo* conditions, providing evidence that DivIVA anchors the ParB-bound origins at the cell poles in *C. glutamicum*.

## Results

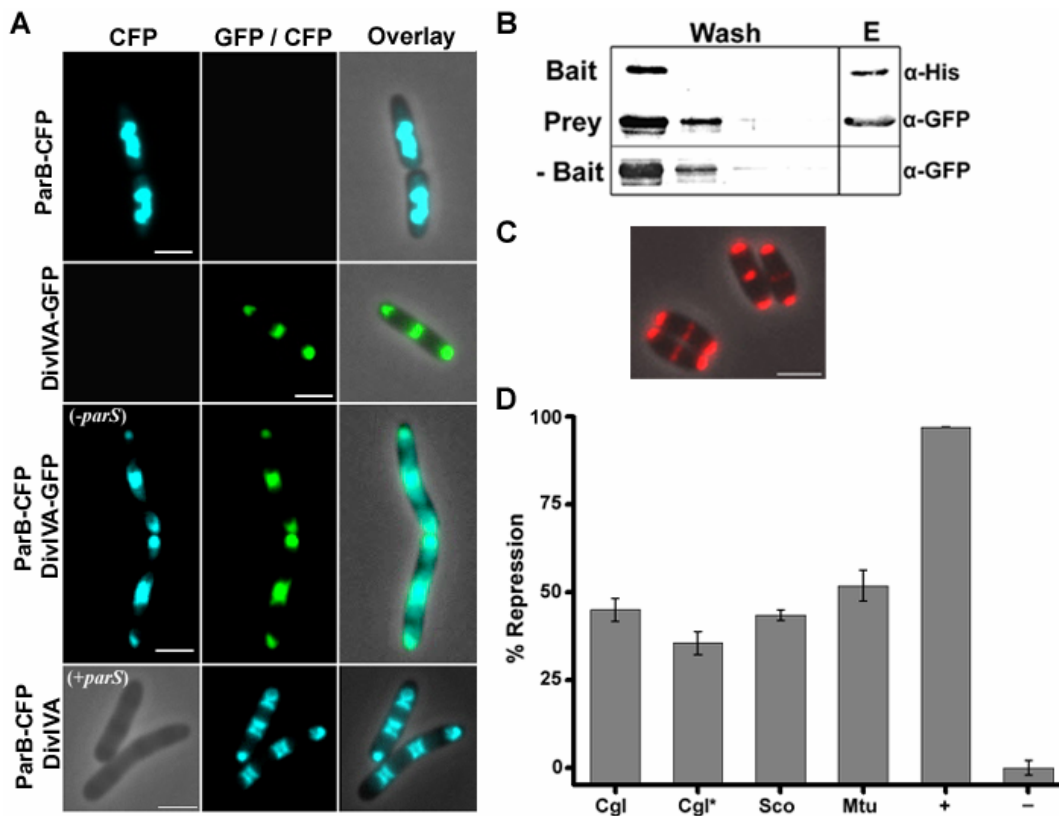


**Figure 2.5: *C. glutamicum* ParB interacts with and is recruited by DivIVA.** (A) *C. glutamicum* ParB-CFP localizes as patches over the chromosome (first panel), while DivIVA-GFP localizes to the cell poles and division septa (second panel) when expressed in *E. coli*. Co-expressed in *E. coli*, ParB-CFP is recruited by DivIVA-GFP to the cell poles and septa and thus, ParB and DivIVA physically interact (third panel). DivIVA recruitment is also observed if ParB is in complex with *parS* DNA (lower panel). Expression was induced with 0.1 mM of IPTG. (B) Co-elution assays show that ParB and DivIVA interact, *in vitro*. Purified His<sub>10</sub>-ParB was used as bait. Bait proteins were detected by immunoblotting using α-Penta-His antibodies. Interacting prey proteins (DivIVA-GFP expressed in *E. coli*), which co-eluted [E] with the bait protein, were detected by immunoblotting using α-GFP antibodies. As a control, prey proteins were incubated with Ni-NTA resin in the absence of bait proteins (- bait). (C) Chromosomal expression of DivIVA-mCherry from the native promoter in *C. glutamicum*. (D) A LexA-based bacterial two-hybrid (Dmitrova *et al.*, 1998) approach was performed to study protein-protein interactions between ParB and DivIVA from Actinobacteria. The experiments were performed in *E. coli* SU202 (*PsuA-lacZ*, *op408/op+*). The proteins of interest were fused to either wild-type LexA DNA binding domain (pMS604) or a mutant LexA DNA binding domain (pDP804). Heterodimerization of the proteins of interest bring the wild-type and mutant portions of the LexA DNA binding domains together, repressing transcription of a LexA-regulated *PsuA-lacZ* fusion, which was measured by β-galactosidase assays. The leucine zipper domains of Fos and Jun fused to the WT and mutant LexA DNA binding domain, respectively, serve as positive control (+). Unrepressed levels of β-galactosidase activity was determined in the presence of empty vector (pMS604 / pDP804) and the LexA DNA binding domain fusion to the test protein, in both combinations (negative control (-)). The % repression of *PsuA-lacZ* of interacting proteins was determined against the negative control. Shown are interaction between *C. glutamicum* ParB and DivIVA (Cgl) (pMS-ParB / pDP-DivIVA, negative control -1761 Miller units), *C. glutamicum* DivIVA144-298 and ParB (Cgl\*) (pMS-DivIVA144-298 / pDP-ParB, negative control - 2011 Miller units), *S. coelicolor* ParB and DivIVA (Sco) (pMS-DivIVA / pDP-ParB, negative control - 2537 Miller units) and *M. tuberculosis* ParB and Wag31 (Mtu) (pMS-ParB / pDP-Wag31, negative control - 1977 Miller units). Standard deviations are derived from three independent experiments. Scale bar, 2 μm.

### DivIVA interacts with ParB, *in vitro*

The direct and specific interaction between ParB and DivIVA was tested *in vitro* by co-elution experiments. Therefore, purified His-tagged ParB (bait protein) was bound to Ni-NTA resin. After removal of unbound protein, bound His<sub>10</sub>-ParB was incubated with the cleared cell lysate of *E. coli* DivIVA-GFP expressing cells (prey protein). After extensive washing, interacting protein complexes were eluted and subsequently analyzed by immunoblot. DivIVA and ParB were detected with α-Penta-His and anti-GFP antibodies, respectively. Similar to the *in vivo* situation, ParB specifically co-eluted with DivIVA (Fig. 2.5 B). To exclude unspecific interactions, the prey protein (DivIVA-GFP) was incubated with the Ni-NTA resin in the absence of bait protein (Fig. 2.5 B (-Bait)). Here, additional evidence is provided for the direct physical *in vitro* interaction of *C. glutamicum* DivIVA and ParB, and subsequent implications in tethering the origins to the cell poles.

### The N-terminal domain of ParB interacts with DivIVA

In several organisms, ParB domains have been attributed specific functions. The N-terminal domain of *C. crescentus* ParB, as well as ParB of plasmid P1 and SopB of F plasmid interact with ParA / SopA (Figge *et al.*, 2003; Radnedge *et al.*, 1998; Ravin *et al.*, 2003), while the C-terminal domain of *C. crescentus* and *Thermus thermophilus* ParB is required for dimerization and subsequent DNA binding (Figge *et al.*, 2003; Leonard *et al.*, 2004). In *B. subtilis*, the N-terminal domain of Spo0J (ParB) stimulates the ATPase activity of Soj (ParA), driving Soj to an ADP-bound monomer which in turn inhibits DNA replication initiation (Scholefield *et al.*, 2011).

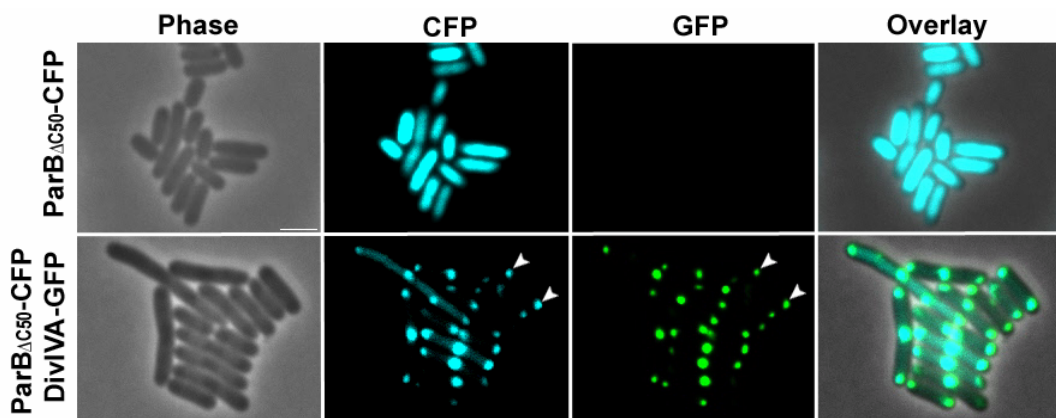


**Figure 2.6: Deletion of the C-terminal 50 amino acids of ParB does not influence interaction with DivIVA.** ParB<sub>ΔC50</sub>-CFP exhibits diffuse cytoplasm localization, in *E. coli* (Upper panel). Co-expression of ParB<sub>ΔC50</sub>-CFP and DivIVA-GFP in *E. coli* demonstrate that the C-terminal domain of ParB is not involved in interaction with DivIVA. Scale bar, 2 μm.

In *C. glutamicum*, ParB domains have not been attributed a specific function, yet. We took advantage of the concentration dependent localization of ParB to the *E. coli* nucleoid and carried out

## Results

mutational analysis to gain additional insight into the function of the ParB domains and interaction with DivIVA. It has been shown that the C-terminal domain of ParB is the initial dimerization domain, and dimerization is a prerequisite for DNA binding (Figge *et al.*, 2003; Leonard *et al.*, 2004; Murray *et al.*, 2006). Truncation of the C-terminal domain of *C. glutamicum* ParB (ParB $_{\Delta C50}$ ) exhibited a diffuse cytoplasmic localization when expressed in *E. coli* (Fig. 2.6), indicating that binding of this ParB mutant to the nucleoid is weakened, if not completely abrogated. As this ParB variant still contained the putative central DNA binding domain (HTH domain), it appears that deletion of the C-terminal impacts on dimerization rather than directly inhibiting binding to DNA. When co-expressed with DivIVA in *E. coli*, recruitment of ParB $_{\Delta C50}$  to the cell poles was not altered (Fig. 2.6). Therefore, we turned our attention to the N-terminal domain of ParB. Thus, a mutant ParB protein, lacking 100 amino acids of the N-terminal region of ParB (ParB $_{\Delta N100}$ -CFP), was expressed in combination with DivIVA, which lacked a fluorescent tag. Interaction of the ParB variant deleted for the N-terminal 100 amino acids and full-length DivIVA was completely abolished (data not shown).

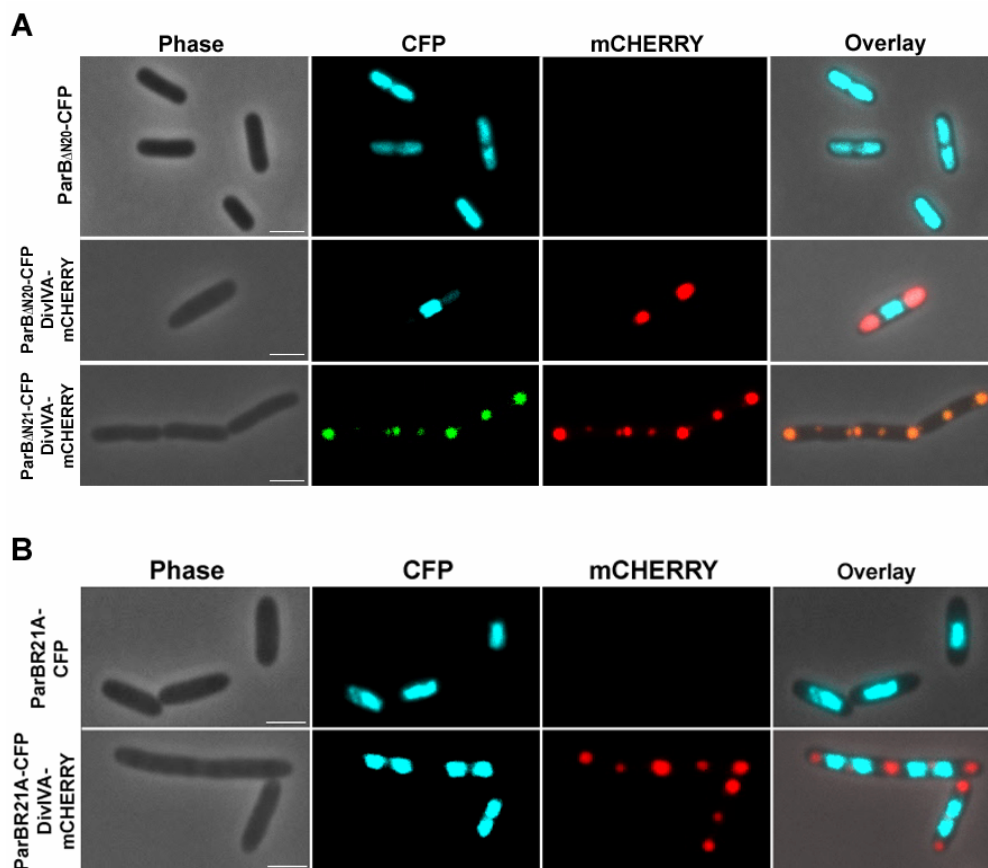


**Figure 2.7: The N-terminal of ParB interacts with DivIVA.** (A) Deletion of the N-terminal 20 (or 21) amino acids of ParB does not alter binding to the nucleoid, when expressed in *E. coli*. However, ParB $_{\Delta N20}$ -CFP no longer interacts with DivIVA. The ParB $_{\Delta N21}$ -CFP variant, which still contains the conserved arginine, can interact with DivIVA, when expressed in *E.* (B) Co-expression of ParBR21A-CFP and DivIVA-mCHERRY, in *E. coli*. Mutation of a conserved arginine (R21) in ParB weakens interaction with DivIVA. Scale bar, 2  $\mu$ m.

## Results

---

In a previous study, sequence alignments of putative ParB (Spo0J) proteins revealed a high degree of conservation of the N-terminal regions (Leonard *et al.*, 2004). Indeed, alignment of *C. glutamicum* ParB and *B. subtilis* Spo0J (ParB) sequences revealed that the N-terminal domains of both sequences contain a conserved stretch of aliphatic residues (Fig. S1). It was hypothesized that one or all of these residues might be required for interaction with DivIVA. Hence, the N-terminal domain of ParB was truncated, deleting the first 21 amino acids (ParB<sub>ΔN21</sub>-CFP). This mutant ParB protein lacks the highly conserved arginine (R21) within the stretch of aliphatic residues, which in other organisms is reported to be imperative for ParA interaction (Leonard *et al.*, 2005). Despite localizing identical to full length ParB in *E. coli*, DivIVA dependent recruitment of ParB<sub>ΔN21</sub>-CFP was completely abolished (Fig. 2.7 A). It was reasoned that the conserved arginine is important for interaction with DivIVA. Therefore, a ParB mutant protein still possessing the conserved arginine but lacking the preceding 20 amino acids (ParB<sub>ΔN20</sub>-CFP) was co-expressed with DivIVA-mCHERRY. Interestingly, ParB<sub>ΔN20</sub>-CFP still interacted with DivIVA, showing that the N-terminal arginine does indeed strongly influence interaction with DivIVA (Fig. 2.7 A). Keeping with this line of investigation, the conserved arginine was mutated to an alanine, in the otherwise wild type protein. Again, this mutant ParB protein (ParBR21A-CFP) localized as patches over the *E. coli* nucleoid, however interaction with DivIVA was eliminated, (Fig. 2.7 B). Thus, the N-terminal motif of ParB (Fig. S1) is essential for interaction with DivIVA.

### **In *C. glutamicum*, mutation of the conserved arginine (R21) of ParB significantly alters interaction with DivIVA.**

The conserved arginine (R21) of the N-terminal motif (Fig. S1) of ParB was identified as an important residue for interaction with DivIVA, when expressed in the heterologous *E. coli* system (Fig. 2.7 B). To further support this finding, two *C. glutamicum* strains expressing ParB-eCFP and ParBR21A-eCFP in a  $\Delta parB$  DivIVA-mCHERRY mutant background were constructed. Expression of ParB-eCFP and ParBR21A-eCFP was induced with 0.5 mM IPTG for 90 minutes before microscopic analysis. The subcellular localization of ParB-eCFP and ParBR21A-eCFP foci were analyzed statistically. The foci were categorized as either, (i) unipolar or bipolar, (ii) bipolar with one or two foci at midcell or cell quarter positions, (iii) unipolar with two foci at midcell or cell quarter positions and (iv) foci localized at midcell or cell quarter cell positions in the absence of polar localized foci. In cells expressing ParB-eCFP, ParB foci were always anchored to the cell poles, either uniquely as polar foci or as polar and midcell / cell quarter foci. In contrast, unipolar or bipolar localization of ParBR21A-eCFP foci was greatly reduced (20 %) compared to ParB-eCFP expressing cells (60 %). Although ParBR21A-eCFP foci were sometimes localized at the cell poles, a significant number of cells (20 %) completely lacked polar localized foci (Fig. 2.8 A and C).

In *C. glutamicum*, deletion of *parB* results in a high frequency of anucleate cells (Fig. 2.1). Expression of ParB-eCFP almost fully complemented the  $\Delta parB$  mutant phenotype. In the absence of inducer, 32.8 % anucleate cells were produced, which was reduced to 1.7 % upon expression of ParB-

## Results

eCFP (Fig. 2.8 B). However, *C. glutamicum* cells expressing ParBR21A-eCFP only partially complemented the *parB* mutant phenotype, producing 10.4 % anucleate cells (Fig. 2.8 B). Thus, mutation of the invariant arginine (R21) of ParB significantly reduces the affinity of ParB for DivIVA and impairs polar anchoring of the chromosome origin.

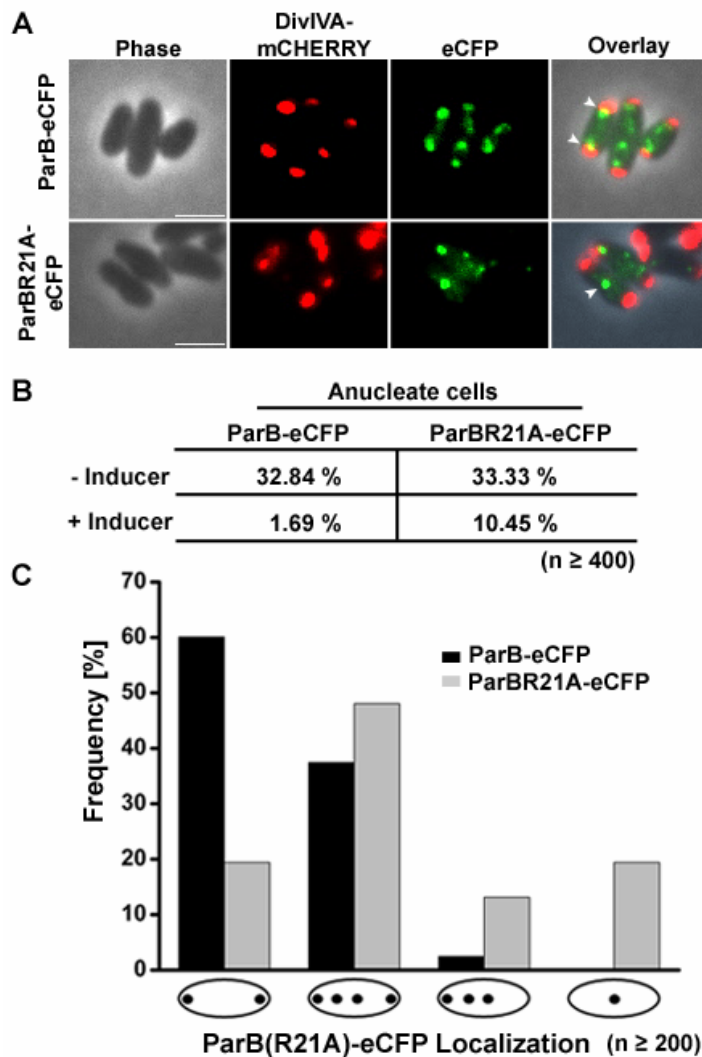


**Figure 2.8: Mutation of the invariant arginine (R21) of ParB alters polar localization of ParB foci in *C. glutamicum*.** (A) Localization of ParB-eCFP and ParBR21A-eCFP expressed from a plasmid in *C. glutamicum* cells in a  $\Delta parB$  DivIVA-mChERRY background. Cells were induced with 0.5 mM IPTG for 90 minutes prior to microscopic analysis. ParB-eCFP foci are localized to the cell poles (upper panel, arrows). In cells expressing ParBR21A-eCFP, foci are often observed that are not anchored to the cell poles (lower panel, arrow). (B) Quantification of anucleate cell production in absence and presence of ParB-eCFP and ParBR21A-eCFP. Expression of ParB-eCFP almost completely complements the anucleate cell phenotype of a  $\Delta parB$  mutant (1.69 % anucleate cells). However, expression of ParBR21A-eCFP only partially complemented the  $\Delta parB$  mutant phenotype, producing 10.45 % anucleate cells. (C) Statistical analysis of ParB-eCFP and ParBR21A-eCFP localization. ParB-eCFP localizes predominantly at the cell poles, exhibiting either exclusive polar localization or polar and midcell / cell quarter localization (black). However, in 20 % of cells expressing ParBR21A-eCFP, the poles are completely devoid of ParB foci (grey). Scale bar, 2  $\mu$ m.

### A central region of DivIVA is necessary for ParB interaction

With the exception of the N-terminal domain, the amino acid sequences of functionally different DivIVA homologues display significant variation (Fig. S2). The Actinobacteria DivIVA is larger, containing a central insertion that is absent in the Firmicutes DivIVA (Lenarcic *et al.*, 2009; Oliva *et al.*, 2010). In sporulating *B. subtilis*, attachment of the origin to the prespore pole is mediated by centromere bound RacA and polar DivIVA (Ben-Yehuda *et al.*, 2003; Ben-Yehuda *et al.*, 2005; Wu and Errington, 2003). Although a *soj* (*parA*) *spo0J* (*parB*) *racA* triple mutant exhibited a higher level of chromosome misorientation than the single *racA* mutant, no direct interaction between membrane associated DivIVA and Spo0J has been shown, to date. The synthetic *E. coli* system was used to test the potential interaction between *B. subtilis* DivIVA (DivIVA<sub>bsu</sub>) and Spo0J. Expressed alone, Spo0J-CFP localized as patches over the *E. coli* nucleoid (Fig. S3). This pattern was not altered when expressed in combination with DivIVA<sub>bsu</sub>, showing that these proteins presumably do not interact physically (Fig. S3). This result highlights the reliability of the synthetic *E. coli* system for assaying protein-protein interactions.

It was speculated that the central region of *C. glutamicum* DivIVA would be important for interaction with ParB. To test this idea, *C. glutamicum* ParB-CFP was co-expressed with DivIVA<sub>bsu</sub> in *E. coli*. Testifying that our postulation was correct, *C. glutamicum* ParB was not recruited to the cell poles and septa by DivIVA<sub>bsu</sub> (Fig. S3). Consequently, part of the central region of *C. glutamicum* DivIVA (amino acids 144 – 298) was deleted. This mutant DivIVA protein (DivIVA<sub>Δ1</sub>-GFP) still localized to the cell poles and division septum when expressed in *E. coli* cells, however, when co-expressed with ParB-CFP, ParB remained bound to the nucleoid (Fig. 2.9 B). To further support the finding that ParB interacts with the central region of DivIVA, potential interaction between the central region of DivIVA (DivIVA<sub>144-298</sub>) and full-length ParB was assayed in a LexA bacterial two-hybrid. The bacterial two-hybrid experiment indicates that DivIVA<sub>144-298</sub> and ParB can interact, however, in comparison to interaction analysis of full-length ParB and DivIVA, the interaction is slightly reduced (Fig. 2.5 D). However, these results indicate that the ParB interaction site lies within this central region of DivIVA.

To pin-point the region of DivIVA that is necessary for ParB interaction, a series of shorter DivIVA truncation mutants were constructed. The various DivIVA truncation mutants generated are shown in figure 2.9 A. All DivIVA truncation mutant proteins localized to the poles and division septa, identical to the full-length protein (Fig. 2.9 B, one example shown), suggesting that these DivIVA variants are functional in respect to membrane binding and oligomerization when expressed in *E. coli*.

These DivIVA truncation mutants were co-expressed with ParB-CFP and subsequently analyzed for interaction. Similar to DivIVA<sub>Δ1</sub>-mCHERRY, deletion of amino acids 144-229 of DivIVA (DivIVA<sub>Δ2</sub>-mCHERRY) inhibited ParB recruitment and interaction (data not shown). As DivIVA<sub>Δ1</sub> and DivIVA<sub>Δ2</sub> mutants lack the C-terminal end of coiled-coil 1 and the N-terminal end of coiled-coil 2, it was speculated that both coiled-coil domains are necessary for ParB recruitment. Co-expression of DivIVA variants lacking the N-terminal end of coiled-coil 2 but still containing the entire coiled-coil 1 domain (DivIVA<sub>Δ3</sub>-mCHERRY, DivIVA<sub>Δ4</sub>-mCHERRY) exhibited weak recruitment of ParB-CFP (Fig. 2.9 B).

## Results

Finally, a DivIVA mutant lacking amino acid 160-200 (DivIVA<sub>Δ5</sub>-mCHERRY) was expressed with ParB-CFP and again exhibited partial recruitment of ParB-CFP. Hence, a short part of both coiled-coil domains of DivIVA are necessary for ParB interaction.

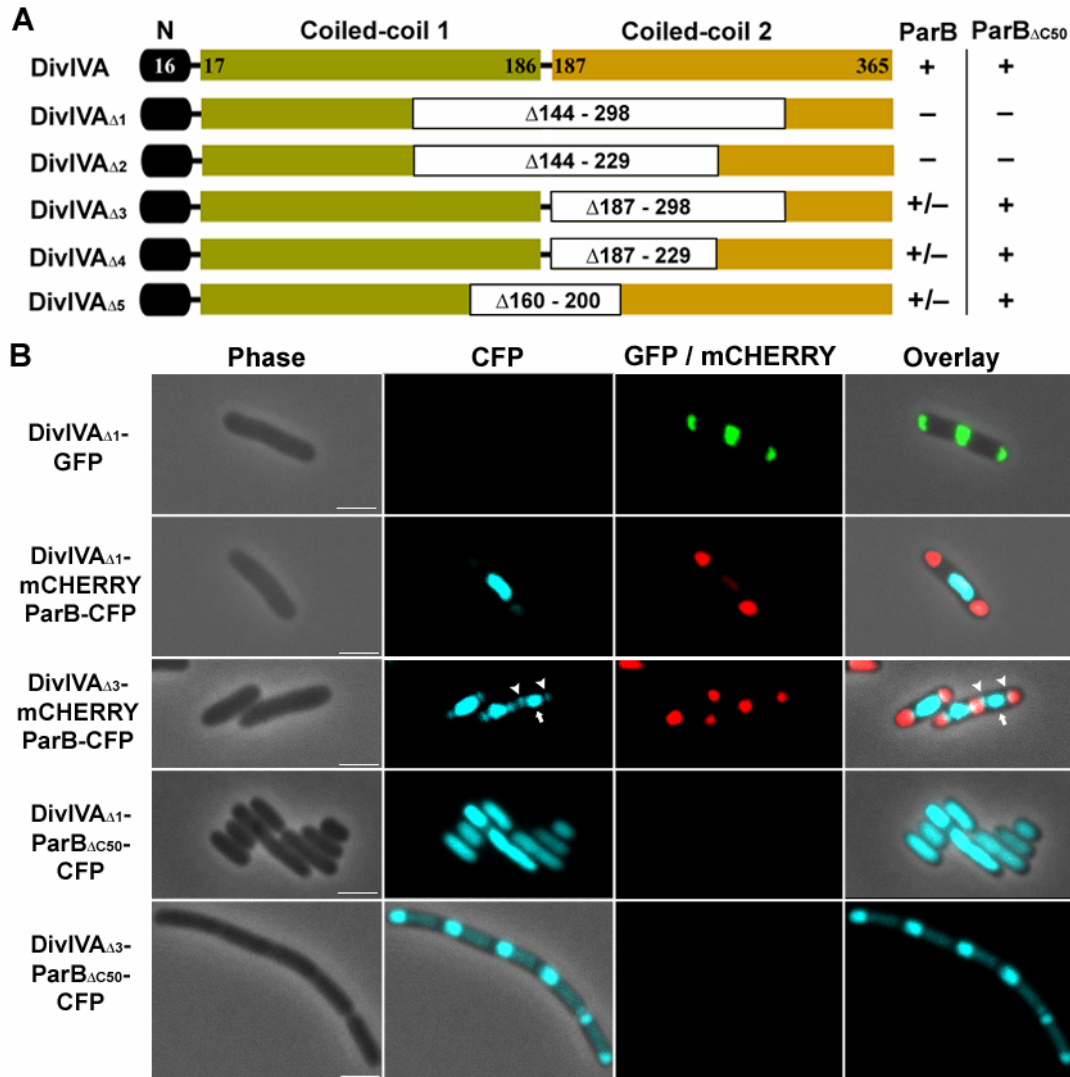


**Figure 2.9: ParB interacts with a central region of DivIVA.** (A) Illustration of the domain architecture of DivIVA and the different DivIVA truncation mutants where central regions were deleted (deleted regions are shown in white together with deleted amino acids). A summary of the interaction potential of the various DivIVA mutants with ParB or ParB<sub>ΔC50</sub> is indicated on the right. ((±) indicates partial recruitment, (+) indicates full recruitment and (-) indicates no recruitment). (B) Examples of the subcellular localization and ParB interaction potential of the various DivIVA truncation mutants when expressed in *E. coli*. DivIVA<sub>Δ1</sub>-GFP, and all other DivIVA truncation mutants, localized to the cell poles and septa, identical to full length DivIVA (first panel). DivIVA<sub>Δ1</sub>-mCHERRY does not recruit ParB-CFP to the cell poles (second panel). DivIVA<sub>Δ3</sub>-mCHERRY shows partial recruitment of ParB-CFP (third panel, arrow heads). ParB remains mostly associated with the nucleoid (arrow). A ParB mutant, defective in DNA binding (ParB<sub>ΔC50</sub>-CFP) and free to diffuse in the cell, is not recruited by DivIVA<sub>Δ1</sub> (fourth panel) but is recruited by DivIVA<sub>Δ3</sub> to the cell poles (lower panel). Scale bar, 2 μm.

### In the synthetic *E. coli* system, ParB interacts with DivIVA via a diffusion-capture mechanism

In the synthetic *E. coli* system, ParB exhibits affinity for the chromosome and, when co-expressed, a stronger affinity for DivIVA. The affinity of the ParB–DivIVA interaction can be eliminated or reduced by mutating the N-terminal domain of ParB or truncating the central region of DivIVA. On the other hand, truncation of the ParB C-terminal domain (ParB<sub>ΔC50</sub>-CFP) results in a diffuse cytoplasmic localization, suggesting that this domain is necessary for DNA binding and also likely dimer formation, which is often a prerequisite for DNA binding (Figge *et al.*, 2003; Leonard *et al.*, 2004).

To unambiguously determine if ParB can interact with the various DivIVA truncation mutants, the different DivIVA mutants were co-expressed with ParB<sub>ΔC50</sub>-CFP, which is free to diffuse in the cytoplasm. If the C-terminal domain of ParB is indeed involved in DNA binding, it would be expected that ParB<sub>ΔC50</sub>-CFP would interact with the DivIVA mutants where full length ParB showed only partial interaction, also supporting the idea of a diffusion-capture mechanism, in *E. coli* cells. Co-expression of ParB<sub>ΔC50</sub>-CFP with DivIVA<sub>Δ1</sub> did not alter the diffuse cytoplasmic localization of ParB (Fig. 2.9 B). However, when expressed in combination with DivIVA<sub>Δ3</sub>, DivIVA<sub>Δ4</sub> or DivIVA<sub>Δ5</sub>, ParB<sub>ΔC50</sub>-CFP was again recruited to the cell poles via interaction with the DivIVA mutants (Fig. 2.9 B, one example shown). These results support the idea that the central region of DivIVA is required for interaction with ParB. Also, the C-terminal domain of ParB is required for DNA binding. Consequently, in the absence of the other components of the Par system, ParB that is free to diffuse in the cytoplasm interacts with DivIVA via a diffusion-capture mechanism, in the synthetic *E. coli* system.

### The ParB-DivIVA interaction is conserved in Actinobacteria

DivIVA-orchestrated apical growth is a distinguishing feature of Actinobacteria. Heterologous DivIVA from either *S. coelicolor* or *M. tuberculosis* can restore apical growth in a *C. glutamicum* DivIVA knock-down mutant, yet *B. subtilis* DivIVA cannot (Letek *et al.*, 2008). This conserved role of DivIVA tempted us to determine if anchoring the origin at the cell pole is additionally a common feature of DivIVA from Actinobacteria. Therefore, two medically and industrially important members, *M. tuberculosis* and *S. coelicolor*, were selected for further analysis.

*M. tuberculosis* is the causative agent of tuberculosis, the world's most deadly bacterial disease. New insights into particular functional aspects of this organism are advantageous, facilitating the search for new antimicrobial targets. Similar to *C. glutamicum*, the chromosome origins, reflected by the localization of ParB, are fixed at the cell poles (Jakimowicz *et al.*, 2007a; Maloney *et al.*, 2009). In addition, overproduction of *M. tuberculosis* ParA<sub>mtu</sub> and ParB<sub>mtu</sub> causes filamentation and multinucleoidity when expressed in *M. smegmatis*, indicating defects in cell cycle progression (Maloney *et al.*, 2009). We heterologously expressed fluorescent fusion constructs of the *M. tuberculosis* DivIVA homologue, Wag31, and ParB in the synthetic *E. coli* system. Similar to the *C. glutamicum* DivIVA, Wag31-mCHERRY localizes to the cell poles and division septa, while *M. tuberculosis* ParB (ParB<sub>mtu</sub>-CFP) formed patches over the *E. coli* nucleoid (Fig. 2.10 A). Expression of

## Results

ParB<sub>mtu</sub>-CFP in combination with Wag31, without a fluorescent tag, again resulted in Wag31 dependent recruitment of ParB<sub>mtu</sub>-CFP to the cell poles and division septa. The interaction between ParB<sub>mtu</sub> and Wag31 could also be shown in a LexA based bacterial two-hybrid (Fig. 2.5 D). These results indicate a direct physical interaction between ParB<sub>mtu</sub> and Wag31 and, thus, anchoring of the chromosome origins to the cell poles (Fig. 2.10 A).

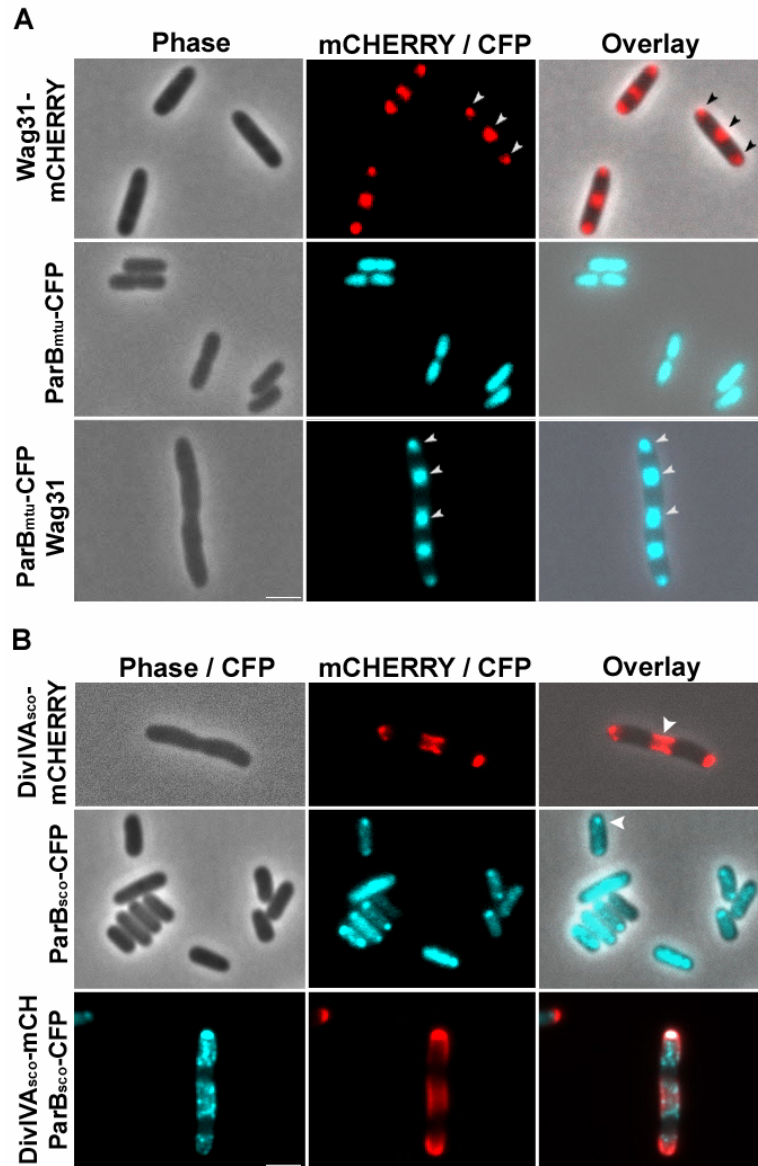


**Figure 2.10: DivIVA mediated recruitment of ParB is conserved in Actinobacteria.** (A) Heterologous expression of *M. tuberculosis* Wag31 and ParB<sub>mtu</sub>-CFP. In *E. coli*, Wag31-mCHERRY localizes to the cell poles and septum (upper panel, arrowheads), while ParB<sub>mtu</sub>-CFP forms patches over the chromosome (middle panel). Expressed in combination, Wag31 recruits ParB<sub>mtu</sub>-CFP to the cell poles and septa (lower panel, arrowheads). (B) Expression of *S. coelicolor* DivIVA and ParB in the synthetic *E. coli* system. DivIVA<sub>sco</sub>-mCHERRY localizes at the cell poles and at the division septum. DivIVA<sub>sco</sub>-mCHERRY localization often extends laterally along the membrane (upper panel, arrow). The *parB*<sub>sco</sub> gene contains a native internal *parS* site, and thus ParB<sub>sco</sub>-CFP forms foci localized mostly near the cell poles (middle panel, arrowhead). Co-expressed, ParB<sub>sco</sub>-CFP is mostly recruited by DivIVA<sub>sco</sub>-mCHERRY (lower panel). Scale bar, 2  $\mu$ m.

## Results

---

The complex life cycle of *Streptomyces* species differs drastically from *C. glutamicum* and *M. tuberculosis*, sharing more similarities with filamentous fungi. *S. coelicolor* cells grow as branching hyphae that form a vegetative mycelium, containing several copies of linear chromosomes (Flårdh and Buttner, 2009). Vegetative hyphal tip extension and initiation of new branching sites is driven by DivIVA<sub>sco</sub>, again highlighting the essential role of DivIVA in setting up a new axis of polarity (Hempel *et al.*, 2008; Wang *et al.*, 2009). In vegetative mycelia, ParB<sub>sco</sub>-eGFP forms irregular foci that are often closely associated with hyphal tips (Jakimowicz *et al.*, 2005). The foci localized close to the hyphal tips have been suggested by the authors to be anchored at these positions, while the non-apical ParB<sub>sco</sub> foci have been implicated in regulating replication initiation (Jakimowicz *et al.*, 2005). During the reproductive phase, chromosome condensation, segregation and multiple septation lead to the development of chains of unigenomic spore compartments. At the onset of sporulation, the expression of ParAB<sub>sco</sub> is up-regulated. ParA<sub>sco</sub>, which accumulates at the hyphal tips, spreading along the hyphae as a pair of helical filaments, appears to be necessary for the proper assembly of segregation complexes (Jakimowicz *et al.*, 2007b). ParB<sub>sco</sub> assembles into regularly spaced foci, usually situated in the middle of the spore (Jakimowicz *et al.*, 2005), however some foci can also be seen close to the septum. The requirement of ParB<sub>sco</sub> (and also ParA<sub>sco</sub>) in chromosome organization is reflected in the increase of anucleate spores in a *parB*<sub>sco</sub> mutant (Kim *et al.*, 1999; Jakimowicz *et al.*, 2005; Jakimowicz *et al.*, 2007b). We hypothesized that ParB<sub>sco</sub> and DivIVA<sub>sco</sub> might interact, which in turn could support chromosome organization in *Streptomyces*.

The interaction potential of DivIVA<sub>sco</sub> and ParB<sub>sco</sub> was tested in the synthetic *E. coli* system. The *S. coelicolor parB* gene contains an internal *parS* site, thus when expressed in *E. coli*, ParB<sub>sco</sub> was often seen as foci localized near the cell pole, but some ParB<sub>sco</sub> was also diffused in the cytoplasm (Fig. 2.10 B). DivIVA<sub>sco</sub>-mCHERRY initially localized as foci at the cell poles, then over time lined the inner membrane of the curved poles and also localized along the lateral axis, beginning around the midcell region then extending laterally. On occasion, some lateral DivIVA<sub>sco</sub>-mCHERRY foci were also seen. In *S. coelicolor*, DivIVA<sub>sco</sub> is predominately localized at the tips of vegetative hyphae and occasionally as bands at sites of septation, however it remains unclear if DivIVA<sub>sco</sub> plays a role in cell division (Flårdh, 2003). In *E. coli*, DivIVA<sub>sco</sub> localized to the division septa. A Z-stack series and subsequent 3-D construction demonstrated that *S. coelicolor* DivIVA forms a ring-like structure at this midcell position, indicating that DivIVA<sub>sco</sub> binds to the curved membrane at the invaginating septum (Fig. 2.10 B and Fig. S4). In general, the behavior of DivIVA<sub>sco</sub> differs from *C. glutamicum* DivIVA when expressed in *E. coli*, highlighting intrinsic properties of DivIVA<sub>sco</sub> in regards to subcellular assembly and organization. In light of the complex life cycle of *S. coelicolor*, multiple additional roles of DivIVA<sub>sco</sub> might also be taken into account. Co-expression of DivIVA<sub>sco</sub>-mCHERRY and ParB<sub>sco</sub>-CFP in *E. coli* did not reveal complete recruitment of ParB<sub>sco</sub> to the cell poles and division septa, however interaction with DivIVA<sub>sco</sub> was often seen (Fig. 2.10 B). Interestingly, ParB<sub>sco</sub> does not contain the conserved arginine seen in ParB<sub>cgl</sub> and ParB<sub>mtu</sub>; however the corresponding stretch of amino acids is aliphatic (Fig. S1). Thus, the entire motif might be necessary for interaction with DivIVA. As ParB<sub>sco</sub> can bind the *parS* site in the native *parB*<sub>sco</sub> coding sequence, reduced cytoplasmic diffusion of ParB<sub>sco</sub>

## Results

---

may perturb interaction with DivIVA<sub>SCO</sub>. Therefore, interaction between ParB<sub>SCO</sub> and DivIVA<sub>SCO</sub> was also assayed in a LexA bacterial two-hybrid (Fig. 2.5 D). Together, in both *M. tuberculosis* and *S. coelicolor*, ParB interacts with and is recruited by DivIVA, providing evidence for a possible role in chromosome organization and / or polar anchoring of the origins.

### ParA interacts with both ParB and DivIVA

In *C. glutamicum*, the interaction between ParB and DivIVA could be sufficient to anchor the newly replicated origins at the cell poles, but only if the ParB bound origin is in the vicinity of the cell pole. In the absence of a “motor protein” the duplicated origin is probably not delivered to the cell pole. Thus, if the ParB bound origins are not directed to the cell poles, then polar tethering of the origins cannot occur. In *V. cholerae*, interaction of ParA with an as-of-yet unidentified polar factor has been speculated to hold the origins at the cell poles (Fogel and Waldor, 2006). In *C. glutamicum*, ParA forms foci localized at the cell poles. This localization pattern is reminiscent of the ParB-oriC nucleoprotein localization and a potential interaction between ParA and ParB has been demonstrated by a bacterial two-hybrid analysis (Fig. 1.5). It seems likely that polar positioned ParA is interacting with ParB, however it is not clear if ParA aids polar anchoring via direct interaction with DivIVA. Thus, it could be postulated that ParA is involved, either directly or indirectly, in tethering the origins to the cell poles.

In *C. glutamicum*, the N-terminal stretch of basic amino acids of ParB is necessary for interaction with DivIVA. In *B. subtilis*, this region of ParB interacts with and stimulates the ATPase activity of ParA (Scholefield *et al.*, 2012). On the other hand, the C-terminal of ParB is required for interaction with ParA in *Pseudomonas aeruginosa* (Bartosik *et al.*, 2004). To test which region of *C. glutamicum* ParB might be necessary for interaction with ParA, co-elution experiments were carried out. To this end, the cleared cell lysate of an *E. coli* strain expressing Strep-ParA was incubated with purified His<sub>10</sub>-ParB, His<sub>10</sub>-ParB $\Delta$ C50, His<sub>10</sub>-ParB $\Delta$ N20, His<sub>10</sub>-ParB $\Delta$ N21 or His<sub>10</sub>-ParBR21A. Thereby, His<sub>10</sub>-ParB, (and the ParB mutant variants) was bound to a Ni-NTA matrix, washed extensively to remove any unbound protein, followed by incubation with Strep-ParA and again washing extensively before elution of interacting complexes. In all cases tested, Strep-ParA bound to and co-eluted with ParB and the mutant variants (Fig. 2.11 A). Although this shows that ParA and ParB interact directly *in vitro*, it does not give any information about the potential interact site. This approach is relatively crude and may not reflect the *in vivo* situation. In addition, it might be more informative to determine if a particular domain of ParB can stimulate ATP hydrolysis of ParA.

## Results

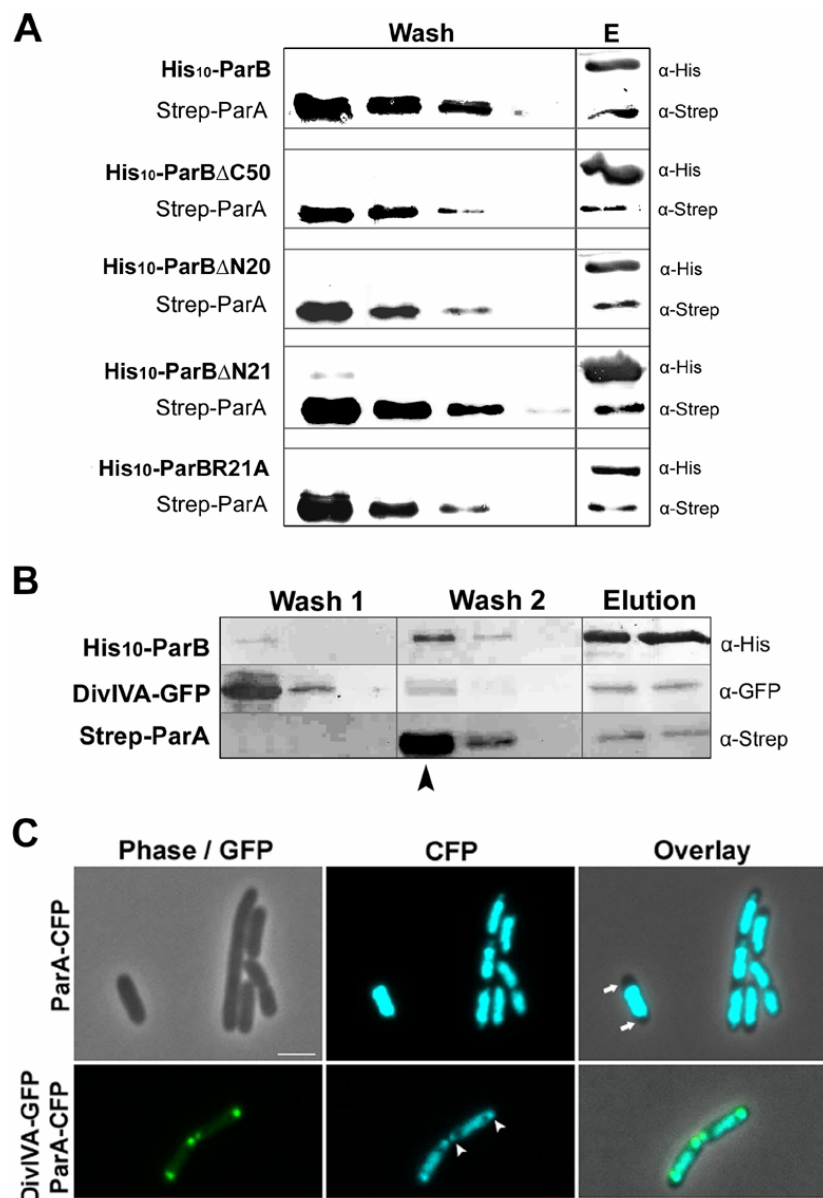


**Figure 2.11. ParA interacts with both ParB and DivIVA.** (A) Co-elution assays demonstrate that ParA and ParB interact, *in vitro*. Purified His<sub>10</sub>-ParB and mutant variants, as indicated in bold on the left, were immobilized on a Ni-NTA resin. The cleared cell lysate of an *E. coli* strain expressing Strep-ParA was incubated with the immobilized His<sub>10</sub>-ParB. Stringent wash steps remove unbound Strep-ParA (Wash). Interacting protein complexes were co-eluted (E) and analyzed by immunoblot. His<sub>10</sub>-ParB was detected with  $\alpha$ -Penta-His antibody and Strep-ParA was detected with  $\alpha$ -Strep antibody, as indicated on the right. (B) ParB interacts simultaneously with ParA and DivIVA, *in vitro*. His<sub>10</sub>-ParB bound to a Ni-NTA resin was incubated with DivIVA-GFP, followed by incubation with Strep-ParA. Again, unbound protein was removed by numerous wash steps. Wash 1 show the removal of unbound DivIVA-GFP and Wash 2 shows the removal of unbound Step-ParA. Note that all unbound protein was removed prior to incubation with the next protein. During the wash steps to remove unbound Strep-ParA, both His<sub>10</sub>-ParB and DivIVA-GFP were also removed (arrowhead). (C) Expression of ParA-CFP and DivIVA-GFP in *E. coli*. ParA-CFP localizes to the nucleoid, when expressed individually in *E. coli* (upper panel). Upon co-expression with DivIVA-GFP some ParA-CFP is recruited to the cell pole (lower panel, arrowheads). Note that in the absence of DivIVA-GFP, the poles are devoid of ParA-CFP (arrows). Scale bar, 2  $\mu$ m.

## Results

---

To determine if ParA can interact directly with DivIVA *in vivo*, in the absence of ParB, expression in the synthetic *E. coli* system was employed. ParA-CFP expressed from a pET-DUET vector localized exclusively to the nucleoid, when expressed alone in *E. coli*. In general, ParA proteins exhibit non-specific DNA binding activity, which can often depend on protein concentration or the nucleotide bound form of ParA (Hester and Lutkenhaus, 2007). Expression of ParA-CFP in combination with DivIVA-GFP in *E. coli* resulted in partial polar recruitment of ParA. However, ParA remained mostly bound to the nucleoid (Fig.2.11 C). It was speculated that in the absence of ParB the nucleotide bound state and activity of ParA is not regulated and thus, ParA remains mostly bound to the nucleoid. It was assumed that interaction of ParA with DivIVA might depend on the regulatory activities of ParB. Subsequently, ParB lacking a fluorescent tag, expressed from a pET derivative vector was co-expressed with ParA-CFP and DivIVA-GFP. However, the localization pattern of ParA was not altered (data not shown). Nevertheless, it seems that ParA can interact with DivIVA.

The *in vivo* and *in vitro* results indicated that ParA can interact with ParB and also DivIVA. Similarly, ParB can also interact with both ParA and DivIVA. We wanted to determine if ParB can interact simultaneously with both proteins. Again, a co-elution approach was employed. Thereby, purified His<sub>10</sub>-ParB was incubated with Ni-NTA resin, then incubated with DivIVA-GFP and finally incubated with Strep-ParA. Extensive wash steps removed unbound protein prior to incubation with the next protein. The Ni-NTA resin was washed until no protein was detected on an immunoblot. Interestingly, both DivIVA-GFP and Strep-ParA co-eluted with His<sub>10</sub>-ParB (Fig. 2.11 B). However, during the wash step to remove unbound Strep-ParA, some His<sub>10</sub>-ParB and DivIVA-GFP was also removed. Thus, it appears that ParA can interact with DivIVA-GFP and His<sub>10</sub>-ParB. In a reciprocal approach, whereby immobilized His<sub>10</sub>-ParB was incubated with Strep-ParA followed by incubation with DivIVA-GFP, a similar result was obtained (data not shown). Although not conclusive, these results indicate that ParA and ParB interact with each other and with DivIVA, and ParA, together with ParB, might play a role in tethering the origin at the cell poles through interaction with DivIVA.

### 2.3 Chromosome organization influences cell growth and division site selection

In the absence of *parA* or *parB* the subcellular organization of the *C. glutamicum* chromosome is perturbed. In addition, under certain growth conditions, the growth rate of these mutants is also severely reduced. It was reasoned that anchoring of the ParB bound origin to the cell pole could influence apical growth. This assumption was based on the interaction between ParB and the polar growth determinant DivIVA, and also the lack of polar cell growth in the *parB* deletion mutant. While growth of *C. glutamicum* cell cultures has been characterized in great detail, growth at the single cell level has not been analyzed. Therefore, to analyze growth of *C. glutamicum* cells at the single cell level a microfluidic chamber was used for live cell imaging (Fig. 2.12). This system provides cells with a continuous supply of nutrients. In addition, the chamber is designed to hold cells at a single focal plane, allowing tracking of single cells over multiple generations. To unambiguously define the cell

## Results

poles and division septum, we made use of a DivIVA-mCHERRY expressing strain, where expression is under the control of the native promoter. Growth of the DivIVA-mCHERRY strains (referred to as wild type) was compared to the *parA* / *parB* mutant strains, in the DivIVA-mCHERRY background. All strains were pre-cultured in BHI medium. Cells were diluted to OD<sub>600</sub> 0.005 – 0.010 prior to loading the microfluidic chamber. Live cell imaging was carried out at 30°C and images were acquired every 5 minutes.

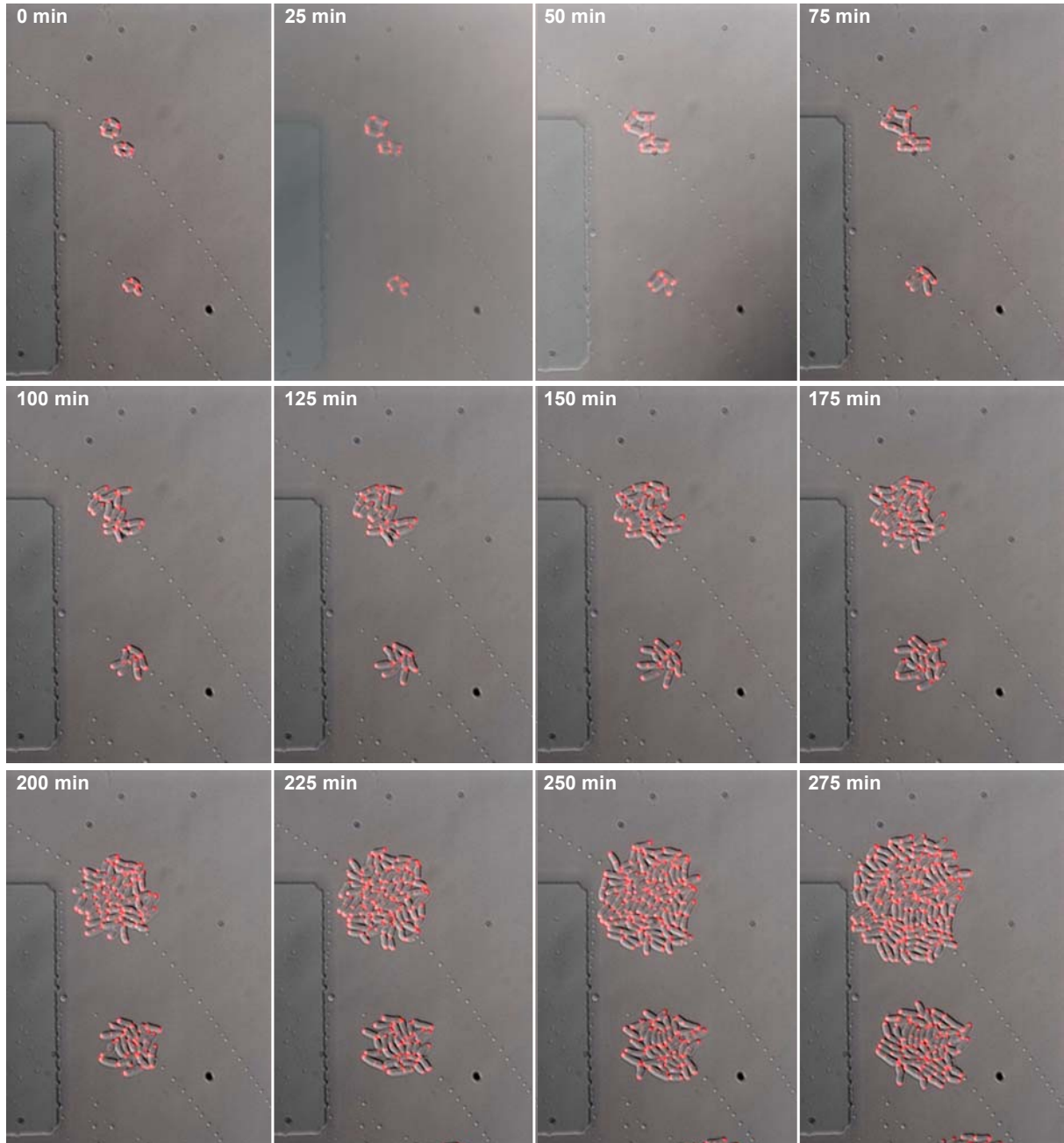


**Figure 2.12: Growth of *C. glutamicum* DivIVA-mCHERRY in a microfluidic chamber.** Prior to time lapse analysis, cells were loaded onto a microfluidic chamber at an OD<sub>600</sub>-0.005-0.01. During the time lapse cells were grown in BHI at 30°C. Images were acquired every 5 minutes. Shown is a selection of images, taken at 25 minute intervals, as indicated. Note the formation of microcolonies.

## Results

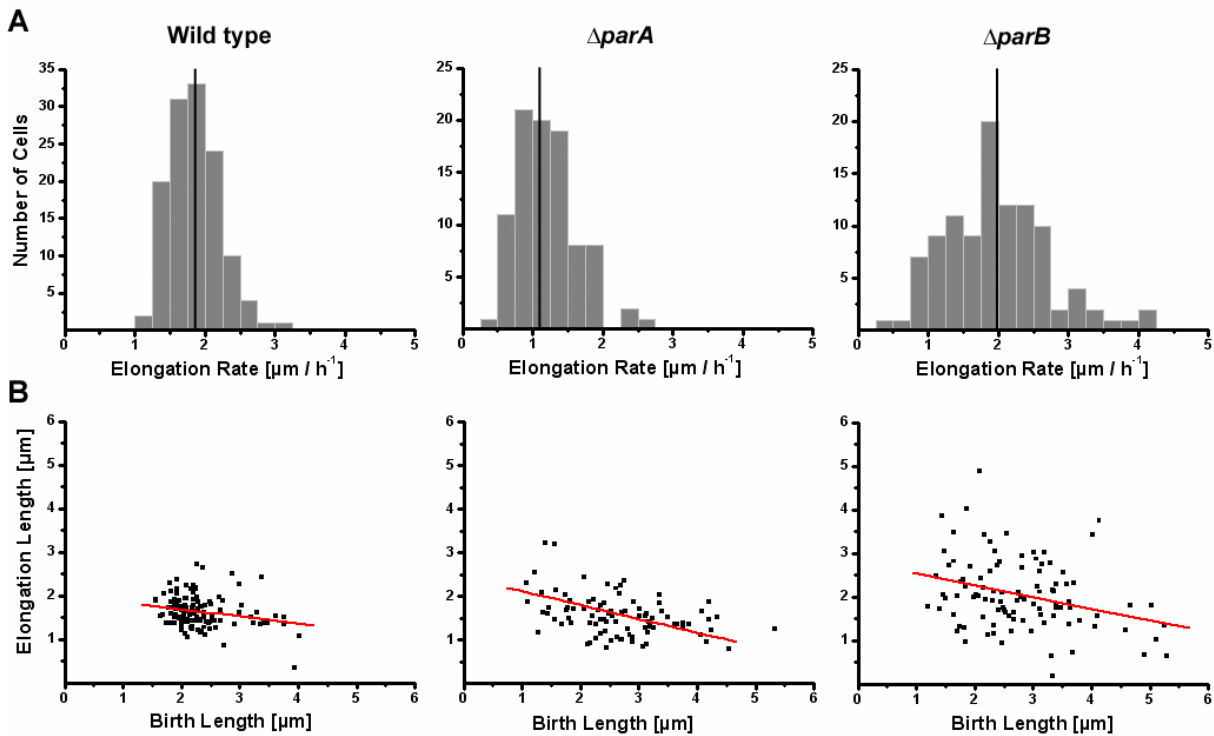


**Figure 2.13: Chromosome disorganization leads to altered cell growth in *C. glutamicum*.** (A) Distribution of elongation rates of wild type,  $\Delta parA$  and  $\Delta parB$  mutant cells. Average elongation rates are indicated by the black line. (B) In wild type cells the birth length and elongation length are relatively constant. In the absence of *parA* or *parB*, there is no correlation between the length of the cell at birth and the cell length before division. Negative correlation between birth and elongation lengths has been previously shown to indicate a size-based cell cycle regulatory mechanism (red line).

Growth of wild type and mutant cells was assessed by measuring the rate of growth in terms of increase in cell length directly after a division event (cell birth) until directly before the next division event. In wild type cells, the elongation rate of most cells is in the range of 1.5 to 2.5  $\mu\text{m} / \text{h}$ , averaging at 1.8  $\mu\text{m} / \text{h}$  (Fig. 2.13 A). In contrast, the elongation rate of cells lacking *parA* or *parB* exhibited much more variability (Fig. 2.13 A). In the absence of *parA*, the rate of cell growth was slightly reduced, while cells lacking *parB* exhibited enormous variability, ranging from less than 0.5  $\mu\text{m} / \text{h}$  to greater than 4  $\mu\text{m} / \text{h}$ . This variability might be due to differing cell lengths at birth and thus give rise to increased or decreased elongation rate. Therefore, the association between birth length and elongation length was measured. In wild type cells there is a high degree of correlation between birth length and elongation rate. The majority of cells have a birth length ranging from 1.5 to 2.5  $\mu\text{m}$  which elongate to a length ranging from 1 to 2.5  $\mu\text{m}$  (Fig. 2.13 B). Thus, wild type cells retain a relatively constant size both at birth and prior to division. The situation is very different in the absence of *parA* or *parB*. In these mutant cells the length of the cell at birth varies greatly and shows little or no correlation with elongation length, giving rise to a population of cells that is extremely heterogeneous in size and elongation rates (Fig. 2.13 B).

## Results

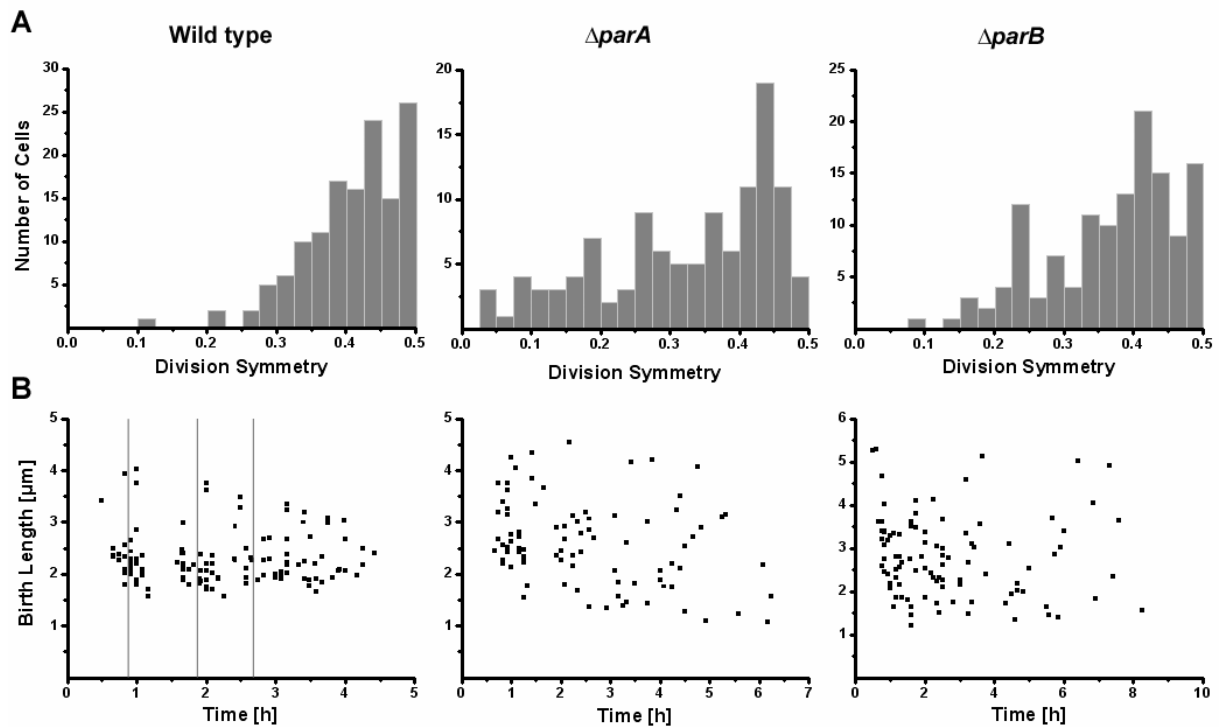


**Figure 2.14: Chromosome miss-organization leads to altered division site placement in *C. glutamicum*.** (A) Distribution of division site placement in wild type,  $\Delta parA$  and  $\Delta parB$  cells. (B) Timing of birth events in wild type,  $\Delta parA$  and  $\Delta parB$  cells. In wild type cells, division occurs at regular intervals, after which a microcolony is formed (grey lines).

The discrepancy of cell length at birth between wild type and *par* mutant cells would suggest that the placement of the divisome is also altered in the *parA* and *parB* mutant strains. Rod-shaped bacteria, such as *E. coli* and *B. subtilis* use regulatory systems, the Min and Noc system, to position the division machinery precisely at midcell. The site of division in wild type *C. glutamicum* cells is not always positioned precisely at midcell. As *C. glutamicum* lacks homologues of the conventional regulatory systems and no other positive or negative regulation of cell division are presently known, we speculated that the subcellular organization of the chromosome might influence division site selection. On a single cell level, division in *C. glutamicum* cells was assessed in terms of division symmetry and timing of birth events. As to be expected, we found that the placement of the division site was not always precisely at midcell in wild type cells, however some regulatory mechanism must exist because in the vast majority of cells division normally occurs in the region between the 1/3 and 2/3 positions of the cell. In the majority of cells, division is restricted to the midcell region in wild type cells (Fig. 2.14 A). However, in the absence of *parA* or *parB*, the placement of the division site varied greatly (Fig 2.14 A). In these mutants the frequency of polar cell division is drastically increased, frequently giving rise to nonviable cells. Tracking division events over a number of generations revealed that division close to the cell poles often occurred repeatedly at the same pole. In almost

## Results

every cell lineage analyzed, in particular in the case of the *parA* mutant, extreme asymmetric division was observed.

In wild type cells, the birth length and elongation rate are relatively constant. Thus, starting from a single cell this would suggest that the timing of birth events would also be relatively synchronous. Indeed, at least for a number of generations, the timing of division events occurs within a defined time window (Fig 2.14 B). It should be pointed out that after some time a microcolony is formed, and in these microcolonies nutrient availability and growth are altered. Thus, it is difficult to compare growth of single cells with that of microcolonies. However, cells lacking *parA* or *parB* have more variable birth lengths and elongation rates, which is also reflected in random timing of birth events (Fig. 2.14 B). Taken together these results strongly indicate that alterations in chromosome organization, as a result of *parA* or *parB* mutation, directly influence apical cell growth and division site placement in *C. glutamicum*.

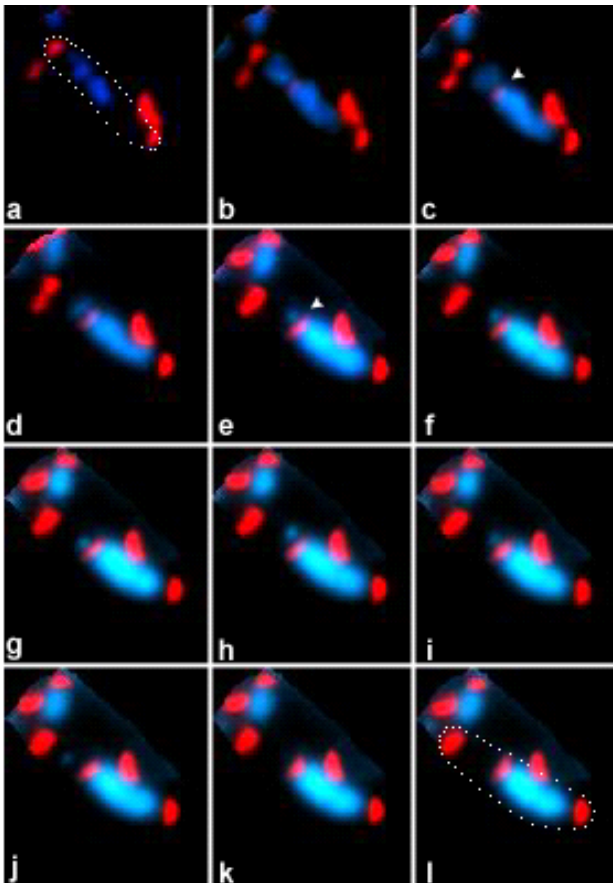


**Figure 2.15: In the absence of *parB*, division occurs over the nucleoid, guillotining part of the chromosome.**

Shown is a time lapse series of DivIVA-mCHERRY expressing cell in the absence of *parB*. Images were acquired every 5 minutes. In frame (a) and (l) the cells are outlined. DNA is stained with Hoechst (blue) and DivIVA-mCHERRY is shown in red. In frame (c) DivIVA-mCHERRY begins to appear at the division septum (arrowhead). Note that the septum forms over the chromosome. The chromosome is pumped in one direction. In frame (e), the division septum constricts, guillotining part of the chromosome (arrowhead).

A major advantage of the microfluidic chamber is that medium can be changed during an experiment. This allowed us to stain growing cells with Hoechst DNA stain and analyze division events in cells lacking *parA* and *parB*. It should be noted that Hoechst DNA stain is slightly toxic for the cells. Additionally, we observed that *C. glutamicum* cells do not grow when exposed to light that is close to the UV range. However, this approach allowed us to get a glimpse at the organization of the

## Results

---

chromosome and determine what happens during cells division. As shown in figure 2.15, we observed cells where the division septum formed and constricted over the nucleoid. Interestingly, we also observed that the DNA was pumped in one direction when the septum started constricting. Normally, DNA translocases, such as FtsK in *E. coli*, coordinate the late stages of cytokinesis and chromosome segregation ensuring that DNA does not get trapped in the inward growing septum. These results show that *C. glutamicum* cells lack a Noc system. Additionally, in cell lacking *parB* the DNA is not always pumped into each daughter cell. It could be speculated that DNA translocases require the *oriC* to be attached to the cell poles. Alternatively, it might be due to the gross disorganization of the chromosome in the absence of *parA* or *parB*.

### 2.4 Characterization of the orphan ParA-like protein, PldP

Although the genome of *C. glutamicum* encodes two ParA proteins, the *in vivo* data presented above demonstrates that each ParA protein fulfills a different role. Based on the *in vivo* localization and phenotype of *pldP*, it appears that the main role of this protein is in cell division and not chromosome segregation. However, our current knowledge of cell division in *C. glutamicum* is very limited, and therefore also how PldP might function in cell division. To address the role of PldP, we began by analyzing PldP, *in vivo* and *in vitro*.

#### PldP exists as a monomer in solution

PldP, containing an N-terminal His<sub>10</sub>-tag fusion, was heterologously overexpressed in *E. coli* BL21(DE3) pLysS cells. Expression of His<sub>10</sub>-PldP was induced with 1mM IPTG, 37°C for 4 hours. Expressing cells were harvested and resuspended in buffer P (50 mM Tris-HCl, pH 7.5, 300 mM NaCl, 10 % glycerol, 1 mM DTT and 10 mM imidazole), supplemented with DNase and protease inhibitor. Cells were disrupted by three passes through a French Press. The cleared cell lysate was loaded onto a 1 ml HisTrap™ FF column, washed with 10 column volumes of buffer A and subsequently eluted by a step gradient of buffer P supplemented with 250 mM imidazole. The affinity purified His<sub>10</sub>-PldP was applied to a Superdex™ 200 10/300 gel filtration column. The predicated molecular weight of His<sub>10</sub>-PldP is approximately 33 kDa. According to the gel filtration elution profile, PldP exists as a monomer in solution (Fig. 2.16 B).

## Results

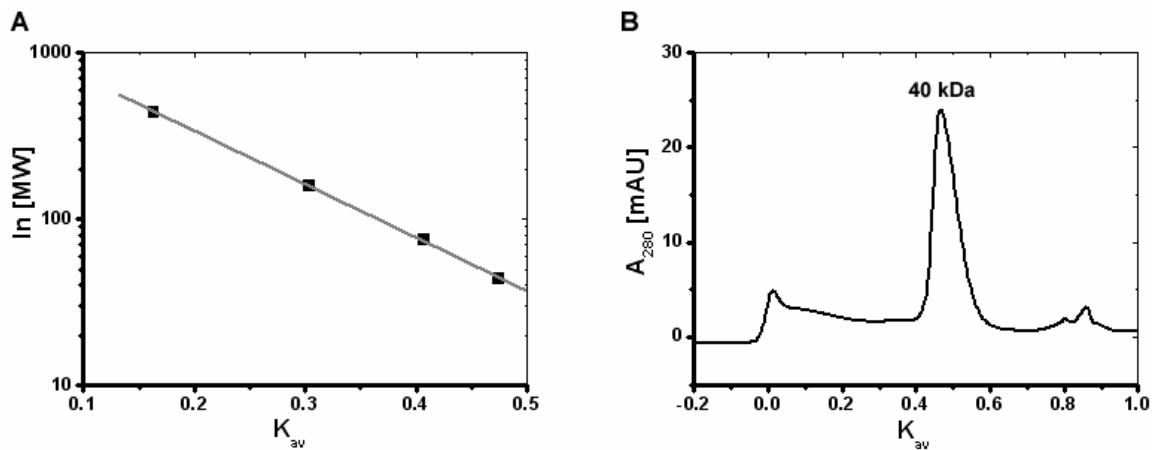


**Figure 2.16: His<sub>10</sub>-PldP exists as a monomer in solution.** (A) Calibration of Superdex™ 200 10/300 gel filtration column with standards - ferritin (440 kDa), aldolase (158 kDa), conalbumin (75 kDa) and ovalbumin (43 kDa) in 50 mM Tris, 200 mM NaCl, pH 7.9. (B) Elution profile of His<sub>10</sub>-PldP. His<sub>10</sub>-PldP elutes at a  $K_{av}$  of 0.47 which corresponds to a molecular weight of 40 kDa.

### PldP binds membranes via a putative C-terminal amphipathic helix

PldP is distantly related to the division site selection protein MinD. A short stretch of the C-terminal of MinD forms an amphipathic  $\alpha$ -helix which targets it to the membrane (Szeto *et al.*, 2002; Hu and Lutkenhaus, 2003). The *in vivo* localization data suggests that PldP is recruited to the membrane. Interestingly, the C-terminal of PldP (amino acids 270-290) is predicted to be amphipathic in nature. Thus, similar to MinD, it was speculated that PldP binds the membrane by insertion of the hydrophobic face of the amphipathic helix into the lipid bilayer.

The membrane-binding potential of PldP was tested in *E. coli* cells expressing a His<sub>10</sub>-PldP variant. In this experiment a number of centrifugation steps is used to determine which cell fraction is occupied by PldP. Following each centrifugation step, the supernatant is removed and the pellet is resuspended in an equal volume of buffer. Samples of both supernatant and pellet were applied to an SDS-PAGE for analysis. The first step entailed a “low speed centrifugation” step which removes protein aggregates or unfolded His<sub>10</sub>-PldP (Fig. 2.17 A). As PldP was found mostly in the supernatant, with only some PldP in the pellet fraction, PldP is not forming inclusion bodies. Next, a “high speed centrifugation step” was employed to isolate the cell membranes. Thereby, the supernatant from the first step was centrifuged at 200,000  $g$  for 1 hour at 4°C. PldP was found in the pellet fraction indicating that it is associated to the membrane (Fig. 2.17 A). If PldP is associated with the membrane, then detergent should solubilize PldP from the membrane. To test this, 1 % DDM was added to the resuspended pellet, which was then mixed for 30 minutes at 4°C and subsequently centrifuged again at 200,000  $g$  for 1 hour at 4°C. Interestingly, the majority of PldP was found in the supernatant indicating that addition of 1 % DDM could partially solubilize PldP and thus, PldP might be a membrane associated protein.

## Results

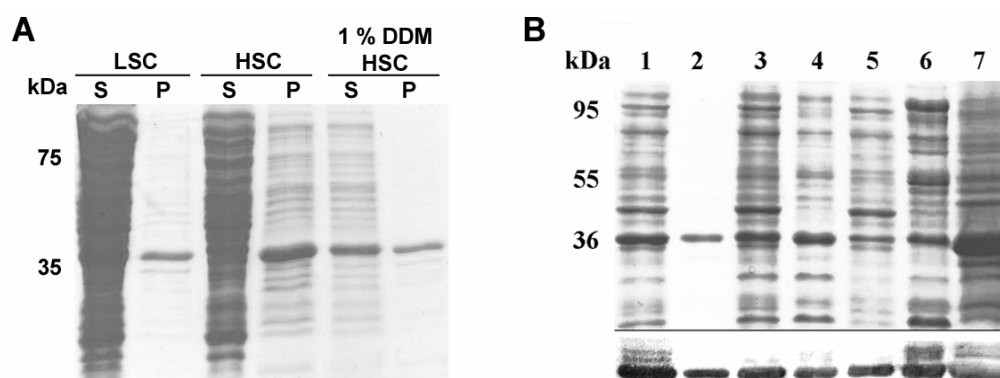


**Figure 2.17: PldP is a membrane associated protein.** (A) A spin-down assay was employed to determine if PldP is associated to membranes. LSC – low speed centrifugation and HSC – high speed centrifugation, S – supernatant and P – pellet. (B) Na<sub>2</sub>CO<sub>3</sub> extraction of PldP. Shown are a coomassie stained SDS gel (top) and detection of His<sub>10</sub>-PldP by immunoblot using  $\alpha$ -Penta-His antibodies (bottom). 1, supernatant after 4,000 g centrifugation, 2, pellet after 10,000 g centrifugation, 3, supernatant after 10,000 g centrifugation, 4, pellet after 204,000 g centrifugation, 5, supernatant after 204,000 g centrifugation, 6, supernatant after Na<sub>2</sub>CO<sub>3</sub> treatment, 7, pellet after Na<sub>2</sub>CO<sub>3</sub> treatment.

To show that PldP associates to the membrane, as opposed to being a membrane integral protein, carbonate extractions were carried out (Fig. 2.17 B) (Renfordt, 2011). Similar to above, His<sub>10</sub>-PldP was heterologously expressed in *E. coli* cells. After removal of cell debris and inclusion bodies, the membranes were isolated and treated with 100 mM Na<sub>2</sub>CO<sub>3</sub> at 4°C. In the presence of Na<sub>2</sub>CO<sub>3</sub> integral membrane proteins remain intact in the membrane while associated proteins are removed. Subsequent to Na<sub>2</sub>CO<sub>3</sub> treatment, the membranes were isolated again. Although PldP was always found to be enriched in the supernatant, indicating that PldP is associated to the membrane, a small fraction of PldP was always found in the pellet fraction. However, Na<sub>2</sub>CO<sub>3</sub> does not extract integral membrane proteins. Together, these *in vitro* results in combination with the *in vivo* localization, strongly suggest that PldP is a membrane associated protein.

### ***In vivo*, PldP binds to the membrane**

To clarify that PldP can associate to the membrane in *C. glutamicum* cells, the localization of PldP was revisited. Thereby, PldP-eCFP was expressed from an ectopic locus in the *pldP* mutant background. The *adhA* (alcohol dehydrogenase) locus was chosen for ectopic integration as it was reasoned that integration at this site could be selected for by lack of growth on ethanol plates. Therefore, homologous sequences of *adhA* were cloned into the pK18mob vector. PldP-eCFP and the upstream promoter region of PldP was cloned into the region between the *adhA* sites on the pK18mob vector. This vector was subsequently transformed into the *pldP* mutant strain background. From microscopic analysis it was clear that ectopic expression of PldP could complement the phenotype of the deletion mutant (Fig. 2.18). Cell lengths were comparable to wild type cells and no anucleate cells were observed.

## Results

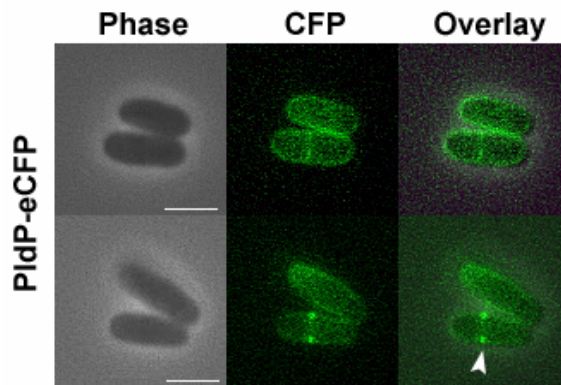


**Figure 2.18:** In *C. glutamicum* PldP-eCFP expressed from an ectopic locus complements the *pldP* mutant phenotype and PldP-eCFP is recruited to the membrane and forms foci at the site of division. PldP-eCFP was expressed from the native promoter at the *adhA* locus. Shown are the localization patterns of unfixed PldP-eCFP cells. Scale bar, 2  $\mu$ m.

We previously observed that the expression of PldP is relatively low and microscopic analysis the PldP-CFP translation fusion proved problematic due to relatively long exposure times and relatively high background fluorescence (Fig. 2.3). Using an enhance CFP to determine the localization, we found that PldP was recruited to the membrane (Fig. 2.18). However, when cells expressing PldP-eCFP were fixed on an agarose pad, PldP-eCFP was mostly bound to the nucleoid (data not shown). PldP-eCFP was still seen as foci at the site of division. It was previously shown that alteration in membrane potential can greatly alter protein localization (Strahl and Hamoen, 2010). Although it remains to be tested if the membrane potential does indeed alter the localization of PldP-eCFP, these results demonstrate that PldP can associate to the *C. glutamicum* membrane, and under certain conditions PldP can bind DNA.

### Identification of potential PldP interaction partners

The evidence so far indications that PldP is primarily involved in cell division. From the *in vivo* localization it appears that PldP could be recruited relatively early to the division site (Fig. 2.3). Apart from the essential cell division protein, such as FtsZ, we do not know how PldP could function in cell division. In an attempt to gain a better insight into the role of PldP, and also identify potential proteins involved in cytokinesis, pull-down assays were carried out (Renfordt, 2011). Thereby, purified His<sub>10</sub>-PldP was used as bait to isolate interacting partners from either whole cell lysate, cytoplasmic or the membrane fraction of *C. glutamicum* cells. His<sub>10</sub>-PldP, and bound interaction partners, was subsequently affinity purified using Ni-NTA resin. Eluted fraction containing potential interacting protein complexes were applied to an SDS-PAGE. Co-eluted protein complexes were analyzed by mass spectrometry. Unspecific interaction with the Ni-NTA matrix was ruled out by incubation with the cleared cell lysate with the matrix. Also, abundant cellular proteins that might interact unspecifically were excluded by carrying out the pull down assay with an unrelated protein (His<sub>10</sub>-AlpC). Using this approach a number of potential interaction partners could be identified. Three proteins were found to always co-elute with PldP, namely glycyl-tRNA synthetase, S-adenosyl-L-homocysteine hydrolase and

## Results

aspartate ammonia-lyase (Table 2.2). The score of these three proteins is relatively high, indicating that the degree of confidence of the mass spectrometry is high. A number of other proteins were identified, however the score was relatively low and they were not always pulled-down from the different cell fractions. Interestingly, ParA consistently co-eluted with PldP. Although the score is very low, previous data has shown that ParA and PldP might interact (Fig 1.5).

**Table 2.2: Summary of potential PldP interaction partners.**

Protein	Cg number	Abbreviation	Score
<b>Whole Cell Lysate</b>			
Glycyl-tRNA synthetase	Cg2499	GlyS	801.4
S-adenosyl-L-homocysteine hydrolase	Cg0860	SahH	433
Aspartate ammonia-lyase	Cg1697	AspA	419.4
Inosine-5'-monophosphate dehydrogenase	Cg0699	GauB2	215.9
Chromosome segregation ATPase	Cg3427	ParA	141.2
<b>Cytoplasmic Fraction</b>			
Glycyl-tRNA synthetase	Cg2499	GlyS	1339.8
Aspartate ammonia-lyase	Cg1697	AspA	425.9
S-adenosyl-L-homocysteine hydrolase	Cg0860	SahH	407.9
Elongation factor G	Cg0583	FusA	240.7
ABC-type transporter	Cg0736		152.5
Dihydroliipoamide dehydrogenase	Cg0441	Lpd	131.6
NAD dependent Aldehyde dehydrogenase	Cg0635		86.5
Chromosome segregation ATPase	Cg3427	ParA	82.9

From a first glance, most of the proteins that co-eluted with PldP would not be assumed to be directly involved in cell division. An interaction between ParA and PldP has been addressed in a bacterial two-hybrid (Fig. 1.5). In an attempt to begin validating these proteins as PldP interaction partners, one of the co-eluted proteins was analyzed in more detail (Renford, 2011). To begin with, we wanted to determine if SahH and PldP occupy similar subcellular positions. Subsequently, SahH-eCFP was extra-chromosomally expressed from a pEKEX2 plasmid. Expression of SahH-eCFP was induced with 1 mM IPTG and cells were grown in LB medium. SahH-eCFP exhibited a diffuse cytoplasmic localization (Fig. 2.19). Although the microscopic analysis would suggest that SahH-eCFP and PldP occupy different subcellular positions, overexpression of SahH also resulted in growth from ectopic sites and low frequency anucleate cell production (Fig. 2.19). Although branching was only observed in a low number of cells, anucleate cell production was similar to that of the *pldP* deletion mutant, approximately 0.75 %. However, further analysis is required to determine the underlying reason for ectopic branching, and also to confirm that SahH, together with PldP, plays a role in cell division.

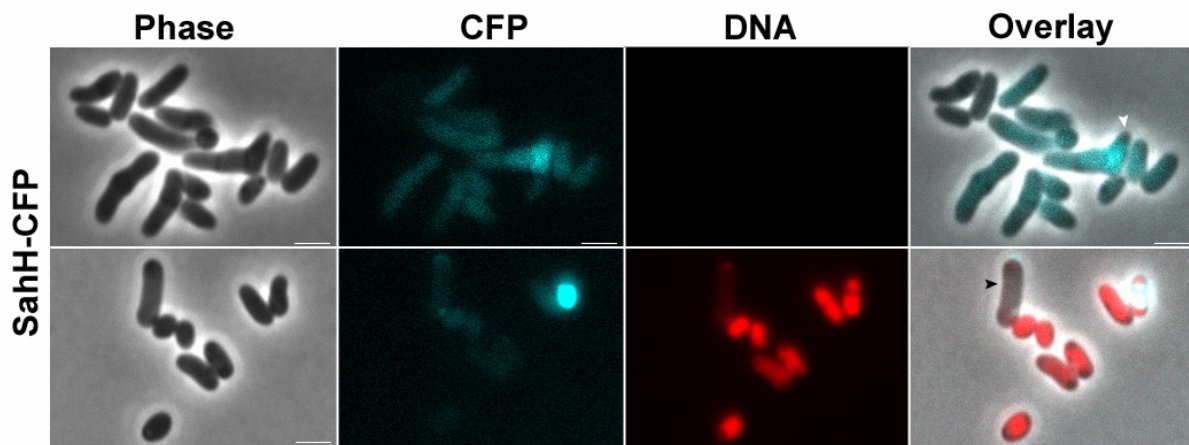


**Figure 2.19: Subcellular localization and overexpression phenotype of SahH-CFP.** SahH-CFP was expressed from a pEKEX2 plasmid, induced with 1 mM IPTG. SahH-CFP exhibits a diffuse cytoplasmic localization in *C. glutamicum*. Overexpression of SahH-CFP results in growth from ectopic sites (top, arrowhead). Additionally, in cells overexpressing SahH-CFP, 0.75 % of cells lack DNA (bottom, arrowhead). Shown are phase contrast (Phase), CFP fluorescence (CFP), DNA stain with Sytox Red (DNA) and an overlay (right). Scale bar, 2  $\mu$ m.

### Chapter II A prophage encoded cytoskeleton protein

AlpC is a novel actin-like protein encoded on the *C. glutamicum* CGP3 prophage. Although AlpC contains the conserved actin signature motifs (Fig 1.7), it is not clear if AlpC shares similar properties to other actin homologues and related proteins, such as *in vivo* filament assembly and dynamics or nucleotide hydrolysis. A large number of actin-like proteins have been identified recently (Derman *et al.*, 2009), but detailed studies have only been undertaken on actin-like proteins encoded on plasmids, revealing their involvement in plasmid segregation. The underlying mechanisms of these partitioning systems share similarities with type I and II segregation systems. The function of actin-like proteins encoded on chromosome integrated prophages has not been studied, to date. It could be speculated that, similar to plasmid encoded counterparts, prophages carry their own machinery for segregation of induced prophages. We began by attempting to answer two important questions; does AlpC share actin-like properties and what is the molecular role of AlpC?

#### 2.5 Does AlpC exhibit actin-like properties?

##### AlpC assembles into filaments, *in vivo*

One of the defining properties of actin and related cytoskeleton proteins is the ability to polymerize forming filamentous structures *in vivo*. In order to determine if the novel *C. glutamicum* actin-like protein shares this characteristic, the subcellular behavior of AlpC was analyzed. Consequently, AlpC-CFP was extra-chromosomally expressed from a pEKEX2 plasmid. Expression of AlpC-CFP was induced with 0.5 mM IPTG and cells were grown in LB medium. Similar to the recently studied Alp7A (Derman *et al.*, 2009), AlpC-CFP readily assembles into filamentous structures, *in vivo* (Fig. 2.20 A). In the majority of cells, AlpC-CFP assembled into numerous long and curved filaments. However, some cells contained either a combination of filaments and foci or only discrete foci. This localization pattern indicates that the AlpC filaments are dynamic. It is tempting to speculate that the foci represent the nucleation point from which the AlpC-CFP filaments elongate. In order to gain more insight into the distribution of the AlpC-CFP filaments within the cell, Z-stacks were carried out. As shown in figure 2.20 B, a number of long, curved filaments extending the length of the cell were observed, some filaments appearing to elongate along the cell membrane. Thus, similar actin and related cytoskeleton proteins AlpC can polymerize forming filamentous structures *in vivo*.

Mutations in the nucleotide binding pocket that eliminate nucleotide hydrolysis do not necessarily inhibit filament formation but can lead to reduced filament dynamics and subsequent stabilization of filaments that do not support plasmid partitioning (Garner *et al.*, 2004). Based on amino acid sequence alignments of actin and actin-like proteins, the conserved aspartic acids of AlpC of the phosphate 2 motif was identified (Fig 1.7). To begin investigating if ATP hydrolysis is a feature of AlpC

## Results

or if it is necessary for polymerization, an amino acid mutation was introduced that changes aspartic acid 301, located in the phosphate 2 sequence, to an alanine (AlpCD301A). This mutant protein, AlpCD301A, was subsequently fused to CFP and expressed extra-chromosomally from the pEKEX2 plasmid. Upon induction with 0.5 mM IPTG, filaments could be observed in some cells (Fig 2.20 A). However, the frequency of filament formation was greatly reduced compared to the wild type protein. The morphology of the AlpCD301A filaments differs from the wild type protein. Filaments were often at the membrane and some cells contained, what appeared to be, large aggregates often found near the cell pole.

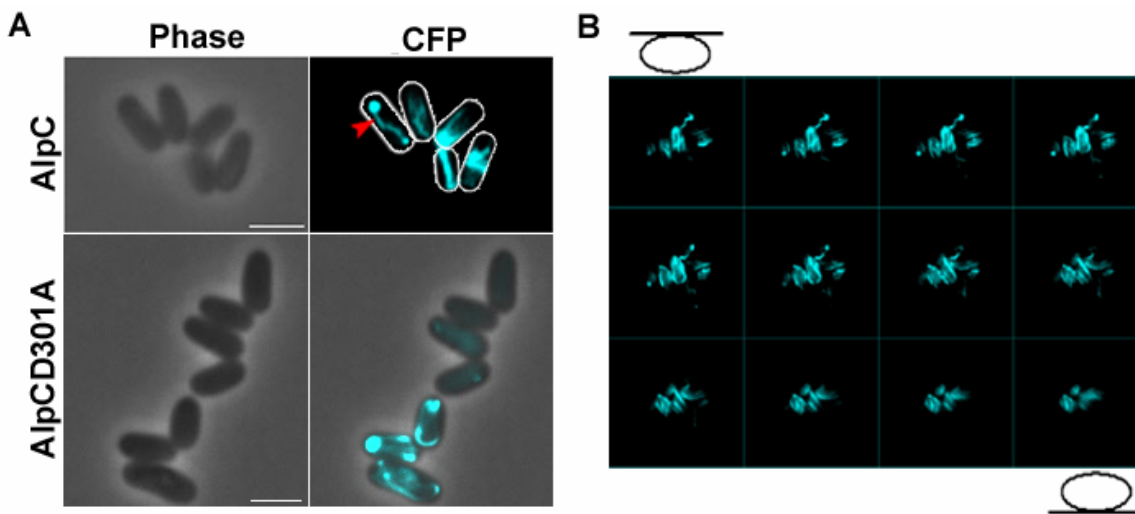


**Figure 2.20: In *C. glutamicum*, AlpC assembles into filaments.** (A) AlpC-CFP forms filaments when overexpressed in *C. glutamicum*. AlpC-CFP sometimes forms foci from which a filament appears to nucleate (upper panel, arrow). Mutation of the conserved aspartic acid of the phosphate 2 motif reduces assembly into filaments (lower panel). Filaments were often seen lining the cell membrane. (B) Z-stack analysis of the subcellular distribution of AlpC-CFP filaments shows that cells contain numerous filaments of various orientation, curvature and length. Images were acquired at different focal planes, as indicated by symbols. Scale bar, 2  $\mu$ m.

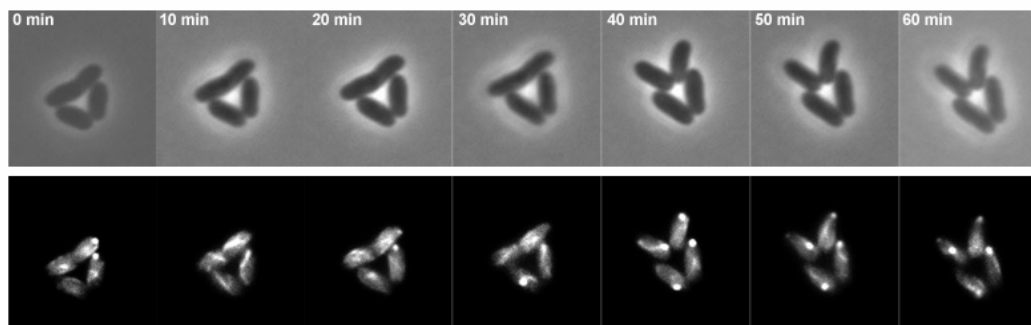


**Figure 2.21: Dynamics of AlpC filaments.** The dynamics of AlpC filaments was analyzed by time-lapse microscopy. Images were acquired every 10 minutes. AlpC assembles into filaments, which disassemble into compact foci. Shown is phase contrast (top) and CFP fluorescence (bottom).

### AlpC filament dynamics

*In vivo*, filaments assembled from ParM subunits are extremely dynamic, undergoing bursts of rapid growth and catastrophic decay (Garner *et al.*, 2004). Although such instability is not a distinguishing feature of actin and actin-like proteins, filament dynamics is essential for protein function. The subcellular localization and behavior of AlpC-CFP expressed from a pEKEX2 plasmid suggests that AlpC could be dynamic. In an attempt to gain a better understanding of the dynamics of AlpC-CFP, time-lapse analysis was carried out. Images were acquired every 10 minutes. As shown in figure 2.21, AlpC filaments are dynamic, often assembling into filaments followed by disassembling into a compact focus.

### AlpC exists as a monodisperse species in solution

The *C. glutamicum* AlpC protein was characterized further, *in vitro*. Thereby, AlpC and AlpCD301A were heterologously expressed and purified. The His<sub>10</sub>-tagged proteins were heterologously overexpressed in BL21(DE3) pLysS cells, induced with 0.4 mM IPTG and expressed at 20°C overnight. Higher expression temperature or inducer concentration resulted in the formation of mostly insoluble inclusion bodies. The recombinant protein was affinity purified using a 1 ml HisTrap™ FF column. At high concentrations, the affinity purified protein had a tendency to form thick gel-like slurry, probably as a consequence of concentration dependent polymerization. The affinity purified proteins were further applied to a Superdex™ 200 10/300 gel filtration column. The predicted molecular weight of His<sub>10</sub>-AlpC is 55 kDa. In the absence of nucleotide, AlpC eluted at an elution constant that corresponds to 74 kDa. An identical elution profile was observed for His<sub>10</sub>-AlpCD301A. Thus, both proteins elute as monodispersed species in solution (Fig. 2.22). The purity of the eluted fractions was analyzed by SDS-PAGE and immunoblotting.

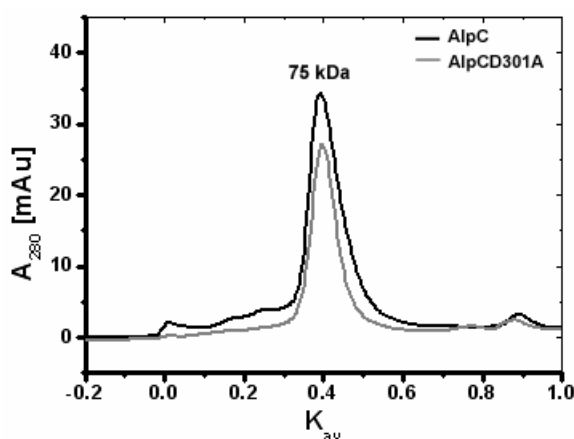


**Figure 2.22: AlpC and AlpCD301A exist as monodisperse species in solution.** Affinity purified AlpC or AlpCD301A was applied to a Superdex™ 200 10/300 gel filtration column. Both proteins elute at a  $K_{av}$  corresponding to approximately 75 kDa.

### AlpC hydrolyzes both ATP and GTP

The dynamic properties of actin filaments depends on the proteins ability of catalyze nucleotide hydrolysis. Many members of the actin superfamily bind and hydrolyze both ATP and GTP (Becker *et al.*, 2006; Galkin *et al.*, 2009). Hydrolysis mutant variants of the plasmid partitioning protein, ParM, form static filaments that do not support plasmid segregation, demonstrating that filament dynamics is essential for the protein function (Garner *et al.*, 2004). The *in vivo* organization into filaments suggests that AlpC can bind and hydrolyze nucleotides. To test if phosphate release is accompanied by AlpC polymerization, a continuous regenerating activity assay was employed. In this assay ATP / GTP is regenerated from ADP / GDP by pyruvate kinase, using phosphoenolpyruvate (PEP) as a substrate (Renosto *et al.*, 1984). In this reaction, pyruvate kinase (PK) produces pyruvate, which, in turn, is reduced to lactate by the enzyme lactate dehydrogenase (LDH) and simultaneously depletes pyruvate's cosubstrate NADH. Depletion of NADH was measured by monitoring absorbance at 340 nm. The change in absorbance over time was used to calculate ATPase or GTPase activity under the initial constant substrate concentration.

The activity of 1  $\mu\text{M}$  of AlpC was assayed with increasing concentrations of ATP / GTP (Fig. 2.23 A-D). Similar to other characterized actin-like proteins, AlpC can hydrolyze both ATP and GTP, and exhibits Michaelis–Menten kinetics. In the presence of ATP, the maximum turnover rate is reached at slightly lower substrate concentrations compared to that of GTP. In the presence of GTP AlpC has a  $V_{\text{max}}$  of  $4.3 \mu\text{M Min}^{-1}$ , compared to  $3.74 \mu\text{M Min}^{-1}$  for ATP (Fig. 2.23 B and D). The measured  $K_m$  is relatively low and does not differ greatly between ATP and GTP,  $0.2 \mu\text{M}$  and  $0.43\mu\text{M}$ , respectively. However, *in vivo* ATP is much more abundant compared to GTP, and thus, ATP is the favored substrate.

In comparison, the mutant variant AlpCD301A that lacks the conserved aspartic acid of the phosphate 2 motif, is defective in nucleotide hydrolysis. Similarly, 1  $\mu\text{M}$  AlpCD301A was assayed with increasing nucleotide concentration (Fig. 2.23 A-D). Thus, the conserved aspartic acid residue of the phosphate 2 motif is essential for nucleotide hydrolysis.

### AlpC polymerization is nucleotide dependent, *in vitro*

To determine if AlpC requires nucleotides for polymerization, the purified protein was subjected to sedimentation assays (Fig. 2.23 E). Thereby, 4  $\mu\text{M}$  of purified protein was mixed with nucleotide in the presence or absence of magnesium and incubated at  $30^\circ\text{C}$  for 30 minutes. Polymerized protein was then separated from non-polymerized protein by centrifugation at 120, 000  $g$  for 10 minutes. Even though aggregated protein was removed by centrifugation prior to experimental setup, to rule out reformation of aggregates at  $30^\circ\text{C}$ , one preparation contained AlpC, only. In the absence of nucleotide, AlpC did not sediment, thus, protein aggregation can be ruled out. Upon addition of ATP or GFP, polymerized AlpC was found in the pellet fraction. AlpC polymerization is also dependent on the presence of  $\text{Mg}^{2+}$ . In principle, AlpCD301A polymerization behavior was similar to the wild type

## Results

protein. The AlpCD301A mutant protein was prone to aggregation and thus, some protein was lost in the initial step to remove aggregates. Consequently, the protein concentrations cannot be compared as most of the AlpCD301A protein was removed at the initial step. However, both AlpC and AlpCD301A exhibit nucleotide dependent polymerization behavior.

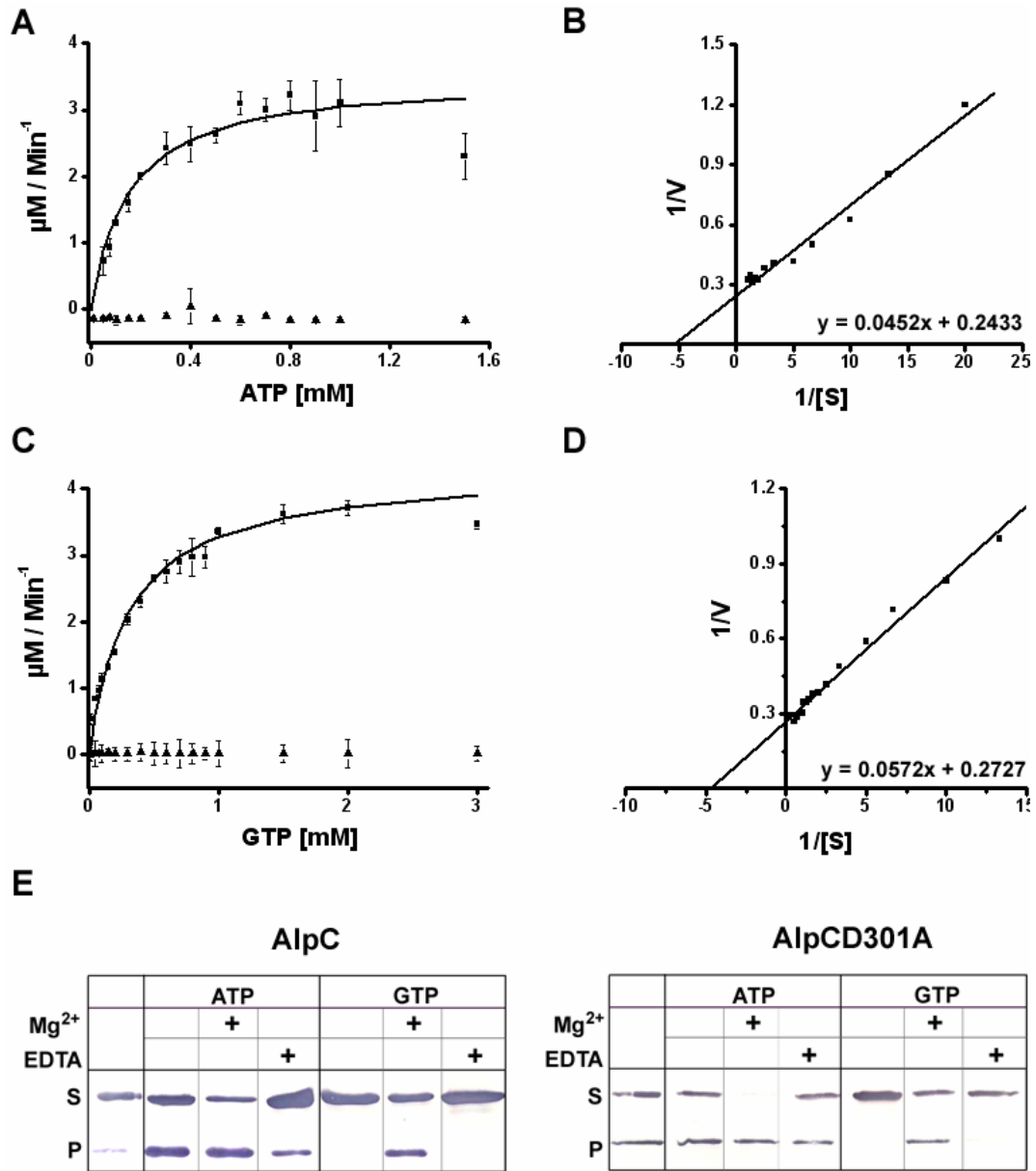


**Figure 2.23: AlpC catalyzes the hydrolysis of both ATP and GTP, *in vitro*.** AlpC exhibits both ATPase and GTPase activity. Shown is the turnover rate of 1  $\mu\text{M}$  of AlpC with increasing concentrations of (A) ATP and (C) GTP. These plots are fitted for Michaelis-Menten kinetics. The  $K_m$  and  $V_{\text{max}}$  were determined using a Lineweaver-Burk plot (B and D). (AlpC (■) and AlpCD301A (▲)). (E) Nucleotide dependent polymerization of AlpC and AlpCD301A. In the absence of nucleotide AlpC does not aggregate (c). Polymerization of 4  $\mu\text{M}$  AlpC was assayed in the presence of 2 mM nucleotide, 2 mM  $\text{Mg}^{2+}$  or 4 mM EDTA, as indicated. AlpCD301A exhibits a nucleotide dependent polymerization behavior similar to wild type proteins. This mutant protein is prone to aggregation, resulting to loss of protein prior to incubation with nucleotides. Experimental setup was identical to AlpC.

### 2.6 What is the molecular role of AlpC in *C. glutamicum*?

#### AlpC filament assembly requires a host specific factor

The actin-like proteins studied to date are encoded on plasmids and often co-transcribed with an adaptor protein, which connects the actin filament with the plasmid. In many cases, the adaptor protein stimulates or stabilizes the actin filaments (Becker *et al.*, 2006; Garner *et al.*, 2007; Salje and Löwe, 2008; Polka *et al.*, 2009). Keeping with this line of thought, the behavior of AlpC was analyzed in a heterologous host. When produced in *E. coli*, AlpC-CFP exhibited diffuse cytoplasmic localization, sometime forming irregularly sized foci (data not shown). The inability of AlpC to organize into filaments in a heterologous host suggests that filament assembly is not solely dependent on the intracellular concentration of AlpC-CFP. Thus, additional elements are required for production of AlpC-CFP filaments, most probably a factor found on the *C. glutamicum* CGP3 prophage.

#### Attempts to identify an AlpC adaptor protein

The CGP3 prophage is relatively large and most of the coding regions encode hypothetical proteins of unknown function (Frunzke *et al.*, 2008). The genetic organization of AlpC does not share any similarities to actin homologues of plasmid partitioning systems. The *alpC* gene is located at the extreme border of the CGP3 prophage region, before a cluster of tRNA genes, flanked by a 26bp direct repeat. Although numerous adaptor protein candidates could exist on the CGP3 prophage, we focused on the gene neighboring AlpC. This gene, *cg1891* shares some similarities to the adaptor protein AlfR from the pLS32 partitioning system, mainly its small size and the relatively high number of charged amino acids. However, at the amino acid sequence level these proteins share little similarity. If Cg1891 is indeed an adaptor protein, then a physical interaction between AlpC and Cg1891 would be expected. Therefore, a LexA bacterial two-hybrid approach was used to test both homo- and hetero-interactions. To this end, both proteins were fused to a wild type LexA DNA binding domain and transformed into the reporter strain SU101. If the protein partners do not interact, binding of the operator does not occur, leading to expression of the downstream *lacZ* gene. Expression of the *lacZ* gene can be determined by grown on MacConkey agar supplemented with 10 % lactose. In the presence of LacZ, the lactose is fermented resulting in a decrease in the pH of the medium and the colonies appear red. Potential interactions between AlpC and Cg1891 were tested in all possible combinations. The appearance of white colonies on MacConkey agar demonstrated that both AlpC and Cg1891 are capable of self-interaction (data not shown). However, no interaction between the AlpC and Cg1891 proteins was detected (Fig. S5). Thus, it can be concluded that Cg1891 is not an AlpC adaptor protein.

### Filament assembly of AlpC at physiological concentration

Overexpression of AlpC resulted in the production of numerous filaments. Growth of this strain in complex medium such as LB or BHI did not appear to have deleterious consequences for the cells, expression of AlpC-CFP in CGXII minimal medium supplemented with 4 % glucoses often resulted in cell lysis. The potent effect AlpC-CFP overexpression is reflected by reduced growth rates compared to wild type cells, when grown in nutrient rich medium (Julia Frunzke and Antonia Heyer, FZ Jülich, personal communications).

Therefore, to resolve the behavior of AlpC at physiological concentration, allelic replacement was carried out. Thereby, eCFP was integrated into the *C. glutamicum* chromosome upstream of the *alpC* gene. The resulting strain has an N-terminal eCFP translation fusion to AlpC that is expressed from the native promoter. This strain exhibited medium dependent expression and organization in filaments and foci. Interestingly, when grown in LB or BHI medium, expression of eCFP-AlpC was relatively low as, apart from some background fluorescence, no fluorescence signal could be detected. It was speculated that AlpC expression or filament formation could be dependent on replication and / or induction of the CGP3 prophage. Therefore, in order to trigger CGP3 prophage induction cells were treated with mitomycin C (0.2 µg / ml), which induces host cell SOS response system. Under these stress conditions, eCFP-AlpC assembled as foci positioned mostly at the cell poles (data not shown). In a few cells, short filaments were observed. Again, a direct link between AlpC and induced CGP3 prophage could be speculated.

In comparison, eCFP-AlpC readily assembled into filaments when grown in a minimal medium (CGXII supplemented with 4 % glucose) (Fig. 2.24 A). AlpC filaments or foci were readily observed in the vast majority of cells. The filaments were varying in length, straight and mostly found running along the long axis of the cells. Previous studies on other prophages have shown that prophage induction is often dependent on and directly triggered by nutrient availability and cell density (McDaniel and Paul, 2005). At least in part, these results suggest that AlpC expression and filament formation occurs in response to cellular stress and also possibly induction of the CGP3 prophage. However, the magnitude to AlpC filaments observed in cells grown in minimal medium make it difficult to reason a direct link between AlpC filament assembly and prophage induction, under these conditions.

### In the absence of *alpC*, prophage induction rate is reduced

Thus far, the *in vivo* data hint that there is a direct connection between AlpC and the CGP3 prophage. In wild type *C. glutamicum* cells, prophage induction occurs in a low fraction of the population (Frunzke *et al.*, 2008). Although this low-scale induction probably occurs randomly, specific signals can lead to large-scale prophage induction. Most of these signals, such as exposure to ultraviolet light, are linked to the SOS response system of the host cell. The antibiotic mitomycin C is a potent DNA cross-linker that leads to the formation of single stranded DNA and subsequent induction of an SOS response. The effect of mitomycin C treatment and host cell SOS response on prophage induction

## Results

---

was tested for wild type *C. glutamicum* cells grown in CGXII medium supplemented with 4 % glucose. Using qPCR, the amount of excised, circular CGP3 prophage DNA molecules was quantified at various time points over a 24 hour time period for both mitomycin C treated and untreated wild type cells (Julia Frunzke and Antonia Heyer, FZ Jülich). Indeed, cells treated with mitomycin C showed approximately a 9-fold increase of circular phage particles compared to untreated cells (Fig. 2.24 C).

The notion that the role of AlpC is directly linked to the CGP3 prophage was tested by analysis and comparison of prophage induction rate between wild type and a mutant deleted for *alpC*. The morphology of the *alpC* null mutant was identical to wild type cells, as was the growth rate in CGXII supplemented with 4 % glucose (Julia Frunzke and Antonia Heyer, FZ Jülich). Again, the amount of excised circular phage particles in the *alpC* deletion strain treated with mitomycin C was determined by qPCR (Julia Frunzke and Antonia Heyer, FZ Jülich). Interestingly, in the *alpC* mutant strain a similar induction profile was observed, however the rate of prophage induction was greatly reduced, approximately 2-fold compared to wild type cells. Thus, AlpC does influence induction and / or replication of the CGP3 prophage.

### ***In vivo* co-visualization of the CGP3 prophage and AlpC**

In light of the finding that some of the other novel actin-like proteins are involved in segregation of plasmid DNA, an analogous role of AlpC was speculated. To test this idea, the CGP3 prophage and eCFP-AlpC were co-visualized *in vivo* by fluorescent microscopy. Visualization of the CGP3 prophage was carried out as described previously (Frunzke *et al.*, 2008). Basically, an array of *tetO* operator regions of transposon *Tn10* was integrated into an intergenic region within the CGP3 prophage region. The resulting strain was then transformed with a pEKEX2-*yfp-tetR* plasmid. This plasmid allows inducible expression of fluorescently tagged TetR, which is a repressor of *Tn10*. The TetR-YFP binds specifically to the *tetO* array, allowing direct visualization of the prophage region. The resulting strain, eCFP-AlpC CGP3-YFP, was grown in CGXII minimal medium supplemented with 4 % glucose and treated with 0.2 µg / ml mitomycin C for 2 hours. Expression of TetR-YFP was induced with 0.1 mM IPTG for 20 to 40 minutes prior to examination under the microscope. As reported previously, some cells contained 2 CGP3 prophage foci, representing chromosome inserted prophages that are replicated with the host chromosome. (Frunzke *et al.*, 2008) In these cells, eCFP-AlpC filaments or foci were readily observed. The eCFP-AlpC foci often colocalized with the CGP3 prophage foci but the positioning of the AlpC filaments showed no direct relationship with the CGP3 prophage. A population of cell contained more than 4 CGP3 prophage foci, representing prophages that have excised out of the chromosome. These foci were normally randomly distributed throughout the cell (Fig. 2.24 B). Interestingly, most of these cells did not contain an AlpC filament. A few cells did contain an AlpC filament. However, the random distribution of the induced CGP3 prophage and lack of co-localization with the AlpC filament make it difficult to reason that AlpC serves as a segregator of the prophage particles. Nevertheless, AlpC does influence induction of the CGP3 prophage.

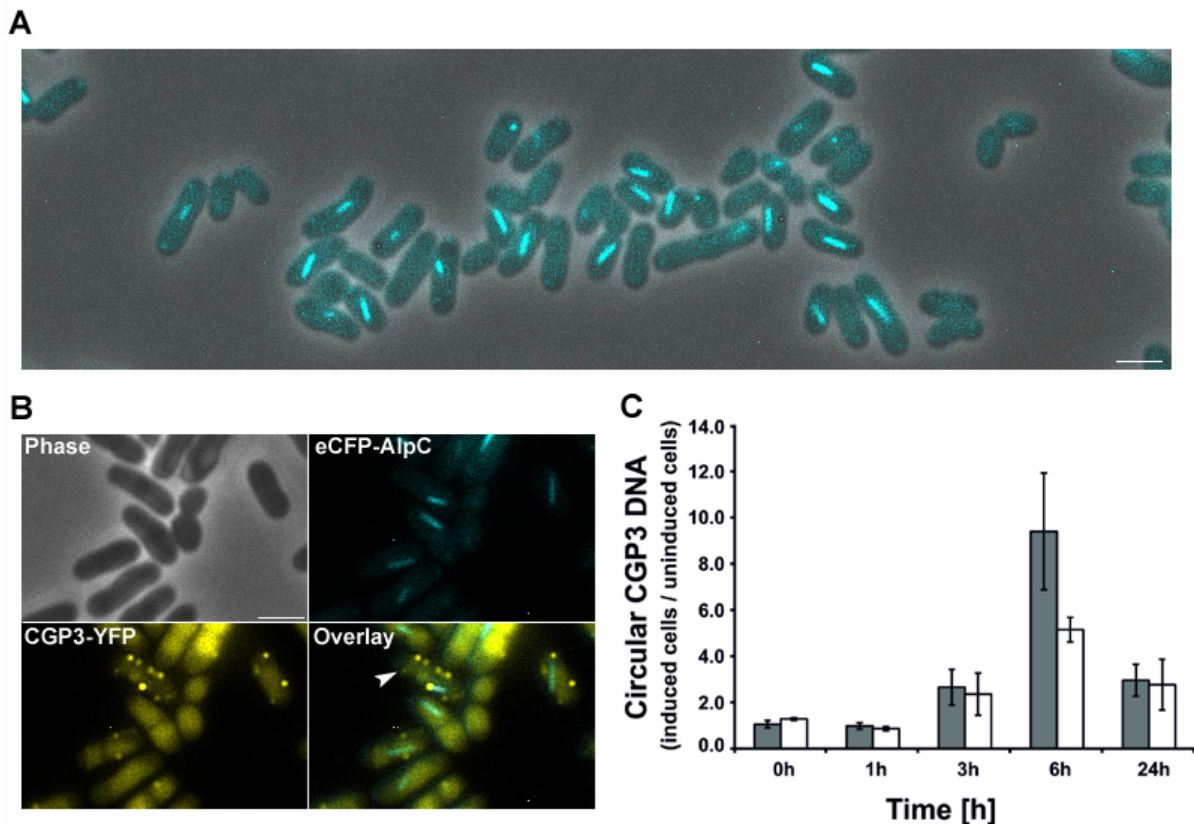


**Figure 2.24: AlpC is required for efficient prophage induction, however eCFP-AlpC filaments do not appear to organize and segregate the induced prophage particles.** (A) When grown in CGXII medium supplemented with 4 % glucose, eCFP-AlpC filaments or foci can be seen in the majority of cells. (B) Co-visualization of eCFP-AlpC and induced CGP3 prophage (CGP3-YFP and arrow) reveal that AlpC filaments do not necessarily organize the induced phage particles. In the example shown the tip of an AlpC filament is connected to a phage particle. However, many cells containing replicated phage particles did not contain AlpC filaments. (C) In the absence of AlpC the induction rate of CGP3 prophage is drastically reduced (Julia Frunzke and Antonia Heyer, FZ Jülich). (wild type is shown in grey and  $\Delta alpC$  is shown in white).

### 3. Discussion

#### Chapter I

#### Cytoskeleton elements involved in chromosome segregation and cell division

All living cells must replicate and segregate their DNA to ensure faithful inheritance of the genetic material. Akin to plasmid segregation system, bacteria use an active system to segregate replicated chromosomes, which subsequently facilitates chromosome organization. The organization of the chromosome changes in accordance with cell cycle progression. The positioning of the chromosome gives the bacterial cell polarity, which further guides cell cycle progression. The localization of the nucleoid itself can help to spatially regulate cell division, as is the case for *C. crescentus*, *E. coli* and *B. subtilis* (Lau *et al.*, 2003; Thanbichler and Shapiro, 2006; Cho *et al.*, 2011). A multitude of systems are involved in organizing the chromosome. The Par system functions to segregate the *oriC* regions of the chromosome and other systems facilitate segregation of the bulk of the chromosome. Rapid pre-segregation of the *oriC* appears to be necessary for subsequent bulk chromosome segregation and organization.

The situation in *C. glutamicum* was relatively unexplored. *C. glutamicum* has the potential to serve as a model organism for the analysis of apical growth, cell division, chromosome segregation and regulation of cell cycle events. Information gathered from exploring certain cell biology aspects of *C. glutamicum* could be used to further our understanding of cell cycle events and growth of other members of the Actinobacteria phylum, including *M. tuberculosis* and *S. coelicolor*. The aforementioned organisms are of medical and industrial importance, however complex life cycles and pathogenicity has hindered detailed studies of these organisms.

Using *C. glutamicum* as a model organism, it could be shown that the Par system of is required for efficient segregation and organization of the *oriC*. The origins are anchored at the cell poles by interaction between the ParB-*oriC* nucleoprotein complex and the apical growth determinant, DivIVA. It appears that this interaction gives the cell polarity which might further influence cell growth and division in *C. glutamicum*. The orphan ParA-like protein, PldP plays a role in cell division; however additional regulatory roles could be speculated upon.

#### 3.1 ParA and ParB: role in chromosome segregation

The subcellular organization and dynamics of the chromosome is distinct for different bacteria. While in *B. subtilis* and *E. coli* the chromosome origins are found at the cell quarter positions, polar positioning of the origin has been observed for *C. crescentus* and *V. cholerae*. (Niki and Hiraga, 1998; Niki *et al.*, 2000; Webb *et al.*, 1998; Mohl and Gober, 1997; Viollier *et al.*, 2004; Fogel and Waldor, 2005; Fiebig *et al.*, 2006) The *oriC* of the rod-shaped actinomycete *C. glutamicum*, is localized at the cell poles (Fig. 1.4 B) (Schwaiger, 2009). Thus, chromosome organization in *C. glutamicum* shares

## Discussion

---

more similarities with *C. crescentus* and *V. cholerae* than with *B. subtilis*. In *C. glutamicum*, the localization pattern of the centromere-binding protein, ParB is reminiscent to the localization of the *oriC*. ParB proteins bind short inverted repeats, *parS* sites, which are clustered around the *oriC*. Phylogenetic analysis has shown that *parS* sites occur in a large number of bacteria and share a conserved consensus sequence. In *C. glutamicum*, three *parS* sites in the origin proximal region have been identified and purified ParB binds selectively to *parS* DNA, *in vitro* (Fig. 1.4 C) (Schwaiger, 2009; Donovan *et al.*, 2010).

ParB proteins are classical helix-turn-helix DNA binding proteins (Leonard *et al.*, 2004). The domain architecture of ParB proteins can be simplified into three domains; a flexible N-terminal, central HTH and a C-terminal domain. While the N-terminal domain has been implicated in interaction with ParA, the C-terminal and HTH domain are essential for dimerization and subsequent DNA binding (Easter and Gober, 2002; Leonard *et al.*, 2004; Leonard *et al.*, 2005; Murray and Errington, 2008; Scholefield *et al.*, 2011). Based on structural analysis, a model has been proposed in which the C-terminal domain of ParB proteins interact, bringing together the N-terminal and HTH domains (Leonard *et al.*, 2004). Together, these domains constitute the secondary dimerization determinant. Interaction between the ParB C-terminal domains is essential for DNA binding. In *C. glutamicum*, ParB variants lacking part of the C-terminal domain failed to bind DNA, when expressed in *E. coli* (Fig. 2.6). While wild type ParB bound tightly to the *E. coli* nucleoid (Fig. 2.5 A), a mutant variant lacking the C-terminal domain was diffuse in the cytoplasm. Thus, it appears that the C-terminal domain is necessary for dimerization and subsequent DNA binding. However, further *in vitro* analysis will have to be carried out to confirm that this ParB mutant variant is unable to bind DNA.

In slow growing *C. glutamicum* cells, polar localized ParB foci are static, while ParB foci bound to the sister origins are dynamic and move towards the opposite cell pole. ParA proteins have been implicated in providing the driving force for either pulling or pushing the ParB bound origins to the cell pole (Fogel and Waldor, 2005; Ptacin *et al.*, 2010; Schofield *et al.*, 2010). In designing the experiment it was aimed to determine if ParA exhibits a localization pattern consistent with a role in chromosome segregation. As expression of a second chromosomal copy resulted in altered cell lengths and a low frequency of anucleate cell production, we aimed to express ParA as a single copy from the native locus. Thereby, allelic replacement was employed to introduce an in-frame C-terminal translational fusion fluorescent tag to *parA*. Although a slight increase in cell length was observed, the protein fusion was deemed functional based on the lack of anucleate cell production (Fig. 2.6). Also, no polar effects on the downstream *parB* gene were observed. In *C. glutamicum*, ParA-CFP exhibited a dynamic localization pattern, localizing as either polar foci or as patches over the nucleoid (Fig. 2.6).

The localization pattern of *C. glutamicum* ParA is reminiscent to ParA proteins from other bacteria, for example *C. crescentus* (Mohl and Gober, 1997). Recently, high resolution microscopy was employed to elucidate the subcellular structure of the ParA “clouds”. Interestingly, super resolution imaging revealed that ParA actually forms a narrow, linear polymer (Ptacin *et al.*, 2010). This observation is consistent with the *in vitro* polymerization behavior of purified ParA (Ptacin *et al.*, 2010; Schofield *et al.*, 2010; Schwaiger, 2009). Additionally, time-lapse analysis in combination with

## Discussion

---

biochemical analysis revealed that depolymerization of the ParA filament, mediated by ATP hydrolysis, segregates replicated origins by a pulling mechanism (Ptacin *et al.*, 2010; Schofield *et al.*, 2010).

The origin pulling mechanism described above requires that ParA filaments are anchored at one end to the cell poles, while the other end interacts with the ParB-*oriC* nucleoprotein complex. This model, however, cannot be applied to all ParA mediated systems, simply because not all ParA homologues assemble into long filaments extending from one pole to the other. Models have been proposed in attempts to explain the mechanism of ParA mediated force generation that is required to segregate origins. Recently, according to *in vitro* data, Vecchiarelli *et al.* (2010) proposed a “diffusion-ratchet” model for ParA mediated segregation of the pB171 plasmid. In this model, ParA-ATP dimers bind unspecifically to the nucleoid. The ParB-bound plasmids interact directly with ParA, and have a higher affinity for regions of highly concentrated nucleoid-bound ParA-ATP. Upon interaction, ParB stimulates the ATPase activity of ParA, leading to its release from the chromosome. The authors observed a time delay between disassociation from the nucleoid and the reacquisition of the nucleoid-binding conformation. This time delay results in reduced local concentration of nucleoid-bound ParA. When ParA-ATP dissociates from the nucleoid, the ParB-bound plasmid experiences a force towards region with high ParA-ATP concentration, leading to movement of the plasmid. However, as ParA-ATP can bind unspecifically to the nucleoid, this model does not explain the directed plasmid movement towards the cell poles. Nevertheless, this model does suggest alternative mechanisms aside from retracting ParA filaments.

Although, ParA filaments were not observed *in vivo* when analyzed by fluorescence microscopy, the resolution might be too low to see such structures. *In vitro*, purified ParA-GFP was found to assemble into long filaments that could be observed under the fluorescence microscope (Schwaiger, 2009). Although it would be tempting to speculate that ParA forms filaments *in vivo*, alternative mechanisms, similar to that proposed for pB171 plasmid segregation, might also hold true.

Nonetheless, the localization pattern of ParA in *C. glutamicum* strongly suggests dynamic behavior, but we gain no additional information regarding the mechanism of segregation. Therefore, time lapse analysis was attempted with the ParA-CFP strain in an endeavor to unravel the potential mechanism of ParA mediated segregation. The microfluidic chamber has proved ideal for live cell analysis of *C. glutamicum* cells (Fig. 2.12). However, we observed that exposure of *C. glutamicum* cells to light that excites cyan fluorophores severely inhibits cell growth. This is likely because the excitation and emission profile of CFP is close to the ultraviolet range. We suspect that of exposure to ultraviolet light causes DNA damage and subsequently induces an SOS response in *C. glutamicum*. Therefore, in the future alternative fluorescent proteins should be used when considering analysis of protein dynamics in *C. glutamicum*. Nevertheless, the localization pattern of ParA-CFP is consistent with a role in chromosome segregation and also dynamic behavior.

But does *C. glutamicum* ParA regulate the pole-ward movement of the replicated *oriC*? ParB-CFP expressed from a plasmid in the wild type background has mostly polar positioned foci (Table 2.1). In the absence of *parA*, ParB foci (and subsequently the origins) are mislocalized, positioned

mostly at the cell quarter positions (Table 2.1). Most of these cells lack polar attached origins. Thus, it appears that ParA does influence the localization of origin proximal regions of the chromosomes. ParB proteins have been implicated in regulating the activities of ParA, leading to the movement and segregation of origins (Marston and Errington, 1999; Quisel *et al.*, 1999; Murray and Errington, 2008; Murray and Errington, 2008). In the ATP bound form, ParA proteins dimerize and bind cooperatively and unspecifically to DNA. Upon interaction with ParB, the ATPase activity of ParA is stimulated driving ParA from a DNA bound dimer to a monomer. *In vitro*, ParA binds DNA only as a dimer (Leonard *et al.*, 2005; Hester and Lutkenhaus, 2007). Also, binding DNA appears to be a prerequisite for polymerization (Leonard *et al.*, 2005). Thus, interaction with ParB can stimulate depolymerization of ParA filaments or 'cloud-like' structures, providing a force that partitions the origin-proximal region of the chromosome.

It is not known, yet, if the situation in *C. glutamicum* is similar. Purified His<sub>10</sub>-ParA exists as a monodispersed species in solution (data not shown). However, the purified protein was not active in terms of ATP hydrolysis. Previous reports have stated that active ParA proteins are only acquired if ATP or ADP is present during the entire purification procedure. By means of co-elution, it was aimed to determine which domain of ParB might be necessary for interaction with ParA. It was found that truncation of the C- terminal or N-terminal of ParB did not alter interaction with ParA (Fig. 2.11 A). Thus, it might be that multiple residues of ParB interact with ParA. However, it would be more informative to determine with domain of ParB is necessary to stimulate hydrolysis of ParA-ATP.

### **ParA has a possible additional role in regulation of chromosome replication initiation.**

Mutation of components of the Par system often leads to a plethora of pleiotropic phenotypes, which has made it difficult to decipher the role of this system in some organisms. However, more recently it has become clear that the Par system is often involved in a number of overlapping systems. In *B. subtilis*, Soj fulfills a regulatory role, either activating or inhibiting the activity of the replication initiation protein, DnaA (Murray and Errington, 2008; Scholefield *et al.*, 2011). Again, the nucleotide bound form of Soj is central to this regulation.

In the experiment described above, where the localization of ParB foci was analyzed in the absence of *parA*, an increased number of ParB foci in cells lacking *parA* was additionally observed (Table 2.1). Assuming that each ParB focus is bound to a single *oriC*, this would mean that replication is overinitiated in cells lacking *parA*. In *B. subtilis*, the interplay between Spo0J and Soj regulates the activity of the replication initiator, DnaA. Mutants deleted for *soj* display only mild chromosome segregation defects; however chromosome replication is overinitiated (Iretton *et al.*, 1994; Murray and Errington, 2008). In *C. glutamicum*, the average number of ParB-CFP foci increased from approximately 2, in the wild type background, to 3 in the absence of *parA* (Table 2.1). Thus, it appears that *C. glutamicum* ParA might be involved in regulating chromosome replication initiation. Indeed, from microscopic analysis the DNA content per cell appeared to be altered in *parA* mutants; however, this is difficult to judge by DNA stain alone.

## Discussion

---

Overinitiation of replication can be quantified by marker frequency analysis, whereby the *oriC*-to-terminus ratio is determined by qPCR (Murray and Errington, 2008). Increased replication initiation leads to more origin firing and thus, altered numbers of replicated origins compared to the terminus. Flow cytometry has also proved useful to measure DNA content per cell and to determine defects in replication initiation. Using this method, we attempted to determine if chromosome replication is overinitiated in the absence of *parA*. Cells were treated with chloramphenicol to inhibit initiation of new rounds of replication initiation, prior to flow cytometry analysis. However, the large variation in cell size of the *par* mutants along with the tendency of *C. glutamicum* cells to clump together made it difficult to obtain reproducible results. Thus, it remains to be clarified if ParA has an additional role in regulation of chromosome replication initiation in *C. glutamicum*.

### **Pleiotropic nature of *parA* and *parB* mutation – possible additional roles**

In some organisms, chromosome replication and segregation is strictly coupled to and required for progression of the cell cycle. This is particularly evident for *C. crescentus*, where chromosome segregation spatially and temporally regulates cell division (Thanbichler and Shapiro, 2006). As a consequence, mutation of the Par system is lethal in this organism. This is not the case for *B. subtilis* (Ireton *et al.*, 1994), implying that there is a great deal of redundancy in regards to chromosome segregation in *B. subtilis*.

In many cases, deletion of one or both partitioning proteins results in various phenotypes, including growth defects, unorganized chromosomes, DNA free cells, increased chromosome content and guillotined chromosomes (Ireton *et al.*, 1994; Autret *et al.*, 2001). Similarly, null deletion mutants of either *parA* or *parB* of *C. glutamicum* lead to severe growth defects, altered cell lengths and the production of anucleate cells, phenotypes that are consistent with a role in chromosome segregation (Fig. 2.1). Similar to *E. coli*, *C. glutamicum* cells can initiate multiple rounds of replication initiation prior to completion of cell division (Schwaiger, 2009). Naturally, under these conditions efficient chromosome segregation machinery is required to organize the multiple origins. The necessity of ParA and ParB under such conditions is reflected by the severe growth disadvantage of *par* deletion mutants when grown in complex rich medium (Fig. 2.1 C). However, the situation is different when cells are grown in a medium that supports slower growth. Mutants deleted for *parA* or *parB* can maintain a growth rate that is comparable to wild type cells, when grown in LB medium. This might be because of the reduced level of replication initiation, in combination with other mechanisms that help organize the chromosome, such that the demands of the segregation machinery can be at least partly compensated.

Even though the *par* deletion mutants can keep pace with wild type cells in terms of growth, microscopic examination of the mutant cells reveal a different picture (Fig. 2.1 A). The average cell length of exponentially growing wild type cells is approximately 2  $\mu\text{m}$ . The average cell lengths of the *parA* and *parB* mutants only contrast slightly from that of wild type cells, however, the distribution profiles of these mutants highlight the degree of cell length variability (Fig. 2.1 D). Cell length variation

## Discussion

---

was most prominent for the *parB* deletion mutant. A high degree of extremely small coccoidal shaped cells, along with some longer cells were observed in cells lacking *parB*. The coccoidal shaped cells were 0.5  $\mu\text{m}$  or less in length, but more interestingly, the chromosomes appeared to extremely compact. A division septum was often placed in the middle of the cell, resembling true coccus cells. Additionally, apical cell growth is altered in *parB* mutants (Fig. 2.2) (see section 3.2).

The deleterious consequence of deletion of *parA* or *parB* is reflected in the high frequency of DNA free cells. Anucleate cells are often a result of cell division defects or unorganized chromosomes. Deletion of *parB* gives rise to an unusually high number of anucleate cells, the frequency of which varies with growth conditions. Almost 45 % of the *parB* mutant cells fail to inherit a chromosome, when grown in medium that supports rapid growth. Consistent with the observation that growth rates are not altered when grown in a medium that supports slower growth, the frequency of anucleate cell in the *parB* mutant decreased dramatically to approximately 12 % when grown in LB medium. In comparison, the growth rate did not dramatically influence the frequency of anucleate cells in the *parA* mutant. Irrespective of the medium composition, almost 18 % of *parA* mutant cells lack a chromosome (Fig. 2.1 B). To our knowledge, mutation of the Par system in other organisms studied to date did not result in such high frequency of DNA free cells.

Simultaneous deletion of *parA* and *parB* appears to be lethal in *C. glutamicum*. This suggests that one or both proteins are involved in other processes, aside from chromosome segregation. However, as single mutants can be generated, this could suggest that potential additional roles might be independent of the partner Par protein. As there appears to be a great deal of interplay between ParA and ParB proteins in other organisms, in the absence of *parB*, ParA is likely locked in the ATP bound form and binds exclusively to the nucleoid, in *C. glutamicum*. The *in vivo* localization of ParA in a *parB* mutant would be expected to be static, solely bound to the nucleoid. Attempts to generate a *C. glutamicum* strain expressing ParA-XFP as a single chromosomal copy in the *parB* mutant background were unsuccessful.

In *B. subtilis*, several lines of evidence suggest that Soj is additionally regulated through interaction with MinD, possibly linking cell division and chromosome segregation (Autret and Errington, 2003; Murray and Errington, 2008). Additional regulators might also be present in *C. glutamicum*. The bacterial two-hybrid data suggest that ParA and PldP might interact (Fig. 1.5 A). As PldP shares some similarities with MinD proteins, and we suspect that PldP has a role in cell division, the interaction between ParA and PldP might couple division site placement and chromosome segregation in *C. glutamicum* (see section 3.3).

There is some evidence that *C. glutamicum* ParA might additionally regulate chromosome replication initiation. However, in other organisms the regulatory activity of ParA is dependent on the interplay with ParB (Murray and Errington, 2008; Scholefield *et al.*, 2011). ParB proteins have additionally been implicated in priming the *oriC* for efficient loading of SMC complexes and subsequent chromosome condensation and segregation (Sullivan *et al.*, 2009; Gruber and Errington, 2009). Mutation of genes of the *smc* complex generate multiple phenotypes, including impaired growth, altered chromosome structure and anucleate cells, all consistent with a role in chromosome

## Discussion

---

organization and segregation (Britton *et al.*, 1998; Jensen and Shapiro, 1999; Mascarenhas *et al.*, 2002; Soppa *et al.*, 2002). However, additional SMC loading sites might exist, as in the absence of *spo0J* chromosome segregation is only mildly affected, which is not the case of *smc* mutants (Ireton *et al.*, 1994; Lee and Grossman, 2006). Thus, it will be interesting to see if *C. glutamicum* ParB and SMC interaction plays a role in chromosome segregation and condensation.

Although bacteria have evolved different systems to spatially and temporally control the site of division placement, these systems depend on the organization of the chromosome. In *B. subtilis* and *E. coli*, the cell poles are relatively free of DNA, and thus the Min system is employed to inhibit cell division from occurring near the poles. The Min system of *B. subtilis* additionally functions in divisome disassembly, preventing reassembly close to an existing site of division (van Baarle and Bramkamp, 2010). In *C. crescentus*, the chromosome is directly anchored at one cell pole, and thus chromosome organization differs from that of *B. subtilis* and *E. coli*. Interestingly, *C. crescentus* does not encode homologues of the Min and nucleoid occlusion system. Instead, an FtsZ inhibitory protein, MipZ, moves with the segregating origin to spatially and temporally regulate the positioning of the Z-ring. Thus, cell division only takes place after the chromosomes have been segregated. Nucleoid occlusion employs DNA binding proteins that inhibit FtsZ polymerization over regions in the cell that are occupied by the nucleoid (Wu and Errington, 2004; Bernhardt and de Boer, 2005). More recent data suggests that the nucleoid occlusion system of *B. subtilis* also functions in signaling the end of chromosome segregation (Wu *et al.*, 2009). The effector protein of nucleoid occlusion, Noc, binds multiple sites around the chromosome, with the exception of the *terC* region. Previous studies suggested that approximately 70 % of the chromosome is replicated before the division septum forms (McGinness and Wake, 1979; Wu *et al.*, 1995). It appears that Noc protects the replicating and segregating chromosome until the vast majority of the chromosome has been replicated, leading to reduced midcell concentration of Noc. Thus, the nucleoid occlusion system also serves as a cell cycle checkpoint such that assembly of the divisome does not precede replication and segregation.

In the absence of a Min and nucleoid occlusion system, how does *C. glutamicum* spatially and temporally regulate division site selection? While potential players remain to be identified, it is clear that the organization of the chromosome impacts on cell division. Although chromosome organization is analogous to *C. crescentus*, unlike *C. crescentus*, *C. glutamicum* can initiate multifork replication. The severe phenotypic consequences of *parA* or *parB* mutants could suggest that, in addition to chromosome segregation and organization defects, regulation of cell division is altered.

### **3.2 Polar anchoring of the *oriC* is mediated by ParB-DivIVA interaction.**

The almost static polar localization of ParB and *oriC* foci at the cell poles of slow growing *C. glutamicum* cells suggested that the chromosome is firmly fixed at this position (Schwaiger, 2009). The origin polar tethering factor, PopZ, in *C. crescentus* forms multimeric structures that accumulate at the cell poles in a cell cycle dependent manner (Bowman *et al.*, 2008; Ebersbach *et al.*, 2008). The

## Discussion

---

cell cycle of *C. crescentus* is rich in polarizing events, and PopZ was shown to be central for numerous polarizing events important for pole morphogenesis, protein localization, cell division and also chromosome attachment. A specific interaction between the ParB-*oriC* nucleoprotein complex and polar associated PopZ was shown to be necessary for tethering the chromosome at the cell poles. Furthermore, the PopZ-mediated polar anchoring of the ParB-*oriC* to the cell poles facilitates spatial and temporal regulation of cell division, ensuring that chromosome replication is initiated only once per cell cycle. Thus, the importance of chromosome organization in cell cycle progression is once again highlighted.

We hypothesized that the apical growth determinant, DivIVA, might function in collaboration with ParB to hold the origins at the cell poles. The first indication that this could be the case came from a bacterial two-hybrid analysis (Fig. 1.5 B). Additionally, the reduced polar growth of the *parB* mutant strongly suggested a functional interdependency between DivIVA and ParB (Fig. 2.1, 2.2).

Orthologues of DivIVA are ubiquitous in Gram-positive bacteria, however functionally DivIVA proteins vary greatly. In vegetative *B. subtilis* cells DivIVA interacts with one of the components of the Min system, MinJ, and, thus, sequestering MinCD to the cell poles (Bramkamp *et al.*, 2008; Patrick and Kearns, 2008). In contrast, during sporulation in *B. subtilis* the RacA protein mediates binding of the replicated origin to the cell pole by binding to recognition sequences around the *oriC* region and together this complex is anchored through interaction with the polar localized DivIVA protein (Wu and Errington, 2003). The crystal structure of the N- and C-terminal of *B. subtilis* DivIVA was solved (Oliva *et al.*, 2010). The N-terminal of DivIVA forms a parallel coiled-coil dimer and also contains another small helix that binds to the sides of the coiled-coil. This arrangement produces a crossed-loop structure on the top (Fig. 3.1 A), with several residues being very exposed to the solvent (residues 16–19). Most striking is exposure of the two hydrophobic phenylalanine residues (F17) to the outside, which has been shown to be essential for membrane binding. Although of lower resolution, the C-terminal domain of DivIVA appears to form a tetramer.

In Actinobacteria, DivIVA is required for coordination of apical growth (Letek *et al.*, 2008; Hempel *et al.*, 2008; Kang *et al.*, 2008; Elouelji-El Kemiri, 2008; Letek *et al.*, 2009). The mode of cell growth of Actinobacteria differs from other rod-shaped bacteria, such as *B. subtilis* and *E. coil*, where peptidoglycan synthesis occurs at the lateral wall (Carballido-Lopez and Formstone, 2007). DivIVA has been implicated in forming a scaffold at the cell poles and division septa leading to the recruitment and regulation of the cell wall synthesis machinery. Null deletion mutants of DivIVA have been reported to be lethal in *C. glutamicum*, however as knock-down mutants exhibit greatly reduced polar growth, with growth only occurring at the site of division, additional roles of DivIVA have been speculated. *C. glutamicum* DivIVA contains a short N-terminal domain that is highly similar to that of *B. subtilis* DivIVA and thus, also likely essential for membrane association. Oligomerization of DivIVA can be mediated through two coiled-coil domains. Purified DivIVA forms SDS resistant dimers (B. Sieger, personal communications). Thus, similar to the *B. subtilis* DivIVA, oligomerization is likely a prerequisite for polar accumulation and function of *C. glutamicum* DivIVA. Irrespective of the organism or function, heterologously expressed DivIVA localizes to curved membranes, specifically to the cell

## Discussion

poles and division septa, suggesting that no other factors are required for localization (Lenarcic *et al.*, 2009; Ramamurthi and Losick, 2009).

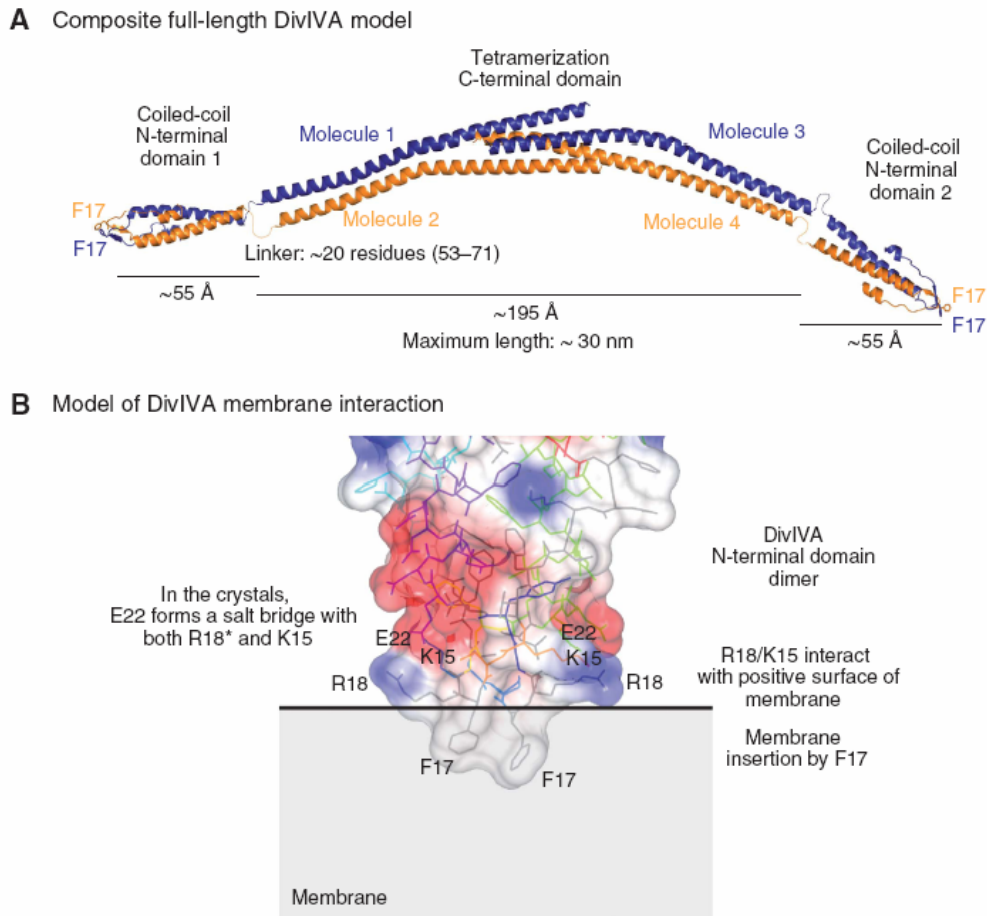


**Figure 3.1: Composite crystal structure of *B. subtilis* DivIVA.** (A) Model of *B. subtilis* DivIVA made from the crystal structures of the N- and C-terminal domains. The domains can be unambiguously joined because they are both parallel coiled-coils. Note F17 and R18, are important for membrane binding, which are exposed at the two tips of the molecule. (B) Model of the interaction of the N-terminal domain with membranes. F17 was shown to be essential for membrane association of DivIVA, proposed to insert into the hydrophobic core of the membrane. This then brings R18 (and K15), also essential for membrane interaction, close to the negatively charged membrane surface, enhancing affinity. (Adopted from Oliva *et al.*, 2010).

Further *in vivo* analysis of the potential ParB-DivIVA interaction in *C. glutamicum* was deemed problematic as DivIVA is an essential protein and slight alteration in the expression level induces gross morphological defects (Letek *et al.*, 2008). Thus, an alternative *in vivo* system was developed. Given that an intrinsic property of DivIVA is to localize, independent of any other factor, to negatively curved membranes (Lenarcic *et al.*, 2009; Ramamurthi and Losick, 2009), we considered *E. coli* as a host to study DivIVA and ParB interaction. The use of *E. coli* cells as a heterologous host is advantageous as homologues of DivIVA and ParB (or ParA) are not encoded. We found that DivIVA and ParB occupied different subcellular localizations when expressed individually in *E. coli*.

Consequently, this appeared to be the ideal system to test interaction, further. Using this system, we could show that DivIVA and ParB interact (Fig 2.5 A). Furthermore, as this minimal system lacks other components of the Par system, DivIVA is necessary and sufficient to recruit ParB to the cell poles and division septa. The DivIVA-ParB interaction was further supported *in vitro* by means of co-elution experiments (Fig. 2.5 B). Thus, DivIVA has an additional role in tethering the chromosome to the cell poles in *C. glutamicum*.

### **The N-terminal of ParB interacts with DivIVA**

The next question; which domains or residues are necessary for interaction? ParB contains a central HTH domain, which likely plays a role in binding DNA. As already discussed above, the C-terminal of *C. glutamicum* ParB is likely the initial dimerization domain, which is a prerequisite for DNA binding (Fig. 2.6). We observed that the N-terminal domain of *C. glutamicum* ParB contains a short stretch of highly conserved basic amino acids (Fig. S1) (Leonard *et al.*, 2004). Co-expression of a ParB truncation variant, lacking the N-terminal 20 amino acids, and DivIVA showed interaction similar to the wild type ParB protein (Fig. 2.7 A). On the other hand, ParB mutants lacking the N-terminal 21 amino acids did not interact with DivIVA (Fig. 2.7 A). This strongly suggested that the highly conserved arginine 21 of ParB influences interaction with DivIVA, at least in the *E. coli* system. Indeed, mutation of arginine 21, in an otherwise wild type ParB, exhibited reduced interaction with DivIVA (Fig. 2.7 B). With this information in hand, we tested if this ParB mutant variant has altered polar localization in *C. glutamicum*. While wild type ParB foci are mostly localized at the cell poles, 20 % of the cells expressing the mutant ParB protein (ParBR21A) completely lacked polar foci (Fig. 2.8 C). The consequence of this aberrant localization is reflected in the high frequency of anucleate cells (10.45 %) (Fig. 2.8 B), and reduced segregation efficiency.

Thus, it appears that ParA is necessary for moving the origin to the opposite cell pole, while, once at the cell pole, ParB interacts with DivIVA tethering the origins at this subcellular position. However, the discrepancy between the ParBR21A-DivIVA interaction in the synthetic *E. coli* system and the *in vivo* situation in *C. glutamicum* cells hints that more complex systems contribute to the polar localization and tethering of the origins.

### **ParA might support polar *oriC* anchoring**

Although the ParB-DivIVA interaction in *E. coli* probably relies on a diffusion capture mechanism, the situation in *C. glutamicum* cells is more complex. *In vivo*, ParB and DivIVA alone are not sufficient for faithful localization of the origins. Once replicated, origin segregation requires the activities of ParA. The requirement of ParA in the segregation of replicated origins is highlighted by the altered localization of ParB foci and increased number of anucleate cells in a *parA* deletion mutant (Fig. 2.1 and Table 2.1). In *C. crescentus*, the specific interaction between ParB and PopZ anchor the origins at the cell poles, while in *V. cholerae* ParA has been implicated, together with an unidentified polar

factor, in a similar role (Fogel and Waldor, 2006; Bowman *et al.*, 2008; Ebersbach *et al.*, 2008). The directed movement of replicated origins in *C. crescentus* is mediated by the polar determinant, TipN. Retracting ParA filaments relocate replicated origins to the opposite cell pole. The unidirectional movement is maintained by the TipN, which holds ParA subunits at the cell pole, preventing reincorporation with the retracting ParA filament (Lam *et al.*, 2006).

The localization of ParA as polar foci in *C. glutamicum* would suggest that ParA is interacting with either, the ParB-*oriC* nucleoprotein complex, DivIVA or with both proteins. It is possible that ParA also plays a role in tethering the origins at the cell poles. Alternatively, DivIVA might function analogous to TipN of *C. crescentus*, holding ParA subunits at the cell pole. However, this seems unlikely as DivIVA remains at the cell poles throughout the cell cycle, which cannot explain release of ParA subunits.

Bacterial two-hybrid data hint that ParA can interact with ParB and DivIVA (Fig. 1.5). Similarly, using a co-elution approach, it was shown that ParA can interact directly with ParB and DivIVA (Fig. 2.11 A and B). However, co-expression of ParA and DivIVA in *E. coli* showed only partial recruitment of ParA to the cell poles and division septa, suggesting that this interaction is weaker than the ParB-DivIVA interaction. The nucleotide bound state of ParA cannot be ignored in this experiment. In the absence of ParB, ParA is likely in the ATP bound form with higher affinity for DNA binding. Although co-expression of ParB, ParA and DivIVA did not influence interaction of ParA and DivIVA, the ratio ParA-ParB *in vivo* is often important for chromosome segregation (Bartosik *et al.*, 2009). Thus, it is not clear if ParA contributes to tethering the origins at the cell poles, however polar localized ParA foci are likely the consequence of interactions with ParB and DivIVA. Nonetheless, a more detailed *in vivo* analysis needs to be carried out in order to understand more fully the molecular consequences of these interactions.

### **ParB interacts with a central region of DivIVA**

At the sequence level, *B. subtilis* and *C. glutamicum* share little similarity, except for the N-terminus region (Fig. S2). The sequence of *C. glutamicum* DivIVA is longer and contains a central region that completely lacks homology to the *B. subtilis* DivIVA protein. Given that these proteins bind curved membranes, even when expressed in a heterologous host (Lenarcic *et al.*, 2009), but have different cellular functions, we speculated that the central insertion of the *C. glutamicum* DivIVA might be required for interaction with ParB and subsequent anchoring of the *oriC* to the cell poles.

Although, specific residues were not identified, it could be shown that part of the central insertion is required for interaction with ParB, using the *E. coli* system (Fig. 2.9 A and B). Part of both coiled-coil domains of DivIVA was found to be necessary for interaction with ParB. The potential interaction between the central region of DivIVA (amino acid 160-298) was additionally demonstrated in a bacterial two-hybrid interaction (Fig. 2.5 D). Interestingly, co-expression of ParB<sub>ΔC50</sub> with a DivIVA truncation mutant that could only support partial recruitment of full length ParB, revealed almost complete recruitment of ParB<sub>ΔC50</sub> to the cell pole and division septa (Fig. 2.9). As the ParB<sub>ΔC50</sub> appears

to have altered dimerization properties, this would suggest that ParB can interact with DivIVA either as a monomer or dimer. However, in *C. glutamicum* the ParB monomer mutants would probably be defect in DNA binding, and subsequently would not support chromosome segregation. In the *E. coli* system, the ParB $_{\Delta C50}$  mutant exhibits a diffuse cytoplasmic localization, showing that binding to the nucleoid is greatly reduced, if not completely abolished (Fig. 2.6). Thus, this mutant proved useful in determining the interaction potential with DivIVA in the absence of a potentially competing DNA interaction.

In contrast, the *B. subtilis* DivIVA homologue, although also involved in anchoring chromosome origins during spore development, requires additional mediator proteins, such as RacA (Ben-Yehuda *et al.*, 2003). In the absence of *soj* and *spo0j*, most prespore compartments capture chromosomal DNA (Sharpe and Errington, 1996; Wu and Errington, 2002; Lee *et al.*, 2003). However, in the absence of *racA*, or *racA* and *soj*, trapping of the *oriC* in the prespore compartment is reduced. Spo0J has been implicated in proper organization and positioning of the *oriC* prior to prespore trapping (Wu and Errington, 2003). Although, Spo0J co-immunoprecipitated with DivIVA in sporulating cells (Perry and Edwards, 2005), it is not clear if DivIVA and Spo0J interact directly, *in vivo*. Interestingly, in the absence of *soj* and *spo0j*, chromosomal regions, termed 'polar localization regions', determine the orientation of the chromosome during sporulation (Wu and Errington, 2002). When tested in the minimal *E. coli* system, *B. subtilis* DivIVA and Spo0J did not interact (Fig. S3). Although both DivIVA from *C. glutamicum* and *B. subtilis* sense and bind negatively curved membranes proteins, this experiment additionally shows that both DivIVA proteins are functionally dissimilar.

The precise role of DivIVA in organizing apical growth in *C. glutamicum* remains unclear. Recently, a *B. subtilis* protein (GpsB) that shares some similarity with DivIVA proteins was identified and found to be involved in directing the localization of a peptidoglycan synthesis proteins, PBP1 (Cleassen *et al.*, 2008). The N-terminus of GpsB is related to the coiled-coil region of DivIVA. The C-terminal of GpsB appears to be unique to this protein. Previously, it was presumed that two independent complexes direct growth at the lateral axis and growth resulting from cell division. However, identification and characterization of GpsB could show that at least some components of the elongation machinery, namely PBP1 actually function in both the cell division and elongation mode of growth. GpsB regulates the localization of PBP1, and therefore also regulates the switch from division to elongation mode of growth. Thus, the mode of action of DivIVA might share some similarities with GpsB.

### **In *C. glutamicum*, DivIVA truncation mutants are viable but acquire suppressor mutations**

Mutation analysis of *C. glutamicum* DivIVA proved very useful as in *E. coli* system as it allowed analysis of the *in vivo* behavior of DivIVA independent of its functional role. Based on localization behavior, deletion of a central region of DivIVA did not inhibit oligomerization or recruitment to the cell poles, when produced in *E. coli*. We speculated that in *C. glutamicum* similar DivIVA truncation

proteins would also be targeted to the cell poles, however it seemed unlikely that these mutants would support polar cell growth. To test this, attempts were made to replace the DivIVA-mCHERRY allele with the truncated DivIVA (DivIVA $\Delta_{1}$ -mCHERRY). This truncation mutant was chosen as it was reasoned that if the largest DivIVA truncation mutant would prove viable then the other truncation mutant would also probably behave similarly. To our surprise, clones were obtained in which the full length DivIVA-mCHERRY locus was replaced by the DivIVA $\Delta_{1}$ -mCHERRY. On agar plates, growth of these mutants was greatly impaired and could easily be distinguished from wild type cells.

Cells of this strain were taken from plate and analyzed microscopically (Fig. S6). Deletion of the central region of DivIVA resulted in a coccoidal morphology, similar to previous observations for a DivIVA knock-down mutant (Letek *et al.*, 2008). However, DivIVA $\Delta_{1}$ -mCHERRY was found exclusively diffused in the cytoplasm (Fig. S6). It could not be reasoned how a *C. glutamicum* coccoidal mutant strain that lacks membrane associated DivIVA and polar growth could be viable. However, after two days the mutant cells began acquiring a rod shape. DivIVA $\Delta_{1}$ -mCHERRY started localizing as foci that were often randomly distributed along the lateral membrane or clustered at one pole. Interestingly, despite the aberrant DivIVA $\Delta_{1}$ -mCHERRY localization, apical cell growth and cell shape was similar to that of wild type cells, suggesting that other redundant mechanisms might exist to direct polar growth. When grown in liquid medium, the DivIVA $\Delta_{1}$ -mCHERRY strain was almost indistinguishable from wild type cells. More interestingly, DivIVA $\Delta_{1}$ -mCHERRY was found almost exclusively at the cell poles and division septa. The acquirement of polarity and recruitment of DivIVA $\Delta_{1}$ -mCHERRY suggests that this mutant strain might have acquired suppresser mutations and also that other factor(s) might be responsible for recruitment of DivIVA to the cell poles and division septa. Based on the localization pattern of DivIVA $\Delta_{1}$ -mCHERRY in *E. coli*, it is tempting to speculate that this mutant DivIVA protein can oligomerize forming higher ordered structures in *C. glutamicum*. However, this remains speculation until the suppressor mutation(s) have been identified.

### 3.3 Regulation of cell division in *C. glutamicum*

The regulation of division site selection in *C. glutamicum* is poorly understood. In stark contrast to *E. coli* and *B. subtilis*, which employ the Min and Noc system to regulation the site of division, *C. glutamicum* lacks homologues of these systems. The situation is similar for other members of the Actinobacteria phylum. Although we have strong evidence that chromosome organization influences the placement of the divisome, other factors, either positive or negative, that regulate the positioning of the Z-ring must exist. The situation in *C. glutamicum* is compounded by the fact that division is often slightly off-centre, unlike the precise midcell positioning of the divisome in *B. subtilis* and *E. coli*. Thus, the temporal and spatial regulation of Z-ring positioning differs greatly in *C. glutamicum*.

*C. glutamicum* encodes a second ParA-like protein, PldP. Similar to other orphan *parA*-like genes, *pldP* is not located at the origin-proximal region and is not co-transcribed with a centromere-binding protein. In fact, in *C. glutamicum* *pldP* is not found in an operon. Analogous to canonical ParA,

## Discussion

---

PldP is Walker-type ATPase and shares a high degree of homology with other ParA proteins. In striking contrast to the mutant deleted for *parA*, growth rates of the *pldP* null mutant were identical to wild type *C. glutamicum* cells irrespective of the growth medium (Fig. 2.1 C). However, the average cell length of this mutant was significantly longer than wild type cells and the cell length distributions were more varied, indicating a role in cell division.

### **PldP: role in cell division**

Indeed, a potential role in cell division was reflected in the localization pattern of PldP, often seen as a two foci at the lateral cell axis of the mature division septum (Fig. 2.3). In general, this localization pattern is indicative of the formation of a ring-like structure. In principle, a Z-stack series and subsequent 3D reconstruction would allow determination of ring formation. In the case of PldP, long exposure times hindered such analysis. Nevertheless, recruitment of PldP to the site of cytokinesis appears to be relatively early, as a band of PldP is observed in some cell prior to visualization of the division septum by Nile red staining. This localization pattern would strongly suggest a role in cell division.

The localization pattern of PldP is strikingly similar to midcell localized MinD. Like canonical ParA proteins, PldP is evolutionary related to the cell division protein, MinD (Fig. 3.2). MinD is one of the components of the Min system, which spatially regulates the positioning of the cytokinetic Z-ring in *E. coli* and *B. subtilis* (Bramkamp and van Baarle, 2009). In *B. subtilis*, MinD is positioned at the cell poles and recruited to the division site where it localizes as either a band or two foci (Marston *et al.*, 1998). In *E. coli*, the components of the Min system oscillate from pole to pole setting up a gradient of the FtsZ inhibitor, MinC which is highest at the cell poles and lowest at midcell (Lutkenhaus, 2008). In the presence of ATP, MinD dimerizes and associates to the membrane (Szeto *et al.*, 2002; Hu and Lutkenhaus, 2003; Lackner *et al.*, 2003; Wu *et al.*, 2011). Membrane associated MinD recruits MinC, while MinE displaces MinC and stimulates the ATPase activity of MinD triggering its release from the membrane. MinD, and the passenger protein MinC reassemble at the opposite cell pole. Repeated cycles of interaction between MinD and MinE set up a gradient of MinC. In the absence of *minD*, or other components of the Min system, aberrant cell division close to the cell poles gives rise to minicells. In these mutants, cytokinesis can take place at midcell, or close to the cell pole. This gives rise to two distinct mutant cell populations, one that is longer than wild type cells and another that is extremely smaller than wild type cells. The smaller cells, referred to as minicells, are the result of unrestricted FtsZ polymerization close to the cell poles producing small round, often DNA-free minicells (de Boer *et al.*, 1988). Thus, as a consequence the sister cell will grow, synthesis more cell division proteins, reaching a cell length that exceeds wild type cells.

Deletion of *pldP* led to a population of cells with varying cell lengths. While the average cell length of the *pldP* mutant strain was significantly longer than wild type cells, a large number of shorter cells (minicells) resulted, also. Although the number of anucleate cells was low, the formation of small round cells that contained DNA was frequent in this mutant strain (Fig. 2.1 A and D). This phenotype is

## Discussion

---

similar to a *minD* mutant and, thus indicates a role in division site selection. However, overexpression of PldP leads to a more dramatic increase in cell length (Schwaiger, 2009), similar to overexpression of MipZ in *C. crescentus*, suggesting a role in spatial regulation of FtsZ.

The C-terminal of MinD is amphipathic in nature and has been shown to mediate direct interaction between MinD and the membrane phospholipids. Truncation of a short part of the C-terminal is sufficient to avert membrane association (Szeto *et al.*, 2003). Also, expression of the C-terminal amphipathic region, fused to GFP is sufficient to recruit GFP to the membrane. Similarly, the C-terminal of PldP is predicted to form an amphipathic  $\alpha$ -helix, and thus might be involved in membrane association (Fig S8). The sequence of this region of PldP deviates greatly from the consensus amphipathic motif of *E. coli* MinD. However, at least in *E. coli* cells, PldP associates with the membrane (Fig. 2.17 A and B). This result is in agreement with the *in vivo* localization of PldP-eCFP, which not only binds to the site of division but is also associated directly to the membrane (Fig. 2.18). However, additional proof that the C-terminal is necessary for membrane association would require testing membrane binding activities of a PldP mutant lacking the putative amphipathic helix.

### **PldP: possible role in regulation of ParA**

Two lines of evidence suggest that PldP and ParA interact. In a bacterial two-hybrid ParA and PldP interacted and also, ParA was consistently pulled-down with PldP (Fig. 1.5 A and Table 2.2). On the other hand, it appears that ParA localization is not dramatically altered in the absence of *pldP* (Fig. 2.2). In *B. subtilis*, Soj is recruited to the cell poles and division septum through interaction with MinD. At the division septum, Soj forms a band. In the absence of *minD*, Soj is diffuse in the cytoplasm, while in the absence of *spo0J* Soj binds tightly and statically to the nucleoid (Murray and Errington, 2008). Furthermore, enrichment of Soj at septa was observed in cell lacking *minC*, suggesting that MinC and Soj might compete for binding with MinD (Murray and Errington, 2008). Although Sop0J regulates the activities of Soj which in turn regulates DNA replication initiation, the altered localization patterns of Soj in a *minD* and *spo0J* mutant would suggest that MinD also regulates the activities of Soj. However, this prospect has not been investigated in detail, to date. It is, however, known that nucleotide hydrolysis deficient *soj* mutants fail to interact with MinD (Murray and Errington, 2008). It appears that the nucleotide binding property of Soj is necessary for interaction with MinD. Also, ATP hydrolysis Soj mutants do not interact with MinD, probably preferentially interacting with DnaA, negatively regulating replication initiation. It could be speculated that the interplay between Soj and MinD acts as a cell cycle regulator, coupling cell division and chromosome segregation.

Although we could show that PldP localizes to the site of division, the low expression level and relatively weak fluorescence of CFP made it difficult to determine if PldP has alternative localization sites. When overexpressed, either as a second chromosomal copy or from a plasmid, PldP was found to localize to the septum along with forming polar foci and patches on the nucleoid (Schwaiger, 2009). We also observed that PldP, expressed as a single copy from the native promoter, might localize as patches over the nucleoid (data not shown). However, what might be the *in vivo* consequence of the

## Discussion

ParA–PldP interaction? As PldP and ParA share some similarities with Soj and MinD, it could also be speculated that both proteins compose a cell cycle regulation system. Although polar localization of PldP might only be an overexpression artifact, at this site PldP could potentially interact with ParA. Additionally, chromosome bound ParA is often enriched at the division septum, where PldP localizes. It could be speculated that PldP binds to defined regions of the chromosome, for example the *terC* which is positioned at the midcell region, to spatially and temporally regulate positioning of the Z-ring. However, further analysis needs to be carried out to determine if PldP functions in regulating the activity of ParA. If this holds true, this would also have general implication for the MinD-Soj based system as a cell cycle regulator.

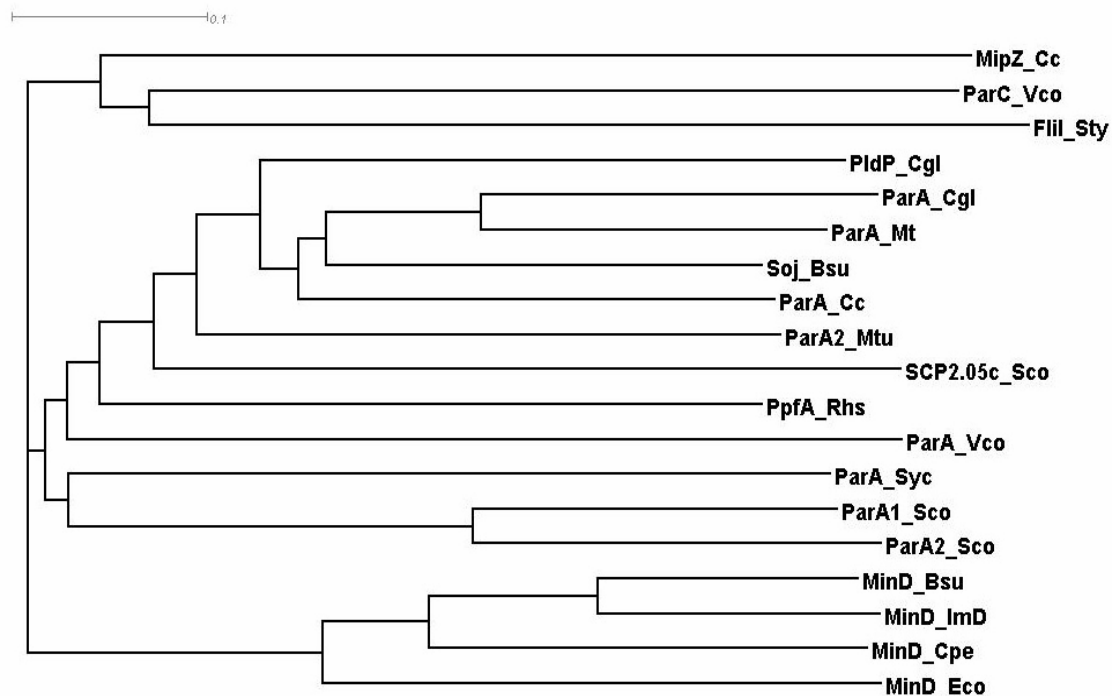


**Figure 3.2: ParA and MinD proteins share an evolutionary relationship.** Many organisms code for more than one ParA protein or have MinD and ParA proteins encoded. MinD proteins clearly cluster together, whereas bona fide ParA/Soj proteins cluster in one group as well. Many *parA*-like genes are closely related to the MinD proteins. At least for the MipZ protein from *Caulobacter crescentus* (MipZ Cc) a role in division site selection has been shown. The dendrogram was calculated by using a CLUSTALW (Larkin *et al.*, 2007) alignment based on the amino acid sequences of various ParA and MinD proteins. Sequences were derived from the genome information broker (<http://gib.genes.nig.ac.jp>). Proteins that were not annotated are shown with their gene codes. Although PldP clusters with ParA, PldP is closer to MinD proteins than ParA. Strain abbreviations: Vco, *Vibrio cholerae* O395; Sco, *Streptomyces coelicolor* A3(2); Mtu, *Mycobacterium tuberculosis* H37Rv; Cgl, *Corynebacterium glutamicum* ATCC 13032; Imc, *Listeria monocytogenes* 4b F2365; Bsu, *Bacillus subtilis* 168; Cc, *Caulobacter crescentus* CB15; Eco, *Escherichia coli* K-12; Rhs, *Rhodobacter sphaeroides*; Sty, *Salmonella enterica* subsp. *enterica* serovar Typhi CT18; Cpe, *Clostridium perfringens* 13.

**Simultaneous deletion of *pldP* and *parB* or *parA* increases growth from ectopic sites.**

## Discussion

---

Even though both *par* deletion mutants and the *pldP* deletion mutant exhibited varying degrees of growth from ectopic sites, simultaneous deletion of *pldP* and either *parA* or *parB* enhanced this branching phenotype (Fig. 2.4 A). Ectopic sites of growth occurred at the long axis of the cell. Interestingly, branching was only observed when cells were grown in LB medium. In these multi-pole mutants the DNA forms a continuous unseparated mass.

Over the past 40 years, reports have popped up describing similar branching phenotypes in *E. coli*. Mutants of cell division proteins, chromosome replication, peptidoglycan synthesis and components of the Min system have all been described to lead to different frequencies of Y-shaped branched *E. coli* cells. Similar to described above, the number of branched cells was generally low but often varied with growth medium. In the past 10 years, the underlying mechanism of shape malformation in *E. coli* has been revisited. Recent evidence has suggested that alterations in the geometry of the Z-rings leads to branched shaped cells (Potluri *et al.*, 2012). In *E. coli*, the Min and Noc system restrict Z-ring formation to midcell, also however, recent evidence suggests that PBP5 (involved in peptidoglycan synthesis), which localizes to the midcell in an FtsZ dependent manner, can fine tune the precise orientation of the Z-ring (Potluri *et al.*, 2010). Mutation of PBP5 leads to slightly tilted Z-ring formation which, after division lead to cells with deformed, slightly slanted poles. The resulting daughter cell can contain a patch of inert peptidoglycan some distance away from the cell pole. As the cell grows, insertion of new peptidoglycan around the patch of inert peptidoglycan can lead to its extrusion, forming a branch.

In *E. coli* and *B. subtilis* cell elongation occurs by intercalation of new peptidoglycan into the wall along the long axis of the cell. The cell poles of these organisms are composed of inert peptidoglycan. The situation in *C. glutamicum* is very different, which grow predominantly from the cell poles and division septa, meaning the lateral axis of cell contains mostly inert peptidoglycan. *Streptomyces* is a member of the Actinobacteria phylum and similar to *C. glutamicum*, uses DivIVA to organize apical cell growth. During vegetative growth, DivIVA can accumulate along the cell sidewall initiating a new zone of polar cell growth. How and what recruits DivIVA to these sites is not know. However, it appears that *Streptomyces* can initiate zones of growth, *de novo*. Another member of the Actinobacteria phylum and close relative of *C. glutamicum*, *Bifidobacterium*, can grow forming branches. Interestingly, *Bifidobacterium* are genetically very similar to *C. glutamicum*. The morphology of these cells are strikingly similar to the *C. glutamicum* mutant branching cells.

We also observed branching cells in a *C. glutamicum* mutant expressing an FtsZ-mCHERRY translational fusion from its native locus. As the localization of FtsZ-mCHERRY was irregular, fusion of mCHERRY to the C-terminal partially inhibits its function. In this mutant, branches were observed along the long axis of the cell. Multiple branching points in filamentous cells were often observed (Fig. S7). One could imagine that abortive Z-rings result in premature recruitment of DivIVA, which sets up a new polar axis. In *C. glutamicum*, branching cells have been observed in mutants of DivIVA, FtsZ, PldP as well as FtsI (a component of the peptidoglycan synthesis machinery, also called PBP3)

(Valbuena *et al.*, 2006). Common to all these mutants is cell division and growth. It will be interesting to examine if PldP influences the localization of the Z-ring in *C. glutamicum*.

### **Orphan ParA-like proteins organize the bacterial subcellular environment**

Numerous ParA-like proteins have been identified on the chromosomes of distantly related bacterial species (Gerdes *et al.*, 2000). While the prototypical ParA proteins are involved in chromosome segregation, orphan Walker-type ParA-like proteins lack any obvious centromere-binding protein. As outlined below, these proteins are involved in diverse cellular functions.

The best characterized orphan-ParA like protein is the *C. crescentus* cell division regulator, MipZ (Thanbichler and Shapiro, 2006). *C. crescentus* does not encode homologues of the Min system. Instead, MipZ, in collaboration with the ParAB partitioning system, synchronizes the formation of a contractile Z-ring with segregation of the origins. MipZ binds the ParB-*oriC* nucleoprotein complex forming a gradient that moves with the segrosome during origin segregation. The stimulatory effect of MipZ on FtsZ GTPase activity, inhibits FtsZ-ring formation close to the cell poles, forcing FtsZ to relocate where MipZ concentration is lowest, namely around the midcell region.

In *Rhodobacter sphaeroides* chemotaxis proteins colocalize in discrete but distinct regions of the cytoplasm (Wadhams *et al.*, 2002; Wadhams *et al.*, 2003). The orphan ParA-like protein PpfA, which is encoded in the chemotaxis operon (*cheOp3*), is required to organize the protein clusters (Thompson *et al.*, 2006). The distribution of these cytoplasmic protein clusters is highly analogous to the subcellular positioning of low copy plasmids of the type I partitioning system. These chemotaxis clusters are located either at midcell or at the cell quarters positions. It is not known if PpfA localizes with the chromosome, however, cells lacking *ppfA* often fail to inherit chemotaxis clusters. Homologues of PpfA can be found in many bacterial species, and interestingly, are often found in the chemotaxis operons. In *V. cholera*, a ParA-like protein designated ParC, modulates the positioning of chemotaxis proteins (Ringgaard *et al.*, 2011). Thus, not only DNA but also protein complexes can be organized within the bacterial cell.

An orphan ParA-like protein of *Synechococcus elongatus* has been implicated in the organization and segregation of carboxysomes (Savage *et al.*, 2010). In cyanobacteria carboxysomes are microcompartments that contain the enzymes required for carbon fixation. Carboxysomes are positioned at regular intervals along the lateral cell axis such that each daughter cell inherits an equal number of the carbon fixing microcompartments after cell division. The fidelity of carboxysome partitioning is greatly perturbed in the absence of *parA*, often resulting in cells completely lacking carboxysomes. Interestingly, cells that fail to inherit carboxysomes divide much later than the corresponding sister cell. Analysis of ParA-GFP localization revealed a dynamic pole to pole oscillation and the formation of dynamic filamentous structures, which formed in-between carboxysomes, suggesting a role in organizing the carboxysomes in the cytoplasm. Cells that lack carboxysomes have greatly reduced cellular fitness, thus an active segregation system would appear logical.

## Discussion

---

Although orphan ParA-like proteins are encoded on many bacterial chromosomes, relatively few have been studied, to date. However, the common theme emerging is that these proteins organize different aspects of the subcellular environment. The orphan ParA-like protein of *C. glutamicum* organizes the cell division machinery, possibly both spatially and temporally.

### 3.4 Proposed model for chromosome segregation in *C. glutamicum*

From the results presented here we propose the following model for chromosome segregation, polar anchoring of the origins and cell division in *C. glutamicum* (Fig. 3.3). In slow growing *C. glutamicum* cells, the chromosome origins are orientated towards the cell pole prior to replication initiation (Fig. 3.3 I). Shortly after replication initiation, the newborn origin is bound by ParB. The daughter origin is subsequently segregated from the old origin and actively moved towards the opposite cell pole (Fig. 3.3 II). Segregation of the daughter origin is most likely mediated by ParA, which moves the origins apart by a pushing or pulling mechanism. The action of ParA is probably highly dependent on the interplay with ParB. Upon reaching the opposite cell pole, the replicated origin is anchored in position through interactions between the ParB-*oriC* nucleoprotein complex and polar DivIVA (Fig. 3.3 III). We speculate that the anchoring of the ParB-*oriC* nucleoprotein complex is an essential step in the cell cycle. Firstly, this step might influence growth of this cell pole. In *C. glutamicum*, growth from the cell poles is slightly asymmetric (B. Sieger, personal communications). The slightly altered rates of polar growth might be important for rapid *oriC* segregation, such that the daughter origin is not chasing after a growing pole. Once anchored at the cell pole, polar growth along with bulk chromosome segregation systems functions to partition the chromosome. Additionally, polar cell growth and chromosome segregation could be tightly linked, serving as a cell cycle checkpoint. Thus, initiation of cell division could be temporally regulated such that it does not occur prior to segregation of the chromosome origins and anchoring at the cell poles. There is some evidence that would suggest that anchoring of the *oriC* to the cell poles is essential for overall chromosome organization, which strongly influences cell division both spatially and temporally. Once the origins are tethered in position at the cell poles, the remainder of chromosome is segregated and condensed resulting in a DNA-free zone around the midcell region. Polymerization of the cell division protein, FtsZ, is initiated, forming the contractile Z ring, on which the cytokinesis apparatus assembles (Fig. 3.3 IV). The orphan ParA-like protein, PldP is recruited at an early stage to the division site, possibly shortly after Z-ring formation. The DivIVA protein is recruited late to the site of cytokinesis, where after completion of septation, DivIVA remains attached to the newly formed cell poles (Fig. 3.3 V and VI).

*C. glutamicum* cells are capable of rapid growth to high cell densities, initiating multiple rounds of replication prior to cell division completion. Although ParB-*parS* nucleoprotein complexes are mostly statically localized at the cell poles, additional ParB-*parS* complexes are often found near the midcell region (Fig. 1.4) (Schwaiger, 2009). At this position, DivIVA localizes to the inward growing membrane. DivIVA is recruited to the division septum before cytokinesis is completed, where it forms

a ring-like structure. The midcell localized ParB bound origins might be held in position through interaction with DivIVA. Interaction of ParB at the growing septum might even be more complex, since a potential interaction between ParB and FtsZ in *C. glutamicum* has been demonstrated earlier (Fig. 1.5 A) (Schwaiger, 2009). As the septum matures and constricts forming the new cell pole, the origins are again tethered at the correct subcellular localization (Fig. 3.3 V and VI).

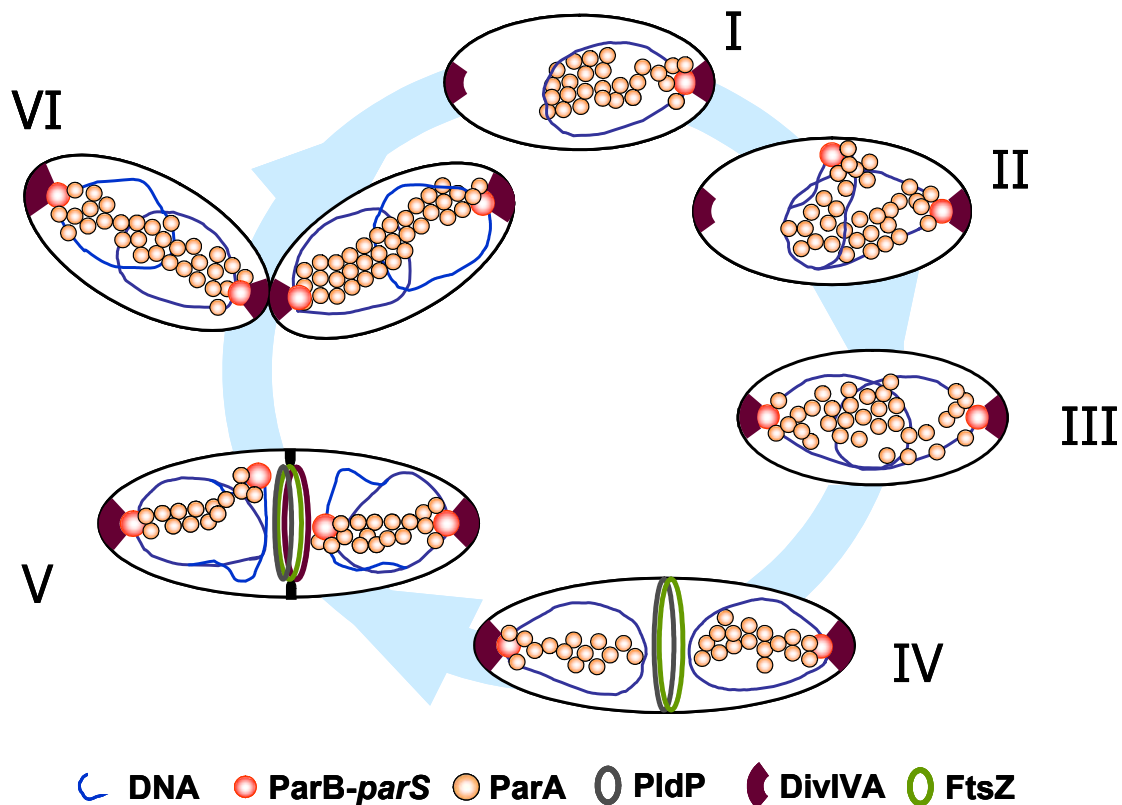


**Figure 3.3: Proposed model for origin anchoring during the cell cycle in *C. glutamicum*.** (I) Prior to replication initiation, the chromosome origin is localized close to one cell pole. (II) After initiation of replication, the polar ParB-origin nucleoprotein complex is segregated towards the opposite cell pole. Active mechanisms help segregate the remaining of the chromosome. (III) When the replicated origin reaches the opposite cell pole, ParB interacts with polar localized DivIVA, tethering the origin at the cell pole. We speculate that the anchoring of the origin at the opposite cell pole influences growth of this cell pole, which in turn could aid the segregation process. (IV) Once the chromosomes have been segregated, FtsZ can polymerize at the internucleoid space and mature to a functional Z-ring. PldP is recruited to the division septum, probably relatively early (V) *C. glutamicum* is capable of fast growth and multiple rounds of replication can be initiated before completion of cell division. In such cases, the newly replicated origins are segregated towards the division site where they eventually stop. DivIVA is recruited late to the division septum. Thus, the ParB-*parS* nucleoprotein complexes are held in position, close to the division septum by interaction with DivIVA. Also, at this stage the division septum matures and grows inwards. PldP is often seen as two foci during the early stages of septum invagination. We think PldP is forming a ring-like structure at this position, as depicted in model. (VI) The division septum matures and constricts, DivIVA is divided between the two new cell poles, tethering the newly replicated origins at the young cell poles.

### 3.5 The ParB-DivIVA interaction is conserved in Actinobacteria

Based on our observations in *E. coli*, we have shown that *C. glutamicum* ParB and DivIVA interact. To support the idea that *C. glutamicum* can be used as a model organism in the study of cell cycle regulation and apical cell growth for other members of the Actinobacteria phylum, we made use of the *E. coli* system to test the interaction between ParB and DivIVA from *M. tuberculosis* and *S. coelicolor*. In *M. tuberculosis* the origins are localized at the cell poles, similar to *C. glutamicum* (Jakimowicz *et al.*, 2007a; Maloney *et al.*, 2009). Thus, similar to the *C. glutamicum* situation, the ParB bound origins might be tethered at the cell poles through interaction with Wag31 in *M. tuberculosis*. In comparison to *C. glutamicum* and *M. tuberculosis*, the interaction of *S. coelicolor* ParB and DivIVA appeared to be weaker. When assayed in a LexA based bacterial two-hybrid the strength of interaction was comparable to *C. glutamicum* and *M. tuberculosis*. Also, the conserved arginine of the N-terminal of ParB is not present in the *S. coelicolor* ParB. Nevertheless, the corresponding stretch of amino acids is aliphatic. Similar to the situation in *C. glutamicum*, the entire motif may be necessary for interaction with DivIVA. In *S. coelicolor* DivIVA and ParB do not directly colocalize in vegetative mycelium (Jakimowicz *et al.*, 2005). Also deletion of *parB* leads to a dramatic increase in anucleate spores (Kim *et al.*, 1999; Jakimowicz *et al.*, 2005; Jakimowicz *et al.*, 2007b). Thus, a meaningful interpretation of the interaction observed in the synthetic *E. coli* system could be that the ParB-DivIVA interaction plays a role during spore development. During sporulation ParB foci are mostly localized in the middle of the spore, however, some foci are localized to the inward growing septum. Although the results presented here hint at a possible interaction between ParB<sub>SCO</sub> and DivIVA<sub>SCO</sub>, a more detailed analysis in *S. coelicolor* cells must be carried out.

Collectively, all the components of the Par system function to aid efficient chromosome segregation. In *Mycobacterium* and *Streptomyces*, ParA promotes binding of ParB to *parS* sites (Jakimowicz *et al.*, 2007a; Jakimowicz *et al.*, 2007b). It has been postulated that ParA provides the driving force that pushes or pulls the replicated origins towards the cell poles. This has been nicely shown for *C. crescentus* and *Vibrio cholerae* where ParA depolymerization, stimulated by ParB, moves the origin to the opposite cell pole (Ptacin *et al.*, 2010; Fogel and Waldor, 2006). The importance of ParA in chromosome segregation cannot be underestimated and a contribution of ParA in origin tethering via interaction with DivIVA cannot be ruled out.

### Chapter II A prophage encoded cytoskeleton protein

Contrary to the long-standing assumption, some *C. glutamicum* strains encode an actin homologue. The *cg1890* gene (designated AlpC, for Actin-Like Protein Corynebacterium) was recently identified as a putative actin-like protein (Derman *et al.*, 2009). The main objective of this study was to determine if the novel AlpC protein possess actin-like properties and is a bona fide cytoskeleton element. As AlpC is one of the first proteins encoded on the CGP3 prophage of *C. glutamicum*, a functional link between AlpC and the prophage was tested.

#### 3.6 AlpC is an actin-like protein

Actin and actin related proteins share limited sequence and structural similarity. In general, to determine if candidate actin-like proteins, that possess the actin signature motif, are true cytoskeleton proteins, a number of characteristic criteria must be met. These features include assembly into dynamic filaments *in vivo* and *in vitro* binding and hydrolysis of nucleotides, in many cases both ATP and GTP. Although numerous actin-like proteins that contain the actin signature motif have been identified, relatively few have been characterized (Derman *et al.*, 2009). Thus, it remains to be clarified if all these protein are indeed cytoskeleton elements.

The formation of dynamic filamentous structures *in vivo* is common to both eukaryotic and prokaryotic homologues. In *C. glutamicum*, AlpC readily assembles into long curved filaments when overexpressed (Fig. 2.20). When expressed at physiological concentration AlpC assembles into short straight filaments, in addition to formation of compact foci (Fig. 2.24 A). The dynamics of actin-like filaments varies and is often linked to the mode of subunit assembly, stability and function of the protein in question (Cabeen and Jackobs-Wagner, 2010). ParM, for example, exhibits extreme dynamic instability, displaying bursts of growth followed by rapid decay (Garner *et al.*, 2004; Garner *et al.*, 2007). Stabilization of the ParM filament requires that both ends of the ParM filament are capped with ParR bound plasmids (Salje and Löwe, 2008) (Fig. 1.6 A). Thus, the dynamic instability of the ParM filament is intrinsic to the mode of action of ParM in plasmid segregation, where it searches the cytoplasmic environment for plasmids. Similarly, the mode of action of Alf7A filaments in plasmid segregation requires that both ends of the filament are capped with a plasmid (Derman *et al.*, 2009). Other actin-like proteins, such as AlfA, assemble into filaments by addition of subunits to one side of the filament only (Polka *et al.*, 2009). Alf7A filaments are more stable and long-lived. Although the mechanism by which AlfA segregates plasmids is not well understood, it differs to ParM mediated segregation (Becker *et al.*, 2006; Polka *et al.*, 2009).

The dynamics of AlpC filaments was analyzed in cells overexpressing AlpC. This strain was used as the relatively low concentration of AlpC expressed from the native promoter required longer exposure times which subsequently led to fluorophore bleaching. Time lapse analysis revealed that AlpC-CFP filaments readily assemble into filaments and disassemble into compact foci (Fig. 2.21). It

## Discussion

---

appears that filament assembly and disassembly is not a rapid process, in comparison to the dynamic nature of ParM filaments. However, nucleation of the AlpC filament seems to occur from compact foci. These compact foci are readily observed in cells either overexpressing AlpC or cells expressing AlpC at physiological concentration (Fig. 2.21 and Fig. 2.24 A). The AlpC foci do not localize to a unique subcellular localization but as these foci are normally slightly off the cell pole, it appears that the AlpC foci could be bound to the chromosome. In other systems, interaction with DNA is often mediated by adaptor proteins that bind specific DNA sequences facilitating interaction between the actin-like protein and chromosome. In plasmid partitioning systems, the adaptor protein is normally co-transcribed with the motor protein (Gerdes and Molin, 1986; Dam and Gerdes, 1994; Becker et al., 2006). Interestingly, *alpC* is not found in an operon and a potential adaptor protein was not identified. Although it could be speculated that AlpC does not require an adaptor protein, the fact that AlpC does not assemble into filaments when expressed in *E. coli* would suggest that additional factors are required and assembly into filaments is not solely dependent on concentration, *in vivo*. Additionally, filament assembly of eCFP-AlpC was severely reduced when expressed in a *C. glutamicum* strain that lacks most of the CGP3 prophage. Thus, factors specific to the phage region are required for the formation of filaments. As AlpC does not contain a DNA binding domain, this would suggest the requirement of an adaptor protein. However, it remains to be tested if AlpC can bind DNA, *in vitro*.

Nucleotide binding and hydrolysis is essential for the dynamic nature of cytoskeleton proteins. *In vitro*, AlpC can hydrolyze both ATP and GTP, with ATP being the most abundant and thus, likely the favored substrate (Fig. 2.23). In the case of ParM filaments, nucleotide hydrolysis is important for filament disassembly. ParM hydrolysis mutants are deficient in plasmid segregation and maintenance (Garner *et al.*, 2004). Mutation of one of the conserved residues in the phosphate 2 (Fig. 1.7) motif abolished nucleotide hydrolysis of AlpC. *In vivo*, the AlpC hydrolysis mutant protein did assemble into filaments, however only in a minority of cells. These filaments were often found close to the membrane and many cells contained large blobs of protein. According to the *in vitro* data, AlpC and the hydrolysis mutant can assemble into filaments, which is dependent on nucleotide and  $Mg^{2+}$  as a cofactor (Fig. 2.23 E). This would suggest that, similar to the situation with ParM, nucleotide hydrolysis is necessary for filament disassembly.

### 3.7 AlpC is necessary for efficient prophage induction.

Derman et al identified a number of actin-like proteins found on the bacterial chromosome, phage genomes and plasmids, however only actin-like proteins of plasmid segregation systems have been studied in detail, to date (Derman *et al.*, 2009). Initially, we speculated that AlpC might function to actively segregate excised prophage particles, akin to plasmid segregation systems. A previous study showed that the CGP3 prophage can excise from the host chromosome and exist as a double stranded circular molecule (Frunzke *et al.*, 2008). However, induction only occurs at low frequency, in approximately 1-2 % of the population. The underlying stimulus that leads to induction of the prophage

is not known. It is, however, interesting that *C. glutamicum* cells have not lost the CGP3 prophage particles, which could occur during cell division giving rise to two different cell populations, one that contains the induced prophages and the other that lack any prophages. Naturally, an alternative to a segregation system might be programmed cell death mediated by addiction molecules or the presence of essential genes on the prophage genome.

To test if AlpC actively segregates induced CP3 prophage DNA, a strain was used in which the prophage was labeled with YFP. To increase the frequency of prophage induction, cells were treated with mitomycin C. Interestingly, we found that AlpC filaments were often absent in cells that contained multiple induced phage particles. In cells that contained both multiple CGP3 foci and AlpC filaments, interaction between the extrachromosomal DNA and filaments was not always observed. These results would suggest that AlpC is probably not involved in segregation of the induced prophage particles. However, the induced prophage particles often appeared to accumulate at the cell membrane (Fig. 2.24 A). It might be that the AlpC filaments organize the phage particles on the host cell membrane. There is an increasing amount of evidence suggesting that plasmid and phage replication occurs at the membrane (Firshein, 1989). It could be speculated that induced phage particles are directed to the membrane where additional rounds of replication occur.

To determine if AlpC is necessary for prophage induction and / or replication, the induction rate was determined and compared for wild type and mutants deleted for *alpC* (Fig. 2.24 C). Induction of the host cell SOS response triggers excision of bacteriophages out of the host chromosome. Similarly, treatment of wild type cells with mitomycin C lead to an enhanced induction of the CGP3 prophage. However, cells lacking *alpC* had a two fold decrease in induced prophage. This would suggest that AlpC plays a role in either CGP3 prophage induction or in organization of the replication machinery.

### 3.8 Host actin related proteins organize phage replication

Replication of circular and linear phages can be grouped into three different mechanisms. These mechanisms are described in detail in the review of Wigel and Seitz, 2006. The *B. subtilis* bacteriophage  $\Phi 29$  has been subject of much study, and now serves as a model for phage replication. The genome of bacteriophage  $\Phi 29$  is linear, containing terminal proteins (TP) covalently linked at the 5' end, which constitute the origins of replication (Blanco and Salas, 1984; Hermoso *et al.*, 1985). The TP ensure that bacteriophage  $\Phi 29$  cannot integrate into the bacterial chromosome and thus, replication and segregation are essential for survival. Transcription of bacteriophage  $\Phi 29$  can be divided into early and late stages. Initiation of replication occurs via the protein-primed mechanism. Replication is initiated upon recognition of the origins, located at both ends of the linear chromosome, by the bacteriophage  $\Phi 29$  DNA polymerase and primer TP. These proteins form a transient heterodimer, which disassociates after the DNA polymerase has catalyzed the addition of dAMP to the TP and subsequent formation of a short DNA primer. Replication is initiated from both ends of the

## Discussion

---

bacteriophage. When the DNA polymerases meet, the nascent DNA molecules are separated and replication proceeds to complete synthesis of the partially replicated template (Mendez *et al.*, 1997). Replication takes place at the bacterial membrane and a number of membrane associated phage proteins have been identified that anchor the machinery close to the membrane. More recently, bacterial host proteins have been implicated in organization of phage DNA replication (Meijer *et al.*, 2000; Meijer *et al.*, 2005; Munoz-Espin *et al.*, 2009). Recent evidence suggests that the MreB cytoskeleton protein influences both replication and distribution of phage particles. After infection, the  $\Phi$ 29 phage rapidly replicates producing multiple copies of the phage.

The subcellular distribution of  $\Phi$ 29 bacteriophage in the host cell is dynamic during its life cycle (Meijer *et al.*, 2000). Initially after infection, the phage DNA particle associates with the host nucleoid. Interestingly,  $\Phi$ 29 bacteriophage contains five *parS* sequences, and thus binding to the host chromosome could be mediated through interactions with the Spo0J-*oriC* nucleoprotein complex. Additionally, specific binding to the *oriC* regions of the host chromosome could facilitate efficient segregation and subsequently proliferation of the  $\Phi$ 29 bacteriophage.

After initiation of replication, the phage particles spread out occupying different sites around the bacterial nucleoid periphery. The p16.7 protein has been shown to be important for redistribution of replicated phage particles (Serna-Rico *et al.*, 2002; Albert *et al.*, 2005). P16.7 is an integral membrane protein that is expressed early during replication. Although not completely essential, replication efficiency is greatly reduced in the absence of p16.7. More recently, the host actin cytoskeleton together with p16.7 were implicated in attaching replicating  $\Phi$ 29 bacteriophage to the membrane (Munoz-Espin *et al.*, 2009). Similar to p16.7 mutants, in the absence of any of the 3 MreB isoforms, replication of the  $\Phi$ 29 bacteriophage is reduced. Thus,  $\Phi$ 29 bacteriophage makes use of both phage encoded and host specific proteins to act as a scaffold to organize replication of its own DNA.

The question arises, does AlpC help organize induced prophage particles and subsequently lead to more efficient replication, similar to that of p16.7 and the *B. subtilis* actin cytoskeleton proteins? To answer this question, we would need to analyze the distribution of the induced prophage particles during the cell cycle. Although phage particles often appear to be membrane associated, the genome of the CGP3 prophage does not encode a p16.7 homologue. Of course, other putative membrane associated proteins might fulfill a similar function. Additionally, unlike the *B. subtilis* actin homologues (MreB, Mbl and MreH), AlpC does not associate with the membrane. However, according to the localization of AlpC filaments and induced prophage particles in some cells (Fig. 2.23) it could be speculated that AlpC functions in directing phage particles to the membrane. Additional rounds of replication might take place at this subcellular position, and thus explain the decrease in prophage particles in cells lacking *alpC*. Therefore, the subcellular distribution of induced prophage particles in cells lacking *alpC* should be analyzed. However, similar to the  $\Phi$ 29 bacteriophage of *B. subtilis*, AlpC is required for efficient replication of the CGP3 prophage.

#### 4. Experimental Procedures

All the chemicals and reagents used in this study, where supplied from GE healthcare (München), Avanti (Alabaster, USA) BioRad GmbH (München), Fluka (Neu-Ulm), Merck (Darmstadt), Millipore (Eschborn), Roth (Karlsruhe), Schleicher and Schuell (Dassel), Serva (Heidelberg), Sigma (Deisendorf) und Qiagen (Hilden).

**Table 4.1: Plasmids used in this study**

Plasmid	Relevant Characteristics	Source
pETDuet-1	<i>bla PT7lac- PT7 lacI</i>	Novagen
pCD002	<i>bla PT7lac-6his-CFP lacI</i>	This study
pCD010	<i>bla PT7lac-6his-parB-CFP lacI</i>	This study
pCD031	<i>bla PT7-divIVA-S lacI</i>	This study
pCD012	<i>bla PT7-divIVA-GFP lacI</i>	This study
pCD004	<i>bla PT7-GFP lacI</i>	This study
pCD074	<i>bla PT7-divIVA-mCHERRY lacI</i>	This study
pCD013	<i>bla PT7lac-6his-parB-CFP PT7-divIVA-GFP lacI</i>	This study
pCD101	<i>bla PT7lac-6his-parB-CFP PT7-divIVA-S lacI</i>	This study
pCD020	<i>bla PT7lac-6his-parBΔC50-CFP lacI</i>	This study
pCD021	<i>bla PT7lac-6his-parBΔC50-CFP PT7-divIVA-GFP lacI</i>	This study
pCD028	<i>bla PT7lac-6his-parBΔN100-CFP lacI</i>	This study
pCD054	<i>bla PT7lac-6his-parBΔN100-CFP PT7-divIVA-S lacI</i>	This study
pCD046	<i>bla PT7lac-6his-parBΔN21-CFP lacI</i>	This study
pCD080	<i>bla PT7lac-6his-parBΔN21-CFP PT7-divIVA-mCHERRY lacI</i>	This study
pCD071	<i>bla PT7lac-6his-parBΔN20-CFP lacI</i>	This study
pCD072	<i>bla PT7lac-6his-parBΔN20-CFP PT7-divIVA-mCHERRY lacI</i>	This study
pCD083	<i>bla PT7lac-6his-parBR21A-CFP lacI</i>	This study
pCD085	<i>bla PT7lac-6his-parBR21A-CFP PT7-divIVA-mCHERRY lacI</i>	This study
pCD040	<i>bla PT7-divIVA(bsu)-S lacI</i>	This study
pCD048	<i>bla PT7lac-6his-parB(cgl)-CFP PT7-divIVA(bsu)-S lacI</i>	This study
pCD033	<i>bla PT7-divIVAΔ144-298-S lacI</i>	This study
pCD034	<i>bla PT7-divIVAΔ144-298-GFP lacI</i>	This study
pCD035	<i>bla PT7lac-6his-parB-CFP PT7-divIVAΔ144-298-S lacI</i>	This study
pCD036	<i>bla PT7lac-6his-parBΔC50-CFP PT7-divIVAΔ144-298-S lacI</i>	This study
pCD075	<i>bla PT7-divIVAΔ144-298-mCHERRY lacI</i>	This study
pCD077	<i>bla PT7lac-6his-parB-CFP PT7-divIVAΔ144-298-mCHERRY lacI</i>	This study
pCD062	<i>bla PT7-divIVAΔ187-298-S lacI</i>	This study

## Experimental Procedures

Plasmid	Relevant Characteristics	Source
pCD066	<i>bla PT7-divIVA<math>\Delta</math>187-298-GFP lacI</i>	This study
pCD076	<i>bla PT7-divIVA<math>\Delta</math>187-298-mCHERRY lacI</i>	This study
pCD079	<i>bla PT7lac-6his-parB-CFP PT7-divIVA<math>\Delta</math>187-298-mCHERRY lacI</i>	This study
pCD063	<i>bla PT7-divIVA<math>\Delta</math>187-229-S lacI</i>	This study
pCD041	<i>bla PT7-divIVA<math>\Delta</math>187-229-GFP lacI</i>	This study
pCD068	<i>bla PT7lac-6his-parB-CFP PT7-divIVA<math>\Delta</math>187-229-S lacI</i>	This study
pCD049	<i>bla PT7lac-6his-parB<math>\Delta</math>C50-CFP PT7-divIVA<math>\Delta</math>187-229 lacI</i>	This study
pCD060	<i>bla PT7-divIVA<math>\Delta</math>144-229-S lacI</i>	This study
pCD064	<i>bla PT7-divIVA<math>\Delta</math>144-229-GFP lacI</i>	This study
pCD061	<i>bla PT7lac-6his-parB-CFP PT7-divIVA<math>\Delta</math>144-229-S lacI</i>	This study
pCD087	<i>bla PT7-divIVA<math>\Delta</math>160-200-S lacI</i>	This study
pCD107	<i>bla PT7-divIVA<math>\Delta</math>160-200-mCHERRY lacI</i>	This study
pCD105	<i>bla PT7lac-6his-parB-CFP PT7-divIVA<math>\Delta</math>160-200-S lacI</i>	This study
pCD050	<i>bla PT7lac-6his-parB(mtu)-CFP lacI</i>	This study
pCD058	<i>bla PT7-wag31-S lacI</i>	This study
pCD043	<i>bla PT7-wag31-mCHERRY lacI</i>	This study
pCD067	<i>bla PT7lac-6his-parBmtu-CFP PT7-wag31-S lacI</i>	This study
pCD103	<i>bla PT7lac-6his-spo0J-CFP lacI</i>	This study
pCD109	<i>bla PT7lac-6his-spo0J-CFP PT7-divIVA(bsu)-S lacI</i>	This study
pCD104	<i>bla PT7lac-6his-parB(sco)-CFP lacI</i>	This study
pCD102	<i>bla PT7-divIVA(sco)-mCHERRY lacI</i>	This study
pCD113	<i>bla PT7lac-6his-parB(sco)-CFP PT7-divIVA(sco)-mCHERRY lacI</i>	This study
pCD017	<i>bla PT7lac-6his-parA-CFP lacI</i>	This study
pCD018	<i>bla PT7lac-6his-parA-CFP PT7-divIVA-GFP lacI</i>	
<b>pBAD33</b>	p15A cat araC pBAD	Guzman <i>et al.</i> , 1995
pCD090	p15A cat araC pBAD parS	This study
<b>pET16(b)</b>	<i>bla PT7lac-10his lacI</i>	Novagen
pCD114	<i>bla PT7lac-10his-parB lacI</i>	This study
pCD115	<i>bla PT7lac-10his-<math>\Delta</math>alpC lacI</i>	This study
pCD116	<i>bla PT7lac-10his-<math>\Delta</math>alpCD301A lacI</i>	This study
<b>pK19mobsacB</b>	Integration vector, ori pUC, Km <sup>R</sup> , mob sacB	Schäfer <i>et al.</i> , 1994
pK19mobsacB-mCHERRY	Integration vector, ori pUC, Km <sup>R</sup> , mob sacB, mCHERRY	This study
pK19mobsacB-eCFP	Integration vector, ori pUC, Km <sup>R</sup> , mob sacB, eCFP	This study
pCD191	Integration vector, ori pUC, Km <sup>R</sup> , mob sacB divIVA-mCHERRY	This study
pCD120	Integration vector, ori pUC, Km <sup>R</sup> , mob sacB, $\Delta$ parB	This study
pCD121	Integration vector, ori pUC, Km <sup>R</sup> , mob sacB, $\Delta$ pldP	This study

## Experimental Procedures

<b>Plasmid</b>	<b>Relevant Characteristics</b>	<b>Source</b>
pCD122	<i>Integration vector, ori pUC, Km<sup>R</sup>, mob sacB, ΔparA</i>	This study
pCD123	<i>Integration vector, ori pUC, Km<sup>R</sup>, mob sacB parA-cfp</i>	This study
pCD124	<i>Integration vector, ori pUC, Km<sup>R</sup>, mob sacB pldP- cfp</i>	This study
pCD125	<i>Integration vector, ori pUC, Km<sup>R</sup>, mob sacB ftsZ-mCHERRY</i>	This study
pCD126	<i>Integration vector, ori pUC, Km<sup>R</sup>, mob sacB divIVA<math>\Delta</math>144-298-mCHERRY</i>	This study
pCD127	<i>Integration vector, ori pUC, Km<sup>R</sup>, mob sacB eCFP-<i>alpC</i></i>	This study
$\Delta$ <i>alpC</i>	<i>Integration vector, ori pUC, Km<sup>R</sup>, mob sacB, ΔalpC</i>	Julia Frunzke & Antonia Heyer (FZ Jülich)
<b>pK18mob</b>	<i>Integration vector, ori pUC, Km<sup>R</sup>, mob</i>	Schäfer <i>et al.</i> , 1994
pCAT	<i>Integration vector, ori pUC, Km<sup>R</sup>, mob, adhA integration</i>	This study
pCD150	<i>Integration vector, ori pUC, Km<sup>R</sup>, mob, adhA integration +150-<i>pldP-eCFP</i></i>	This study
pEKEX2-CFP	<i>Km<sup>R</sup>, P<sub>tac</sub> lacI<sup>f</sup> pBL1 oriV<sub>C.g</sub>, pUC18 oriV<sub>E.c</sub>, CFP</i>	This study
pEKEX2-eCFP	<i>Km<sup>R</sup>, P<sub>tac</sub> lacI<sup>f</sup> pBL1 oriV<sub>C.g</sub>, pUC18 oriV<sub>E.c</sub>, eCFP</i>	This study
pCD128	<i>Km<sup>R</sup>, P<sub>tac</sub> lacI<sup>f</sup> pBL1 oriV<sub>C.g</sub>, pUC18 oriV<sub>E.c</sub>, ParB<sup>+</sup>-CFP</i>	This study
pCD192	<i>Km<sup>R</sup>, P<sub>tac</sub> lacI<sup>f</sup> pBL1 oriV<sub>C.g</sub>, pUC18 oriV<sub>E.c</sub>, ParB<sup>+</sup>-eCFP</i>	This study
pCD193	<i>Km<sup>R</sup>, P<sub>tac</sub> lacI<sup>f</sup> pBL1 oriV<sub>C.g</sub>, pUC18 oriV<sub>E.c</sub>, ParBR21A<sup>+</sup>-eCFP</i>	This study
pCD129	<i>Km<sup>R</sup>, P<sub>tac</sub> lacI<sup>f</sup> pBL1 oriV<sub>C.g</sub>, pUC18 oriV<sub>E.c</sub>, AlpC<sup>+</sup>-CFP</i>	This study
pCD130	<i>Km<sup>R</sup>, P<sub>tac</sub> lacI<sup>f</sup> pBL1 oriV<sub>C.g</sub>, pUC18 oriV<sub>E.c</sub>, AlpCD301A<sup>+</sup>-CFP</i>	This study
pCD142	<i>Km<sup>R</sup>, P<sub>tac</sub> lacI<sup>f</sup> pBL1 oriV<sub>C.g</sub>, pUC18 oriV<sub>E.c</sub>, SahH<sup>+</sup>-CFP</i>	This study
<b>pMS604</b>	<i>Tc<sup>R</sup>, LexADBD(WT) -Fos leu zipper</i>	Dmitrova <i>et al.</i> , 1998
<b>pDP804</b>	<i>Ap<sup>R</sup>, LexADBD(mutant) -Jun leu zipper</i>	Dmitrova <i>et al.</i> , 1998
pCD131	<i>Tc<sup>R</sup>, LexADBD(WT)-<i>parB</i></i>	This study
pCD132	<i>Ap<sup>R</sup>, LexADBD(mutant)-<i>divIVA</i></i>	This study
pCD133	<i>Tc<sup>R</sup>, LexADBD(WT)-<i>divIVA</i><sub>144-298</sub></i>	This study
pCD134	<i>Tc<sup>R</sup>, LexADBD(WT)-<i>divIVA</i><sub>sco</sub></i>	This study
pCD135	<i>Ap<sup>R</sup>, LexADBD(mutant)-<i>parB</i><sub>sco</sub></i>	This study
pCD136	<i>Tc<sup>R</sup>, LexADBD(WT)-<i>divIVA</i><sub>mtu</sub></i>	This study
pCD137	<i>Ap<sup>R</sup>, LexADBD(mutant)-<i>wag31</i></i>	This study
pCD138	<i>Tc<sup>R</sup>, LexADBD(WT)-<i>alpC</i></i>	This study
pCD139	<i>Tc<sup>R</sup>, LexADBD(WT)-<i>cg1891</i></i>	This study
pCD140	<i>Ap<sup>R</sup>, LexADBD(mutant)-<i>alpC</i></i>	This study
pCD141	<i>Ap<sup>R</sup>, LexADBD(mutant)-<i>cg1891</i></i>	This study

Parental plasmids used are indicated in boldfacing.

## Experimental Procedures

**Table 4.2: Oligonucleotides used in this study**

<b>Oligonucleotides</b>	<b>5' - 3'</b>	<b>Restriction Enzyme</b>
CFP-Sall-F	CATGTCGACATGGTTTCAAAGGCGAA	Sall
CFP-ms-Hind-R	CATAAGCTTTTACTTATAAAGTTCGTC	HindIII
ParB-Bam-F	CAGGGATCCGATGGCTCAGAACAAGGG	BamHI
ParB-Sall-R	CAGGTCGACTTGGCCCTGGATCAAGGA	Sall
ParB-D-N100	CAGGGATCCGCAGCAGGAAGCGCCGCAG	BamHI
ParB-D-N21	CATGGATCCGGGTCTGGCCGCACTTATT	BamHI
ParB-D-N20	CATGGATCCGCGCGGTCTGGCCGCACTT	BamHI
ParB-R21A-F	CGTAAGGGCGGTCTGGGGGCTGGTCTGGCCGCACTTATT	
ParB-R21A-R	AATAAGTGCGGCCAGACCAGCCCCAGACCGCCCTTACG	
ParB-DC-50-R	CAGGTCGACGGAGTTGCAGCCTTTTCG	Sall
DivIVA-NdeI-F	CAGGATATCGATGCCGTTGACTCCAGC	NdeI
DivIVA-EcoRV-R	CAGGATATCGCCTCACCAGATGGCTT	EcoRV
Div-up-R-OH	<b>GGAATGGAGTATGGAAGTTGGGGCCTTTTCAGCTTC</b>	OH
Div-D-F-OH	<b>CCAACTTCCATACTCCATTCCCTCCAGGCAGACGCAGA</b>	OH
Div2-up-R-OH	<b>GGAATGGAGTATGGAAGTTGGCGCTGCCTGCATGTGGGT</b>	OH
Div3-D-F-OH	<b>CCAACTTCCATACTCCATTCCAACCGCACTCTGGAAGAT</b>	OH
Div5-D-F-OH	<b>AGCACCCTAAGGCAGCAGCGTCAGAGGCTCGCTCCGAA</b>	OH
Div-B.s-NdeI-F	CAGCATATGATGCCATTAACGCCAAAT	NdeI
Div-B.s-EcoRV-R	CATGATATCGCTTCTTTTCTCAAATAC	EcoRV
Div-Mt-NdeI-F	CATCATATGATGCCGCTTACACCTGCC	NdeI
Div-Mt-EcoRV-R	CATGATATCGCGTTTTTGCCTCGGTTGAA	EcoRV
Sco-Div-NdeI-F	CAGCATATGCCGTTGACCCCCGAG	NdeI
Sco-Div-EcoRV-R	CAGGATATCGCGTTGTCGTCCTCGTCGAT	EcoRV
B-Mt-SacI-F	CATGAGCTCGATGACCCAGCCGTCACGC	SacI
B-Mt-Sall-R	CATGTCGACCAGAGCGTCCCTGTGCAG	Sall
Spo0J-Bam-F	CAGGGATCCGATGAAGCATTCTCTCT	BamHI
Spo0J-Sall-R	CAGGTCGACTTTTGGTATGCGAATCGT	Sall
Sco-ParB-Eco-F	CAGGAATTCGATGCCGCTGCTACCGAAC	EcoRI
Sco-ParB-Ascl-R	ATAGGCGCGCCGCGGACTCGGCGTCCCCGTC	Ascl
GFP-AatII-F	CATGACGTCATGAGTAAAGGAGAAGAA	AatII
GFP-KpnI-R-ms	CTGGGTACCCTATTTGTATAGTTC	KpnI
mCH-AsiSI-F	GCGATCGCGATGGTGAGCAAGGGCGAG	AsiSI
mCH-KpnI-R	GGTACCCTTACTTGTACAGCTCGTC	KpnI
parS-1-SphI	CTGTTCCACGTGAAACAACCTCGCTCGAGCATGTCA	SphI / HindIII (cut)
parS-1-HindIII	AGCTTGACATGCTCGAGCGAAGTTGTTTACGTTGGAACAGCATG	HindIII / SphI (cut)

## Experimental Procedures

<b>Oligonucleotides</b>	<b>5' - 3'</b>	<b>Restriction Enzyme</b>
divIVA Eco91I F	GCTGGTCACCGGATGCCGTTGACTCCAGCTGATGTG	Eco91I
divIVA EcoRI R	GCTGAATTCCTACTACCAGATGGCTTGTTGTT	EcoRI
mCH-XbaI-F	CATTCTAGAAATGGTGAGCAAGGGCGAG	XbaI
mCH-SalI-Rms	CATGTCGACTTACTTGTACAGCTCGTC	SalI
B-10-SalI-F	CATGTCGACCGTCTAAGAGCGATGGCTCAGAAC	SalI
ParB-BamHI-R	CAGGGATCCTTGCCCTGGATCAAGGA	BamHI
ParB-Eco91I-F	CAGGGTGACCATGGCTCAGAACAAG	Eco91I
parB-XhoI R	CAGCTCGAGTTATTGGCCCTGGATCAA	XhoI
Div-BssHII-F	CAGGCGCGCATGCCGTTGACTCCA	BssHII
Div-Sac-R	CAGGAGCTCTTACTCACCAGATGG	SacI
DivDm1-604-F	CAGGGTGACCAAGGCTGAAGCTAAG	Eco91I
DivDm1-604-R	CAGCTCGAGTTAGAGGGCGTTTGCCTT	XhoI
Dsco-BstEII-F	CAGGGTGACCATGCCGTTGACCCCCGA	Eco91I
Dsco-604-Xho-R	CAGCTCGAGTCAGTTGTCGTCCTC	XhoI
Bsco-804-Xho-F	CAGCTCGAGATGCCGCTGCTACCG	XhoI
Bsco-604-BglII-R	CAGAGATCTTCAGGACTCGGCGTC	BglII
Bmtu-604-F	CAGCCTGCAGGCGATGACCCAGCCGTCA	SbfI
Bmtu-AflII-R	CAGCTTAAGTTACAGAGCGTCCCT	AflII
Wag-625-F	CTTGAAGGCCCGCTAGAGCAGCTGCGT	
Wag-625-R	ACGCAGCTGCTCTAGGCGGCCTTCAAG	
Wag-804-Xho-F	CAGCTCGAGATGCCGCTTACACCT	XhoI
Wag-804-BglII-R	CAGAGATCTCTAGTTTTTGCCTCG	BglII
SahH-ex-F	CAGGGATCCAAAGGAGCTCGCCAGGACATGGCA	BamHI
SahH-ex-R	CAGGGTACCGTAGCGGTAGTGCTCCGGC	KpnI
Δ-ParA-1-F	CAGAAGCTTCTATCGCACGCCAGATC	HindIII
Δ-ParA-1-R	GGAATGGAGTATGGAAGTTGGCGACGTCAACCATCCCTA	OH
ΔParA-2-F	CCAACTTCCATACTCCATTCCAGTAACTTCTTTGAATA	OH
Δ-ParA-2-R	CAGTCTAGACACCAACTCGTCAAGTGC	XbaI
Δ-PldP-1-F	CAGAAGCTTAGGTGTATGACAGGGAAA	HindIII
Δ-PldP-1-R	GGAATGGAGTATGGAAGTTGGAGTCAAACCTTCTTCCTT	OH
Δ-PldP-2-F	CCAACTTCCATACTCCATTCCCACGCCTCCTTGTGCGG	OH
Δ-PldP-2-R	CAGTCTAGACGCGGGAGCAGGCGAGCT	XbaI
Δ-ParB-1-F	CAGAAGCTTGACTGCCACCGTCTTTG	HindIII
Δ-ParB-1-R	<b>GGAATGGAGTATGGAAGTTGGCGCTCTTAGACGCACCTT</b>	OH
ΔParB-2-F	<b>CCAACTTCCATACTCCATTCTTTAAGTTTGGCGCCAT</b>	OH
Δ-ParB-2-R	CAGTCTAGACCTCCACATCAATCAGGC	XbaI
ParA-1-F	CAGAAGCTTGTGGCGGATGCGTTG	HindIII

## Experimental Procedures

<i>Oligonucleotides</i>	5' - 3'	Restriction Enzyme
ParA-1-R	CAGGAATTCTTTTCGCAGGTTTTAGGCC	EcoRI
ParA-2-F	CAGACTAGTTAGCAGTAACTTCTTTG	SpeI
ParA-2-R	CAGTCTAGAACCAACTCGTCAAGTGCC	XbaI
PldP-1-F	CAGAAGCTTTATTGACTTGTCCGCTGC	HindIII
PldP-1-R	CAGGAATTCGTCGTTGACGCGGCTGAT	EcoRI
PldP-2-F	CAGACTAGTTAGGTTGTTTTCTAAAA	SpeI
PldP-2-R	CAGTCTAGACGCAACTTGGTGCACGTG	XbaI
DivIVA-1-F	CAGAAGCTTATGGCAGACCGCCTGACC	HindIII
DivIVA-1-R	CAGGCATGCCTCACCAGATGGCTTGTT	SphI
DivIVA-2-F	CAGTCTAGATAAAAAGAAAGATTAGTT	XbaI
DivIVA-2-R	CAGGAATTCGCTTCCCTTCGTTGACAC	EcoRI
mCH-Sall-F	CAGGTCGACATGGTGAGCAAGGGCGA	Sall
mCH-XbaI-Rms	CATCTCGAGTTACTTGTACAGCTCGTC	XbaI
Z-KI-HinD-upF	CAGAAGCTTGAAGTCAACGCAGCTGCA	HinDIII
FtsZ-KI-SaL-upR	CATGTCGACCTGGAGGAAGCTGGGTAC	Sall
FtsZ-KI-SmaL-dF	CAGCCCGGGTTAAGAAGGAGAATAGAC	SmaI
FtsZ-KI-EcoR-dR	CAGGAATTCGCACCCATGAGCGCATG	EcoRI
Div-D144-298-uF	CAGAAGCTTATGCCGTTGACTCCA	HindIII
Div-D144-298-uR	<b>GGAATGGAGTATGGAAGTTGGGGCCTTTTCAGCTTC</b>	OH
Div-D144-298-dF	<b>CCAACTTCATACTCCATTCCAGGCAGACGCAGAGCGC</b>	OH
mCH-XbaI-R-ms	GCGTCTAGATTACTTGTACAGCTCGTC	XbaI
Alp-up-Hind-F	CAGAAGCTTTGTGGGTGAAGTACT	HindIII
Alp-up-Sal-R	CAGGTCGACCTTGCGTGCTTTTCGC	Sall
Alp-D-Xba-F	CAGTCTAGATAATTAATACCTAGTT	XbaI
Alp-D-Bam-F	CATGGATCCCACTCATTACCGCC	BamHI
eCFP-Sall-F	CATGTCGACATGGTGAGCAAGGGC	Sall
eCFP-XbaI-R	CATCTCGAGCTTGTACAGCTCGTC	XbaI
pEKEX2-B-F	CAGGTCGACATGGCTCAGAACAAGGGT	Sall
ParB-BamHI-R-ns	CAGGGATCCTTGCCCTGGATCAAGGA	BamHI
CFP-SacI-F	CAGGAGCTCATGGTGAGCAAGGGCGAG	SacI
cfp EX2 Eco R mS	GCGGAATTCTTACTTGTACAGCTCGTC	EcoRI
eCFP-SacI-F	CAGGAGCTCATGGTGAGCAAGGGCGA	SacI
eCFP-EcoRI-R	GCGGAATTCTTACTTGTACAGCTCGTC	EcoRI
AlpC-Sall-F	CAGGTCGACATGACCAGCGCTGTGAAT	Sall
AlpC-BamHI-os-R	CAGGGATCCCTTGCGTGCTTTTCGCTGC	BamHI
1890-D301A-F	CGCCACACAATCGGTGTGGCCGTGGGTGAAGGTACTG	
1890-D301A-R	CAGTACCTTCACCCACGGCCACACCGATTGTGTGGCG	

## Experimental Procedures

<b>Oligonucleotides</b>	<b>5' - 3'</b>	<b>Restriction Enzyme</b>
AlpC-et-F	CAG <u>CTCGAG</u> ATGACCAGCGCTGTG	XhoI
AlpC-et-R	CAGGGATC <u>CCTTACTT</u> GCGTGCTTTTCGC	BamHI
Delta-cg1890_1	ATAATGA <u>ATTCTT</u> GTTTTGTCGCTGAATACGGTG	EcoRI
Delta-cg1890_2	<b>CCCATCCACTAAACTTAAACAC</b> ACATTACAGCGCTGGTCATAATC	
Delta-cg1890_3	<b>TGTTTAAGTTTAGTGGATGGG</b> CGCTCGATTGCAGCGAAAGCACG	
Delta-cg1890_4	TATATAGGAT <u>CCAGCGCG</u> CCAAAGAAAACACAGAG	BamHI
Phage-LC-for	CCCACGTTACCCCCACAAACG	
Phage-LC-rev	CTAAAATGAAGCCATCGCGACC	
ddh-LC-for	ACGTGCTGTTCCCTGTGCATGG	
ddh-LC-rev	GCTCGGCTAAGACTGCCGCT	
AdhA-5'-F	CATGA <u>ATTCGGC</u> ACCTGCGAATACTG	EcoRI
AdhA-5'-R	CATGGTAC <u>CCGCAATG</u> ACACGCATGCCCA	KpnI
AdhA-3'-F	CATAAG <u>CTTGTAG</u> ATATTGCCGATGAC	HindIII
AdhA-3'-R	CAGGCTAG <u>CGGCCA</u> AGTCTTGGCGGGT	NheI
+150-PldP-F	CATGGTAC <u>CGTATTGT</u> GGTCGCGGAGA	KpnI
PldP-R-ns	CAT <u>TCTAGAG</u> TCGTTGACGCGGCTGAT	XbaI
eCFP-1-F	CATGT <u>CGACAT</u> GGTGAGCAAGGGCGAG	Sall
eCFP-1-Rms	CATAAG <u>CTTTTACT</u> TGTACAGCTCGT	HindIII

Homologous sequences for crossover PCR (OH) are indicated by boldfacing; restriction sites are indicated by underlining, amino acid mutations on mutagenesis primers are indicated in grey boldfacing.

## Experimental Procedures

**Table 4.3: Bacterial strains used in this study**

Strain	Relevant Characteristics	Source
<i>Corynebacterium glutamicum</i>		
RES 167	restriction deficient <i>C. glutamicum</i> mutant, otherwise considered wild type	Tauch <i>et al.</i> , 2002
ATCC 13032	Biotin-auxotrophic wild type	Kinoshita <i>et al.</i> , 1957
CDC001	RES 167 derivative with in-frame deletion of <i>parA</i>	This study
CDC002	RES 167 derivative with in-frame deletion of <i>pldP</i>	This study
CDC003	RES 167 derivative with in-frame deletion of <i>parB</i>	This study
CDC004	RES 167 derivative with <i>parA</i> -CFP	This study
CDC005	RES 167 derivative with <i>pldP</i> -CFP	This study
CDC006	CDC002 <i>parA</i> -CFP	This study
CDC007	RES 167 derivative with IPTG-inducible extrachromosomal copy of <i>parB</i> -CFP, Kan <sup>R</sup>	This study
CDC008	CDC001 with IPTG-inducible extrachromosomal copy of <i>parB</i> -CFP, Kan <sup>R</sup>	This study
CDC009	CDC002 with IPTG-inducible extrachromosomal copy of <i>parB</i> -CFP, Kan <sup>R</sup>	This study
CDC010	RES 167 derivative with <i>DivIVA-mCHERRY</i>	This study
CDC011	Res 167 $\Delta$ <i>parB</i> , IPTG-inducible extra-chromosomal copy of <i>parB</i> -CFP, Kan <sup>R</sup>	This study
CDC012	Res 167 $\Delta$ <i>parB</i> , <i>divIVA</i> -mCHERRY	This study
CDC013	Res 167 $\Delta$ <i>parB</i> , <i>divIVA</i> -mCHERRY, IPTG-inducible extra-chromosomal copy of <i>parB</i> -eCFP, Kan <sup>R</sup>	This study
CDC014	Res 167 $\Delta$ <i>parB</i> , <i>divIVA</i> -mCHERRY, IPTG-inducible extra-chromosomal copy of <i>parBR21A</i> -eCFP, Kan <sup>R</sup>	This study
CDC015	RES 167 derivative with in-frame deletion of <i>parA</i> and <i>pldP</i>	This study
CDC016	RES 167 derivative with in-frame deletion of <i>parB</i> and <i>pldP</i>	This study
CDC017	RES 167 derivative with <i>DivIVA</i> $\Delta$ 144-298-mCHERRY	This study
CDC018	RES 167 derivative with <i>FtsZ</i> -mCHERRY	This study
CDC019	CDC001 + Res 167 $\Delta$ <i>parB</i> , <i>divIVA</i> -mCHERRY	This study
$\Delta$ <i>alpC</i>	ATCC 13032 with in-frame deletion of <i>alpC</i>	Julia Frunzke and Antonia Heyer (FZ Jülich)
CDC020	ATCC 13032 with eCFP- <i>alpC</i>	This study
CDC021	ATCC 13032, IPTG-inducible extra-chromosomal copy of <i>alpC</i> -CFP, Kan <sup>R</sup>	This study
CDC022	ATCC 13032, IPTG-inducible extra-chromosomal copy of <i>alpCD301A</i> -CFP, Kan <sup>R</sup>	This study
13032::pLAU44-CGP3-Spec	13032 derivative containing plasmid pLAU44-CGP3-Spec integrated into the cg1905-cg1906 intergenic region	Frunzke <i>et al.</i> , 2008
CDC023	CDC20, 13032 derivative containing plasmid pLAU44-CGP3-Spec integrated into the cg1905-cg1906 intergenic region	This study
CDC024	RES 167 derivative with IPTG-inducible extrachromosomal copy of <i>sahH</i> -CFP, Kan <sup>R</sup>	This study
CDC025	CDC002, <i>adhA</i> ::+150- <i>pldP</i> -eCFP Kan <sup>R</sup>	This study

## Experimental Procedures

Strain	Relevant Characteristics	Source
<i>Escherichia coli</i>		
DH5 $\alpha$	F- $\phi$ 80 <i>lacZ</i> .M15( <i>lacZYA-argF</i> )U169 <i>recA1 endA1 hsdR17</i> ( $r_k^-$ , $m_k^+$ ) <i>phoA supE44 thi-1 gyrA96 relA1</i> $\lambda^-$	Invitrogen
BL21(DE3)	F <sup>-</sup> <i>ompT gal dcm lon hsdS<sub>B</sub></i> ( $r_B^-$ $m_B^-$ ) $\lambda$ (DE3 [ <i>lacI lacUV5-T7gene 1 ind1 sam7 nin5</i> ])	Studier and Moffatt, 1986
BL21(DE3)pLysS	F <sup>-</sup> <i>ompT hsdS<sub>B</sub></i> ( $r_B^-$ $m_B^-$ ) <i>gal dcm met</i> (DE3) pLysS (Cam <sup>R</sup> )	Studier and Moffatt, 1986
<i>E. coli</i> SU101	Tn9 Cm <sup>R</sup> for selection of F <sup>+</sup> plasmid, JL1434 lambda-lysogen with <i>lexA</i> operator (wt/wt) <i>sulA</i> -promoter- <i>lacZ</i> fusion, JL1434 <i>lexA71::Tn5(Def)sulA211</i> $\Delta$ <i>lacU169</i> , F' <i>[lacI<sup>q</sup> lacZ</i> $\Delta$ M15::Tn9]	Dmitrova <i>et al.</i> , 1998
<i>E. coli</i> SU202	Tn9 Cm <sup>R</sup> for selection of F <sup>+</sup> plasmid, JL1434 lambda-lysogen with <i>lexA</i> operator (408/wt) <i>sulA</i> -promoter- <i>lacZ</i> fusion, JL1434 <i>lexA71::Tn5(Def)sulA211</i> $\Delta$ <i>lacU169</i> , F' <i>[lacI<sup>d</sup> lacZ</i> $\Delta$ M15::Tn9]	Dmitrova <i>et al.</i> , 1998

**Table 4.4: Overview of *C. glutamicum* strains constructed in this study**

Strain	Plasmid	Primer pairs
CDC001	pCD122	( $\Delta$ -ParA-1- F, $\Delta$ -ParA-1-R) ( $\Delta$ ParA-2- F- $\Delta$ -ParA-2-R)
CDC002	pCD121	( $\Delta$ -PldP-1-F, $\Delta$ -PldP-1-R) ( $\Delta$ -PldP-2-F, $\Delta$ -PldP-2-R)
CDC003	pCD120	( $\Delta$ -ParB-1- F, $\Delta$ -ParB-1-R) ( $\Delta$ ParB-2- F, $\Delta$ -ParB-2-R)
CDC004	pCD123	(ParA-1-F, ParA-1-R) (ParA-2-F, ParA-2-R)
CDC005	pCD124	(PldP-1-F, PldP-1-R) (PldP-2-F, PldP-2-R)
CDC007	pCD128	(pEKEX2-B-F, ParB-BamHI-R-ns) (CFP-SacI-F, cfp EX2 Eco R mS)
CDC010	pCD125	(DivIVA-1-F, DivIVA-1-R) (DivIVA-2-F, DivIVA-2-R) (mCH-Sall-F, mCH-XbaI-Rms)
CDC017	pCD126	(Div-D144-298-uF, Div-D144-298-uR) (Div-D144-298-dF, mCH-XbaI-R-ms)
CDC018	pCD125	(Z-KI-HinD-upF, FtsZ-KI-SaL-upR) (FtsZ-KI-SmaL-dF, FtsZ-KI-EcoR-dR)
CDC020	pCD127	(Alp-up-Hind-F, Alp-up-Sal-R) (Alp-D-Xba-F, Alp-D-Bam-F) (eCFP-Sall-F, eCFP-XbaI-R)
CDC021	pCD129	(AlpC-Sall-F, AlpC-BamHI-os-R) (CFP-SacI-F, cfp EX2 Eco R mS)
CDC022	pCD130	(AlpC-Sall-F, AlpC-BamHI-os-R) (CFP-SacI-F, cfp EX2 Eco R mS) (1890-D301A-F, 1890-D301A-R)
CDC024	pCD142	(SahH-ex-F, SahH-ex-R) (CFP-SacI-F, cfp EX2 Eco R mS)
$\Delta$ <i>alpC</i>	$\Delta$ <i>alpC</i>	(Delta-cg1890_1, Delta-cg1890_2) (Delta-cg1890_3, Delta-cg1890_4)
CDC025	pCD150	(AdhA-5'-F, AdhA-5'-R) (+150-PldP-F, PldP-R-ns) (eCFP-1-F, eCFP-1-Rms) (AdhA-3'-F, AdhA-3'-R)

### 4.1 Strain construction

For the construction of *C. glutamicum* deletion mutants, the method of allelic replacement described by Schäfer *et al.*, 1994, was used (Table 4.4). Derivatives of the vector pK19mobsacB were constructed using the method of cross over PCR after Link *et al.*, 1997. For the allelic replacement, competent *C. glutamicum* cells were transformed with pK19mobsacB derivatives by means of electroporation (van der Rest *et al.*, 1999). Plasmid integration into the genome was verified by selecting kanamycin-resistant and sucrose-sensitive colonies (the expression of the *sacB* gene encoding the levansucrase is toxic in sucrose containing media). To promote re-excision of the plasmid DNA, positive clones were grown overnight in LB broth and subsequently plated on LB agar supplemented with 10 % (w/v) sucrose in different dilutions. Positive colonies obtained from the subsequent selection ( $Km^S$ ,  $Suc^R$ ) were tested for allelic replacement by PCR.

Similarly, to generate *C. glutamicum* stains expressing XFP fusion proteins, as a single copy from the native promoter allelic replacement was employed. pK19mobsacB plasmid derivatives were generated containing homologous sequences of approximately 500 bp upstream and downstream of the desired integration site. The gene encoding the fluorescent protein was cloned in-between the homologous up- and downstream sequences. Allelic replacement was carried out as described above. All strains were confirmed by PCR.

### 4.2 Plasmid construction

Plasmid **pCD010** allows expression of ParB-CFP from pETDuet-1 in *E. coli*. This plasmid was generated by amplifying the CFP gene including the stop codon via PCR from pDR200 (gift from Dr. David Rudner, Harvard Medical School) using primer pair CFP-Sall-F and CFP-ms-Hind-R. The purified fragment was digested with Sall and HindIII and ligated into an equally treated pETDuet-1 vector, giving rise to **pCD002**. The *parB* gene excluding the stop codon was PCR-amplified from *C. glutamicum* genomic DNA using primer pair ParB-Bam-F and ParB-Sall-R. The resulting fragment was digested with BamHI and Sall and ligated into an equally treated pCD002 vector.

Plasmid **pCD031** allows expression of DivIVA with a 3' S-tag fusion from pETDuet-1 in *E. coli*. The *divIVA* gene was amplified from *C. glutamicum* genomic DNA using primer pair DivIVA-NdeI-F and DivIVA-EcoRV-R, purified and digested with NdeI and EcoRV. The resulting product was ligated into an identically cut pETDuet-1 vector, giving rise to an in-frame DivIVA-S-tag expression vector.

Plasmid **pCD012** allows expression of DivIVA-GFP from pETDuet-1 in *E. coli*. The GFP gene including the stop codon was amplified from pSG1154 (Lewis and Marston, 1999) using primer pair GFP-AatII-F and GFP-KpnI-R. The purified product was digested with AatII and KpnI. The pETDuet-1 vector was identically digested and ligated with the digested GFP fragment, giving rise to **pCD004**. A *divIVA* fragment was isolated from pCD031 by restriction digest with NdeI and EcoRV. The resulting

## Experimental Procedures

---

product was ligated into an identically cut pETDuet-1-GFP vector, giving rise to an in-frame DivIVA-GFP expression vector.

Plasmid **pCD074** allows expression of DivIVA-mCHERRY from pETDuet-1 in *E. coli*. The mCHERRY gene including the stop codon was amplified using primer pair mCH-AsiSI-F and mCH-kpnI-R. The purified product was digested with AsiSI and KpnI and ligated into an identically cut pCD031 vector to create an in-frame fusion of mCHERRY to the C-terminus of DivIVA.

Plasmid **pCD013** allows co-expression of ParB-CFP and DivIVA-GFP from pETDuet-1 in *E. coli*. This plasmid was generated by isolating a *parB*-CFP fragment from pCD10 by restriction digestion with BamHI and HindIII. The purified fragment was ligated into an identically cut pCD012 vector.

Plasmid **pCD101** allows co-expression of ParB-CFP and DivIVA-S-tag from pETDuet-1 in *E. coli*. This plasmid was generated by isolating a *parB*-CFP fragment from pCD10 by restriction digestion with BamHI and HindIII. The purified fragment was ligated into an identically cut pCD031 vector.

Plasmid **pCD020** allows expression of ParB $_{\Delta C50}$ -CFP from pETDuet-1 in *E. coli*. Thereby, a *parB* fragment lacking 50 amino acids of the C-terminal domain was amplified with primers ParB-Bam-F and ParB-DC-50-R. The purified product was digested with BamHI and Sall and ligated into an identically cut pCD002 vector.

Plasmid **pCD021** allows co-expression of *parB* $_{\Delta C50}$ -CFP and DivIVA-GFP from pETDuet-1 in *E. coli*. A *parB* $_{\Delta C50}$ -CFP fragment was isolated from pCD020 by restriction digest with BamHI and HindIII. The purified fragment was ligated into an identically cut pCD012 vector.

Plasmid **pCD028** allows expression of ParB $_{\Delta N100}$ -CFP from pETDuet-1 in *E. coli*. Thereby, a *parB* fragment lacking 100 amino acids of the N-terminal domain was amplified with primers ParB-D-N100 and ParB-Sall-R. The purified product was digested with BamHI and Sall and ligated into an identically cut pCD002 vector.

Plasmid **pCD054** allows co-expression of ParB $_{\Delta N100}$ -CFP and DivIVA-S-Tag from pETDuet-1 in *E. coli*. A *parB* $_{\Delta N100}$ -CFP fragment was isolated from pCD028 by restriction digest with BamHI and HindIII. The purified fragment was ligated into an identically cut pCD031 vector.

Plasmid **pCD046** allows expression of ParB $_{\Delta N21}$ -CFP from pETDuet-1 in *E. coli*. A *parB* fragment lacking 21 amino acids of the N-terminal domain was amplified with primers ParB-D-N21 and ParB-Sall-R. The purified fragment was digested with BamHI and Sall and ligated into an identically cut pCD002 vector.

Plasmid **pCD080** allows expression of ParB $_{\Delta N21}$ -CFP and DivIVA-mCHERRY from pETDuet-1 in *E. coli*. A *parB* $_{\Delta N21}$ -CFP fragment was isolated from pCD046 by restriction digest with BamHI and HindIII and ligated into an identically cut pCD074 vector.

Plasmid **pCD071** allows expression of ParB $_{\Delta N20}$ -CFP from pETDuet-1 in *E. coli*. A *parB* fragment lacking 20 amino acids of the N-terminal domain was amplified with primers ParB-D-N20 and ParB-Sall-R. The purified fragment was digested with BamHI and Sall and ligated into an identically cut pCD002 vector.

## Experimental Procedures

---

Plasmid **pCD072** allows co-expression of ParB<sub>ΔN20</sub>-CFP and DivIVA-mCHERRY from pETDuet-1 in *E. coli*. A *parB*ΔN20-CFP fragment was isolated from pCD071 by restriction digest with BamHI and HindIII and ligated into an identically cut pCD074 vector.

The **pCD083** plasmid contains a ParB variant where arginine 21 has been mutated to an alanine and is fused to CFP. Site-directed mutagenesis to create a ParBR21A mutant was done using the QuikChange Site-Directed Mutagenesis Kit (Stratagene) as per the instruction manual. Primer pair ParB-R20A-F and ParB-R20A-R was used for PCR amplification using pCD010 as template.

Plasmid **pCD085** allows co-expression of ParBR21A-CFP and DivIVA-mCHERRY from pETDuet-1 in *E. coli*. A *parBR21A*-CFP fragment was isolated from pCD083 by restriction digest with BamHI and HindIII and ligated into an identically cut pCD074 vector.

Plasmid **pCD040** allows expression of *B. subtilis* DivIVA-S-tag from pETDuet-1 in *E. coli*. The *B. subtilis* *divIVA* gene was PCR amplified using primers Div-B.s-NdeI-F and Div-B.s-EcoRV-R using *B. subtilis* 168 genomic DNA as template. The purified product was digested with NdeI and EcoRV and ligated into an identically cut pETDuet-1 vector.

Plasmid **pCD048** allows expression of *C. glutamicum* ParB-CFP and *B. subtilis* DivIVA-S-tag from pETDuet-1 in *E. coli*. This plasmid was generated by isolating a *parB*-CFP fragment from pCD10 by restriction digestion with BamHI and HindIII. The purified fragment was ligated into an identically cut pCD040 vector.

Plasmids **pCD033** and **pCD034** allows expression of DivIVA<sub>Δ144-298</sub>-S-tag and DivIVA<sub>Δ144-298</sub>-GFP from pETDuet-1 in *E. coli*, respectively. Deletion of a central region of DivIVA (amino acid 144 -298) was carried out as follows; the regions upstream and downstream of the site to be deleted were amplified with prime pair Div-NdeI-F / Div-up-R-OH and Div-D-F-OH / Div-EcoRV-R, respectively. These fragments were designed to contain complementary overhangs (Table 2, bold) and overlap extension PCR was then used to fuse the two fragments. The resulting fragment was restriction digested with NdeI and EcoRV and ligated into an identically cut pETDuet-1 and pCD004 vector, giving rise to pCD033 and pCD034, respectively.

Plasmid **pCD035** allows co-expression of ParB-CFP and DivIVA<sub>Δ144-298</sub>-S-tag from pETDuet-1 in *E. coli*. This plasmid was generated by isolating a *parB*-CFP fragment from pCD010 by restriction digestion with BamHI and HindIII. The purified fragment was ligated into an identically cut pCD033 vector.

Plasmid **pCD036** allows co-expression of ParB<sub>ΔC50</sub>-CFP and DivIVA<sub>Δ144-298</sub>-S-tag from pETDuet-1 in *E. coli*. A ParB<sub>ΔC50</sub>-CFP fragment was isolated from pCD020 by restriction digest with BamHI and HindIII. The purified fragment was ligated into an identically cut pCD033 vector.

Plasmid **pCD077** allows co-expression of ParB-CFP and DivIVA<sub>Δ144-298</sub>-mCHERRY from pETDuet-1 in *E. coli*. A *divIVA*<sub>Δ144-298</sub> fragment was isolated from pCD033 by restriction digest with NdeI and EcoRV and ligated into an identically cut pCD074 vector, replacing full-length *divIVA*, and generating **pCD075**. A *parB*-CFP fragment was isolated from pCD010 by restriction digestion with BamHI and HindIII. The purified fragment was ligated into an identically cut pCD075 vector giving rise to pCD077.

## Experimental Procedures

---

Plasmids **pCD062** and **pCD066** allow expression of DivIVA $_{\Delta 187-298}$ -S and DivIVA $_{\Delta 187-298}$ -GFP from pETDuet-1 in *E. coli*, respectively. The cloning strategy used was similar to generation of pCD033. For fragment amplification primer pairs Div-NdeI-F / Div2-up-R-OH and Div-D-F-OH / Div-EcoRV-R were used. The resulting fragment was restriction digested with NdeI and EcoRV and ligated into an identically cut pETDuet-1 and pCD004 vector, giving rise to pCD062 and pCD066, respectively.

Plasmid **pCD079** allows co-expression of ParB-CFP and DivIVA $_{\Delta 187-298}$ -mCHERRY from pETDuet-1 in *E. coli*. A *divIVA* $_{\Delta 187-298}$  fragment was isolated from pCD062 by restriction digest with NdeI and EcoRV and ligated into an identically cut pCD074 vector, replacing full-length *divIVA*, and generating **pCD076**. Next, a *parB*-CFP fragment was isolated from pCD010 by restriction digestion with BamHI and HindIII and ligated into an identically cut pCD076 plasmid.

Plasmids **pCD063** and **pCD041** allow expression of DivIVA $_{\Delta 187-229}$ -S-tag and DivIVA $_{\Delta 187-229}$ -GFP, respectively from pETDuet-1 in *E. coli*. The cloning strategy used to generate the DivIVA $_{\Delta 187-229}$  is as described for pCD033. Primer pairs Div-NdeI-F / Div2-up-R-OH and Div3-D-F-OH / Div-EcoRV-R were used for PCR amplification. The resulting fragment was restriction digested with NdeI and EcoRV and ligated into an identically cut pETDuet-1 and pCD004 vector, giving rise to pCD063 and pCD041, respectively.

Plasmids **pCD068** and **pCD049** allows co-expression of ParB-CFP and DivIVA $_{\Delta 187-229}$ -S-tag, and ParB $_{\Delta C50}$ -CFP and DivIVA $_{\Delta 187-298}$ -S-tag, respectively from pETDuet-1 in *E. coli*. A *parB*-CFP fragment from pCD010 and a *parB* $_{\Delta C50}$ -CFP fragment from pCD020 were isolated by restriction digestion with BamHI and HindIII. The purified fragment(s) was ligated into an identically cut pCD063 vector.

Plasmids **pCD060** and **pCD064** allow expression of DivIVA $_{\Delta 144-229}$ -S-tag and DivIVA $_{\Delta 144-229}$ -GFP, respectively from pETDuet-1 in *E. coli*. The cloning strategy used to generate the DivIVA $_{\Delta 144-229}$  is as described for pCD033. Primer pairs Div-NdeI-F / Div-up-R-OH and Div3-D-F-OH / Div-EcoRV-R were used for fragment amplification. The resulting fragment was restriction digested with NdeI and EcoRV and ligated into an identically cut pETDuet-1 and pCD004 vector, generating pCD060 and pCD064, respectively.

Plasmid **pCD061** allows co-expression of ParB-CFP and DivIVA $_{\Delta 144-229}$ -S-tag from pETDuet-1 in *E. coli*. This plasmid was generated by isolating a *parB*-CFP fragment from pCD10 by restriction digestion with BamHI and HindIII. The purified fragment was ligated into an identically cut pCD060 vector.

Plasmids **pCD087** and **pCD107** allow expression of DivIVA $_{\Delta 160-200}$ -S-tag and DivIVA $_{\Delta 160-200}$ -mCHERRY from pETDuet-1 in *E. coli*. The cloning strategy used to generate the DivIVA $_{\Delta 160-200}$  is as described for pCD033. Primer pairs Div-NdeI-F / Div3-up-R-OH and Div5-D-F-OH / Div-EcoRV-R were used for fragment amplification. This fragment was restriction digested with NdeI and EcoRV and ligated into an identically cut pETDuet-1 or pCD074 (replacing the full-length *divIVA*), generating pCD087 and pCD107, respectively.

Plasmid **pCD105** allows co-expression of ParB-CFP and DivIVA $_{\Delta 160-200}$ -S-tag from pETDuet-1 in *E. coli*. This plasmid was generated by isolating a *parB*-CFP fragment from pCD10 by restriction

## Experimental Procedures

---

digestion with BamHI and HindIII. The purified fragment was ligated into an identically cut pCD087 vector.

Plasmid **pCD050** allows expression of ParB<sub>mtu</sub>-CFP from pETDuet-1 in *E. coli*. This plasmid was generated by PCR amplifying the ParB<sub>mtu</sub> gene using primer pair B-Mt-SacI-F and B-Mt-SalI-R. The purified fragment was digested with SacI and HindIII and ligated into an equally treated pCD002 vector.

Plasmid **pCD058** allows expression of Wag31-S-tag from pETDuet-1 in *E. coli*. Wag31 was PCR amplified by primer pair Div-Mt-NdeI-F and Div-Mt-EcoRV-R. The purified fragment was digested with NdeI and EcoRV and ligated into an equally treated pETDuet-1 vector.

Plasmid **pCD043** allows expression of Wag31-mCHERRY from pETDuet-1 in *E. coli*. The mCHERRY gene including the stop codon was amplified from pCHYC-2 (Thanbichler *et al.*, 2007) using primer pair mCH-AsiSI-F and mCH-kpnI-R. The purified product was digested with AsiSI and KpnI restriction enzymes and subsequently ligated into an identically cut pCD058 vector to create an in-frame fusion of mCHERRY to the C-terminus of Wag31.

Plasmid **pCD067** allows co-expression of ParB<sub>mtu</sub>-CFP and Wag31-S-tag in *E. coli* from pETDuet-1. A wag31 fragment was isolated from pCD058 by restriction digest with NdeI and EcoRV and ligated into an equally digest pCD050 vector.

Plasmid **pCD103** allows expression of Spo0J-CFP from pETDuet-1 in *E. coli*. A *spo0J* fragment was PCR amplified using primer pair Spo0J-Bam-F and Spo0J-SalI-F. The purified fragment was restriction digested with BamHI and SalI and ligated into an identically treated pCD002 vector.

Plasmid **pCD109** allows co-expression of Spo0J-CFP and DivIVA<sub>bsu</sub>-S-tag from pETDuet-1 in *E. coli*. A *spo0J*-CFP fragment was isolated from pCD103 by restriction digest with BamHI and HindIII and ligated into an identically treated pCD040 vector.

Plasmid **pCD104** allows expression of ParB<sub>sco</sub>-CFP from pETDuet-1 in *E. coli*. A *parB* fragment was PCR amplified using primer pair Sco-ParB-Eco+1F and Sco-ParB-Ascl-R. The purified fragment was digested with EcoRI and Ascl and ligated into an identically treated pCD002 vector.

Plasmid **CD102** allows expression of DivIVA<sub>sco</sub>-mCHERRY from pETDuet-1 in *E. coli*. A *divIVA*<sub>sco</sub> fragment was PCR amplified using primer pair Sco-Div-NdeI-F and Sco-Div-EcoRV-R. The purified fragment was restriction digested with NdeI and EcoRV and ligated into an equally treated pETDuet-1 vector. mCHERRY was subsequently cloned into the resulting vector to create an in-frame fusion of mCHERRY to the C-terminus of DivIVA<sub>sco</sub>.

Plasmid **pCD113** allows co-expression of ParB<sub>sco</sub>-CFP and DivIVA<sub>sco</sub>-mCHERRY from pETDuet-1 in *E. coli*. A *parB*<sub>sco</sub>-CFP fragment was isolated from pCD104 by restriction digestion with EcoRI and Ascl and ligated into an equally treated pCD102 plasmid.

Plasmid **pCD090** contains a consensus *C. glutamicum parS* sequence. Primer pair parS-1-SphI and parS-1-HindIII, which contain the SphI and HindIII cut overhangs were annealed. This fragment was ligated with a SphI / HindIII digested pBAD33. Insertion of *parS* DNA was confirmed by sequencing.

To generate plasmid **pCD191**, which allows allelic replacement at the *divIVA* locus, integrating mCHERRY in frame to the C-terminus of DivIVA, an mCHERRY fragment was amplified by PCR using

## Experimental Procedures

---

primer pair mCHERRY-Sall-F and mCHERRY-XbaI-R-ms. The purified fragment was restriction digested with Sall and XbaI and ligated into an identically cut pK19mobsacB vector. The resulting vector (pK19mobsacB-mCHERRY) is used for allelic replacement, integrating mCHERRY at the C-terminus of a desired locus. Subsequently, homologous flanking sequences 500 base pairs upstream and downstream of the mCHERRY insertion site were amplified using primer pairs DivIVA-HinD-upF / DivIVA-SphI-upR and DivIVA-XbaI-D-F / DivIVA-EcoR-D-R, respectively. The resulting fragments were purified and restriction digested with HindIII / SphI and XbaI / EcoRI, respectively. The upstream and downstream fragments were sequentially ligated into pK19mobsacB-mCHERRY.

Plasmid **pCD192** allows extra-chromosomal, IPTG (isopropyl- $\beta$ -D-thiogalactopyranoside)-inducible expression of ParB with a C-terminal eCFP fusion was constructed by PCR amplification of the *parB* gene, including the ribosome binding site, using the primer pair B-10-Sall-F and ParB-BamHI-R. The purified fragment was ligated into an identically digested pEKEX2-eCFP plasmid.

Plasmid **pCD193** allows extra-chromosomal, IPTG (isopropyl- $\beta$ -D-thiogalactopyranoside)-inducible expression of ParBR21A with a C-terminal eCFP fusion. This plasmid was generated by PCR amplification of the *parBR21A* gene including the ribosome binding site, using pCD083 as template and the primer pair B-10-Sall-F and ParB-BamHI-R. The purified fragment was ligated into an identically digested pEKEX2-eCFP plasmid.

### 4.3 Media and cultivation conditions

*Escherichia coli* cells were grown at 37°C in LB (Luria Bertani) medium (Sambrook *et al.*, 1989) supplemented with, where appropriated, kanamycin 25  $\mu\text{g ml}^{-1}$ , carbenicillin 100  $\mu\text{g ml}^{-1}$  or chloramphenicol 10  $\mu\text{g ml}^{-1}$ . pETDuet-1 plasmids were routinely transformed fresh into *E. coli* BL21(DE3) cells and grown in LB medium prior to microscopic analysis. Cells were grown at 37°C in LB medium to OD<sub>600</sub> 0.5-1.0. Protein expression from the pETDuet-1 vector was induced with 0.1 mM IPTG for 1 hour before analysis, unless otherwise stated.

*C. glutamicum* cells were grown at 30°C in brain-heart-infusion (BHI) medium (Becton-Dickenson), LB medium, CGXII minimal medium with 4 % (w / v) glucose as the carbon and energy source (Keilhauer *et al.*, 1993) or MM1 medium supplemented with 4 % glucose (Nottebrock *et al.*, 2003).

For growth analysis, all strains were cultivated during the day in 5 ml of LB medium and diluted in 10 ml of desired medium and grown overnight. The following day the cultures were diluted to OD<sub>600</sub> of 1.0 and resuspended in fresh medium. Growth of bacterial cultures was measured photometrically at 600 nm (OD<sub>600</sub>). Expression from the pEKEX2 plasmid was induced by addition of 0.5 mM IPTG to the growth medium, for approximately 90 min, unless otherwise stated.

### 4.4 Molecular biological techniques

#### General cloning techniques

DNA was PCR amplified using Phusion polymerase (New England Biolabs). Amplified DNA fragments were purified by use of the NucleoSpin Extract II kit (Macherey-Nagel). Restriction digest was carried out according to the manufacturer's recommendations (NEB, Fermentas). DNA fragments were ligated using T4 DNA ligase at 18°C for one hour (Fermentas). Ligated DNA products were then transformed into *E. coli* DH5 $\alpha$ . Plasmids were verified by sequencing.

#### DNA amplification

*In vitro* amplification of DNA was carried out by polymerase chain reaction (PCR). Template DNA was purified using NucleoSpin® Plasmid Kit (Macherey-Nagel). Oligonucleotides were synthesized by Eurofins MWG Operon. Oligonucleotides were diluted to 10 mM in sterile H<sub>2</sub>O. The amplification was carried out using Phusion polymerase enzyme (New England Biolabs, Ipswich, England) as in the case of fragment amplification. *Taq*-Polymerase (*Taq* PCR Master Mix Kit; Qiagen,) was used to determine correct construct. The PCR reactions consisted of 30 cycles of amplification with a denaturing temperature of 98°C, an annealing temperature ranging between 55°C and 65°C degrees, and an extension temperature of 72°C.

#### Agarose gel electrophoresis and gel extraction

The separation of DNA, plasmids and restriction fragments was carried out, according to Sambrook *et al.*, 1989, in 1 % TAE agarose gel. DNA separation was carried out in 1 x TAE buffer at 100 volts for 45 minutes. Determination of DNA fragment size was determined by a 1-10 kb DNA ladder (GeneRuler™, 1 kb /10 kb DNA Ladder; Fermentas). Where required DNA was extracted from the gel or directly purified using NucleoSpin®-Extract II Kit (Macherey-Nagel).

#### Sequencing

The sequencing of DNA fragments was carried out by GATC Biotech. 300-500 ng of DNA and 10 pmol primers were used for sequencing reactions.

#### Site-directed mutagenesis

Site-directed mutagenesis was carried out using the QuikChange®II Site-Directed Mutagenesis Kit (Stratagene) as per instruction manual.

### DNA quantification

DNA concentration was determined by absorbance measurement in a Tecan NanoQuant plate at 280 nm.

### Overlap extension PCR

Cross over PCR was performed according to Link *et al.*, 1997.

### Preparation of competent cells and transformation

Competent *E. coli* cells were prepared according to Inoue *et al.*, 1990. Competent cells were thawed on ice, incubated with DNA for 30 min on ice and heat shocked for 30-40 s at 42°C. After 10 min cooling on ice, cells were outgrown for 30-60 min at 37°C in 800 ml LB and plated on selective media. Competent *C. glutamicum* cells were prepared as described by Liebl *et al.*, 1989, and transformed by electroporation (2.5 kV, 600  $\Omega$ , 2.5  $\mu$ F) with a MICRO PULSERTM (Bio-Rad, München) (van der Rest *et al.*, 1999).

### Fluorescence microscopy

For phase contrast and fluorescence microscopy, 1-3  $\mu$ l of a culture sample was placed on a microscope slide coated with a thin 1 % agarose layer and covered by a cover slip. Images were taken on a Zeiss AxioImager M1 equipped with a Zeiss AxioCam HRm camera. GFP fluorescence was monitored using filter set 38 HE eGFP, BG-430 fluorescence and CFP (eCFP) were monitored using filter 47 HE CFP, red fluorescence (membrane stain) was monitored by using filter 43 HE Cy3 and DAPI / Hoechst fluorescence was examined with filter set 49. An EC Plan-Neofluar 100x/1.3 Oil Ph3 objective was used. Digital images were acquired and analyzed with the AxioVision 4.6 software (Carl Zeiss). Final image preparation was done using Adobe Photoshop 6.0 (Adobe Systems Incorporated).

### Time-lapse microscopy with microfluidic chamber

Live cell imaging was carried out in B04A microfluidic chamber (Omix, CellASIC). *C. glutamicum* cells were grown in BHI medium overnight. The next morning, cultures were diluted to an OD<sub>600</sub> 1.0 and grown further in shaking flasks to approximately OD<sub>600</sub> 5.0. Cultures were diluted to OD<sub>600</sub> 0.005 – 0.01 prior to loading microfluidic chamber. Cells were loaded to wells with 5 psi for 10 seconds. Nutrient supply was maintained at 3 psi. The temperature was maintained at 30°C. Cells were grown in BHI during time lapse analysis and images were acquired at five minute intervals. Images were taken on a Delta Vision microscope (Applied Precision), using the sofworX software. Final image preparation was done using Velocity and Adobe Photoshop 6.0 (Adobe Systems Incorporated).

### Bacterial Two-Hybrid and $\beta$ -galactosidase -assay

Protein-protein interactions were analyzed by a LexA-based bacterial two-hybrid analysis (Dmitrova *et al.*, 1998). *E. coli* strain SU101 or SU202 was co-transformed with derivatives of pDP804 and pMS604. Heterodimerization of two heterologous proteins was determined by  $\beta$ -galactosidase assays. Therefore, a 5 ml LB culture supplemented with appropriate antibiotics and 1 mM IPTG were inoculated ( $OD_{600}$  0.05) with an overnight culture also containing 1 mM IPTG. After reaching an  $OD_{600}$  of 0.5 - 0.6, 20  $\mu$ l of culture were mixed with 80  $\mu$ l permeabilization buffer (100 mM  $Na_2HPO_4$ , 20 mM KCl, 2 mM  $MgSO_4$ , 0.8 mg  $ml^{-1}$  CTAB, 0.4 mg  $ml^{-1}$  deoxycholic acid (sodium salt), 5.4  $\mu$ l  $ml^{-1}$   $\beta$ -mercaptoethanol) and incubated for 30 min at 30°C. Afterwards 600  $\mu$ l pre-warmed substrate solution (30°C) (60 mM  $Na_2HPO_4$ , 40 mM  $NaH_2PO_4$ , 1 mg  $ml^{-1}$  o-nitrophenyl- $\beta$ -D-galactopyranoside (ONPG), 2  $\mu$ l  $ml^{-1}$   $\beta$ -mercaptoethanol) were added. When the samples turned yellow, the reaction was stopped by adding 700  $\mu$ l of stop solution (1 M  $Na_2CO_3$ ). Subsequently, the samples were centrifuged and the supernatant was measured photometrically at 420 nm. Water was used as blank. Miller units were calculated with the following equation:  $1000 * (OD_{420} / (OD_{600} * \text{volume (0.02 ml)} * \text{reaction time [min]}))$ .

### Determination of circular phage DNA using quantitative PCR

The amount of circular phage DNA was determined by qPCR (Julia Frunzke & Antonia Heyer, FZ Jülich) (Frunzke *et al.*, 2008)

## 4.5 Biochemical methods

### Polyacrylamid gel electrophoresis

SDS-PAGE was performed according to Laemmli (1970) with resolving gels of 5 to 14 % acrylamide / bisacrylamide and 4 % stacking gels (37.5:1, Rotiphorese Gel 30 solution). Samples were prepared by addition of 4 $\times$  sample buffer (150 mM Tris/HCl pH 7.0 / 25° C, 12 % SDS, 6 % 2-mercaptoethanol, 30 % glycerol, 0.05 % Coomassie G-250) and incubation for 30 min at RT. Gels were run in a BioRad Mini-PROTEAN chamber at ~200 V. Coomassie Brilliant Blue (CBB) staining was performed for 15-60 min in 0.02 % Coomassie G-250, 25 % methanol, 10 % acetic acid with subsequent destaining in 10 % acetic acid and a cellulose tissue.

### Immunoblotting

The PVDF membranes were activated a solution consisting 60 % methanol and electrotransfer was performed in 10 mM CAPS, 10 % methanol, pH 11 / 25°C in a semidry blotting chamber at 75 mA per gel for 1 h. Unspecific binding sites were blocked by incubation in 4 % blocking buffer. Subsequently, the membrane was incubated with the primary antibody in TBSM (50 mM Tris, 150 mM NaCl, 5 % fat free milk powder, pH 7.5 / 25°C) at room temperature for 1 h. The membrane was washed three times for 5 min in TBS (50 mM Tris, 150 mM NaCl, pH 7.5 / 25°C) before incubation with alkaline

## Experimental Procedures

phosphatase conjugated secondary antibodies (1:10,000) in TBSM for 30 min. After a second washing cycle, the membrane was developed with NBT/BCIP in 100 mM Tris, 100 mM NaCl, 5 mM MgCl<sub>2</sub>, pH 9.5 / 25°C.

**Table 4.5: Primary antibodies used in this study**

Antibody	Concentration	Source	Reference
α-PentaHis	1:2,000	mouse	Quiagen
α-Strep mAb	1:1,000	mouse	IBA
α-GFP	1:5000	rabbit	lab stock

### Heterologous overexpression and protein purification

#### ParB purification

His<sub>10</sub>-ParB was heterologously overexpressed in BL21 (DE3). Expression was induced by addition of 0.5 mM IPTG and cells were grown in LB medium at 30°C for 3 h. Cells were collected by centrifugation at 5000 *g* (4°C) for 10 min, resuspended in buffer B (50 mM Tris/HCl (pH 7.5), 150 mM NaCl, 150 mM KCl, 10 % glycerol) supplemented with DNase I and protease inhibitor (Complete Roche). Cells were disrupted by using an Emulsiflex C4 (Avestin). Cell debris was removed by centrifugation at 31,000 *g* (4°C) for 45 min. The cleared cell lysate was applied to a 1 ml His Trap™ FF column (GE Healthcare), washed with 20 ml of buffer B and the bound protein was eluted with buffer B supplemented with 250 mM imidazole. Fractions were analyzed by SDS-PAGE and relevant fractions were pooled. The pooled fractions were applied to a Superdex 200 gel filtration column (GE Healthcare) pre-equilibrated with ParB gel filtration buffer (50 mM Tris/HCl (pH 7.5), 150 mM NaCl, 150 mM KCl, 1 mM DTT, 5 mM EDTA, 10 % glycerol). Relevant fractions were analyzed by SDS-PAGE. Purification procedure of ParB mutants was identical.

#### PldP purification

His<sub>10</sub>-PldP was heterologously overexpressed in BL21 (DE3). Expression of His<sub>10</sub>-PldP was induced with 1mM IPTG, at 37°C for 4 hours. Cells were collected by centrifugation at 5000 *g* (4°C) for 10 min, resuspended in buffer P (50 mM Tris-HCl, pH 7.5, 300 mM NaCl, 10 % glycerol, 1 mM DTT and 10 mM imidazole), supplemented with DNase and protease inhibitor. Cells were disrupted by three passes through a French Press. The cleared cell lysate was loaded onto a 1 ml HisTrap™ FF column, washed with 10 column volumes of buffer P and subsequently eluted by a step gradient of buffer P supplemented with 250 mM imidazole. The affinity purified His<sub>10</sub>-PldP was applied to a Superdex™ 200 10/300 gel filtration column and eluted with buffer P. Purity was monitored by SDS-PAGE and immunoblotting.

## Experimental Procedures

---

### AlpC purification

His<sub>10</sub>-AlpC was heterologously overexpressed in BL21 (DE3) pLysS. Expression was induced with 0.4 mM IPTG and expressed at 20°C overnight. Cells were collected by centrifugation at 5000 *g* (4°C) for 10 min, resuspended in buffer A (100 mM Tris-HCl, pH 7.5, 150 mM KCl, 150 mM NaCl, 10 % glycerol and 10 mM imidazole), supplemented with DNase I and protease inhibitor. Cells were disrupted by three passes through a French Press. The cleared cell lysate was applied to a 1 ml HisTrap™ FF column, washed with 10 column volumes of buffer A and subsequently eluted by a step gradient of buffer B supplemented with 500 mM imidazole. The affinity purified AlpC protein was further applied to a Superdex™ 200 10/300 gel filtration column. The purity of the eluted fractions was analyzed by SDS-PAGE and immunoblotting.

### Concentration by ultrafiltration

Protein was concentrated by centrifugation at 3,200 *g* in Amicon concentrators (Millipore) with a MWCO of 10,000. The solutions were mixed repeatedly by pipetting during the concentration process.

### Nucleotide hydrolysis assay

ATPase and GTPase activity was measured in a coupled enzyme assay constantly regenerating GTP (Ingerman *et al.*, 2005). Nucleotide hydrolysis rate of 1 μM protein was measured in a total volume of 100 μl containing varying nucleotide concentration (as indicated in the results section), equimolar MgSO<sub>4</sub>, 50 mM Tris/HCl, 200 mM NaCl, 10 % glycerol, 1 mM PEP, 0.6 mM NADH, 20 U/ml pyruvate kinase and 20 U/ml lactate dehydrogenase. The samples were setup in a 96-well microtiter plate and the absorbance of NADH was monitored at 340 nm for 1 hour at 30°C (Tecan Plate Reader, software: I-control). All data were obtained from triplicate determination and corrected for nucleotide auto-hydrolysis.

### Co-elution assay

Purified His<sub>10</sub>-ParB was applied to a Ni-NTA resin (Macherey-Nagel) and incubated at 4°C for 1 hour. Unbound protein was removed by wash steps with buffer B. The cleared cell lysate of DivIVA-GFP expressing *E. coli* BL21 (DE3) cells was added and incubated for 1 hour at 4°C. Unbound protein was removed by wash steps with buffer B. Interacting protein complexes were eluted with buffer B containing 500 mM imidazole and subsequently analyzed by immunoblotting. His<sub>10</sub>-ParB was detected with α-Penta-His antibody and DivIVA-GFP was detected with α-GFP antibody.

### Pull Down Assay

Pull down assays were carried out using metal affinity chromatography. Thereby, 500  $\mu$ l Ni-NTA resin (Quiagen) was washed 3x with H<sub>2</sub>O and 2x with Pull-down binding buffer. (Centrifugation for 4 min, 2000 g at 4°C). Purified His<sub>10</sub>-PldP was incubated with the Ni-NTA resin on a roller for 1 hour at 4°C. (Centrifugation 3000 g at 4°C).

Wild type *C. glutamicum* cells were resuspended in pull-down buffer supplemented with DNase I and protease inhibitor (Roche) and lysed by Fast Prep (Speed 6.5, for 30 sec, 7x). Cell debris was removed by centrifugation at 8000 g for 5 min at 4°C. 2ml of the whole cell lysate was applied to the His<sub>10</sub>-PldP bound Ni-NTA resin and incubated for 1 hour at 4°C. *C. glutamicum* membranes were isolated by centrifugation at 204,000 g for 1 hour at 4°C. The supernatant containing the cytosolic fraction was used for the pull-down assay. The pellet fraction containing membranes was resuspended in pull-down buffer (10 ml buffer per 1 g membrane), and solubilization was carried out by mixed with 1 % DDM, with stirring for 1 hour at 4°C. Solubilized membranes were isolated by centrifugation at 204,000 g for 30 min at 4°C. The supernatant containing solubilized membranes was used for the pull-down assays. 500  $\mu$ l of each cell fraction was applied to the His<sub>10</sub>-PldP bound Ni-NTA. As a control, His<sub>10</sub>-AlpC was used. The Ni-NTA resin was washed 2x with pull-down buffer. As a negative control each cell fraction was incubated with Ni-NTA in the absence of His<sub>10</sub>-PldP.

Sample and control were incubated for 1 hour at 4°C, rolling. The Ni-NTA was washed 2x with pull-down buffer. (centrifugation for 4 min at 3000 g at 4°C). Complexes were eluted 2x with pull-down buffer supplemented with 500 mM imidazole and 1x with pull-down buffer supplemented with 1 M imidazole. Thereby, the Ni-NTA sample and control were incubated for 10 min in elution buffer at 4°C on a roller (centrifugation 4 min, 3000 g, 4°C). Sample were taken for each wash and elution step and analyzed by SDS-PAGE and immunoblotting. Potential interaction partners were identified by mass spectrometry at the CMMC.

#### **Pull-down buffer**

50 mM Tris-HCl (pH 7.5)  
100 mM NaCl  
1 mM DTT  
10 % glycerol

#### **Pull-down Elution buffer**

50 mM Tris-HCl (pH 7.5)  
100 mM NaCl  
1 mM DTT  
10 % glycerol  
0.5 - 1 M imidazole

### PldP membrane binding

*E. coli* cells expressing His<sub>10</sub>-PldP were resuspended in membrane buffer and disrupted by 3x passes through a French press. Cell debris was removed by centrifugation at 4000 g at 4°C for 10 min. Inclusion bodies were isolated by centrifugation at 10,000 g for 30 min at 4°C. The supernatant was

## Experimental Procedures

---

centrifugation at 204,000 *g* for 1 hour at 4°C to isolate membranes. The pellet fraction containing membranes was resuspended in an equal volume of membrane buffer. Membranes were solubilized with 1 % DDM, gentle stirring at 4°C for 1 hour. Solubilized proteins were isolated centrifugation at 204,000 *g* for 1 hour at 4°C. Samples of supernatant and pellet from each step were analyzed by SDS-PAGE.

### Membrane buffer

50 mM Tris-HCl (pH7.5)

300 mM NaCl

5 mM MgCl<sub>2</sub>

5 mM ATP

1 mM DTT

### Sodium carbonate extraction

Membranes of *E. coli* expressing His<sub>10</sub>-PldP were isolated by centrifugation at 204,000 *g* for 1 hour at 4°C. The membranes were incubated with 500 µl 0.1 M Na<sub>2</sub>CO<sub>3</sub> for 3 hours, stirring at 4°C. Integral membrane proteins were separated from membrane associated proteins by centrifugation at 204,000 *g* for 1 hour at 4°C. Samples were analyzed by SDS-PAGE and immunoblotting.

#### 4. Literature

- Abeles**, A.L., Friedman, S.A., Austin, S.J. 1985. Partition of unit-copy miniplasmids to daughter cells. III. The DNA sequence and functional organization of the P1 partition region. *J Mol Biol* **185**: 261-272.
- Adams**, D.W., Errington, J. 2009. Bacterial cell division: assembly, maintenance and disassembly of the Z-ring. *Nat Rev Microbiol* **7**: 642-653.
- Albert**, A., Muñoz-Espín, D., Jiménez, M., Asenio, J.L., Hermoso, J.A., Salas, M., Meijer, W.J. 2005. Structural basis for membrane anchorage of viral phi 29 DNA during replication. *J Biol Chem* **208**: 42486-42488.
- Aukerlund**, A., Nordström, K., Bernander, R. 1993. Branched *Escherichia coli* cells. *Mol Microbiol* **10**: 849-858.
- Ausmees**, N., Kuhn, J.R., Jacobs-Wagner, C. 2003. The bacterial cytoskeleton: an intermediate filament-like function in cell shape. *Cell* **115**: 705-713.
- Austin**, S., Abeles, A. 1983a. Partition of unit-copy miniplasmids to daughter cells. I. P1 and F miniplasmids contain discrete, interchangeable sequences sufficient to promote equipartition. *J Mol Biol* **169**: 353-372.
- Austin**, S., Abeles, A. 1983b. Partition of unit-copy miniplasmids to daughter cells. II. The partition region of miniplasmid P1 encodes an essential protein and a centromere-like site at which it acts. *J Mol Biol* **169**: 373-387.
- Austin**, S., Nordstrom, K. 1990. Partition-mediated incompatibility of bacterial plasmids. *Cell* **60**: 351-354.
- Autret**, S., Errington, J. 2003. A role for division-site-selection protein MinD in regulation of internucleoid jumping of Soj (ParA) protein in *Bacillus subtilis*. *Mol Microbiol* **47**: 159-169.
- Bartosik**, A.A., Mierzejewska, J., Thomas, C.M., Jagura-Burdzy, G. 2009. ParB deficiency in *Pseudomonas aeruginosa* destabilizes the partner protein ParA and affects a variety of physiological parameters. *Microbiol* **155**: 1080-1092.
- Becker**, E., Herrera, N.C., Gunderson, F.Q., Derman, A.I., Dance, A.L., Sims, J., Larsen, R.A., Pogliano, J. 2006. DNA segregation by the bacterial actin AlfA during *Bacillus subtilis* growth and development. *EMBO J* **25**: 5919-5931.
- Ben-Yehuda**, S., Rudner, D.Z., Losick, R. 2003. RacA, a bacterial protein that anchors chromosomes to the cell poles. *Science* **299**: 532-536.
- Ben-Yehuda**, S., Fujita, M., Liu, X.S., Gorbatyuk, B., Skoko, D., Yan, J., Marko, J.F., Liu, J.S., Eichenberger, P., Rudner, D.Z., Losick, R. 2005. Defining a centromere-like element in *Bacillus subtilis* by identifying the binding sites for the chromosome-anchoring protein RacA. *Mol Cell* **17**: 773-782.
- Bernhardt**, T.G., de Boer, P.A. 2005. SlmA, a nucleoid-associated, FtsZ binding protein required for blocking septal ring assembly over chromosomes in *E. coli*. *Mol Cell* **18**: 555-564.
- Bi**, E.F., Lutkenhaus, J. 1991. FtsZ-ring structure associated with division in *Escherichia coli*. *Nature* **354**: 161-164.
- Blanco**, L., Salas, M. 1984. Characterization and purification of a phage phi 29-encoded DNA polymerase required for the initiation of replication. *Proc Natl Acad Sci U S A* **81**: 5325-5329.

- Bork**, P., Sander, C., Valencia, A. 1992. An ATPase domain common to prokaryotic cell cycle proteins, sugar kinases, actin, and hsp70 heat shock proteins. *Proc Natl Acad Sci U S A* **89**: 7290-7294.
- Bowman**, G.R., Comolli, L.R., Zhu, J., Eckart, M., Koenig, M., Downing, K.H., Moerner, W.E., Earnest, T., Shapiro, L. 2008. A polymeric protein anchors the chromosomal origin/ParB complex at a bacterial cell pole. *Cell* **134**: 945-955.
- Bramkamp**, M., Emmins, R., Weston, L., Donovan, C., Daniel, R.A., Errington, J. 2008. A novel component of the division-site selection system of *Bacillus subtilis* and a new mode of action for the division inhibitor MinCD. *Mol Microbiol* **70**: 1556-1569.
- Bramkamp**, M., van Baarle, S. 2009. Division site selection in rod-shaped bacteria. *Curr Opin Microbiol* **12**: 683-688.
- Britton**, R.A., Chi-Hong Lin, D., Grossman, A.D. 1998. Characterization of a prokaryotic SMC protein involved in chromosome segregation. *Genes Dev* **12**: 1254-1259.
- Brune**, I., Werner, H., Hueser, A.T., Kalinowski, J., Puehler, A., Tauch, A. 2006. The DtxR protein acting as dual transcription regulator directs a global regulatory network involved in iron metabolism of *Corynebacterium glutamicum*. *BMC Genomics* **7**:21.
- Cabeen**, M.T., Jacobs-Wagner, C. 2010. The bacterial cytoskeleton. *Ann Rev Genet* **44**: 365-392.
- Carballido-Lopez**, R., Errington, J. 2003. The bacterial cytoskeleton: *in vivo* dynamics of the actin-like protein Mbl of *Bacillus subtilis*. *Dev Cell* **4**: 19-28.
- Carballido-Lopez**, R., Formatone, A. 2007. Shape determination in *Bacillus subtilis*. *Curr Opin Microbiol* **10**: 611-616.
- Cha**, J.H., Stewart, G.C. 1997. The *divIVA* minicell locus of *Bacillus subtilis*. *J Bacteriol* **179**: 1671-1683.
- Cho**, H., McManus, H.R., Dove, S.L., Bernhardt, T.G. 2011. Nucleoid occlusion factor SlmA is a DNA-activated FtsZ polymerization antagonist. *Proc Natl Acad Sci U S A* **108**: 3773-3778.
- Claessen**, D., Emmins, R., Hamoen, L.W., Daniel, R.A., Errington, J. Edwards, D.H. 2008. Control of the cell elongation-division cycle by shuttling of PBP1 protein in *Bacillus subtilis*. *Mol Microbiol* **68**: 1029-1046.
- Cooper**, S., Helmstetter C.E. 1968. Chromosome replication and the division cycle of *Escherichia coli* B / r. *J Mol Biol* **31**: 519-540.
- Dam**, M., Gerdes, K. 1994. Partitioning of plasmid R1. Ten direct repeats flanking the *parA* promoter constitute a centromere-like partitioning site *parC*, that expresses incompatibility. *J Mol Biol* **236**: 1289-1298.
- Daniel**, R.A, Errington, J. 2003. Control of cell morphogenesis in bacteria: how distinct was to make a rod-shaped cell. *Cell* **113**: 767-776.
- Danilova**, O., Reyes-Lamothe, R., Pinskaya, M., Sherratt, D., Possoz, C. 2007. MukB colocalizes with the *oriC* region and is required for organization of the two *Escherichia coli* chromosome arms into separate cell halves. *Mol Microbiol* **65**: 1485-1492.
- Davey**, M.J., Funnell, B.E. 1994. The P1 plasmid partition protein ParA. A role for ATP in site-specific DNA binding. *J Biol Chem* **269**: 29908-29913.
- Davey**, M.J., Funnell, B.E. 1997. Modulation of the P1 plasmid partitioning protein ParA by ATP, ADP and P1 ParB. *J Biol Chem* **272**: 15286-15292.

## Literature

---

- Davis**, M.A., Martin, K.A., Austin, S.J. 1992. Biochemical activities of the ParA partitioning protein of the P1 plasmid. *Mol Microbiol* **6**: 1141-1147.
- de Boer**, P.A., Crossley, R.E., Rothfield, L.I. 1988. Isolation and properties of *minB*, a complex genetic locus involved in correct placement of the division site in *Escherichia coli*. *J Bacteriol* **170**: 2106-2112.
- de Boer**, P.A., Crosskey, R.E., Rothfield, L.I. 1989. A division inhibitor and a topological specificity factor coded by the minicell locus determine proper placement of the division septum in *E. coli*. *Cell* **56**: 641-649.
- de Boer**, P.A., Crosskey, R.E., Hand, A.R., Rothfield, L.I. 1991. The MinD protein is a membrane ATPase required for the correct placement of the *Escherichia coli* division site. *Embo J* **10**: 4371-4380.
- de Pedro**, M.A., Donachie, W.D., Höltje, J.V. Schwarz, H. 1997. Constitutive septal murein synthesis in *Escherichia coli* with impaired activity of the morphogenetic protein RodA and penicillin-binding protein 2. *J Bacteriol* **183** : 4115-26.
- Derman**, A. I., Becker, E. C., Truong, B. D., Fujioka, A., Tucey, T. M., Erb, M. L., Patterson, P. C., Pogliano, J. 2009. Phylogenetic analysis identifies many uncharacterized actin-like proteins (Alps) in bacteria: regulated polymerization, dynamic instability and treadmilling in Alp7A. *Mol Microbiol*. **73**: 534-552.
- Dmitrova**, M.G., Younes-Cauet, P., Oertel-Buchheit, D., Porte, M., Schnarr, M., Granger-Schnarr, M. 1998. A new LexA-based genetic system for monitoring and analyzing protein heterodimerization in *Escherichia coli*. *Mol Gen Genet* **257**: 205-212.
- Donovan**, C., Schwaiger, A., Krämer, R., Bramkamp, M. 2010. Subcellular localization and characterization of the ParAB system from *Corynebacterium glutamicum*. *J Bacteriol* **192**: 3441-3451.
- Easter**, J. Jr., Gober, J.W. 2002. ParB-stimulated nucleotide exchange regulates a switch in functionally distinct ParA activities. *Mol Cell* **10**: 427-434.
- Ebersbach**, G., Ringgaard, S., Møller-Jensen, J., Wang, Q., Sherratt, D.J., Gerdes, K. 2006. Regular cellular distribution of plasmids by oscillating and filament-forming ParA ATPase of plasmid pB171. *Mol Microbiol* **61**: 1428-1442.
- Edgar**, R., Biek, D., Yarmolinsky, M. 2006. P1 plasmid partition: *in vivo* evidence for the ParA- and ParB-mediated formation of an anchored *parS* complex in the absence of a partner *parS*. *Mol Microbiol* **59**: 276-287.
- Edwards**, D.H., Errington, J. 1997. The *Bacillus subtilis* DivIVA protein targets to the division septum and controls the site specificity of cell division. *Mol Microbiol* **24**: 905-915.
- Ebersbach**, G., Briegel, A., Jensen, G.J., Jacobs-Wagner, C. 2008. A self-associating protein critical for chromosome attachment, division, and polar organization in *Caulobacter*. *Cell* **134**: 956-68.
- Eikmanns**, B.J., Kleinertz, E., Liebl, W., Sahm, H. 1991. A family of *Corynebacterium glutamicum* / *Escherichia coli* shuttle vectors for cloning, controlled gene expression, and promoter probing. *Gene* **102**: 93–98.
- Elouelji-El Kemiri**, S. 2008. Morphologie und Zellteilung in *Corynebacterium glutamicum*. Diplom Thesis, University of Cologne.
- Erdmann**, N., Petroff, T., Funnell, B.E. 1999. Intracellular localization of Pi ParB protein depends on ParA and *parS*. *Proc Natl Acad Sci U S A* **96**: 1490-14910.
- Erickson**, H.P., Taylor, D.W., Taylor, K.A., Bramhill, D. 1996. Bacterial cell division protein FtsZ assembles into protofilament sheets and minirings, structural homologues of tubulin polymers. *Proc Natl Acad Sci U S A* **93**: 519-523.

- Fennell-Fezzie**, R., Gradia, S.D., Akey, D., Berger, J.M. 2005. The MukF subunit of *Escherichia coli* condensing: architecture and functional relationship to kleisins. *EMBO J* **24**: 1921-1930.
- Fiebig**, A., Keren, K., Theriot, J.A. 2006. Fine-scale time-lapse analysis of the biphasic, dynamic behaviour of the two *Vibrio cholerae* chromosomes. *Mol Microbiol* **60**: 1164-1178.
- Figge**, R.M., Easter, J., Gober, J.W. 2003. Productive interaction between the chromosome partitioning proteins, ParA and ParB, is required for the progression of the cell cycle in *Caulobacter crescentus*. *Mol Microbiol* **47**:1225-37.
- Figge**, R.M., Divakaruni, A.V., Gober, J.W. 2004. MreB, the cell shape-determining bacterial actin homologue, co-ordinates cell wall morphogenesis in *Caulobacter crescentus*. *Mol Microbiol* **51**: 1321-1332.
- Firshein**, W. 1989. Role of DNA/membrane complex in prokaryotic DNA replication. *Ann Rev Microbiol* **43**: 89-120.
- Flårdh**, K., Buttner, M.J. 2009. *Streptomyces* morphogenetics: dissecting differentiation in a filamentous bacterium. *Nat Rev Microbiol* **7**: 36-49.
- Fogel**, M.A., Waldor, M.K. 2005. Distinct segregation dynamics of the two *Vibrio cholerae* chromosomes. *Mol Microbiol* **55**: 125-136.
- Fogel**, M.A., Waldor, M.K. 2006. A dynamic mitotic-like mechanism for bacterial chromosome segregation. *Genes Dev* **20**: 3269-3282.
- Friedman**, S.A., Austin, S.J. 1998. The P1 plasmid-partition system synthesizes two essential proteins from an autoregulated operon. *Plasmid* **19**: 103-112.
- Frunzke**, J., Bramkamp, M., Schweitzer, J.E., Bott, M. 2008. Population heterogeneity in *Corynebacterium glutamicum* ATCC 13032 caused by prophage CGP3. *J Bacteriol.* **190**: 5111-5119.
- Fu**, X., Shih, Y.L., Zhang, Y., Rothfield, L.I. 2001. The MinE ring required for proper placement of the division site is a mobile structure that changes its cellular location during the *Escherichia coli* division cycle. *Proc Natl Acad Sci U S A* **98**: 980-985.
- Funnell**, B.E. 1987. Mini-P1 plasmid partitioning: Excess ParB protein destabilizes plasmids containing the centromere *parS*. *J Bacteriol* **170**: 954-960.
- Galkin**, V.E., Orlova, A., Rivera, C., Mullins, R.D., Egelman, E.H. 2009. Structural polymorphism of the ParM filament and dynamic instability. *Structure* **17**: 1253-1264.
- Garner**, E.C., Cambell, C.S., Mullins, R.D. 2004. Dynamic instability in a DNA-segregation prokaryotic actin homolog. *Science* **306**: 1021-1025.
- Garner**, E.C., Cambell, C.S., Weibel, D.B., Mullins, R.D. 2007. Reconstitution of DNA segregation driven by assembly of a prokaryotic actin homolog. *Science* **315**: 1270-1274.
- Gautier**, R., Douguet, D., Antony, B., Drin, G. 2008. HELIQUEST : a web server to screen sequences with specific  $\alpha$ -helical properties. *Bioinformatics* **24**: 2101-2102.
- Gerdes**, K., Molin, S. 1986. Partitioning of plasmid R1. Structural and functional analysis of the *parA* locus. *J Mol Biol* **190**: 269-279.
- Gerdes**, K., Møller-Jensen, J., Bugge Jensen, R. 2000. Plasmid and chromosome partitioning: surprises from phylogeny. *Mol Microbiol* **37**: 455-466.

## Literature

---

- Glaser**, P., Sharpe, M.E., Raether, B., Perego, M., Ohlsen, K., Errington, J. 1997. Dynamic, mitotic-like behaviour of a bacterial protein required for accurate chromosome partitioning. *Genes Dev* **11**: 1160-1168.
- Goley**, E.D., Iniesta, A.A., Shapiro, L. 2007. Cell cycle regulation in *Caulobacter*: location, location, location. *J Cell Sci* **120**: 3501-3507.
- Gorbatyuk**, B., Marczynski, G.t. 2005. Regulated degradation of chromosome replication proteins DnaA and CtrA in *Caulobacter crescentus*. *Mol Microbiol* **55**: 1233-1245.
- Gordon**, G.S., Sitnikow, D., Webb, C.D., Teleman, A., Straight, A., Losick, R., Murray, A.W., Wright, A. 1997. Chromosome and low copy plasmid segregation in *E. coli*: visual evidence for distinct mechanisms. *Cell* **90**: 1113-1121.
- Gouet**, P., Courcelle, E., Stuart, D.I., Metz, F. 1999. ESPript: multiple sequence alignments in PostScript. *Bioinformatics*. **15**: 305-308.
- Gray**, D.I., Gooday, G.W., Prosser, J.I. 1990. *Apical hyphal extension in Streptomyces coelicolor A3(2)*. *J Gen Microbiol* **136**: 1077-1084.
- Gruber**, S., Errington, J. 2009. Recruitment of condensin to replication origin regions by ParA/Spo0J promotes chromosome segregation in *B. subtilis*. *Cell* **137**: 685-696.
- Gullbrand**, B., Akerlund, T., Nordström, K. 1999. On the origin of branches in *Escherichia coli*. *J Bacteriol* **181**: 6607-6614.
- Guzman**, L.M., Belin, D., Carson, M.J., Beckwith, J. 1995. Tight regulation, modulation, and high-level expression by vectors containing the arabinose P<sub>BAD</sub> promoter. *J Bacteriol* **177**: 4121-4130.
- Harry**, E.J. 2001. Bacterial cell division: regulating Z-ring formation. *Mol Microbiol* **40**: 795-803.
- Hayama**, R., Marians, K.J. 2010. Physical and functional interaction between the condensin MukB and the decatenase topoisomerase IV in *Escherichia coli*. *Proc Natl Acad Sci U S A* **107**: 18826-18831.
- Hayes**, F., Radnedge, L., Davis, M.A., Austin, S.J. 1994. The homologous operons for P1 and P7 plasmid partitioning are autoregulated from dissimilar operator sites. *Mol Microbiol* **11**: 249-260.
- Heidelberg**, J.F., Eisen, J.A., Nelson, W.C., Clayton, R.A., Gwinn, M.L., Dodson, R.J., Haft, D.H., Hickey, E.K., Peterson, J.D., Umayam, L., Gill, S.R., Nelson, K.E., Read, T.D., Tettelin, H., Richardson, D., Ermolaeva, M.D., Vamathevan, J., Bass, S., Qin, H., Dragoi, I., Sellers, P., McDonald, L., Utterback, T., Fleishmann, R.D., Nierman, W.C., White, O., Salzberg, S.L., Smith, H.O., Colwell, R.R., Mekalanos, J.J., Venter, J.C., Fraser, C.M. 2000. DNA sequence of both chromosomes of the cholera pathogen *Vibrio cholerae*. *Nature* **406**: 477-483.
- Hempel**, A.M., Wang, S.B., Letek, M., Gil, J.A., Flärdh, K. 2008. Assemblies of DivIVA mark sites for hyphal branching and can establish new zones of cell wall growth in *Streptomyces coelicolor*. *J Bacteriol* **190**: 7579-7583.
- Hermoso**, J.M., Mendez, E., Soriano, F., Salas, M. 1985. Location of the serine residue involved in the linkage between the terminal protein and the DNA of phage phi 29. *Nucleic Acids Res* **13**: 7715-7728.
- Hester**, C.M., Lutkenhaus, J. 2007. Soj (ParA) DNA binding is mediated by conserved arginines and is essential for plasmid segregation. *Proc Natl Acad Sci U S A* **104**: 20326-20331.
- Hirano**, M., Mori, H., Onogi, T., Yamazoe, M., Niki, H., Ogura, T., Hiraga, S. 1998. Autoregulation of the partition genes of the mini-F plasmid and the intercellular localization of their products in *Escherichia coli*. *Mol Genet* **257**: 392-403.

**Hirano, M., Hirano, T.** 2004. Positive and negative regulation of SMC-DNA interactions by ATP and accessory proteins. *EMBO J* **23**: 2664-2673.

**Hirano, M., Hirano, T.** 2006. Opening closed arc: long-distance activation of SMC ATPase by hinge-DNA interactions. *Mol Cell* **21**: 175-186.

**Hu, Z., Lutkenhaus, J.** 1999. Topological regulation of cell division in *Escherichia coli* involves rapid pole to pole oscillation of the division inhibitor MinC under the control of MinD and MinE. *Mol Microbiol* **34**: 82-90.

**Hu, Z., Lutkenhaus, J.** 2000. Analysis of MinC reveals two independent domains involved in interaction with MinD and FtsZ. *J Bacteriol* **182**: 3965-3971.

**Hu, Z., Lutkenhaus, J.** 2003. A conserved sequence at the C-terminus of MinD is required for binding to the membrane and targeting MinC to the septum. *Mol Microbiol* **47**: 345-355.

**Hu, Z., Mukherjee, A., Pichoff, S., Lutkenhaus, J.** 1999. The MinC component of the division site selection system in *Escherichia coli* interacts with FtsZ to prevent polymerization. *Proc Natl Acad Sci U S A* **96**: 14819-14824.

**Inoue, H., Nojima, H., Okayama, H.** 1990. High efficiency transformation of *Escherichia coli* with plasmids. *Gene* **96**: 23-28.

**Iretton, K., Gunther IV, N.W., Grossman, A.D.** 1994. *spo0J*, is required for normal chromosome segregation as well as the initiation of sporulation in *Bacillus subtilis*. *J Bacteriol* **176**: 5320-5329.

**Jakimowicz, D., Gust, B., Zakrzewska-Czerwinska, J., Chater, K.F.** 2005. Developmental-stage-specific assembly of ParB complexes in *Streptomyces coelicolor* hyphae. *J Bacteriol* **187**: 3572-3580.

**Jakimowicz, D., Brzostek, A., Rumijowska-Galewicz, A., Zydek, P., Dolzblasz, A., Smulczyk-Krawczynszyn, A., Zimniak, T., Wojtasz, L., Zawilak-Pawlik, A., Kois, A., Dziadek, J., Zakrzewska-Czerwinska, J.** 2007a. Characterization of the mycobacterial chromosome segregation protein ParB and identification of its target in *Mycobacterium smegmatis*. *Microbiology* **153**: 4050-4060.

**Jakimowicz, D., Zydek, P., Kois, A., Zakrzewska-Czerwinska, J., Chater, K.F.** 2007b. Alignment of multiple chromosomes along helical ParA scaffolding in sporulating *Streptomyces* hyphae. *Mol Microbiol* **65**: 625-41.

**Janniere, L., Canceill, D., Suski, C., Kanga, S., Balmais, B., Lestini, R., Monnier, A.F., Chapuis, J., Bolotin, A., Titok, M., Le Chatelier, E., Ehrlich, S.D.,** 2007. Genetic evidence for a link between glycolysis and DNA replication. *PLoS ONE* **2**: e447.

**Jensen, R.B., Lurz, R., Gerdes, K.** 1998. Mechanism of DNA segregation in prokaryotes: replicon pairing by *parC* of plasmid R1. *Proc Natl Acad Sci U S A* **95**: 8550-8555.

**Jensen, R.B., Shapiro, L.** 1999. The *Caulobacter crescentus smc* gene is required for cell cycle progression and chromosome segregation. *Proc Natl Acad Sci U S A* **96**: 10661-10666.

**Jensen, R.B., Wang, S.C., Shapiro, L.** 2001. A moving DNA replication factory in *Caulobacter crescentus*. *EMBO J* **20**: 4952-4963.

**Jones, L.J., Carballido-Lopez, R., Errington, J.** 2001. Control of cell shape in bacteria: helical, actin-like filaments in *Bacillus subtilis*. *Cell* **104**: 913-922.

**Kabsch, W., Holmes, K. C.** 1995. Protein motifs. The actin fold. *FASEB J.* **9**: 167-174.

**Kadoya, R., Baek, J.H., Sarker, A., Chatteraj, D.K.** 2011. Participation of chromosome segregation protein ParA1 of *Vibrio cholerae* in chromosome replication. *J Bacteriol* **193**: 1504-1514.

## Literature

---

- Kaguni, J.M.** 2006. DnaA: controlling the initiation of bacterial DNA replication and more. *Annu Rev Microbiol* **60**: 351-375.
- Kalinowski, J.** 2005. The genomes of amino acid-producing corynebacteria, p. 37–56. In L. Eggeling and M. Bott (ed.), *Handbook of Corynebacterium glutamicum*. CRC Press, Boca Raton, FL.
- Kang, C.M., Nyayapathy, S., Lee, J.Y., Suh, J.W., Husson, R.N.** 2008. Wag31, a homologue of the cell division protein DivIVA, regulates growth, morphology and polar cell wall synthesis in mycobacteria. *Microbiology* **154**: 725-735.
- Keilhauer, C., Eggeling, L., Sahn, H.** 1993. Isoleucine synthesis in *Corynebacterium glutamicum*: molecular analysis of the *ilvB-ilvN-ilvC* operon. *J Bacteriol* **175**: 5595-55603.
- Keijser, B.J., Noens, E.E., Kraal, B., Koerten, H.K., van Wezel, G.P.** 2003. The *Streptomyces coelicolor ssgB* gene is required for early stages of sporulation. *FEMS Microbiol Lett* **225**: 59-67.
- Kim, S.K., Wang, J.C.** 1999. Localization of F plasmid SopB protein to positions near the poles of *Escherichia coli* cells. *Proc Natl Acad Sci U S A* **95**: 1523-1527.
- Kinoshita, S., Udaka, S., Shimono, M.** 1957. Studies on the amino acid fermentation. Part I production of L-glutamic acid by various microorganisms. *J Gen Appl Microbiol* **3**: 193-205.
- Kirkpatrick, C.L., Viollier, P.H.** 2010. A polarity factor takes the lead in chromosome segregation. *EMBO J* **29**: 3035-3036.
- Kruse, T., Bork-Jensen, J., Gerdes, K.** 2005. The morphogenetic MreBCD proteins of *Escherichia coli* form an essential membrane-bound complex. *Mol Microbiol* **55** : 78-89.
- Lackner, L.L., Raskin, D.M., de Boer, P.A.** 2003. ATP-dependent interactions between *Escherichia coli* Min proteins and the phospholipid membrane *in vitro*. *J Bacteriol* **185**: 735-749.
- Laemmli, U.K.** 1970. Cleavage of structural proteins during the assembly of the head of bacteriophage T4. *Nature* **227**: 680-685.
- Lam, H., Schofield, W.B., Jacobs-Wagner, C.** 2006. A landmark protein essential for establishing and perpetuating the polarity of a bacterial cell. *Cell* **124**: 1011-1023.
- Larkin, M.A., Blackshields, G., Brown, N.P., Chenna, R., McGettigan, P.A., McWilliam, H., Valentin, F., Wallace, I.M., Wilm, A., Lopez, R., Thompson, J.D., Gibson, T.J., Higgins, D.G.** 2007. ClustalW and ClustalX version 2. *Bioinformatics* **23**: 2947-2948.
- Larson, R.A., Cusumano, C., Fujioka, A., Lim-Fong, G., Patterson, P., Pogliano, J.** 2007. Treadmilling of a prokaryotic tubulin-like protein, TubZ, required for plasmid stability in *Bacillus thuringiensis*. *Genes Dev* **21**: 1340-1352.
- Lau, I.F., Filipe, S.R., Søballe, B., Økstad, O-A., Bare, F-A., Sherratt, D.J.** 2003. Spatial and temporal organization of replicating *Escherichia coli* chromosomes. *Mol Micro* **49**: 731-743.
- Lawler, M.L., Brun, Y.V.** 2007. Advantages and mechanisms of polarity and cell shape determination in *Caulobacter crescentus*. *Curr Opin Microbiol* **10**: 630-637.
- Le, Q.B., Ghigo, J.M.** 2009. BcsQ is an essential component of the *Escherichia coli* cellulose biosynthesis apparatus that localizes at the bacterial cell pole. *Mol Microbiol* **72**: 724-740.
- Lee, P.S., Lin, D.C., Moriya, S., Grossman, A.D.** 2003. Effects of the chromosome partitioning protein Spo0J (ParB) on *oriC* positioning and replication initiation in *Bacillus subtilis*. *J Bacteriol* **185**: 1326-1337.

## Literature

---

- Lee, P.S., Grossman, A.D.** 2006. The chromosome partitioning proteins Soj (ParA) and Spo0J (ParB) contribute to accurate chromosome partitioning, separation of replicated sister origins, and regulation of replication in *Bacillus subtilis*. *Mol Microbiol* **60**: 853-869.
- Lenarcic, R., Halbedel, S., Visser, L., Shaw, M., Wu, L.J., Errington, J., Marenduzzo, D., Hamoen, L.W.** 2009. Localisation of DivIVA by targeting to negatively curved membranes. *Embo J.* **28**: 2272-2282.
- Leonard, T.A., Butler, P.J., Löwe, J.** 2004. Structural analysis of the chromosome segregation protein Spo0J from *Thermus thermophilus*. *Mol Microbiol* **53**: 419-432.
- Leonard, T.A., Butler, P.J., Löwe, J.** 2005. Bacterial chromosome segregation: structure and DNA binding of the Soj dimer: a conserved biological switch. *EMBO J* **24**: 270-283.
- Letek, M., Ordóñez, E., Vaquera, J., Margolin, W., Flärdh, K., Mateos, L.M., Gil, J.A.** 2008. DivIVA is required for polar growth in the MreB-lacking rod-shaped actinomycete *Corynebacterium glutamicum*. *J Bacteriol* **190**: 3283-3292.
- Letek, M., Fiuza, M., Ordóñez, E., Villadangos, A.F., Flärdh, K., Mateos, L.M., Gil, J.A.** 2009. DivIVA uses an N-terminal conserved region and two coiled-coil domains to localize and sustain the polar growth *Corynebacterium glutamicum*. *FEMS Microbiol Lett* **297**:110-116.
- Lewis, P.J., and Marston, A.L.** 1999. GFP vectors for controlled expression and dual labelling of protein fusions in *Bacillus subtilis*. *Gene* **227**: 101-110.
- Li, Y., Stewart, N.K., Berger, A.J., Vos, S., Schoeffler, A.J., Berger, J.M., Chait, B.T., Oakley, M.G.** 2010. *Escherichia coli* condensin MukB stimulates topoisomerase IV activity by a direct physical interaction. *Proc Natl Acad Sci U S A* **107**: 18832-18837.
- Libante, V., Thion, L., Lane, D.** 2001. Role of the ATP-binding site of SopA protein in partitioning of the F plasmid. *J Mol Biol* **314**: 387-399.
- Liebl, W., Bayerl, A., Schein, B., Stillner, U., Schleifer, K.H.** 1989. High efficiency electroporation of intact *Corynebacterium glutamicum* cells. *FEMS Microbiol Lett* **53**: 299-303.
- Lin, D.C.-H., Levin, P.A., Grossman, A.D.** 1997. Bipolar localization of a chromosome partitioning protein in *Bacillus subtilis*. *Proc Natl Acad Sci U S A* **94**: 4721-4726.
- Lin, D.C.-H., Grossman, A.D.** 1998. Identification and characterization of a bacterial chromosome partitioning protein in *Bacillus subtilis*. *Proc Natl Acad Sci U S A* **92**: 675-685.
- Lindow, J.C., Kuwano, M., Moriya, S., Grossman, A.D.** 2002. Subcellular localization of the *Bacillus subtilis* structural maintenance of chromosomes (SMC) protein. *Mol Microbiol* **46**: 997-1009.
- Link, A.J., Phillips, D., Church, G.M.** 1997. Methods for generating precise deletions and insertions in the genome of wild-type *Escherichia coli*: application to open reading frame characterization. *J Bacteriol* **179**: 6228-6237.
- Livny, J., Yamaichi, Y., Waldor, M.K.** 2007. Distribution of centromere-like *parS* sites in bacteria: insights from comprehensive genomics. *J Bacteriol* **189**: 8693-8703.
- Löwe, J., Amos, L.A.** 1998. Crystal structure of the bacterial cell-division protein FtsZ. *Nature* **391**: 203-206.
- Löwe, J., Cordell, S.C., van den Ent, F.** 2001. Crystal structure of the SMC head domain: an ABC ATPase with 900 residues antiparallel coiled coil inserted. *J Mol Biol* **360**: 25-35.
- Lutkenhaus, J.** 2008. Min oscillation in bacteria. *Adv Exp Med Biol* **641**: 49-61.

## Literature

---

- Maciag**, M., Nowicki, D., Janniére, L., Szalewska-Palasz, A., Wegrzyn, G., 2011. Genetic response to metabolic fluctuations: correlation between central metabolism and DNA replication in *Escherichia coli*. *Microbial Cell Factories* **10**:19.
- Maloney**, E., Madiraju, M., Rajagopalan, M. 2009. Overproduction and localization of *Mycobacterium tuberculosis* ParA and ParB proteins. *Tuberculosis (Edinb)* **89**: S65-69.
- Marston**, A.L., Thomaidés, H.B, Edwards, D.H., Sharpe, M.E., Errington, J. 1998. Polar localization of the MinD protein of *Bacillus subtilis* and its role in selection of the mid-cell division site. *Genes Dev* **12**: 3419-3430.
- Marston**, A.L., Errington, J. 1999. Dynamic movement of the ParA-like Soj protein of *B. subtilis* and its dual role in nucleoid organization and development regulation. *Mol Cell* **4**: 672-682.
- Mascarenhas**, J., Soppa, J., Strunnikov, A.V., Graumann, P.L. 2002. Cell cycle-dependent localization of two novel prokaryotic chromosome segregatin and condensation proteins in *Bacillus subtilis* that interact with SMC protein. *EMBO J* **21**: 3108-3018.
- McCormick**, J.R., Su, E.P., Driks, A., Losick, R. 1994. Growth and viability of *Streptomyces coelicolor* mutant for the cell division gene *ftsZ*. *Mol Microbiol* **14**: 243-254.
- McCormick**, J.R., Losick, R. 1996. Cell division gene *ftsQ* is required for efficient sporulation but not growth and viability in *Streptomyces coelicolor* A3(2). *J Bacteriol* **178**: 5295-5301.
- McDaniel**, L., Paul, J.H. 2005. Effect of nutrient addition and environmental factors on prophage induction in natural populations of marine *synechococcus* species. *Appl Environ Microbiol* **71**: 842-850.
- McGinness**, T., Wake, R.G. 1979. Division septation in the absence of chromosome termination in *Bacillus subtilis*. *J Mol Biol* **134**: 251-264.
- McNeil**, M.R., Brennan, P.J. 1991. Structure, function and biogenesis of the cell envelope of mycobacteria in relation to bacterial physiology, pathogenesis and drug resistance; some thoughts and possibilities arising from recent structural information. *Res Microbiol* **142**: 451-463.
- Meijer**, W.J., Lewis, P.J., Errington, J., Salas, M. 2000. Dynamic relocalization of phage phi 29 DNA during replication and the role of the viral protein p16.7. *EMBO J* **19**: 4182-4190.
- Meijer**, W.J., Castilla-Llorente, V., Villar, L., Murray, H., Errington, J., Salas, M. 2005. Molecular basis for the exploitation of spore formation as survival mechanism by virulent phage phi 29. *EMBO J* **24**: 3647-3657.
- Mendez**, J., Blanco, L., Salas, M. 1997. Protein-primed DNA replication: a transition between two modes of priming by a inique DNA polymerase. *EMBO J* **16**: 2519-2527.
- Messer**, W. 2002. The bacterial replication initiator DnaA. DnaA and *oriC*, the bacterial mode to initiate DNA replication. *FEMS Microbiol Rev* **26**: 355-374.
- Mohl**, D.A., Gober, J.W. 1997. Cell-cycle dependent polar localization of chromosome partitioning proteins in *Caulobacter crescentus*. *Cell* **88**: 675-684.
- Mohl**, D.A., Easter, J.Jr., Gober, J.W. 2001. The chromosome partitioning protein, ParB, is required for cytokinesis in *Caulobacter crescentus*. *Mol Microbiol* **42**: 741-755.
- Møller-Jensen**, J., Jensen, R.B., Löwe, J., Gerdes, K. 2002. Prokaryotic DNA segregation by an actin-like filament. *EMBO J* **21**: 3119-3127.
- Møller-Jensen**, J., Borch, J., Dam, M., Jensen, R.B., Roepstorff, P., Gerdes, K. 2003. Bacterial mitosis: ParM of plasmid R1 moves DNA by an actin-like insertional polymerization mechanism. *Mol Cell* **12**: 3119-3127.

## Literature

---

- Muñoz-Espín, D, Daniel, R., Kawai, Y., Carballido-López, R., Castilla-Llorente, V., Errington, J., Meijer, W.J., Salas, M.** 2009. The actin-like MreB cytoskeleton organizes viral DNA replication in bacteria. *Proc Natl Acad Sci U S A* **160**: 13347-13352.
- Murray, H., Ferreira, H., Errington, J.** 2006. The bacterial chromosome segregation protein Spo0J spreads along DNA from *parS* nucleation sites. *Mol Microbiol* **61**: 1352-1361.
- Murray, H., Errington, J.** 2008. Dynamic control of the DNA replication initiation protein DnaA by Soj/ParA. *Cell* **135**: 74-84.
- Naito, T., Kusano, K., Kobayashi, I.** 1995. Selfish behaviour of restriction modification systems. *Science* **267**: 897-899.
- Nguyen, L., Scherr, N., Gatfield, J., Walburger, A., Pieters, J., Thompson, C.J.** 2007. Antigen 84, an effector of pleiomorphism in *Mycobacterium smegmatis*. *J Bacteriol* **189**: 7896-7910.
- Nielsen, H.J., Youngren, B., Hansen, F.G., Austin, S.** 2007. Dynamics of *Escherichia coli* chromosome segregation during multifork replication. *J Bacteriol* **189**: 8660-8666.
- Niki, H., Jaffe, A., Imamura, R., Ogura, T., Hiraga, S.** 1991. The new gene *mukB* codes for a 177 kd protein with coiled-coil domains involved in chromosome partitioning in *E. coli*. *EMBO J* **10**: 183-193.
- Niki, H., Hiraga, S.** 1998. Polar localization of the replication origin and terminus in *Escherichia coli* nucleoids during chromosome partitioning. *Genes Dev* **12**: 1036-1045.
- Niki, H., Yamaichi, Y., Hiraga, S.** 2000. Dynamic organization of chromosomal DNA in *Escherichia coli*. *Genes Dev* **14**: 212-223.
- Nishida, S., Fujimistu, K., Sekimizu, K., Ohmura, T., Ueda, T., Katayama, T.** 2002. A nucleotide switch in the *Escherichia coli* DnaA protein initiates chromosomal replication: evidence from a mutant DnaA protein defective in regulatory ATP hydrolysis *in vitro* and *in vivo*. *J Biol Chem* **227**: 14986-14995.
- Nguyen, L., Scherr, N., Gatfield, J., Walburger, A., Pieters, J., Thompson, C.J.** 2007. Antigen 84, an effector of pleiomorphism in *Mycobacterium smegmatis*. *J Bacteriol* **189**: 7896-7910.
- Nottebrock, D., Meyer, U., Kramer, R., Morbach, S.** 2003. Molecular and biochemical characterization of mechanosensitive channels in *Corynebacterium glutamicum*. *FEMS Microbiol Lett* **218**: 305-309.
- Ogura, T., Hiraga, S.** 1983. Partition mechanism of F plasmid: two plasmid gene-encoded products and a *cis*-acting region are involved in partition. *Cell* **32**: 351-360.
- Oliva, M.A., Halbedel, S., Freund, S.M., Dutow, P., Leonard, T.A., Veprintsev, D.B., Hamoen, L.W., Löwe, J.** 2010. Features critical for membrane binding revealed by DivIVA crystal structure. *Embo J* **29**: 1988-2001.
- Patrick, J.E., Kearns, D.B.** 2008. MinJ (YvjD) is a topological determinant of cell division in *Bacillus subtilis*. *Mol Microbiol* **70**: 1166-1179.
- Perry, S.E., Edwards, D.H.** 2006. The *Bacillus subtilis* DivIVA protein has a sporulation-specific proximity to Spo0J. *J Bacteriol* **188**: 6039-6043.
- Polka, J.K., Kollman, J.M., Agard, D.A., Mullins, R.D.** 2009. The structure and assembly dynamics of plasmid actin AlfA imply a novel mechanism of DNA segregation. *J Bacteriol* **191**: 6219-6230.
- Popp, D., Xu, W., Narita, A., Brzoska, A.J., Skurray, R.A., Firth, N., Goshdastider, U., Maéda, Y., Robinson, R. C., Schumacher, M. A.** 2010. Structure and filament dynamics of the pSK41 actin-like ParM protein: implications for plasmid DNA segregation. *J Biol Chem*. **285**: 10130-1040.

- Potluri, L.,** Karczmarek, A., Verheul, J., Piette, A., Wilkin, J.M., Werth, N., Banzhaf, M., Vollmer, W., Young, K.D., Nguyen-Disteche, M., den Blaauwen, T. 2010. Septal and lateral wall localization of PBP5, the major D,D-carboxypeptidase of *Escherichia coli*, requires substrate recognition and membrane attachment. *Mol Microbiol* **77**: 300-323.
- Potluri, L.,** de Pedro, M., Young, K.D. 2012. *E. coli* molecular weight penicillin binding proteins help orient FtsZ, and their absence leads to asymmetric cell division and branching. DOI: 10.1111/j.1365-2958.2012.08023.
- Prentki, P.,** Chandler, M., Caro, L. 1997. Replication of the prophage P1 during the cell cycle of *Escherichia coli*. *Mol Gen Genet* **152**: 71-76.
- Ptacin, J.L.,** Lee, S.F., Garner, E.C., Toro, E., Eckart, M., Comolli, L.R., Moerner, W.E., Shapiro, L. 2010. A spindle-like apparatus guides bacterial chromosome segregation. *Nat Cell Biol* **12**: 791-798.
- Quisel, J.D.,** Lin, D.C.-H., Grossman, A.D. 1999. Control of development by altered localization of a transcription factor in *B. subtilis*. *Mol Cell* **4**: 665-672.
- Radnedge, L.,** Youngren, B., Davis, M.A., Austin, S.A. 1998. Probing the structure of complex macromolecular interactions by homolog specificity scanning: the P1 and P7 plasmid partitioning system. *EMBO J* **17**: 6076-6085.
- Ramamurthi, K.S.,** Losick, R. 2009. Negative membrane curvature as a cue for subcellular localization of a bacterial protein. *Proc Natl Acad Sci U S A* **106**: 13541-13545.
- Ravin, N.V.,** Rech, J., Lane, D. 2003. Mapping of functional domains in F plasmid partition proteins reveals a bipartite SopB-recognition domain in SopA. *J Mol Biol* **329**: 875-889.
- Renfordt, L.** 2011. Funktionelle Charakterisierung der Walker-Typ ATPase PldP aus *Corynebacterium glutamicum*. Bachelor Thesis, University of Cologne.
- Rest, van der, M. E.,** Lange, C., Molenaar, D. 1999. A heat shock following electroporation induces highly efficient transformation of *Corynebacterium glutamicum* with xenogeneic plasmid DNA. *Appl Microbiol Biotechnol* **52**: 541-545.
- Reyes-Lamothe, R.,** Possoz, C., Danilova, O. Sherratt, D.J. 2008. Independent positioning and action of *E. coli* replication forks in living cells. *Cell* **133**: 90-102.
- Ringgaard, S.,** van Zon, J., Howard, M., Gerdes, K. 2009. Movement and equipositioning of plasmids by ParA filament disassembly. *Proc Natl Acad Sci U S A* **106**: 19369-19374.
- Ringgaard, S.,** Schirmer, K., Davis, B.M., Waldor, M.K. 2011. A family of ParA-like ATPases promotes cell pole maturation by facilitating polar localization of chemotaxis proteins. *Genes Dev* **25**: 1544-1555.
- Saitoh, N.,** Goldberg, I.G., Wood, E.R., Earnshaw, W.C. 1994. ScII: an abundant chromosome scaffold protein is a member of a family of putative ATPases with an unusual predicted tertiary structure. *J Cell Biol* **127**: 303-318.
- Salje, J.,** Löwe, J. 2008. Bacterial actin: architecture of the ParMRC plasmid DNA partitioning complex. *EMBO J* **27**: 2230-2238.
- Salje, J.,** Gayathri, P., Löwe, J. 2010. The ParMRC system: molecular mechanism of plasmid segregation by actin-like filaments. *Nat Rev Microbiol* **8**: 683-692.
- Sambrook, J.,** Fritsch, E.F., Maniatis, T. 1989. Molecular cloning: a laboratory manual (2<sup>nd</sup> edition). Cold Spring Harbor Laboratory Press, New York.

## Literature

---

- Savage**, D.F., Afonso, B., Chen, A.H., Silver, P.A. 2010. Spatially ordered dynamics of the bacterial carbon fixation machinery. *Science* **327**: 1258-1261.
- Schwaiger**, A. 2009. Zellteilung und Chromosomensegregation in *Corynebacterium glutamicum*. PhD Thesis, University of Cologne.
- Schäfer**, A., Schwarzer, A., Kalinowski, J., Pühler, A. 1994. Cloning and characterization of a DNA region encoding a stress-sensitive restriction system from *Corynebacterium glutamicum* ATCC 13022 and analysis of its role in intergeneric conjugation with *Escherichia coli*. *J Bacteriol* **176**: 7309-7319.
- Schofield**, W.B., Lim, H.C., Jacobs-Wagner, C. 2010. Cell cycle coordination and regulation of bacterial chromosome segregation dynamics by polarly localized proteins. *EMBO J* **29**: 3068-3081.
- Scholefield**, G., Whiting, R., Errington, J. Murray, H. 2011. Spo0J regulates the oligomeric state of Soj to trigger its switch from an activator to an inhibitor of DNA replication initiation. *Mol Microbiol* **79**: 1365-2958.
- Scholefield**, G., Errington, J. Murray, H. 2012. Soj/ParA stalls DNA replication by inhibiting helix formation of the initiator protein DnaA. *EMBO J* **31**: 1542-1555.
- Schwartz**, M.A., Shapiro, L. 2011. An SMC ATPase mutant disrupts chromosome segregation in *Caulobacter*. *Mol Microbiol* **82**: 1359-1374.
- Schwedock**, J., McCormick, J.R., Angert, E.R., Nodwell, J.R., Losick, R. 1997. Assembly of the cell division protein FtsZ into ladder like structures in the aerial hyphae of *Streptomyces coelicolor*. *Mol Microbiol* **25**: 847-858.
- Serna-Rico**, A., Salas, M., Meijer, W.J. 2002. The *Bacillus subtilis* phage phi 29 protein p16.7 involved in phi 29 DNA replication, is a membrane-localized single-stranded DNA-binding protein. *J Biol Chem* **277**: 6733-3342.
- Sheldrich**, G.M., Jones, P.G., Kennard, O., Williams, D.H., Smith, G.A. 1978. Structure of vancomycin and its complex with acetyl-D-alanyl-D-alanine. *Nature* **271**: 233-225.
- Sherratt**, D. 2003. Bacterial chromosome dynamics. *Science* **301**: 780-785.
- Soppa**, J., Kobayashi, K., Noirot-Gros, M.F., Oesterhelt, D., Ehrlich, S.D., Dervyn, E., Ogasawara, N., Moriya, S. 2002. Discovery of two novel families of proteins that are proposed to interact with prokaryotic SMC proteins, and characterization of the *Bacillus subtilis* family members ScpA and ScpB. *Mol Microbiol* **45**: 59-71.
- Strahl**, H., Hamoen, L.W. 2010. Membrane potential is important for bacterial cell division. *Proc Natl Acad Sci U S A* **107**: 12281-12286.
- Studier**, F.W., Moffatt, B.A. 1986. Use of bacteriophage T7 RNA polymerase to direct selective high-level expression of cloned genes. *J Mol Biol* **189**: 113-130.
- Sullivan**, N.L., Marquis, K.A., Rudner, D.Z. 2009. Recruitment of SMC to the origin by ParB-parS organizes the origin and promotes efficient chromosome segregation. *Cell* **137**: 697-707.
- Sutton**, M.D., Carr, K.M., Vicente, M., Kaguni, J.M., 1998. *Escherichia coli* DnaA protein: the N-terminal domain and loading of DnaB helicase at the *E. coli* chromosomal origin. *J Biol Chem* **273**: 34255-34262.
- Surtees**, J.A., Funnell, B.E. 1999. P1 ParB domain structure includes two independent multimerization domains. *J Bacteriol* **181**: 5898-5908.

- Szeto**, T.H., Rowland, S.L., Rothfield, L.I., King, G.F. 2002. Membrane localization of MinD is mediated by a C-terminal motif that is conserved across eubacterial, archaea, and chloroplasts. *Proc Natl Acad Sci U S A* **99**: 15693-15698.
- Tanaka**, T. 2010. Functional analysis of the stability determinant AlfB of pBET131, a miniplasmid derivative of *Bacillus subtilis* (natto) plasmid pLS32. *J Bacteriol* **192**: 1221-1230.
- Tauch**, A., Kirchner, O., Löffler, B., Götter, S., Pühler, A., Kalinowski, J. 2002. Efficient electrotransformation of *Corynebacterium diphtheriae* with a Mini-Replicon derived from the *Corynebacterium glutamicum* plasmid pGA1. *Current Microbiology* **45**: 362–367.
- Thanbichler**, M., Shapiro, L. 2006. MipZ, a spatial regulator coordinating chromosome segregation with cell division in *Caulobacter*. *Cell* **126**: 147-162.
- Thompson**, S.R., Wadhams, G.H., Armitage, J.P. 2006. The positioning of cytoplasmic protein clusters in bacteria. *Proc Natl Acad Sci U S A* **103**: 8209-8214.
- van Baarle**, S., Bramkamp, M. 2010. The MinCDJ system in *Bacillus subtilis* prevents minicell formation by promoting divisome disassembly. *PLoS ONE* 5: e9850.
- van den Ent**, F., Löwe, J. 2000. Crystal structure of the cell division protein FtsA from *Thermotoga maritime*. *EMBO J* **19**: 5300-5307.
- van den Ent**, F., Amos, L., Löwe, J. 2001. Prokaryotic origin of the actin cytoskeleton. *Nature* **413**: 39-44.
- van den Ent**, F., Møller-Jensen, J., Amos, L.A., Löwe, J. 2002. F-actin-like filaments formed by plasmid segregation protein ParM. *EMBO J* **21**: 6935-6943.
- van Wezel**, G.P., van der Meulen, J., Taal, E., Koerten, H., Kraal, B. 2000. Effects of increased and deregulated expression of cell division genes on the morphology and on antibiotic production of streptomycetes. *Antonie van Leeuwenhoek* **78**: 269-276.
- Vecchiarelli**, A.G., Han, Y-W., Tan, X., Mizuuchi, M., Ghirlando, R., Biertümpfel, C., Funnell, B.E., Mizuuchi, K. 2010. ATP control of dynamic P1 ParA-DNA interactions: a key role for the nucleoid in plasmid partition. *Mol Microbiol* **78**: 78-91.
- Viollier**, P.H., Thanbichler, M., McGrath, P.T., West, L., Meewan, M., McAdams, H.H., Shapiro, L. 2004. Rapid and sequential movement of individual chromosomal loci to specific subcellular locations during bacterial DNA replication. *Proc Natl Acad Sci U S A* **101**: 9257-9262.
- Volkov**, A., Mascarenhas, J., Andrei-Selmer, C., Ulrich, H.D., Graumann, P.L. 2003. A prokaryotic condensin/cohesin-like complex can actively compact chromosomes from a single position on the nucleoid and binds to DNA as a ring-like structure. *Mol Microbiol* **23**: 5638-5650.
- Wang**, X., Lutkenhaus, J. 1993. The FtsZ protein of *Bacillus subtilis* is localized at the division site and has GTPase activity that is dependent upon FtsZ concentration. *Mol Micro* **9**: 435-442.
- Wang**, S.B., Cantlay, S., Nordberg, N., Letek, M., Gil, J.A., Flärdh, K. 2009. Domains involved in the *in vivo* function and oligomerization of apical growth determinant DivIVA in *Streptomyces coelicolor*. *FEMS Microbiol Lett* **297**: 101-109.
- Wang**, X., Sherratt, D.J. 2010. Independent segregation of the two arms of the *Escherichia coli* ori region requires neither RNA synthesis nor MreB dynamics. *J Bacteriol* **129**: 6143-6153.
- Webb**, C.D., Teleman, A., Gordon, S., Straight, A., Belmont, A., Lin, D.C., Grossman, A.D., Wright, A., Losick, R. 1997. Bipolar localization of the replication origin regions of chromosomes in vegetative and sporulating cells of *B. subtilis*. *Cell* **88**: 667-674.

## Literature

---

- Webb**, C.D., Graumann, P.L., Kahana, J.A., Teleman, A.A., Silver, P.A., Losick, R. 1998. Use of time-lapse microscopy to visualize rapid movement of the replication origin region of the chromosome during the cell cycle in *Bacillus subtilis*. *Mol Microbiol* **28**: 883-892.
- Wennerhold**, J., Bott, M. 2006. The DtxR regulon of *Corynebacterium glutamicum*. *J Bacteriol* **188**: 2907-18.
- Williams**, K.P. 2002. Integration sites for genetic elements in prokaryotic tRNA and tmRNA genes: sublocation preference of integrase subfamilies. *Nucleic Acid Res* **30**: 866-875.
- Willemse**, J., Borst, J.W., de Waal, E., Bisseling, T., van Wezel, P. 2010. Positive control of cell division: FtsZ is recruited by SsgB during sporulation of *Streptomyces*. *Genes Dev* **25**: 89-99.
- Woldringh**, C.L., Zaritsky, A., Grover, N.B. 1994. Nucleoid partitioning and the division plane in *Escherichia coli*. *J Bacteriol* **176**: 6030-6038.
- Woldringh**, C.L., Mulder, E., Valkenburg, J.A.C., Wientjes, F.B., Zaritsky, A., Nanninga, N. 1990. Role of nucleoid in toporegulation of division. *Res Microbiol* **141**: 39-49.
- Wu**, L.J., Errington, J. 1998. Use of asymmetric cell division and *spolIIE* mutants to probe chromosome orientation and organization in *Bacillus subtilis*. *Mol Microbiol* **27**: 777-786.
- Wu**, L.J., Errington, J. 2003. RacA and the Soj-Spo0J system combine to effect polar chromosome segregation in sporulating *Bacillus subtilis*. *Mol Microbiol* **49**: 1463-1475.
- Wu**, L.J., Errington, J. 2004. Coordination of cell division and chromosome segregation by a nucleoid occlusion protein in *Bacillus subtilis*. *Cell* **117**: 915-925.
- Wu**, L.J., Ishikawa, S., Kawai, Y., Oshima, T., Ogasawara, N., Errington, J. 2009. Noc protein binds to specific DNA sequences to coordinate cell division with chromosome segregation. *EMBO J* **28**: 1940-1952.
- Wu**, W., Park, K.T., Holyoak, T., Lutkenhaus, J. 2011. Determination of the structure of the MinD-ATP complex reveals the orientation of MinD on the membrane and the relative location of the binding sites for MinE and MinC. *Mol Microbiol* **79**: 1515-1528.
- Yamanaka**, K., Ogura, T., Niki, H., Hiraga, S. 1996. Identification of two new genes, *mukE* and *mukF*, involved in chromosome partitioning in *Escherichia coli*. *Mol Gen Genet* **250**: 241-251.
- Yamaichi**, Y., Niki, H. 2000. Active segregation by the *Bacillus subtilis* partitioning system in *Escherichia coli*. *Proc Natl Acad Sci U S A* **97**: 14656-14661.
- Yamaichi**, Y., Fogel, M.A., Mcleod, S.M., Hui, M.P., Waldor, M.K. 2007. Distinct centromere-like *parS* sites on the two chromosomes of *Vibrio spp.* *J Bacteriol* **198**: 5314-5324.
- Young**, K.D. 2003. Bacterial shape. *Mol Microbiol* **49**: 571-580.

6. Supplementary Figures

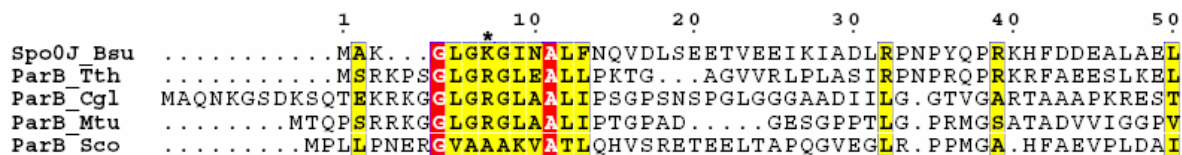


**Figure S1: Sequence alignment of ParB proteins.** Sequence alignments of the N-terminal regions of ParB proteins demonstrate a highly conserved stretch of aliphatic residues. Interestingly, except for *S. coelicolor* ParB, all sequences contain a universally conserved basic (Lys/Arg) residue. In *C. glutamicum*, the N-terminal region of ParB is necessary for interaction with DivIVA. (Bsu – *Bacillus subtilis*, Tth – *Thermus thermophilus*, Cgl – *Corynebacterium glutamicum*, Mtu – *Mycobacterium tuberculosis*, Sco – *Streptomyces coelicolor*). Alignments were generated with ClustalW (Larkin *et al*, 2007) and the figure was prepared using the program ESPript (Gouet *et al*, 1999).

## Supplementary Figures

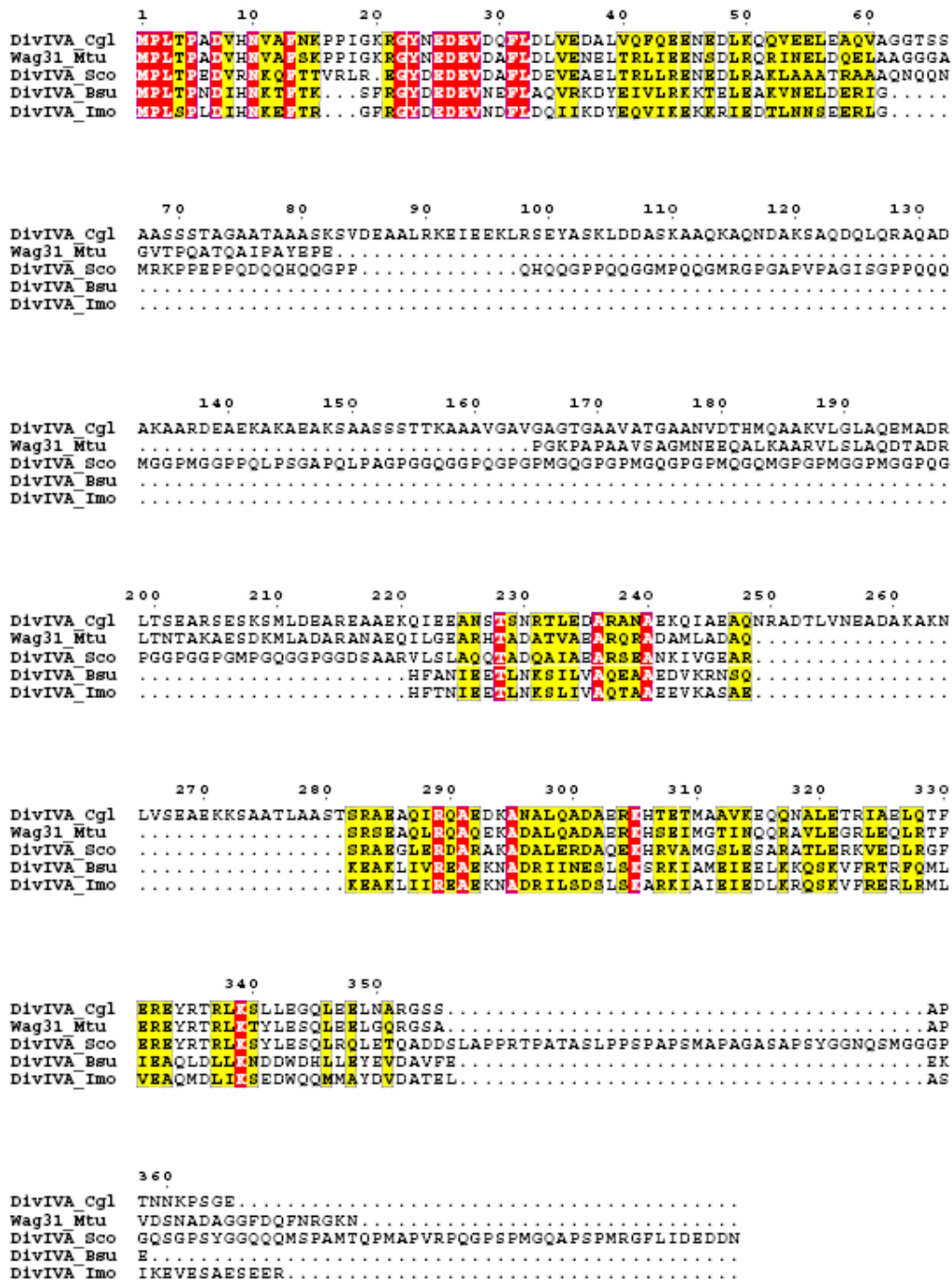


**Figure S2: Sequence alignment of various DivIVA homologues from different species.** The N-terminal regions exhibit a high degree of homology, likely required for membrane association (Lenarcic *et al.*, 2009; Oliva *et al.*, 2010). The Actinobacteria DivIVA proteins contain central insertions that are absent in *B. subtilis* and *L. monocytogenes* DivIVA. In *C. glutamicum* this central region of DivIVA is necessary for ParB interaction. *S. coelicolor* DivIVA contains a PQG rich domain that is specific for *Streptomyces* (Wang *et al.*, 2009). (Cgl – *Corynebacterium glutamicum*, Mtu – *Mycobacterium tuberculosis*, Sco – *Streptomyces coelicolor*, Bsu – *Bacillus subtilis* and Imo – *Listeria monocytogenes*). Alignments were generated with ClustalW (Larkin *et al.*, 2007) and the figure was prepared using the program ESPript (Gouet *et al.*, 1999).

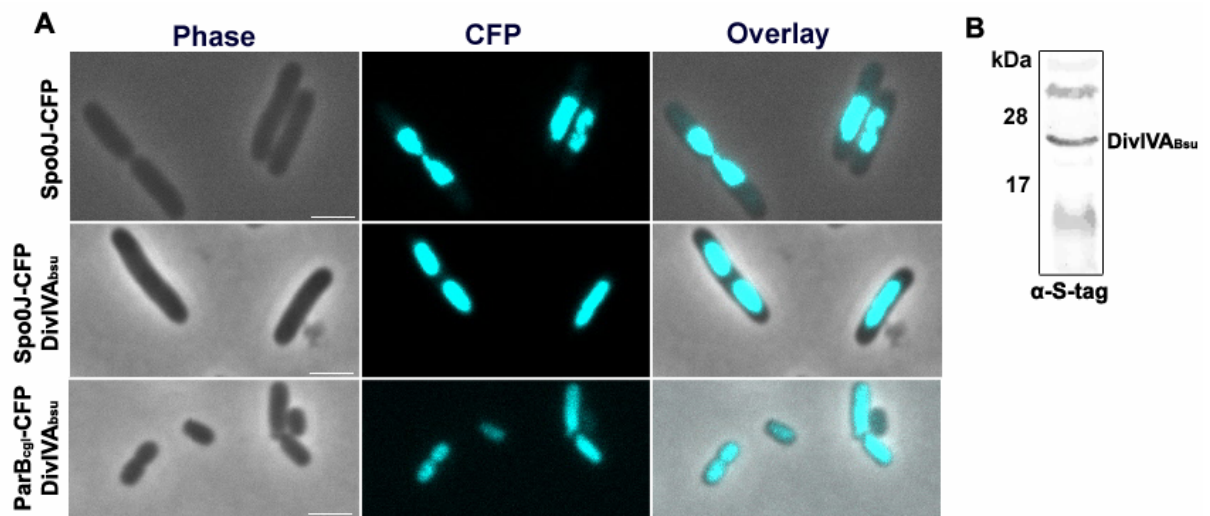


**Figure S3: *B. subtilis* DivIVA does not interact directly with Spo0J and does not recruit *C. glutamicum* ParB.** (A) Spo0J-CFP localizes as patches over the chromosome in *E. coli* (upper panel). (B) Co-expression of *B. subtilis* DivIVA (DivIVA<sub>bsu</sub>), without a fluorescent tag, and Spo0J-CFP in *E. coli* reveal that these proteins do not interact directly (middle panel). As a control, DivIVA<sub>bsu</sub> was co-expressed with *C. glutamicum* ParB-CFP (ParB<sub>cgl</sub>). In *E. coli*, these proteins do not interact (lower panel). (B) DivIVA<sub>bsu</sub> expression was verified by immunoblotting and detection with α-S-tag antibodies (right). Scale bar, 2 μm.

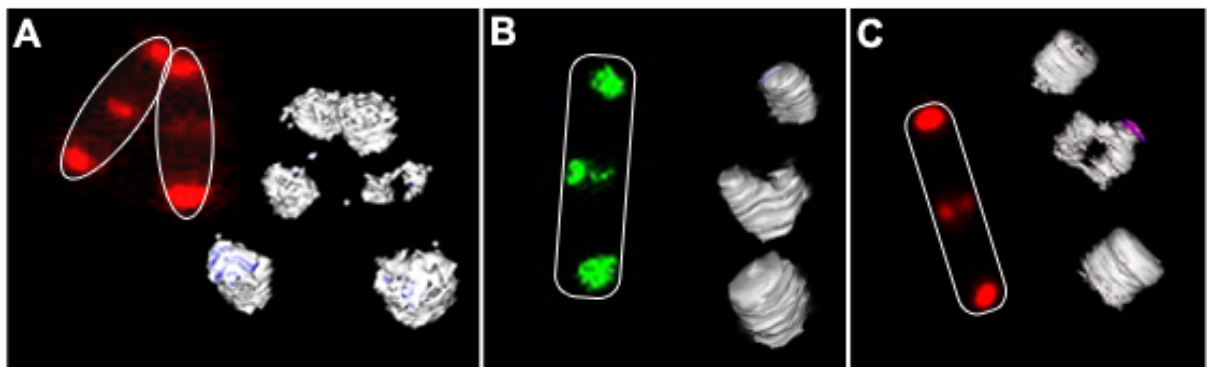


**Figure S4: DivIVA is recruited to the division septum, prior to septum closure.** (A) In *C. glutamicum*, DivIVA localizes as two foci at the midcell position. A three dimensional (3D) reconstruction of a series of Z-stacks reveals that DivIVA is recruited to the division septum before septum constriction and thus forms a ring-like structure at the midcell. (B) When expressed in *E. coli*, *C. glutamicum* DivIVA is also recruited early to the division septum, forming a ring-like structure. (C) A 3D reconstruction of a series of Z-stacks shows that the *S. coelicolor* DivIVA is recruited early to the division septum, forming a ring, when expressed in *E. coli*.

## Supplementary Figures

---

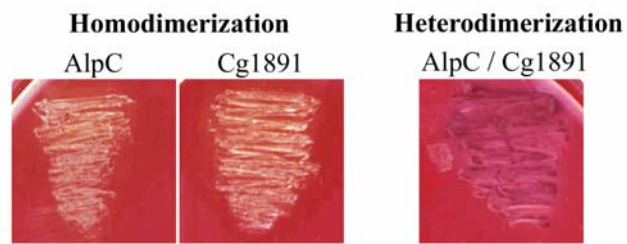


**Figure S5: Protein-protein interaction study between AlpC and Cg1891.** A bacterial-two-hybrid approach was employed to determine if AlpC and Cg1891 interact. To this end, both proteins were fused to a wild-type LexA DNA binding domain and transformed into the reporter strain SU101. If no interaction takes place, there is no binding of the operator and the *lacZ* gene is expressed. When grown on MacConkey agar containing 10 % lactose, the lactose can be fermented resulting in a decrease in the pH of the medium and the colonies appear red. Both AlpC and Cg1891 showed self interaction (left). However, AlpC does not interact with Cg1891.

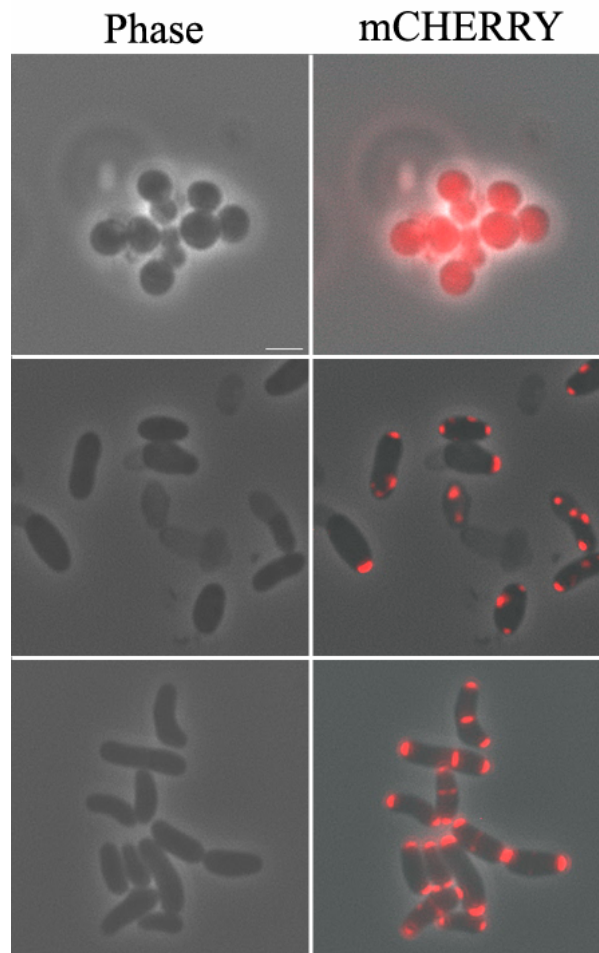


**Figure S6: In *C. glutamicum*, a DivIVA truncation mutant is viable but rapidly acquires suppressor mutations.** In freshly transformed cells, DivIVA $\Delta$ 144-298-mCHERRY does not localize and cells have coccoidal morphology, indicative of apical growth defects (top). After a few days, DivIVA $\Delta$ 144-298-mCHERRY begins to localize, often at irregular positions, and cells begin to acquire polarity and rod-shape (middle). When grown in liquid medium (BHI), the morphology of the majority of cells is almost identical to wild type cells, and DivIVA $\Delta$ 144-298-mCHERRY localization is at the poles and division septa, similar to the wild type protein. Scale bar, 2 $\mu$ m.

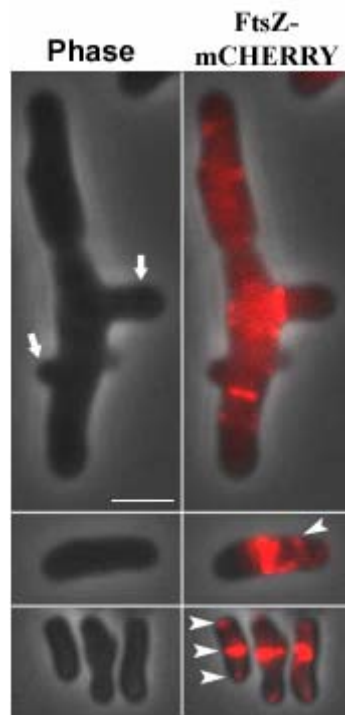


**Figure S7:** In *C. glutamicum*, a partially functional FtsZ mutant exhibits growth from ectopic sites. Shown are *C. glutamicum* cells expressing FtsZ-mCHERRY as the only copy from the native promoter. Scale bar, 2 $\mu$ m.

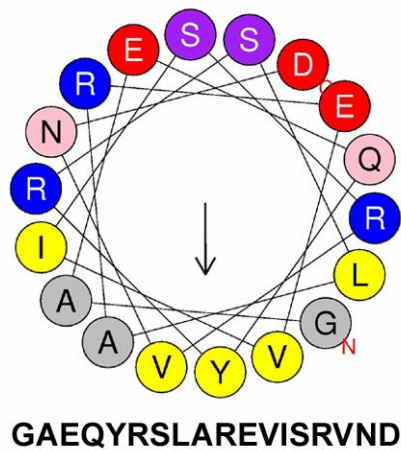


**Figure S8:** The C-terminal of PlpP is predicted to be amphipathic. The amino acid sequence of the C-terminal of PlpP (amino acid 270-290) is shown. Amphipathic Helix predictions were derived from HELIQUEST (<http://heliquet.ipmc.cnrs.fr>) (Gautier *et al.*, 2008).

## 7. Scientific Activities

### 7.1 Publications

Bramkamp, M., Emmins, R., Weston, L., **Donovan, C.**, Daniel R.A., Errington, J. 2008. A novel component of the division-site selection system of *Bacillus subtilis* and a new mode of action for the division inhibitor MinCD. *Mol Microbiol* **70**: 1556-15569.

**Donovan, C.**, Bramkamp, M. 2009. Characterization and subcellular localization of a bacterial flotillin homologue. *Microbiology* **155**: 1789-1799.

\***Donovan, C.**, Schwaiger, A., Krämer, R., Bramkamp, M. 2010. Subcellular localization and characterization of the ParAB system from *Corynebacterium glutamicum*. *J Bacteriol* **192**: 3441-3451.

\***Donovan, C.**, Sieger, B., Krämer, R., Bramkamp, M. 2012. A synthetic *Escherichia coli* system identifies a conserved origin tethering factor in Actinobacteria. *Mol Microbiol* **84**: 105-116.

\* Part of these publications were used in this thesis.

### 7.2 Manuscripts in preparation

Donovan, D., Heyer, A., Krämer, R., Frunzke, J., Bramkamp, M. 2012. Identification of a novel prophage encoded actin-like protein in *Corynebacterium glutamicum*.

Donovan, C., Krämer, R., Bramkamp, M. 2012. Chromosome organization influences cell growth and division in *Corynebacterium glutamicum*.

### 7.3 Conference participation

2009: Jahrestagung Vereinigung für Allgemeine und Angewandte Mikrobiologie (VAAM) in Bochum. Poster Presentation: "A bacterial flotillin homologue involved in the early stages of sporulation in *Bacillus subtilis*".

2010: Jahrestagung Vereinigung für Allgemeine und Angewandte Mikrobiologie (VAAM) in Hannover. Poster Presentation: "Chromosome segregation and cell division in *Corynebacterium glutamicum*".

Bacterial Cell Biology. Puerto Morelos, Mexico. Poster Presentation: "Chromosome segregation and cell division in *Corynebacterium glutamicum*".

2011: Jahrestagung Vereinigung für Allgemeine und Angewandte Mikrobiologie (VAAM) in Karlsruhe. Oral Presentation: "A synthetic *in vivo* system identifies a chromosome tethering factor in *Corynebacterium glutamicum*".

2012: Jahrestagung Vereinigung für Allgemeine und Angewandte Mikrobiologie (VAAM) in Tübingen. Poster Presentation: "Identification of a polar tethering factor in *Corynebacterium glutamicum*".

### 7.4 Awards

2009: Klaus-Liebrecht Preis: "Characterization of the *Bacillus subtilis yuaG* gene; a bacterial flotillin homologue".

2010: Jenny Gusyk-Preis: Travel grant for Bacterial Cell Biology conference, Mexico.

2012: Jahrestagung Vereinigung für Allgemeine und Angewandte Mikrobiologie (VAAM) Tübingen. Posterpreis: "Identification of a polar tethering factor in *Corynebacterium glutamicum*".

### 8. Acknowledgements

I would like to acknowledge the following people:

Prof. Krämer for giving me the opportunity to work in this lab and for the scientific input.

Prof. Marc Bramkamp, thank you for taking a chance on me. Thank you for giving me the faith in myself to achieve my goal. You always took time to discuss problems with the project, after which I usually gained a higher level of optimism and enthusiasm.

Very special thanks to all my wonderful colleagues in the cell division group (Anja, Suey, Inga, Frank, Juri, Boris and Gabi). The wonderful atmosphere you created in the lab made it possible to endure the periods of little or no success. Everyone was always willing to help solve the scientific problems. When the problems were solved, everyone was willing to have a laugh.

To the whole AG Krämer working group, thank you all for your help, kindness and friendliness, for making everyday more interesting than the next and for all the fun times.

To my parents I am so grateful for your support and encouragement, for all you sacrificed for me. I am so blessed to have such wonderful parents. Also, Debra, Aonrai and Mairead, over the years you have helped me so much.

I would especially like to thank Yassine for making it possible for me to study in Cologne. Without you none of this would have been possible.

## 9. Erklärung

Ich versichere, dass ich die von mir vorgelegte Dissertation selbständig angefertigt, die benutzten Quellen und Hilfsmittel vollständig angegeben und die Stellen der Arbeit – einschließlich Tabellen, Karten und Abbildungen –, die anderen Werken im Wortlaut oder dem Sinn nach entnommen sind, in jedem Einzelfall als Entlehnung kenntlich gemacht habe; dass diese Dissertation noch keiner anderen Fakultät oder Universität zur Prüfung vorgelegen hat; dass sie – abgesehen von unten angegebenen Teilpublikationen – noch nicht veröffentlicht worden ist sowie, dass ich eine solche Veröffentlichung vor Abschluß des Promotionsverfahrens nicht vornehmen werde.

Die Bestimmungen dieser Promotionsordnung sind mir bekannt. Die von mir vorgelegte Dissertation ist von Prof. Dr. Krämer betreut worden.

### Nachfolgend genannte Teilpublikationen liegen vor:

**Donovan, C.,** Schwaiger, A., Krämer, R., Bramkamp, M. 2010. Subcellular localization and characterization of the ParAB system from *Corynebacterium glutamicum*. *J Bacteriol* **192**: 3441-3451.

**Donovan, C.,** Sieger, B., Krämer, R., Bramkamp, M. 2012. A synthetic *Escherichia coli* system identifies a conserved origin tethering factor in Actinobacteria. *Mol Microbiol* **84**: 105-116.

Ich versichere, dass ich alle Angaben wahrheitsgemäß nach bestem Wissen und Gewissen gemacht habe und verpflichte mich, jede, die obigen Angaben betreffende Veränderung dem Dekanat unverzüglich mitzuteilen.

.....  
Datum

.....  
Unterschrift

### 10. Curriculum Vitae

#### Personal Details

Name	Catriona Donovan
Date of Birth	28 March 1980
Nationality	Irish
Address	Reinold Str. 8, 50676 Köln

#### University Education

- 2009-2012:** Dissertation at the institute of Biochemistry, University of Cologne, Germany in the group of Prof. Dr. Reinhard Krämer. Research project: "Cytoskeleton proteins involved in chromosome segregation and cell division in *Corynebacterium glutamicum*".
- 2006-2008:** M.Sc Biological Science at the University of Cologne, Germany. Research project: "Characterization of the *B. subtilis* gene *yuaG*; a bacterial flotillin homologue".
- 1998-2004:** B.Sc Applied Biology at the Institute of Technology Tralee, Co. Kerry, Ireland.

#### School Education

- 1992-1998:** St. Mary's Secondary School, Moyderwell, Tralee, Co. Kerry, Ireland.